BAD Phosphorylation:
A Novel Link between Apoptosis and Cancer

BAD Phosphorylierung:
Eine Neue Verbindung zwischen Apoptose und Krebs

Doctoral Thesis for Submission to a Doctoral Degree

at the Graduate School of Life Sciences,

Julius Maximilian University of Würzburg

Sections

Infection & Immunity

and

Biomedicine

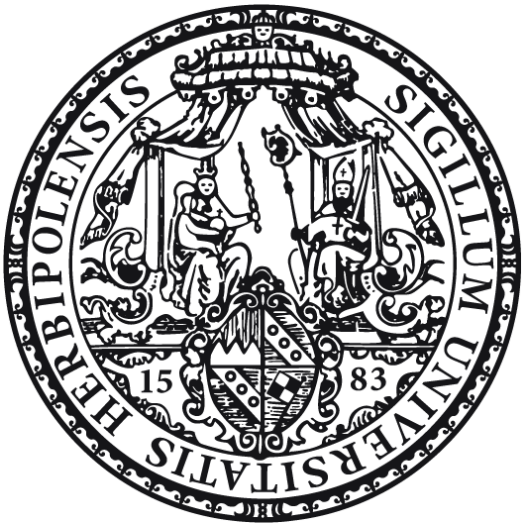

submitted by

Lisa Polzien

from

Würzburg

Würzburg, 2011

Submitted on: February 18th, 2011

Office stamp

Members of the Promotionskomitee:

Chairperson:	Prof. Dr.Thomas Dandekar
Primary Supervisor:	Prof. Dr. Dr. h.c. Roland Benz
Supervisor (second):	Prof. Dr. Thomas Rudel
Supervisor (third):	PD Dr. Mirko Hekman

Day of Rigorosum: 25.05.2011

Certificates were handed out on: ……..

The thesis is based on the following manuscripts:

1. **Polzien L**, Baljuls A, Rennefahrt UE, Fischer A, Schmitz W, Zahedi RP, Sickmann A, Metz R, Albert S, Benz R, Hekman M, Rapp UR (2009) Identification of novel *in vivo* phosphorylation sites of the human pro-apoptotic protein BAD: pore-forming activity of BAD is regulated by phosphorylation. *J. Biol. Chem*. **284,** 28004-28020

2. **Polzien L**, Benz R, Rapp UR (2010) Can BAD pores be good? New insights from examining BAD as a target of RAF kinases. *Adv. Enzyme Regul*. **50,** 147-159

3. **Polzien L**, Baljuls A, Roth HM, Kuper J, Benz R, Schweimer K, Hekman M, Rapp UR (2010) Pore-forming activity of BAD is regulated by specific phosphorylation and structural transitions of the C-terminal part. *Biochim. Biophys Acta*. **1810,** 162-169

4. **Polzien L**, Baljuls A, Albrecht M, Hekman M, Rapp UR (2011) BAD contributes to RAF-mediated proliferation and cooperates with B-RAF-V600E in cancer signaling. *J. Biol. Chem*. [Epub ahead of print]

„Dissertation unter Einschluss mehrerer Manuskripte“ in der GSLS –
Erklärung zu Eigenanteilen an Publikationen und Zweitpublikationsrechten
(ggf. weitere Blätter dieses Formblatts verwenden)

Publikation (Vollständiges Zitat): **Polzien L**, Baljuls A, Rennefahrt UE, Fischer A, Schmitz W, Zahedi RP, Sickmann A, Metz R, Albert S, Benz R, Hekman M, Rapp UR (2009) Identification of novel *in vivo* phosphorylation sites of the human proapoptotic protein BAD: pore-forming activity of BAD is regulated by phosphorylation. *J. Biol. Chem.* **284,** 28004-28020

Beteiligt an	**Autoren-Initialen,** Verantwortlichkeit abnehmend von links nach rechts				
Planung der Untersuchungen	MH	LP	URR, RB	UER	AB
Datenerhebung	LP	UER	RM	AF, SA	WS, RPZ, AS
Daten-Analyse und Interpretation	LP	MH	URR, RB	UER	AB
Schreiben des Manuskripts	MH	LP	URR	AB	

Publikation (Vollständiges Zitat): **Polzien L**, Benz R, Rapp UR (2010) Can BAD pores be good? New insights from examining BAD as a target of RAF kinases. *Adv. Enzyme Regul*. **50,** 147-159

Beteiligt an	**Autoren-Initialen,** Verantwortlichkeit abnehmend von links nach rechts				
Planung der Untersuchungen	LP	RB	URR		
Datenerhebung	LP				
Daten-Analyse und Interpretation	LP	RB	URR		
Schreiben des Manuskripts	LP	URR	RB		

Publikation (Vollständiges Zitat): **Polzien L**, Baljuls A, Roth HM, Kuper J, Benz R, Schweimer K, Hekman M, Rapp UR (2010) Pore-forming activity of BAD is regulated by specific phosphorylation and structural transitions of the C-terminal part. *Biochim. Biophys. Acta*. **1810,**162-169

Beteiligt an	**Autoren-Initialen,** Verantwortlichkeit abnehmend von links nach rechts				
Planung der Untersuchungen	LP	MH	AB, RB	URR	
Datenerhebung	LP	HMR	JK	KS	
Daten-Analyse und Interpretation	LP	MH, RB	AB	HMR	JK, KS
Schreiben des Manuskripts	MH	LP	AB		

Publikation (Vollständiges Zitat): **Polzien L**, Baljuls A, Albrecht M, Hekman M, Rapp UR (2011) BAD contributes to RAF-mediated proliferation and cooperates with B-RAF-V600E in cancer signaling. *J. Biol. Chem.* [Epub ahead of print]

Beteiligt an	**Autoren-Initialen,** Verantwortlichkeit abnehmend von links nach rechts				
Planung der Untersuchungen	LP	MH	MA	AB	URR
Datenerhebung	LP	MA			
Daten-Analyse und Interpretation	LP	MH	MA		
Schreiben des Manuskripts	LP	MH	MA	AB	

Für alle in dieser „Dissertation unter Einschluss mehrerer Manuskripte“ verwendeten Manuskripte liegen die notwendigen Genehmigungen der Verlage und Co-Autoren für die Zweitpublikation vor.
Mit meiner Unterschrift bestätige ich die Kenntnisnahme und das Einverständnis meines direkten Betreuers.

Lisa Polzien, 18.02.2011,
Name Kandidat(in), Datum, Unterschrift

Content

Summary

BAD (Bcl-2 antagonist of cell death, Bcl-2 associated death promoter) is a pro-apoptotic member of the Bcl-2 protein family that is regulated by phosphorylation in response to survival factors. Although much attention has been devoted to the identification of phosphorylation sites in murine BAD (mBAD), little data are available with respect to phosphorylation of human BAD (hBAD) protein. In this work, we investigated the quantitative contribution of BAD targeting kinases in phosphorylating serines 75, 99 and 118 of hBAD (**Chapter 3.1**). Our results indicate that RAF kinases phosphorylate hBAD *in vivo* at these established serine residues. RAF-induced phosphorylation of hBAD was not prevented by MEK inhibitors but could be reduced to control levels by use of the RAF inhibitor Sorafenib (BAY 43-9006). Consistently, expression of active RAF suppressed apoptosis induced by hBAD and the inhibition of colony formation caused by hBAD could be prevented by RAF. In addition, using surface plasmon resonance technique we analyzed the direct consequences of hBAD phosphorylation by RAF with respect to complex formation of BAD with 14-3-3 proteins and Bcl-X_L. Phosphorylation of hBAD by active RAF promotes 14-3-3 protein association, whereby the phosphoserine 99 represents the major binding site. Furthermore, we demonstrate in this work that hBAD forms channels in planar bilayer membranes *in vitro*. This pore-forming capacity is dependent on phosphorylation status and interaction with 14-3-3 proteins. Additionally, we show that hBAD pores possess a funnel-shaped geometry that can be entered by ions and non-charged molecules up to 200 Da (**Chapter 3.2**). Since both lipid binding domains of hBAD (LBD1 and LBD2) are located within the C-terminal region, we investigated this part of the protein with respect to its structural properties (**Chapter 3.3**). Our results demonstrate that the C-terminus of hBAD possesses an ordered β-sheet structure in aqueous solution that adopts helical disposition upon interaction with lipid membranes. Additionally, we show that the interaction of the C-terminal segment of hBAD with the BH3 domain results in the formation of permanently open pores, whereby the phosphorylation of serine 118 proved to be necessary for effective pore-formation. In contrast, phosphorylation of serine 99 in combination with 14-3-3 association suppresses formation of channels. These results indicate that the C-terminal part of hBAD controls hBAD function by structural transitions, lipid binding and phosphorylation.

Using mass spectrometry we identified in this work, besides the established *in vivo* phosphorylation sites at serines 75, 99 and 118, several novel hBAD phosphorylation sites (serines 25, 32/34, 97, 124 and 134, **Chapter 3.1**). To further analyze the regulation of hBAD function, we investigated the role of these newly identified phosphorylation sites on BAD-mediated apoptosis. We found that in contrast to the N-terminal phosphorylation sites, the C-terminal serines 124 and 134 act in an anti-apoptotic manner (**Chapter 3.4**). Our results further indicate that RAF kinases and PAK1 effectively phosphorylate BAD at serine 134. Notably, in the presence of wild type hBAD, co-expression of survival kinases, such as RAF and PAK1, leads to a strongly increased proliferation,

whereas substitution of serine 134 by alanine abolishes this process. Furthermore, we identified hBAD serine 134 to be strongly involved in survival signaling in B-RAF-V600E containing tumor cells and found phosphorylation of this residue to be crucial for efficient proliferation in these cells. Collectively, our findings provide new insights into the regulation of hBAD function by phosphorylation and its role in cancer signaling.

Zusammenfassung

BAD (Bcl-2 antagonist of cell death, Bcl-2 associated death promoter) ist ein pro-apoptotisches Mitglied der Bcl-2 Proteinfamilie und wird in Abhängigkeit von Wachstumsfaktoren durch Phosphorylierung reguliert. Obwohl der Identifizierung von Phosphorylierungsstellen in murinem BAD (mBAD) in den vergangenen Jahren viel Aufmerksamkeit gewidmet wurde, ist die Phosphorylierung des humanen BAD (hBAD) Proteins kaum charakterisiert. In der vorliegenden Arbeit wird der quantitative Beitrag unterschiedlicher Kinasen in Bezug auf die Phosphorylierung der etablierten Phosphorylierungsstellen Serin 75, 99 und 118 von hBAD dargestellt (**Kapitel 3.1**). Unsere Ergebnisse deuten darauf hin, dass RAF-Kinasen hBAD *in vivo* an diesen etablierten Stellen phosphorylieren. Die RAF-bedingte Phosphorylierung konnte nicht durch MEK-Inhibitoren beeinflusst werden, dagegen bewirkte die Gabe des RAF-Inhibitors Sorafenib (BAY 43-9006) eine Reduktion der Phosphorylierung auf das Niveau der Kontrollproben. Übereinstimmend konnte durch die Expression von aktiven RAF-Kinasen die BAD-induzierte Apoptose sowie die BAD-bedingte Inhibierung der Koloniebildung unterdrückt werden. Zusätzlich verwendeten wir Oberflächen-Plasmon-Resonanz-Spektroskopie um die Auswirkungen der RAF-bedingten BAD-Phosphorylierung auf die Komplexbildung von hBAD mit 14-3-3-Proteinen und Bcl-X_L zu analysieren. Dabei wurde festgestellt, dass die Phosphorylierung von hBAD durch aktive RAF-Kinasen die Assoziierung von 14-3-3 begünstigt, wobei Phosphoserin 99 die Hauptbindungsstelle darstellt.

Weiterhin gelang der Nachweis, dass hBAD *in vitro* Poren in Lipid-Doppelschicht-Membranen bilden kann. Wir wiesen nach, dass die Fähigkeit von hBAD Poren zu bilden phosphorylierungsabhängig ist und durch die Interaktion mit 14-3-3-Proteinen beeinflusst wird. Außerdem demonstrieren wir in dieser Arbeit, dass die BAD-Poren eine zylinderförmige Geometrie aufweisen und sowohl für Ionen als auch für ungeladene Moleküle mit einer Größe von bis zu 200 Da zugänglich sind (**Kapitel 3.2**). Da beide Lipid-Bindungsstellen (LBD1 und LBD2) am C-Terminus des hBAD lokalisiert sind, charakterisierten wir des Weiteren diesen Teil des Proteins in Hinblick auf seinen strukturellen Aufbau (**Kapitel 3.3**). Unsere Ergebnisse demonstrieren, dass der hBAD-C-Terminus in wässriger Lösung eine geordnete β-Faltblattstruktur aufweist und bei Eintritt in eine Lipidumgebung helikale Elemente ausbildet. Zusätzlich zeigen wir in dieser Arbeit, dass die Interaktion des C-terminalen hBAD-Segments mit der BH3-Domäne zur Ausbildung von permanent offenen Poren führt, wobei die Phosphorylierung an Serin 118 eine Notwendigkeit für effektive Porenbildung darstellt. In Gegensatz dazu bewirkte die Phosphorylierung von Serin 99 in Kombination mit der Assoziierung von 14-3-3-Protein eine Inhibierung der Porenbildung. Diese Ergebnisse weisen darauf hin, dass der C-terminale Teil von hBAD durch strukturelle Veränderungen, Lipidbindung und Phosphorylierung entscheidend die Funktion von hBAD reguliert.

Mit Hilfe von Massenspektroskopie konnten wir im Rahmen dieser Arbeit, zusätzlich zu den etablierten Phosphorylierungsstellen Serin 75, 99 und 118, einige neue *in vivo*

Phosphorylierungsstellen von hBAD identifizieren (Serin 25, 32/34, 97, 124 und 134, **Kapitel 3.1**). Um die Regulierung der Funktion von hBAD weiter zu analysieren, untersuchten wir die Rolle dieser neu identifizierten Phosphorylierungsstellen in Bezug auf die BAD-induzierte Apoptose (**Kapitel 3.4**). Wir fanden heraus, dass im Gegensatz zu den N-terminalen Phosphorylierungsstellen, die Phosphorylierungsstellen am C-Terminus an der Apoptoseregulation mitwirken. Weiterhin weisen unsere Ergebnisse darauf hin, dass RAF-Kinasen, neben PAK1, an der Phosphorylierung von Serin 134 von hBAD beteiligt sind. Interessanterweise bewirkte die Co-Expression von RAF oder PAK1 mit dem wildtypischen hBAD eine erhebliche Verstärkung der Zellproliferation. Diese verstärkte Proliferation konnte durch einen Serin-zu-Alanin-Austausch in hBAD an der Stelle 134 vollständig verhindert werden. Weiterhin entdeckten wir, dass die Phosphorylierung dieser Stelle in B-RAF-V600E enthaltenden Tumorzellen bei der Regulation der Zellproliferation mitwirkt und für eine effiziente Proliferation entscheidend ist. Zusammenfassend gewähren unsere Ergebnisse neue Einblicke in die Regulierung der Funktion von hBAD durch Phosphorylierung sowie in die Rolle von hBAD bei der Krebsentwicklung.

1. General Introduction

1.1. Apoptosis

Apoptosis is a genetically encoded program leading to cell death that is essential for normal development and homeostasis in multicellular organisms. Deregulation of this process has far-reaching effects by causing illnesses such as tumor development and autoimmune diseases (Danial and Korsmeyer 2004; Reed *et al.* 2004; Wang and Youle 2009). The morphological characterization of apoptosis includes cell shrinkage, chromatin condensation, nuclear fragmentation, and membrane blebbing. All of these phenomena are due to the proteolytic activity of the caspase proteases (Kerr *et al.* 1972; Taylor *et al.* 2008).

Apoptotic caspases can be divided into two classes, termed initiator and executioner caspases. Initiator caspases (caspases 2, 8, and 9) play an apical role during the process of apoptosis and their activation is typically required for the activation of executioner caspases (caspase 3, 6, and 7). Initiator caspases have a limited number of substrates including self-cleavage, the Bcl-2 family protein Bid as well as executioner caspases. In contrast, executioner caspases target hundreds of different substrates and are largely responsible for the phenotypic changes observed during apoptosis. The caspase-mediated protein cleavage ultimately leads to the phagocyte recognition and engulfment of the dying cell.

In apoptosis progression, mitochondria constitute a convergence point (Wang and Youle 2009; Wang 2001; Youle and Strasser 2008). However, the importance of this organelle differs, since in vertebrates apoptosis can occur through two different signaling pathways: the intrinsic or the extrinsic pathway (Fig. 1). Both Pathways converge on activating the executioner caspases 3 and 7 (Tait and Green 2010).

Figure 1 (right): Intrinsic and extrinsic pathways of apoptosis.
Intrinsic apoptotic stimuli, such as endoplasmic reticulum (ER) stress or DNA damage, activate BH3-only proteins which, in turn, activate Bak and Bax leading to mitochondrial outer membrane permeabilization. Anti-apoptotic Bcl-2 proteins inhibit this process by binding BH3-only proteins as well as Bak or Bax. Mitochondrial outer membrane permeabilization enables the release of various proteins from the mitochondrial intermembrane space promoting caspase activation and apoptosis. Cytochrome C binds apoptotic protease-activating factor 1 (APAF1) and induces its oligomerization resulting in the formation of a structure termed the apoptosome. The apoptosome recruits and activates the initiator caspase 9 that cleaves and activates the executioner caspases 3 and 7, leading to apoptosis. Mitochondrial release of the proteins SMAC (also known as DIABLO) and OMI (also known as HTRA2) antagonizes the caspase inhibitory function of XIAP. The extrinsic apoptotic pathway is initiated by stimulation of death receptors resulting to the recruitment of adaptor molecules such as FADD and then caspase 8. The consequence is dimerization and activation of caspase 8, which subsequently cleaves and activates the caspases 3 and 7, leading to apoptosis. Crosstalk between the extrinsic and intrinsic pathway is required in some cell types to induce receptor-induced apoptosis and occurs through caspase 8-mediated cleavage and activation of Bid. FasL, Fas ligand; tBid, truncated Bid; PM, plasma membrane; TNF, tumour necrosis factor; TRAIL, TNF-related apoptosis-inducing ligand. Adapted from Tait and Green (2010).

In the intrinsic pathway, the crucial event driving initiator caspase activation and apoptosis represents the permeabilization of the outer mitochondrial membrane, which leads to the release of pro-apoptotic proteins from the mitochondrial intermembrane space (Tait and Green 2010). One of these proteins is cytochrome C (Liu *et al.* 1996), which subsequently binds to apoptotic protease activating factor-1 (APAF1) and thereby induces conformational change and oligomerization of this protein (Li *et al.* 1997; Tait and Green 2010). The result is the formation of a caspase activation platform termed the apoptosome. The apoptosome recruits, dimerizes and activates the initiator

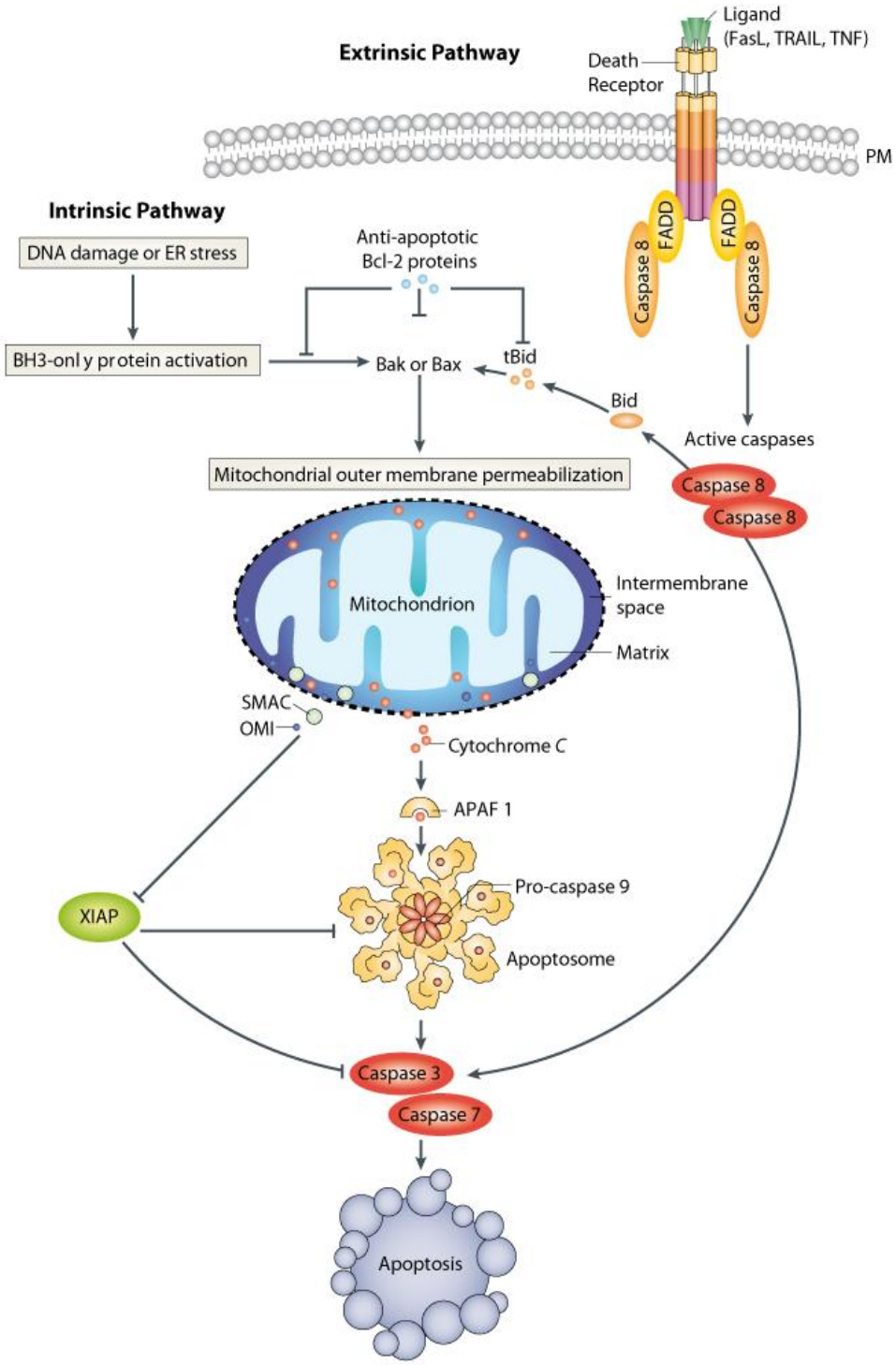

caspase 9, which, in turn, cleaves and activates the executioner caspases 3 and 7. Additionally, inhibition of caspase activity by X-linked inhibitor of apoptosis protein (XIAP) is blocked by mitochondrial release of second mitochondria-derived activator of caspase (SMAC; also known as DIABLO) (Du *et al.* 2000; Verhagen *et al.* 2000) and OMI (also known as HTRA2)(Yang *et al.* 2003). Mitochondrial outer membrane permeabilization is a highly regulated process that is primarily controlled through interactions between pro- and anti-apoptotic members of the Bcl-2 family of proteins.

In the extrinsic pathway, death receptor stimulation causes the recruitment of adaptor molecules, such as Fas-associated death domain protein (FADD), which bind, dimerize and activate the initiator caspase 8. Adjacent, activated caspase 8 cleaves and activates the executioner caspases 3 and 7 (Fig. 1). In so-called type I cells, caspase 8-mediated activation of the executioner caspases is sufficient for apoptosis induction (Barnhart *et al.* 2003). In contrast, type II cells require mitochondrial outer membrane permeabilization to induce apoptosis. In the extrinsic cascade, mitochondrial outer membrane permeabilization can be initiated though crosstalk between the extrinsic and intrinsic pathway by caspase 8-mediated activation of the Bcl-2 family protein Bid (Barnhart *et al.* 2003). The difference between type I and type II cells in death receptor-mediated apoptosis could be ascribed to the requirement for mitochondrial outer membrane permeabilization to antagonize the protein XIAP (Jost *et al.* 2009; Yin *et al.* 1999).

Normally, mitochondrial outer membrane permeabilization leads to a rapid activation of caspases and apoptosis. However, in the absence of caspase activity (for example in caspase 9- and APAF1-deficient backgrounds), certain cells undergo caspase-independent cell death (Cecconi *et al.* 1998; Hakem *et al.* 1998; Yoshida *et al.* 1998). During this process, the mitochondrial outer membrane permeabilization represents a point of no return that causes cell death either by the release of intermembrane space proteins, like Endonuclease G and AIF, or through a progressive decline of mitochondrial function leading, among other effects, to ATP depletion (Tait and Green 2008).

1.2. The Bcl-2 Family of Proteins

Proteins of the Bcl-2 (B-cell lymphoma 2) family are crucial regulators of apoptosis at the level of mitochondria. Bcl-2 proteins are characterized by the presence of at least one of the four Bcl-2 homology (BH) domains: BH1-BH4. The multi-BH domain family members of the Bcl-2 proteins are either anti- or pro-apoptotic (Adams and Cory 1998; Gross *et al.* 1999; Youle and Strasser 2008) (Fig. 2A). In general, the anti-apoptotic members (e.g. Bcl-2, Bcl-X_L, Mcl-1 or Bcl-w) display sequence homology in all four BH domains, whereas the pro-apoptotic multi-BH domain Bcl-2 proteins (e.g. Bak, Bax or Bok) have homologous BH1-3 domains. Deletion and mutagenesis studies demonstrated that the BH3 domain is critical for the pro-apoptotic and heterodimerization function of pro-apoptotic Bcl-2 proteins (Opferman and Korsmeyer 2003). The importance of the BH3 domain for mediating

pro-apoptotic function is further supported by the discovery of a subset of the pro-apoptotic Bcl-2 family members collectively known as the BH3-only proteins (e.g. Bid, Bik, Bim, Bmf, Puma, Noxa, Hrk/DP5, and BAD) that share sequence homology only in the BH3 domains (Huang and Strasser 2000; Youle and Strasser 2008) (Fig. 2A). Several Bcl-2 family proteins contain a carboxy-terminal membrane anchor that may facilitate binding to plasma- or intracellular membranes.

Upon activation by apoptotic stimuli, the pro-apoptotic Bcl-2 family proteins are capable of forming heterodimers with anti-apoptotic Bcl-2 family members. Solution structure of Bcl-X_L reveals that the BH1-3 domains form an elongated hydrophobic groove, which is the docking site for the BH3 domains of its pro-apoptotic binding partners (Sattler *et al.* 1997) (see also Fig. 2A). There is a growing body of evidence that anti-apoptotic Bcl-2 family proteins function, at least in part, by interacting with and antagonizing pro-apoptotic family members (Cory and Adams 2002; Opferman and Korsmeyer 2003). The pro-apoptotic Bcl-2 family proteins can be sub-divided into effector proteins that actually cause mitochondrial outer membrane permeabilization and the BH3-only proteins as sensors that relay the apoptotic signal to the effectors. Two prominent models of the activation of Bak and Bax have been proposed: the *direct* (or neutralization) and the *hierarchy model* (Letai *et al.* 2002; Willis *et al.* 2005) (Fig. 2B). In the *direct model*, Bak and Bax are bound in a constitutively active state by anti-apoptotic Bcl-2 proteins and can be released through competitive

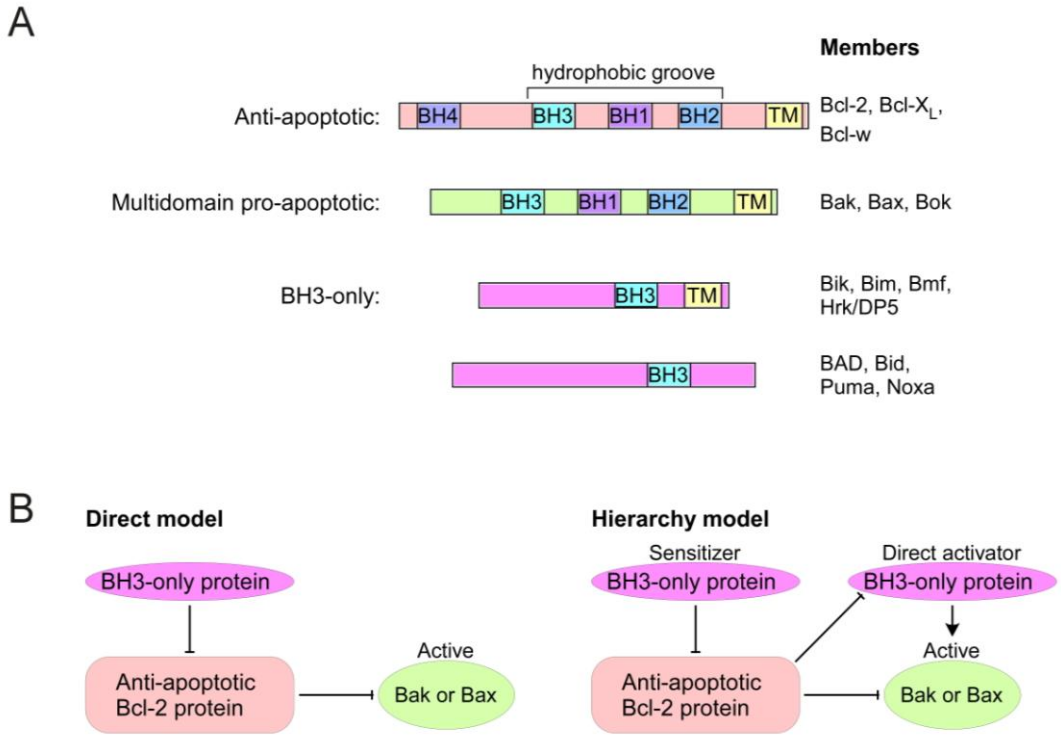

Figure 2: The Bcl-2 family of proteins.
A, The organization of the four Bcl-2 homology (BH) domains among the family members is illustrated. Many Bcl-2 family proteins also harbor a carboxy-terminal hydrophobic region that is thought to act as a transmembrane domain (TM) to facilitate association of the proteins with membranes. B, Two models of the activation of Bak and Bax have been proposed, the direct and the hierarchy model (Letai *et al.* 2002; Willis *et al.* 2005). For details see text. Adapted from Tait and Green (2010).

interactions of BH3-only proteins with these anti-apoptotic Bcl-2 family members resulting in induction of apoptosis. The *hierarchy model* asserts that Bak and Bax are activated following interaction with a subset of BH3-only proteins, the direct activators. According to this model, anti-apoptotic Bcl-2 family members prevent mitochondrial outer membrane permeabilization either by sequestering the activating BH3-only proteins or by inhibiting activated Bak and Bax. Additionally, a second subset of BH3-only proteins, the sensitizers, cannot directly activate Bak and Bax but neutralize anti-apoptotic Bcl-2 proteins. Definitive evidence for one of these models has proved to be challenging since aspects of both models are correct.

The exact modes and the mechanisms of the pathways that involve Bcl-2 family proteins are still not completely elucidated (Youle and Strasser 2008). Beyond apoptosis control, several proteins of the Bcl-2 family contribute in the regulation of various other physiological processes such as autophagy, mitochondrial respiration and glucose metabolism (for Review see (Danial 2008)).

1.2.1. Pore-Forming Activity of the Bcl-2 Family Proteins

During apoptosis, Bcl-2 family proteins, such as Bak and Bax, have been shown to induce permeabilization of the outer mitochondrial membrane, allowing proteins from the mitochondrial intermembrane space to escape into the cytosol, where they can initiate caspase activation and cell death (Antignani and Youle 2006; Kuwana *et al.* 2002; Opferman and Korsmeyer 2003; Wolter *et al.* 1997; Zamzami and Kroemer 2003). The mechanism whereby Bcl-2 proteins affect outer membrane permeability is still under investigation (Antignani and Youle 2006). Based on its crystal structure (Muchmore *et al.* 1996) it has been found that Bcl-X_L bears a resemblance to the translocation domain of diphtheria toxin (Choe *et al.* 1992), a domain that can form pores in artificial lipid bilayers. This observation provoked the predominant view that upon commitment to apoptosis, pro-apoptotic Bcl-2 family proteins form channels in the outer mitochondrial membrane (Martinou and Green 2001). Indeed, Bcl-X_L was shown to form pores in synthetic lipid membranes (Minn *et al.* 1997). Since then, a number of pro- and anti-apoptotic Bcl-2 family proteins like Bcl-2, Bax and the BH3-only protein Bid have been reported to have channel-forming activity (Minn *et al.* 1997; Schendel *et al.* 1999; Schendel *et al.* 1997). The question how many molecules of Bak or Bax are required to induce mitochondrial outer membrane permeabilization is controversially discussed. One study describes that four Bax molecules are sufficient to permeabilize an artificial membrane, whereas another report identified much larger Bax oligomers in apoptotic cells (Nechushtan *et al.* 2001; Saito *et al.* 2000). Recently, using single-cell imaging, the number of Bax molecules in a complex that induces mitochondrial membrane permeabilization was estimated to more than one hundred (Zhou and Chang 2008). However, limits of optical resolution prevented the detection of smaller complexes in this study.

In general, the channels formed by the different members of the Bcl-2 protein family can be divided into two different types: proteinaceous channels of defined size and ion specificity (Antonsson *et al.* 1997; Minn *et al.* 1997; Polzien *et al.* 2009; Schendel *et al.* 1999; Schendel *et al.* 1997; Schlesinger *et al.* 1997) and large lipid pores that allow free diffusion of up to 2-megadalton macromolecules (Basanez *et al.* 1999; Kuwana *et al.* 2002).

1.2.2. BH3-only Proteins as Sensors for Distinct Apoptotic Pathways

The BH3-only proteins are a sub-class of the pro-apoptotic Bcl-2 family proteins that share sequence homology only at the BH3 domain. The BH3 domain (and flanking residues) forms an amphipathic helix that associates with a hydrophobic groove of several members of the Bcl-2 family proteins (Fesik 2000; Petros *et al.* 2004). The large number of BH3-only proteins exhibit unique subcellular localization and diverse modes of activation suggesting a high level of specialization of their pro-apoptotic function.

BH3-only proteins react quickly to changes of cellular health and reach their pro-apoptotic potential by several means. These mechanisms include the increase of the protein level through transcriptional control, regulation of the protein stability (Domina *et al.* 2004; Oda *et al.* 2000), post-

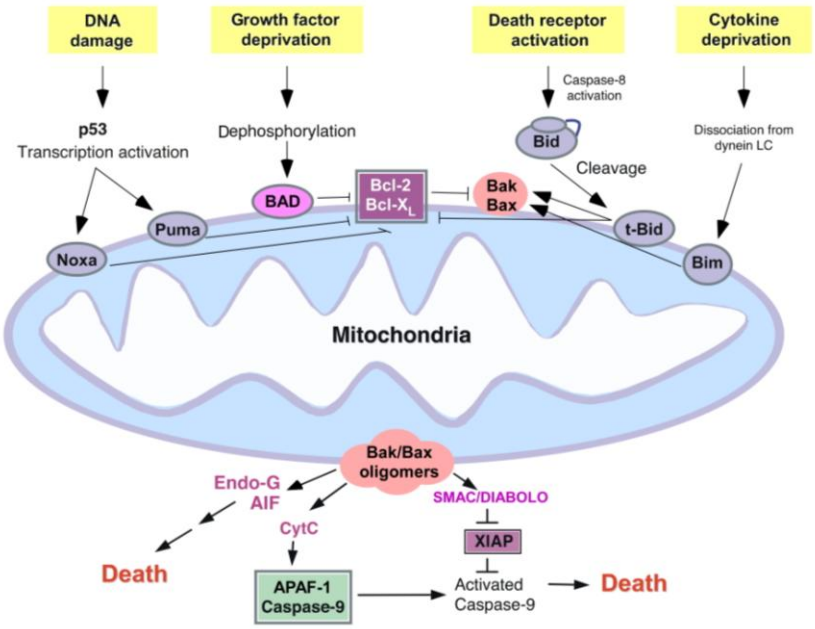

Figure 3: Schematic diagram of the putative function and regulation of selected Bcl-2 family members in apoptosis signaling.
The BH3-only proteins are sensors for various apoptotic stimuli and serve to transmit signals to the mitochondria upon activation. At the mitochondria, the BH3-only proteins act directly on the multidomain pro-apoptotic proteins or antagonize the function of the anti-apoptotic proteins, such as Bcl-2 or Bcl-X_L. Multidomain pro-apoptotic Bak and Bax oligomerize and facilitate permeabilization of the mitochondrial outer membrane and the release of apoptogenic factors like cytochrome C (CytC), apoptosis-inducing factor (AIF), endonuclease G (Endo-G), and SMAC/DIABOLO. Subsequently, these factors execute cell death through caspase dependent or -independent mechanisms. APAF-1, apoptotic protease activating factor-1; LC, light chain. Adapted from Chan and Yu (2004).

translational protein modifications (Zha *et al.* 1996; Zha *et al.* 2000), and changes in their subcellular distribution (Galmiche *et al.* 2008; Puthalakath *et al.* 1999). Therefore, BH3-only proteins were proposed to function as sentinels of the cellular health status by connecting proximal death signals to the core apoptotic pathway. Interestingly, individual BH3-only proteins are regulated by distinct mechanisms (Fig. 3). The genes of the BH3-only proteins Puma and Noxa, for instance, are transcription targets of the transcription factor p53 (Nakano and Vousden 2001; Oda *et al.* 2000; Yu *et al.* 2001), which is thought to induce or repress gene products that have a role in regulating apoptosis (Vousden 2000). Another BH3-only protein that was demonstrated to be regulated transcriptionally is Hrk/DP5. During embryogenesis, expression of Hrk/DP5 is induced in neuronal tissues that contain a relatively large number of apoptotic cells (Imaizumi *et al.* 1999).

The BH3-only proteins Bmf and Bim sense intracellular damage by their localization to distinct cytoskeletal structures. Three isoforms of Bim were described initially (BimEL, BimL and BimS) (O'Connor *et al.* 1998). In healthy cells, BimEL and BimL are maintained in an inactive status through binding to the microtubule-associated dynein motor complex. Certain damage signals, such as cytokine removal or exposure to taxol, a microtubule-polymerizing drug, can trigger that these proteins are released from microtubules, translocate to mitochondria and associate with Bcl-2 and Bcl-X_L to presumably neutralize their anti-apoptotic activity (Puthalakath *et al.* 1999). Additionally, Bim was demonstrated to be essential for the execution of trophic factor-induced apoptosis in the lymphoid cell lineage (Bouillet *et al.* 1999) as well as for the initiation of apoptosis during thymocyte negative selection (Bouillet *et al.* 2002). BimS as well as BimAD isoform (Marani *et al.* 2002) are normally not found in healthy tissue and may be controlled at the transcriptional level. Bmf has been described to be sequestered to myosin V motors in healthy cells. Some apoptotic stimuli, such as loss of cell attachment (anoikis), unleash Bmf, allowing it to translocate to the mitochondria and bind pro-survival Bcl-2 proteins (Puthalakath *et al.* 2001).

Under non-apoptotic conditions, the BH3-only protein Bid is localized in the cytosol. There, Bid is kept in its inactive form via an intramolecular bridge between the BH3 domain and the C-terminus of the protein (Tan *et al.* 1999). Binding of specific ligands to death receptors leads to an activation of caspase-8, that cleaves the inactive Bid conformer (Li *et al.* 1998; Luo *et al.* 1998). Caspase cleavage of Bid leads to the exposition of a glycine that is N-myristoylated (Zha *et al.* 2000). This cleaved Bid targets mitochondria with dramatically enhanced efficiency to trigger apoptosis (Zha *et al.* 2000). In addition to binding anti-apoptotic members of Bcl-2 family, Bid is able to induce allosteric activation and homo-oligomerization of Bak and Bax resulting in permeabilization of the outer mitochondrial membrane and the release of cytochrome C (Wei *et al.* 2000). Beside caspase-8, other proteases, such as lysozyme, granzyme B, and calpain have been shown to cleave and activate Bid (Heibein *et al.* 2000; Stoka *et al.* 2001; Sutton *et al.* 2000) indicating that multiple pathways exist in cells to activate this protein. The kinase JNK was demonstrated to induce caspase-8-independent cleavage of Bid at a

specific site to generate the Bid cleavage product jBid that translocates to mitochondria and leads to the release of SMAC/DIABLO, but not cytochrome C (Deng *et al.* 2003).

Since the different BH3-only proteins have very distinct modes of regulation, for many of these proteins it is not completely known which apoptotic signals they 'sense' and how their 'activities' are regulated. In addition, different cell types may require specific BH3-only proteins to regulate the apoptosis machinery in response to distinct conditions of stress (Chan and Yu 2004).

1.2.3. The BH3-only Protein BAD

The BH3-only protein BAD (Bcl-2 antagonist of cell death, Bcl-2 associated death promoter) was originally described to promote apoptosis by forming heterodimers with the pro-survival proteins Bcl-2 and Bcl-X_L, thus, preventing them from binding to Bax (Yang *et al.* 1995). In this process, phosphorylation of BAD protein plays a crucial role and leads to inactivation of its pro-apoptotic function. The importance of phosphorylation events was demonstrated by a knock-in approach in mice using a mutant of BAD that was non-phosphorylatable at serines 112, 136 and 155 (Datta *et al.* 2002). In cells expressing this BAD mutant, growth factors were unable to block apoptosis induced by either the intrinsic or extrinsic death pathway. Amino acid sequence of the human BAD protein (hBAD), all identified phosphorylation sites and the most important regulatory domains are illustrated in Fig. 26.

A death stimulus, such as growth factor withdrawal, results in dephosphorylation of BAD by calcineurin (Chiang *et al.* 2001) or protein phosphatase 2A (Zha *et al.* 1996) (Fig. 3). Dephosphorylated BAD translocates to mitochondria and associates with the anti-apoptotic proteins Bcl-2 or Bcl-X_L leading to induction of apoptosis. Therefore, the non-phosphorylated status of BAD was described to be its active state. Phosphorylation of murine BAD (mBAD) at Ser-155 (that corresponds to Ser-118 of human BAD) within its BH3 domain disrupts the complex formation with Bcl-2 or Bcl-X_L promoting cell survival (Datta *et al.* 2000). Accordingly, phosphorylation of Ser-112 and Ser-136 of mBAD or the corresponding phosphorylation sites Ser-75 and Ser-99 of hBAD results in association with 14-3-3 proteins and subsequent cytoplasmic sequestration of BAD (Hekman *et al.* 2006; Zha *et al.* 1996). Therefore, the phosphorylation status of BAD regulates its subcellular localization as well as the association with other proteins and reflects a checkpoint for cell death or survival (see also Fig. 38).

Although C-RAF was the first reported BAD kinase (Wang *et al.* 1996), its target sites were not clearly defined. In the meantime, there is a growing body of evidence for direct participation of RAF in regulation of apoptosis *via* BAD (Jin *et al.* 2005; Kebache *et al.* 2007; Panka *et al.* 2006). In addition, also other kinases, such as PKA (Harada *et al.* 1999), Akt/PKB (Datta *et al.* 1997), PAK (Gnesutta *et al.* 2001; Jin *et al.* 2005; Schurmann *et al.* 2000), Cdc2 (Konishi *et al.* 2002), RSK (She *et al.* 2002; Shimamura *et al.* 2000), CK2 (Klumpp *et al.* 2004) and PIM (Macdonald *et al.* 2006) were

shown to be involved in BAD phosphorylation. Also JNK is discussed to participate in BAD phosphorylation (Donovan *et al.* 2002; Yu *et al.* 2004; Zhang *et al.* 2005). Taken together, five serine phosphorylation sites (at positions 112, 128, 136, 155 and 170) and two threonines (117 and 201) have been identified and characterized in murine BAD so far. On the other hand, only few data were available regarding the role of phosphorylation in regulation of human BAD protein.

Presently, there is no crystallographic or NMR-based structural data for the full length BAD available. The only structural analysis of BAD describes the mode of molecular association between the anti-apoptotic protein Bcl-X_L and a 25-residue peptide derived from its BH3 domain (Petros *et al.* 2000). Recently, Hinds *et al*. (2007) suggested that in the absence of binding partners, BAD is an intrinsically unstructured protein. However, Yang *et al*. (1995) showed that the amino-terminus of BAD contains two PEST-sequences, suggestive of a high protein turnover (Rogers *et al.* 1986). Moreover, Hekman *et al.* (2006) observed that hBAD associates with unchanged efficiency with non-treated and protein-depleted mitochondria. Although the amino acid sequence of hBAD does not reveal a typical C-terminal transmembrane domain, hBAD was found to bind to model membranes with high affinity, predominantly to negative charged phospholipids and cholesterol-rich membranes (see also Fig. 38). These authors identified two lipid binding domains (LBD1 and LBD2) with different binding preferences, both located in the C-terminal part of the hBAD protein (Hekman *et al.* 2006). Interestingly, addition of the 25-residue peptide derived from the BAD BH3 domain increased considerably the association of Bcl-X_L with lipid vesicles (Hekman *et al.* 2006). This observation underlines recent findings concerning the role for BAD in mitochondrial targeting and membrane insertion of Bcl-X_L (Billen *et al.* 2008; Jeong *et al.* 2004).

1.3. RAF Kinases

Protein kinases play a central role in almost every aspect of cell biology. In humans, the family of protein kinases consists of 518 genes thereby making it one of the largest gene families (Manning *et al.* 2002). These enzymes are classified as serine/threonine kinases (385 members), tyrosine kinases (90 members), and tyrosine-kinase like proteins (43 members). RAF kinases are serine/threonine kinases that regulate the highly conserved Ras-RAF-MEK-ERK pathway (Daum *et al.* 1994; Mark and Rapp 1984; Rapp *et al.* 2006; Roskoski 2010; Wellbrock *et al.* 2004). This cascade mediates transduction of extracellular mitogenic signals through activated Ras GTPases to a MAP kinase module. Diverse cellular processes important for development including proliferation, survival, metabolism, migration and senescence are coordinated by this pathway. Consequently, deregulation is frequently found in tumors (Yeang *et al.* 2008). The first identified isoform of the RAF kinase family was C-RAF. It was discovered by retrovirus transduction experiments that led to isolation of the acutely transforming virus carrying the *v-raf* oncogene (3611-MSV) (Rapp *et al.* 1983). Mammalian RAF kinases belong to a family that includes A-, B-, and C-RAF. Team work between these enzymes

as well as specific interaction partners refines RAF signaling by targeting the mitogenic cascade to different subcellular compartments (Rapp *et al.* 2006; Udell *et al.* 2011).

All three RAF kinase isoforms are ubiquitously expressed in mammals, but they differ in their expression levels (Storm *et al.* 1990). Differential regulation of RAF kinase activity (Wellbrock *et al.* 2004) and varying phenotypes of RAF knockout mice indicate specialized functions of each isoform (Pritchard *et al.* 1996; Wojnowski *et al.* 2000; Wojnowski *et al.* 1997). Whereas C-RAF$^{-/-}$ as well as B-RAF$^{-/-}$ mice die early in embryonic development, A-RAF$^{-/-}$ animals are viable although they display neurological and intestinal abnormalities (Pritchard *et al.* 1996). The knockout of B-RAF in mice leads to overall growth retardation and increased apoptosis in endothelial tissues resulting in death from vascular hemorrhage between day 10.5 and 12.5 (Wojnowski *et al.* 1997). C-RAF$^{-/-}$ embryos exhibit disturbed development of the placenta and embryonic organs, in particular of the liver and the hematopoietic compartment (Huser *et al.* 2001; Mikula *et al.* 2001; Wojnowski *et al.* 2000). Embryonic lethality of C-RAF$^{-/-}$ mice occurred in midgestation and may be due to a high apoptosis rate in the liver (Huser *et al.* 2001; Mikula *et al.* 2001) that is also observed in cell culture experiments (Zhong *et al.* 2001).

1.3.1. Structure of the RAF Kinases

All RAF kinase isoforms share three conserved regions (CR1, CR2 and CR3) and two functional parts: the regulatory and the catalytic part (Daum *et al.* 1994; Roskoski 2010; Wellbrock *et al.* 2004). CR1 comprises a Ras-binding domain (RBD) and a cysteine-rich domain (CRD), which can bind two zinc ions. CR1 interacts with Ras as well as with membrane phospholipids. CR2 is a serine/threonine

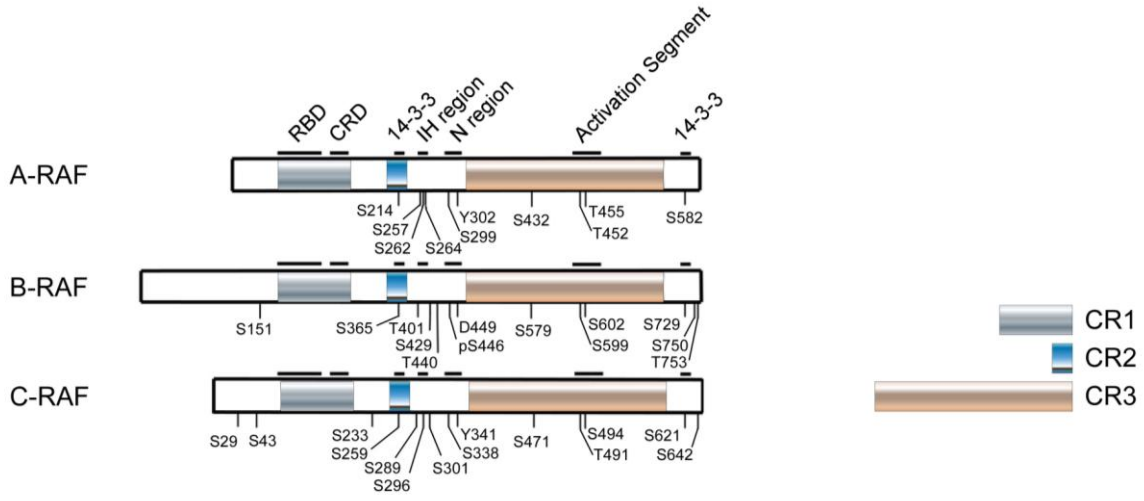

Figure 4: Organization of the RAF kinases.
CR1, CR2, and CR3 indicate the location of the three conserved regions that occur in all three enzymes. CR3 represents the protein kinase domain that contains an activation segment. Numbers indicate the location of selected serine (S), threonine (T), and tyrosine (Y) phosphorylation sites. In B-RAF, pS446 is a constitutively phosphorylated serine residue. Two independent 14-3-3 binding sites have been confirmed in all RAF kinase isoforms. See text for details. Adapted from Roskoski (2010).

rich domain containing a specific serine residue that can bind to 14-3-3 proteins in its phosphorylated state. Binding of 14-3-3 proteins to this phosphorylated site is inhibitory with respect to the kinase activity of the RAF kinases. CR3, which is located near the C-terminus, represents the protein kinase domain (Fig. 4).

The RAF protein kinase domain contains a large C-terminal lobe that is found in all protein kinases and an additional characteristic small N-terminal lobe (Fig. 5) (Wan *et al.* 2004). The large C-lobe is mainly α-helical and binds to the substrates of the RAF kinases. The N-terminal lobe exhibits an antiparallel β-sheet structure and anchors as well as orients ATP. It comprises a glycine-rich ATP-phosphate-binding loop, the so-called P-loop. The catalytic site lies in the cleft between the large and small lobes. In Fig. 5, the catalytic site is occupied by Sorafenib, an ATP-competitive inhibitor of RAF that has been approved for the treatment of advanced kidney and liver cancer (Wilhelm *et al.* 2008).

Movement of the two lobes leads to opening or closing of the catalytic cleft. The open state allows access of ATP and release of ADP. The closed state brings residues into the catalytically active position. Each lobe contains a polypeptide segment that can switch between active and inactive conformations (Seeliger *et al.* 2009). This segment represents the major α-helix of the small lobe, the so-called αC-helix. Within the large lobe, the activation segment adjusts to make or break part of the ATP-binding site.

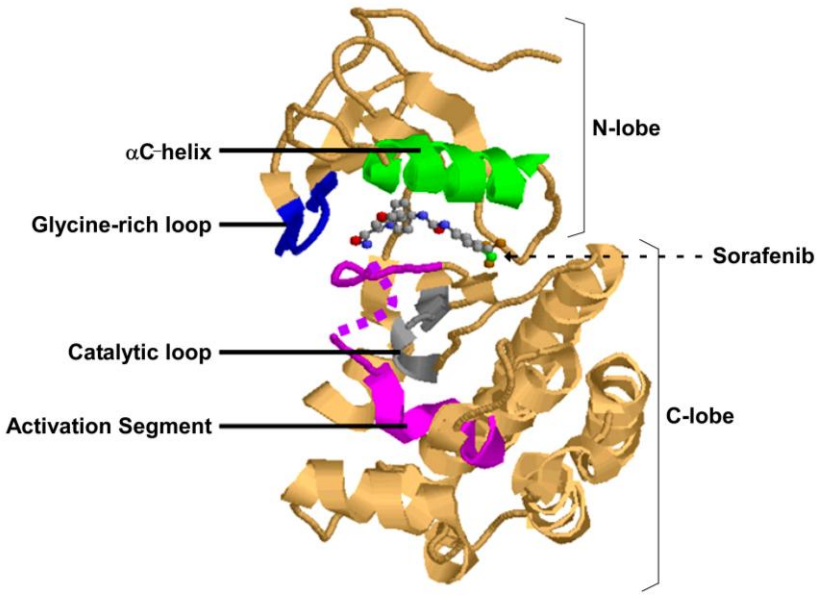

Figure 5: Ribbon diagram of the structure of human B-RAF kinase domain (CR3) associated to the RAF inhibitor Sorafenib.
The activation loop is displayed in its inactive conformation. Sorafenib (in the ball and stick format) is located in the catalytic cleft between the N- and C-lobes. Part of the activation segment, which is disordered, is shown by the dotted lines connecting its N-terminal (top) and C-terminal (bottom) components. The ribbon diagram was prepared from protein data bank file 1UWH. Adapted from Wan *et al.* (2004).

1.3.2. Regulation of RAF Kinase Activity

The basal activity of B-RAF is greater than that of C-RAF, which is greater than that of A-RAF. The regulation of activity of RAF kinases involves several steps including conformational changes, protein-protein interactions, phosphorylations and dephosphorylations (Rapp *et al.* 2006; Udell *et al.* 2011; Wellbrock *et al.* 2004). Under non-stimulatory conditions, two serine residues within the 14-3-3 binding domains are phosphorylated and occupied by 14-3-3 proteins (Fig. 4). Beside interaction of Ras-GTP with the RBD, that is necessary but not sufficient to activate RAF, each RAF isoform reveals additional specific activation mechanisms (see bottom).

The RAF kinases can form both homo- and heterodimers (Roskoski 2010; Rushworth *et al.* 2006; Weber *et al.* 2001). Concerning B- and C-RAF, it was reported that B-RAF/C-RAF heterodimers are more active than either homodimers (Rushworth *et al.* 2006). The dimerization of RAF kinase domains involves the αC-helix, an important determinant of active and inactive conformations (Rajakulendran *et al.* 2009). In cell lines and xenografts that harbor activated mutant B-RAF-V600E, some RAF kinase inhibitors effectively block MEK and ERK phosphorylation and activation (Hatzivassiliou *et al.* 2010; Heidorn *et al.* 2010; Poulikakos *et al.* 2010). Heidorn *et al*. (2010) found, however, that the B-RAF specific inhibitor 885-A leads to an unexpected increase in ERK phosphorylation in four human melanoma cell lines bearing activated N-Ras mutations. Two additional studies address this issue, and the common finding is that the binding of ATP competitive inhibitors to RAF kinases promote Ras-dependent C-RAF homo- or heterodimerization and leads to the so-called paradoxical activation (Hatzivassiliou *et al.* 2010; Poulikakos *et al.* 2010).

1.3.2.1. Regulation of C-RAF Activation

The regulation of C-RAF involves inter- and intramolecular protein interactions as well as direct phosphorylation (Chong *et al.* 2003; Dhillon and Kolch 2002; Roskoski 2010). In quiescent cells, C-RAF is located in its inactive state in the cytosol. The inactive conformation of C-RAF is maintained by autoinhibitory interactions occurring between the regulatory N-terminal and the catalytic C-terminal domains as well as by binding of 14-3-3 proteins to phosphorylated Ser-259 and Ser-621 (Fig. 4). In contrast to these inhibitory sites, phosphorylation of Ser-491 and Ser-494, which occur within the activation segment, as well as Ser-338 and Tyr-341, that are located in the N-region, is stimulatory for C-RAF activity (Chong *et al.* 2001). In addition, phosphorylation of Ser-471, which is located within the catalytic loop, is required for the interaction of C-RAF with its substrate MEK (Zhu *et al.* 2005). Active C-RAF can be down-regulated by ERK-mediated inhibitory feedback phosphorylation in positions Ser-29, Ser-43, Ser-289, Ser-296, Ser-301 and Ser-642 (Dougherty *et al.* 2005)

1.3.2.2. Regulation of A-RAF Activation

Perhaps due to its relatively low basal and inducible activity, little attention has been devoted to the regulation of A-RAF activation. Recently, Baljuls *et al*. (2008) investigated A-RAF phosphorylation and identified 35 phosphorylation sites in human A-RAF. Two of these newly identified phosphorylation sites could be ascribed as the inferred 14-3-3 binding sites (Ser-214 and Ser-582, Fig. 4). The authors showed that the degree of Ras/Lck-induced activation of serine 582 to alanine mutant was lower than that of A-RAF wild type. In addition, they found that A-RAF kinase activity is considerably increased in the serine 214 to alanine mutant when compared with the A-RAF wild type. Both results support a crucial role for 14-3-3 binding in the regulation of A-RAF kinase activity. Furthermore, Baljuls *et al*. (2008) found that Ser-432 within the potential MEK binding domain is essential for A-RAF signaling, whereas the importance of phosphorylation within the activation segment (Thr-452 and Thr-455) is restricted to the Ras/Lck-mediated stimulation of A-RAF. Additionally, seven novel phosphorylation sites within a tryptic peptide corresponding to A-RAF(248–267) were identified in this study. This regulatory domain was designated as the IH segment (Isoform-specific Hinge segment). The authors discovered three of the phosphorylation sites within this segment to be strongly involved in the positive regulation of A-RAF activity (Ser-257, 262, and 264). A spatial model of an A-RAF fragment, including residues between Ser-246 and Gln-277, revealed a switch of charge at the molecular surface of the IH region upon phosphorylation. This indicates a mechanism in which the high accumulation of negative charges leads to an electrostatic destabilization of protein-membrane interaction resulting in depletion of A-RAF from the plasma membrane upon prolonged stimulation (Baljuls *et al.* 2008).

1.3.2.3. Regulation of B-RAF Activation

In B-RAF, phosphorylation of Ser-365 within the CR2 region and Ser-729 near the C-terminus is required for 14-3-3 binding (Fig. 4). Phosphorylation of Thr-599 and Ser-602, which are located within the activation segment, is essential for B-RAF activation (Chong *et al.* 2003; Wellbrock *et al.* 2004). In addition, phosphorylation of Ser-579, which occurs in the catalytic loop, is essential for anchoring of RAF substrate MEK (Zhu *et al.* 2005). Activation of A-RAF and C-RAF requires protein-kinase catalyzed phosphorylation of residues in the N-region. In contrast, the N-region of B-RAF contains Asp-448 and Asp-449, which bear negative charges. Moreover, in B-RAF, Ser-446 is constitutively phosphorylated. Consequently, the N-region of B-RAF contains negative charges and does not require additional modifications to become negatively charged during activation. Deactivation of B-RAF can be achieved by feedback inhibition through ERK-induced phosphorylation of Ser-151, Thr-401, Ser-750, and Thr-753 (Ritt *et al.* 2010).

B-RAF mutants occur in a variety of human cancers while mutants of the other two RAF isoforms in cancers are rare. The majority of B-RAF mutations occur in the glycine-rich loop or in the activation segment (Davies *et al.* 2002). These mutations disrupt the inactive state to favor the active

one. A valine to glutamic acid exchange in position 600 accounts for ≈90% of all known B-RAF mutations. This mutation occurs within the activation segment of B-RAF where the introduction of negative charges favors the formation of an active conformation.

1.4. The Family of 14-3-3 Proteins

14-3-3 proteins are ubiquitous eukaryotic adapter proteins involved in the regulation of a variety of cellular processes such as protein trafficking, cell-cycle control, signal transduction and apoptosis (Aitken 2006; Hermeking and Benzinger 2006). 14-3-3 proteins regulate cellular processes through several different mechanisms such as altering protein localization, modulating enzymatic activity, promoting protein stability, preventing dephosphorylation and inhibiting or mediating protein interactions (Aitken 2006; Dougherty and Morrison 2004). For example, 14-3-3 proteins stabilize the tumor suppressor p53 (Rajagopalan *et al.* 2010; Schumacher *et al.* 2010) and regulate the activity of the cell-cycle phosphatase Cdc25 (Conklin *et al.* 1995; Peng *et al.* 1997), the transcriptional modulator TAZ (Hong *et al.* 2005) and RAF (Fantl *et al.* 1994; Fischer *et al.* 2009; Freed *et al.* 1994; Fu *et al.* 1994; Hekman *et al.* 2004; Light *et al.* 2002). Importantly, 14-3-3 proteins have been implicated in a variety of human diseases. They were shown to participate in diverse cancers (Hermeking 2003; Tzivion *et al.* 2006) and have been associated with the virulence of human pathogenic organisms (Fu *et al.* 1993; Ottmann *et al.* 2007) and the development of neurodegenerative diseases (Berg *et al.* 2003).

Mammals contain at least seven 14-3-3 isoforms each encoded by a distinct gene (Aitken 2006). The crystal structures of the seven different human isoforms reveal that all 14-3-3 proteins share a similar tertiary structure which consists of nine α-helices (Gardino *et al.* 2006). Two 14-3-3 protein molecules form biologically functional homo- and heterodimers, resembling a U-shaped structure (see Fig. 6). Four amino-terminal α-helices mediate dimerization and form a platform to which five carboxy-terminal helices have a rectangular orientation, representing the walls of the U-shaped dimer (Obsil *et al.* 2001). The 14-3-3 dimer forms an amphipathic groove, wherein most of the conserved amino acids are located in the interior side and the variant chains point towards the outside.

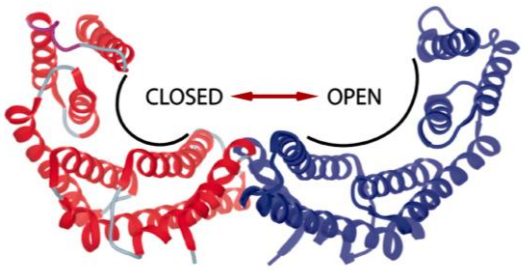

Figure 6: Dynamic nature of the 14-3-3 protein dimers.
Crystal structure of 14-3-3 β, looking down the peptide binding grooves, which are demonstrated open and closed for the individual monomers. Adapted from Yang *et al.* (2006).

14-3-3 proteins bind to defined peptide motifs, two of which (RS-X-pS-X-P and R-XXX-pS-X-P) are highly conserved and recognized by all 14-3-3 isoforms. Normally, binding occurs only if a specific site within the motif is phosphorylated, but some 14-3-3 interactions are independent of phosphorylation (Aitken 2006). The phosphorylated serine/threonine residue of the ligand contacts amino acids that form a basic pocket in the otherwise acidic 14-3-3 molecule, explaining the ability of substrate phosphorylation to act as a molecular switch, controlling ligand binding (Aitken 2006; Obsil *et al.* 2001).

1.4.1. 14-3-3 Proteins as Key Regulators of RAF Kinases

RAF kinases contain two high-affinity phosphoserine sites that mediate binding to a 14-3-3 dimer. These are in C-RAF Ser-259 in the CR2 and Ser-621 at the C-terminal end of the kinase domain. In A-RAF, they correspond to Ser-214 and Ser-582, respectively, whereas in B-RAF these sites are Ser-365 and Ser-729. In C-RAF, an additional 14-3-3 binding site surrounding Ser-233 has been proposed (Dumaz and Marais 2003). Additionally, an atypical 14-3-3 binding site positioned at the C-terminal part of C-RAF-CRD and close to RBD (comprising the residues RKT in position 143–145) has been identified (Clark *et al.* 1997). Near this 14-3-3 binding site, in the hydrophobic region LAF (positions 149–151), occurs a contact domain for farnesyl residue of Ras proteins. Therefore, it is feasible that the interaction of the farnesyl residue with this domain is necessary to remove sterical hindrances caused by 14-3-3 proteins.

Hekman *et al.* (2004) analyzed 14-3-3 interaction with purified full-length RAF kinases and showed that RAF isozymes differ in their 14-3-3 association rates. They demonstrated that the C-terminal 14-3-3 binding site (pSer-621) represents the high-affinity binding site, whereas the pSer-259 epitope mediates lower affinity binding. Importantly, they visualized the dynamic changes of C-RAF phosphorylation events, including 14-3-3 binding, that occur in response to growth factor stimulation (Hekman *et al.* 2004). Hagemann and Rapp (1999) suggested a hypothetical model, in which 14-3-3 proteins stabilize the inactive as well as the fully active conformation of RAF. In this model, a 14-3-3 dimer binds to the conserved 14-3-3 binding sites to keep RAF in a closed inactive conformation. Binding of Ras-GTP to the RBD displaces 14-3-3 from the phosphoserine site in the CR2 domain. This results in a conformational rearrangement, which subsequently, could cause a basal activation of RAF. Finally, the fully active RAF conformation might be stabilized by binding of 14-3-3 dimers (Hagemann and Rapp 1999). More recent studies provide additional details to this regulation model. It has been demonstrated that serine dephosphorylation within the CR2 domain represents a prerequisite for RAF activation in growth factor-stimulated cells (Ory *et al.* 2003). Thus, an additional function of 14-3-3 dimer might be to mask regions on RAF that are required for translocation and subsequent activation of RAF by Ras. In addition, it was demonstrated that, during the C-RAF activation process, the 14-3-3 dimer can be replaced from the internal binding site of C-RAF by the scaffold prohibitin (PHB) (Fischer *et al.* 2009). Although the discussed regulation mechanism was conceptualized on the

basis of interaction studies with 14-3-3 and C-RAF, the highly conserved 14-3-3 binding sites presented in A- and B-RAF suggest that this mechanism can be generalized for all RAF kinases. Concerning A-RAF, co-immunoprecipitation of overexpressed 14-3-3 with A-RAF (Hagemann 1999) as well as isolation of the 14-3-3 isoforms β, ε, ζ, τ and η in a two-hybrid screen using A-RAF as a bait reinforce the assumption that A-RAF, just like B- and C-RAF, might be regulated by 14-3-3 proteins. Indeed, our group demonstrated recently that A-RAF associates *in vivo* with at least two 14-3-3 isoforms, epsilon and tau (Fischer *et al.* 2009).

Mutations within the internal 14-3-3 binding domain of C-RAF (surrounding the Ser-259) have been shown to cause severe human disorders, such as Noonan and LEOPARD syndrome (Pandit *et al.* 2007; Razzaque *et al.* 2007). Recently, in collaboration with our group, Molzan *et al*. (2010) further characterized the nature of Noonan syndrome. We showed that the reported mutations in the N-terminal 14-3-3 binding site mediate plasma membrane recruitment of C-RAF by wild-type Ras, thereby confirming the essential negatively regulatory role of 14-3-3. These observations are of prime importance, since they suggest the possibility of addressing the 14-3-3/C-RAF complex in diseases that involve an overactive Ras-RAF-MAPK pathway.

1.4.2. 14-3-3 Proteins Control Apoptosis

The ability of 14-3-3 proteins to stimulate protein–protein interactions as well as the control that 14-3-3 proteins exert on the subcellular localization of their binding partners is crucial for apoptosis regulation (Fig. 7). 14-3-3 proteins sequester various pro-apoptotic proteins. For example, they interact with Fkhrl1 (Brunet *et al.* 1999), Bax (Nomura *et al.* 2003), Ask1 (Zhang *et al.* 1999), Yap (Basu *et al.* 2003) and BAD (Zha *et al.* 1996). Phosphorylated Fkhrl1 associates with 14-3-3 proteins and is therefore retained in the cytoplasm. Upon deprivation from survival signals, dephosphorylation of Fkhrl1 leads to its dissociation from 14-3-3 and translocation to the nucleus, resulting in the activation of apoptotic genes. Phosphorylated Yap is also retained in the cytoplasm by binding to 14-3-3, resulting in a displacement from the nucleus where it functions as a co-activator of p73-mediated apoptosis (Basu *et al.* 2003). Similarly, association with 14-3-3 antagonizes the death-promoting activity of Ask1 independent of Ask1 kinase activity (Zhang *et al.* 1999). Interaction of Bax with 14-3-3 occurs in a phosphorylation-independent manner, negatively regulating pro-apoptotic activity of Bax (Nomura *et al.* 2003).

During apoptosis control, 14-3-3 proteins play an important role in the regulation of the BH3-only protein BAD as well. As mentioned above, phosphorylation of Ser-112 and Ser-136 of mBAD or the corresponding phosphorylation sites Ser-75 and Ser-99 of hBAD results in association with 14-3-3 proteins and subsequent cytoplasmic sequestration of BAD preventing the association of BAD with the mitochondrially localized Bcl-2 and Bcl-X_L, and therefore inhibiting apoptosis (Hekman *et al.* 2006; Zha *et al.* 1996). Furthermore, in this work we show that 14-3-3 proteins are able to terminate the pore-forming activity of hBAD (Polzien *et al.* 2009).

Whereas 14-3-3 promotes the cytoplasmic localization of Fkhrl1, Yap and BAD, interaction of 14-3-3 with the catalytic subunit of telomerase that prevents apoptosis, Tert, promotes its retention in the nucleus (Seimiya *et al.* 2000; Zhang *et al.* 2003). Additionally, a role of 14-3-3 proteins as adapter molecules has been implicated for the binding of A20, a zinc-finger protein that inhibits apoptosis induced by TNFα. It was demonstrated that A20 and RAF do not interact directly, but require 14-3-3 for their interaction to take place (Vincenz and Dixit 1996). Furthermore, 14-3-3 influences the subcellular localization of A20 by keeping it in the cytoplasm (Muslin and Xing 2000; van Hemert *et al.* 2001). 14-3-3 proteins seem also to be involved in promoting apoptosis, since interaction of Nade with p75 neurotrophin receptor (p75NTR) might recruit 14-3-3 proteins, resulting in an induction of caspase-3 activation and cell death (Kimura *et al.* 2001).

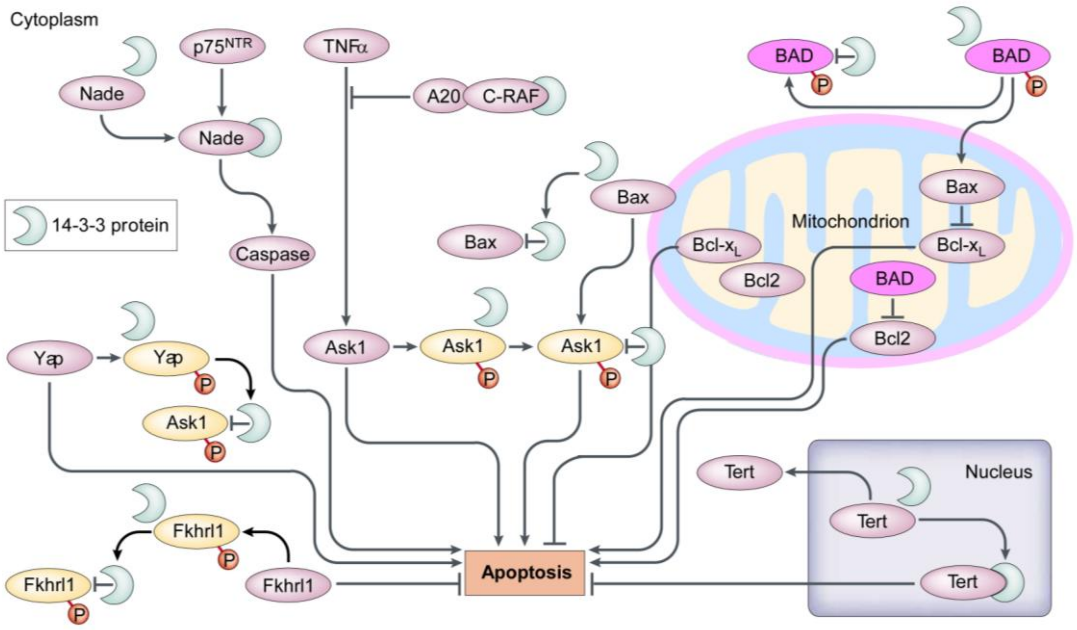

Figure 7: Regulation of apoptosis by 14-3-3 proteins.
By binding to various interaction partners involved in apoptosis, 14-3-3 proteins (green) modulate the apoptotic process through various mechanisms, such as sequestration and control of the subcellular localization of phosphorylated and non-phosphorylated pro- and anti-apoptotic proteins. The pro-apoptotic protein BAD binds to the anti-apoptotic proteins Bcl-2 and Bcl-X_L resulting in cell death. Once phosphorylated, BAD can be complexed by 14-3-3 proteins in the cytoplasm, which prevents the association with Bcl-2 and Bcl-X_L and therefore inhibits apoptosis. Similarly, phosphorylated Fkhrl1 and phosphorylated Yap are retained in the cytoplasm. On the other hand, interaction of 14-3-3 with the catalytic subunit of telomerase that prevents apoptosis (Tert) promotes its retention in the nucleus. In addition, the death-promoting activity of Ask1 and Bax is antagonized by its binding to 14-3-3 proteins. Ligand-dependent binding of the p75 neurotrophin receptor (p75NTR)-associated cell death executor (Nade) to p75NTR has been demonstrated to occur. Interaction of Nade and p75NTR might recruit 14-3-3 proteins, leading to an induction of caspase-3 activation and apoptosis. A role of 14-3-3 proteins as adapter molecule has been implicated for the binding of A20 that inhibits apoptosis induced by TNFα. A20 and RAF do not interact directly, but require 14-3-3 for their interaction to take place. Additionally, 14-3-3 influences the subcellular localization of A20, keeping it in the cytoplasm. Adapted from Berg *et al.* (2003).

1.5. Bcl-2 Proteins are Substrates of RAF and Play a Role in Human Diseases

The proteins of the Bcl-2 family display important targets of the RAF pathway. The Ras-RAF-MEK-ERK cascade was suggested to directly phosphorylate the anti-apoptotic protein Bcl-2 and thereby enhance its apoptosis suppressing properties (Deng *et al.* 2000). Moreover, pro-apoptotic Bcl-2 proteins like Bim and BAD were shown to be targets of the RAF pathway as well. The phosphorylation of these proteins results in an inactivation of their pro-apoptotic properties. Concerning Bim, phosphorylation can lead to degradation of the protein (Ewings *et al.* 2007; Ley *et al.* 2003; Luciano *et al.* 2003). As mentioned above, the phosphorylation of BAD leads to its sequestration into the cytosol (Scheid *et al.* 1999; Zha *et al.* 1996).

Table 1: Involvement of Bcl-2 proteins in selected human diseases.

Disease and involvement of Bcl-2 proteins	Ref.
Neurodegenerative disease	
Bax expression is increased in the brain of Parkinson patients and ablation of Bax prevents dopaminergic neurodegeneration in a mouse model of Parkinson disease.	(Tatton 2000; Vila *et al.* 2001)
Atherosclerosis	
A high level of Bax and p53 was identified in smooth muscle cells from the atherosclerotic plaque.	(Kockx *et al.* 1998)
Cancer	
1. Bcl-2 is frequently overexpressed in many types of cancers.	(Reed 1999)
2. Studies of patients with acute lymphoblastic leukemia, acute myelogenous leukemia, non-Hodgkin's lymphomas, chronic lymphocytic leukemia, and multiple myeloma indicate that a high-level expression of anti-apoptotic Bcl-2 family members, such as Bcl-2, Bcl-X_L, and Mcl-1, represents a clinically important chemoresistant phenotype on cancer cells.	(Reed 1999)
3. The *Bax* gene was shown to exhibit a frameshift mutation or a decreased expression in colon, gastric and haematopoietic cancers. The frameshift mutation within the *Bax* gene was demonstrated to confer a selection advantage during tumor clonal evolution.	(Brimmell *et al.* 1998; Rampino *et al.* 1997)
4. The *Bak* gene is mutated in some human gastric and colorectal cancers.	(Ionov *et al.* 2000; Kondo *et al.* 2000)
5. Amplification of *Akt/PKB* gene was observed frequently in solid tumors. Since it phosphorylates BAD and renders it non-apoptotic, hyperactivation of Akt/PKB induces resistance to apoptotic drugs.	(Datta *et al.* 1999)
6. BAD was identified to be a direct target of B-RAF that was demonstrated to be activated through mutation in many types of cancer. In addition, it was demonstrated that BAD plays an exclusive role in survival signaling of cancer cells harboring mutated B-RAF (B-RAF-V600E).	This work (Polzien *et al*. 2011, *J. Biol. Chem.* [Epub ahead of print])

Analogous to Bim, phosphorylation via C-RAF can also promote BAD polyubiquitination leading to an increase of the turn-over of this protein through proteasomal degradation (Fueller *et al.* 2008).

The finding that BAD is phosphorylated by RAF is of particular importance, since highly active B-RAF has been demonstrated to represent one of the crucial players in cancer development (Davies *et al.* 2002). Importantly, deregulation of specific proteins of the Bcl-2 family was also demonstrated to be involved in many human diseases, especially during development of cancer (Table 1). Unfortunately, for many pathological conditions, it is difficult to decipher the cause and effect relationship. Further studies are required to unravel function and regulation of the Bcl-2 family of proteins.

1.6. Aim of the Project

The mammalian RAF kinases (A-, B- and C-RAF) play a central role in the conserved Ras-RAF-MEK-ERK signaling pathway and mediate cellular responses induced by growth factors (Daum *et al.* 1994; Rapp *et al.* 2006; Wellbrock *et al.* 2004). Consequently, aberrant regulation of this cascade is frequently found in tumors (Yeang *et al.* 2008). The proteins of the Bcl-2 family are crucial regulators of apoptosis that have been shown to be involved in various human diseases as well, especially during development of cancer (see Table 1). Direct involvement of C-RAF in inhibition of pro-apoptotic properties of BAD established the first link between signal transduction and apoptosis control (Rapp *et al.* 2004; Troppmair and Rapp 2003). However, whether BAD is a direct substrate of RAF kinases as well as the exact RAF target sites within BAD protein have not been investigated so far (Wang *et al.* 1996).

In my work, I examined whether hBAD serves as a direct substrate of RAF isoforms. A main focus of my project was to investigate the quantitative contribution of RAF kinases to hBAD phosphorylation *in vivo*. Therefore, I examined hBAD phosphorylation by RAF and other kinases like PKA, Akt/PKB and PAK1 concerning phosphosite specificity and their phosphorylation efficiency. As RAF kinases make crucial contributions to hBAD phosphorylation, I further explored whether hBAD phosphorylation by RAF is accompanied by decreased apoptosis. Additionally, I investigated whether phosphorylation of hBAD by RAF regulates the interaction of BAD with 14-3-3 proteins and Bcl-X_L. To unravel whether other serines contribute to the regulation of hBAD in addition to the established phosphorylation sites serines 75, 99 and 118, I analyzed the whole hBAD protein by mass spectrometry and examined whether the newly identified phosphorylation sites are involved in the regulation of apoptosis. Subsequently, a main focus of this work was to investigate whether specific phosphorylation of hBAD plays a role in survival signaling in naturally occurring tumor cell lines.

To further elucidate the mechanisms of BAD mediated apoptosis, another goal of this work was to examine whether hBAD is able to form channels in planar bilayer membranes. In this respect, I explored whether this pore-formation is dependent on BAD's phosphorylation status and interaction

between BAD and 14-3-3 proteins. Additionally, I decided to elucidate the origin of the extraordinary high affinity of the C-terminal part of hBAD for membrane lipids. Toward this end, I deciphered the secondary structure of a peptide corresponding to the C-terminal part of hBAD and containing the lipid binding domain LBD1 by use of CD and NMR spectroscopy. An important feature of hBAD is that, depending on its phosphorylation state, it changes its location from the cytoplasm to membranes. Therefore, I analyzed the structure of the hBAD C-terminal part in both, aqueous solution and lipid environment. In addition, I examined whether the C-terminal part of hBAD is sufficient for formation of open pores in lipid bilayers.

Knowledge derived from the understanding of the function and regulation of the Bcl-2 family of proteins may allow us to develop novel therapeutic strategies for human diseases with inaccurate apoptosis signaling. Therefore, in summary, the aim of this work was to provide new insights into the regulation of BAD function by phosphorylation and its role in cancer signaling.

2. General Experimental Procedures

The methods described in this section are all based upon today's standard molecular and cellular biology techniques.

2.1. Materials

2.1.1. Instruments

Hardware	***Manufacturer***
Bacterial incubator shaker	TR-125, Infors AG, Bottingen
BIAcore-X or BIAcore-J system	Biacore AB, Uppsala, Sweden
Bruker APEX II FT-ICR mass spectrometer	Bruker Daltonic GmbH, Bremen
Cell culture hood	M630, Ceag Schirp Reinraumtechnik, Selm-Bork
Cell culture incubator	Heraeus Instrument
Centrifuges	Centrifuge 5417 R, Eppendorf; Megafuge 1.0R, Heraeus Instrument
Electrophoresis power supply	EV202, Peqlab
Film developing machine	Ecomax X-Ray Film Processor, Protec GmbH & Co. KG, Oberstenfeld
LTQ XL mass analyzer	Thermo Scientific, Dreieich
Magnetic stirrer	SB161, Bibby Scientific, Staffordshire, UK
PCR machine	T3 Thermocycler, Biometra
pH meter	pH 720, InoLab, Weinheim
Protein gel system	Mini Trans Blot, Biorad
Qstar Elite mass analyzer	Applied Biosystems, Darmstadt
Semi dry blotting system	PerfectBlue Semi-Dry Electro Blotter, Peqlab
Shakers	See-saw rocker SSL4, Bibby Scientific, Staffordshire, UK
Spectrophotometer	NanoDrop NP-1000, Peqlab
Thermoshaker for microfuge tubes	Mixing Block MB-102, Bioer, Hangzhou, China
Typhoon 9200 imager	GE Healthcare
UV/Visible Spectrophotometer	Ultrospec 3000, Pharmacia Biotech
Vortex	Vortex-genie 2, Scientific Industries, New York, USA
Western Blot Imager	ChemoCam HR16-3200, Intas, Göttingen

2.1.2. Chemical Reagents and General Materials

Reagent	*Purchased from*
Acrylamide (30%)/Bisacrylamide (0.8%)	Roth
Adenosin-5'-triphosphate (ATP)	Sigma
Agarose (ultra pure)	Roth
Ammonium peroxydisulfate (APS)	Roth
Ampicillin	Roth
Antipain	AppliChem
Aprotinin	Sigma
Asolectin	Sigma
Sorafenib (BAY-43-9006)	Bayer
Benzamidine	Sigma
β-Glycerophosphate	Roth
β-Mercaptoethanol	Roth
Bovine serum albumin (BSA)	Roth
Bromphenol Blue	Roth
1-Butanol	Roth
C18 ZipTip	Millipore
Cardiolipin	Sigma
CHAPS	Sigma
CI1040	Axon Medchem
Coomassie Protein Assay Reagent	Pierce
Coumaric acid	Sigma
dNTP Mix (2mM)	Fermentas
Dimethyl sulfoxide (DMSO)	Roth
Diphytanoylphosphatidylcholine	Avanti Polar Lipids
Dithiothreitol (DTT)	Sigma
EDTA (Ethylenediaminetetraacetic acid-disodium salt)	Roth
EGTA (Ethylene glycol-bis-(-aminoethylether)-N,N,N',N'-tetraacetic acid)	AppliChem
Empigen BB	Calbiochem
Ethanol (p. A.)	AppliChem
Ethanol (denatured with 1% MEK)	AppliChem
Ethidium bromide	Roth
Glutathione	Sigma
Glutathione Sepharose	Amersham Bioscinces

Glycerol	Roth
Glycine	Roth
H-89	Sigma
HEPES	Roth
Hydrochloride (HCl)	AppliChem
Hydrogen peroxide	Sigma
Isobutylmethylxanthine (IBMX)	Sigma
Isopropanol	Roth
Lambda DNA/Eco91I Marker, 15	Fermentas
LB-Agar	Roth
Leupeptin	Sigma
Lipofectamine	Invitrogen
Lipofectamine 2000	Invitrogen
Luminol	Biomol
LY294002	Promega
Magnesium chloride hexahydrate ($MgCl_2 \times 6H_2O$)	Roth
Magnesium sulfate heptahydrate ($MgSO_4 \times 7H_2O$)	Roth
Manganese (II) chloride tetrahydrate ($MnCl_2 \times 4H_2O$)	Roth
Methanol	Roth
Milk powder (nonfat)	AppliChem
MitoTracker Deep Red	Invitrogen
Ni^{2+}-nitrilotriacetic acid-agarose	Quiagen
Nitrocellulose membrane	Protran, Whatman
Nonidet P40 (NP-40)	Sigma
PD98059	Promega
PD0325901	Santa Cruz Biotechnology
PepMap trapping column	Dionex
PepMap nano-LC column	Dionex
Pepstatin	Roth
Phenylmethylsulfonyl fouoride (PMSF)	Sigma
Phosphatidylcholine	Sigma
Phosphatidylehanolamine	Sigma
Phosphatidylinositol	Sigma
Phosphatidylserine	Simga

PIPES	Sigma
Potassium chloride (KCl)	Roth
Prestained Protein Ladder PageRuler,	Fermentas
Protein G-Agarose	Roche
Sucrose	Roth
Sodium chloride (NaCl)	Roth
Sodium dodecyl sulfate (SDS, ultra pure)	Roth
Sodium fluoride (NaF)	Roth
Sodium hydroxide (NaOH)	Roth
Sodium orthovanadate (Na_3VO_4)	Sigma
Sodium pyrophosphate ($Na_4P_2O_7$)	Roth
Sphingomyelin	Sigma
TEMED (N,N,N',N'-Tetramethylethylenediamine)	Roth
Thrombin	Sigma
Trifluoroethanol (TFE)	Sigma
Tris (Tris-(hydroxymethyl)-aminomethan)	Roth
Tween 20	Roth
U0126	Promega
Whatman 3MM Paper	Schleicher & Schüll
Wortmannin	Santa Cruz Biotechnology
X-ray film	Pierce
Xylene cyanol	Roth

2.1.3. Cell Culture Materials

Reagent	***Source***
Dulbecco's Modified Eagle Medium (DMEM)	Invitrogen
Epidermal growth factor (EGF)	Invitrogen
Fetal calf serum (FCS)	Invitrogen
Forskolin	Alexis
Giemsa dye	Sigma
jetPEI and 150 mM NaCl	Biomol
L-Glutamine	Invitrogen
Neomycin	Calbiochem
OptiMEM	Invitrogen
Phosphate buffered saline (PBS)	Invitrogen
Penicillin/streptomycin	Invitrogen
Puromycin	Calbiochem

Trypsin-EDTA	Invitrogen
Trypan blue	Sigma

2.1.4. Antibodies used for Western Blotting and Immunoprecipitation

Antibody	***Source***
Anti-phospho-ERK antibodies	#9106; Cell Signaling Technology and sc-7393; Santa Cruz Biotechnology
Phosphospecific antibodies against mBAD phosphoserines 112, 136 and 155	#9296S, 9295S and 9297S; Cell Signaling Technology
Phosphospecific antibody against hBAD phosphoserine 134	Abnova
Anti-actin	A2066; Sigma
Anti-Akt/PKB	#9272; Cell Signaling Technology
Anti-BAD antibodies	sc-943 and sc-8044; Santa Cruz Biotechnology
Anti-PAK antibody	sc-881; Santa Cruz Biotechnology
Anti-B-RAF antibody	sc-166; Santa Cruz Biotechnology
Anti-PKA antibody	sc-903; Santa Cruz Biotechnology
Pan-RAF antibody	30K; Institute for Medical Radiation and Cell Research
Anti-Myc	sc-40; Santa Cruz Biotechnology
Horseradish peroxidase conjugated polyclonal anti-rabbit and anti-mouse IgG	Amersham Biosciences

2.1.5. Enzymes

Items	***Source***
Phusion high fidelity DNA polymerase	Finnzymes
EcoRI restriction enzyme	New England BioLabs
Not I restriction enzyme	New England BioLabs
Sac II restriction enzyme	New England BioLabs
StuI restriction enzyme	New England BioLabs
T4 DNA ligase	New England BioLabs
PfuUltra DNA polymerase	Stratagene
Dpn I restriction enzyme	Stratagene

2.1.6. Kits

Items	*Source*
ProteoExtract subcellular proteome extraction kit	Calbiochem
QIAquick gel extraction kit	Qiagen
QIAquick PCR purification kit	Qiagen
QIAprep spin miniprep kit	Qiagen
QIAGEN plasmid midi kit	Qiagen
QIAGEN plasmid maxi kit	Qiagen
QuikChange sitedirected mutagenesis kit	Stratagene

2.1.7. Plasmids

Human origin of genes within the plasmids is indicated by "h" prior to the respective gene name. Site-specific mutations were introduced using QuikChange site-directed mutagenesis kit (Stratagene) according to the manufacturer's instructions. The accuracy of mutants was confirmed by DNA sequencing using standard sequencing oligonucleotides for the respective plasmid.

Plasmid	*Source*
pcDNA3.1 (vector)	Invitrogen
pcDNA3/hC-RAF-myc-His	U.R. Rapp
pcDNA3/HA-hBAD	U.R. Rapp
pcDNA3/hBAD	U.R. Rapp
pcDNA3/Flag-hBAD	U.R. Rapp
pcDNA3/hBAD(S99A/FAA)	U.R. Rapp
pcDNA3/hBAD-His	U.R. Rapp
pcDNA3/hBAD(S25A)-His	L. Polzien
pcDNA3/hBAD(S32A)-His	L. Polzien
pcDNA3/hBAD(S34A)-His	L. Polzien
pcDNA3/hBAD(S75A)-His	L. Polzien
pcDNA3/hBAD(S91A)-His	L. Polzien
pcDNA3/hBAD(S97A)-His	L. Polzien
pcDNA3/hBAD(S99A)-His	L. Polzien
pcDNA3/hBAD(S118A)-His	L. Polzien
pcDNA3/hBAD(S124A)-His	L. Polzien
pcDNA3/hBAD(S134A)-His	L. Polzien

pcDNA3/hBAD(S75A/S99A)-His	L. Polzien
pcDNA3/hBAD(S75A/S118A)-His	L. Polzien
pcDNA3/hBAD(S99A/S118A)-His	L. Polzien
pcDNA3/hBAD(S75A/S99A/S118A)-His	L. Polzien
pcDNA3/hBAD(S75A/S118A/S134A)-His	L. Polzien
pcDNA3/His-hC-RAF	U.R. Rapp
pcDNA3/hH-Ras12V	U.R. Rapp
pcDNA3/myc-His-hA-RAF	A. Baljuls
pcDNA3/myc-His-hC-RAF	A. Baljuls
pcDNA3/myc-His-hA-RAF(Y301D/Y301D)	A. Baljuls
pcDNA3/hBcl-2	U.R. Rapp
pcDNA3/hBcl-X_L	U.R. Rapp
pcDNA3myc (vector)	U.R. Rapp
pcDNA3myc/hA-Raf	U.R. Rapp
pcDNA3myc/hA-Raf(YY301/302DD)	U.R. Rapp
pcDNA3myc/His-hB-RAF	U.R. Rapp
pcDNA3myc/His-hC-RAF	U.R. Rapp
Fast Bac1/h14-3-3 epsilon	U.R. Rapp
Fast Bac1/h14-3-3 zeta	U.R. Rapp
Fast Bac/GST 4T-2 hA-RAF(YY301/302DD)	U.R. Rapp
Fast Bac/GST 4T-1 hC-RAF	U.R. Rapp
Fast Bac/GST 4T-2 hB-RAF-His	U.R. Rapp
Fast Bac/GST 4T-2 hB-RAF-His(K482A)	U.R. Rapp
Fast Bac/GST 4T-2 hB-RAF(V600E)	U.R. Rapp
Fast Bac/GST 4T-2 hC-RAF-His	U.R. Rapp
Fast Bac HTa/hC-RAF	U.R. Rapp
Fast Bac HTa/hC-RAF-His	U.R. Rapp
Fast Bac HTb/hPAK1(T423E)- His	U.R. Rapp
Fast Bac HTb/hPKB(T308D/S473D)	U.R. Rapp
pAC2GT GST/hC-RAF-BXB	U.R. Rapp
pAC2GT GST/hC-RAF-BXB(YY340/341DD)	U.R. Rapp

pAdenoX/hBAD	U.R. Rapp
pAdenoX/hBAD(S136A)	U.R. Rapp
pAdenoX/hBAD(S136A/S155A)	U.R. Rapp
pAdenoX/hC-RAF- BXB-301(K375W)	U.R. Rapp
pBabePuro/hBclX_L	U.R. Rapp
pBabePuro/hBcl-2	U.R. Rapp
pBabePuro/hC-RAF-BXB	U.R. Rapp
pBabePuro/Ha-hRas	U.R. Rapp
pBabePuro/hC-RAF(R89L)	U.R. Rapp
pBabePuro/hC-RAF(YY340/341DD)	U.R. Rapp
pBI-5/hC-RAF-HA-BXB	U.R. Rapp
KRSPA/hLck	U.R. Rapp
KRSPA/HA-hC-RAF	U.R. Rapp
pGEX2T (vector)	Pharmacia
pGEX-4T1/hBAD	U.R. Rapp
pGEX-4T1/hBAD(S75A)	U.R. Rapp
pGEX-4T1/hBAD(S99A)	U.R. Rapp
pGEX-4T1/hBAD(S118A)	U.R. Rapp
pGEX-4T1/hBAD(S75A/S99A)	U.R. Rapp
pGEX-4T1/hBAD(S75A/S99A/S118A)	U.R. Rapp
pcMV5/hB-RAF	U.R. Rapp
pCMV5/hPKBα(308/473DD)	U.R. Rapp
pcMV5/hPKBα(K179A)	U.R. Rapp

2.1.8. Oligonucleotides

Name	***Sequence***
hBAD-S25A-for	GAGAGGGGCCTGGGCCCCGCCCCCGCAGGGGAC
hBAD-S25A-rev	GTCCCCTGCGGGGGCGGGGCCCAGGCCCCTCTC
hBAD-S32A-for	CAGGGGACGGGCCCGCAGGCTCCGGCAAGCATCATC
hBAD-S32A-rev	GATGATGCTTGCCGGAGCCTGCGGGCCCGTCCCCTG
hBAD-S34A-for	GACGGGCCCTCAGGCGCCGGCAAGCATCATC
hBAD-S34A-rev	GATGATGCTTGCCGGCGCCTGAGGGCCCGTC
hBAD-S75A-for	GAGTCGCCACAGCGCCTACCCCGCGGGGAC

hBAD-S75A-rev	GTCCCCGCGGGGTAGGCGCTGTGGCGACTC
hBAD-S91A-for	GATGGGGGAGGAGCCCGCCCCCTTTCGGGGCCGCTC
hBAD-S91A-rev	GAGCGGCCCCGAAAGGGGGCGGGCTCCTCCCCCATC
hBAD-S97A-for	CTTTCGGGGCCGCGCGCGCTCGGCGCC
hBAD-S97A-rev	GGCGCCGAGCGCGCGCGGCCCCGAAAG
hBAD-S99A-for	GGCCGCTCGCGCGCGGCGCCCCCCAAC
hBAD-S99A-rev	GTTGGGGGGCGCCGCGCGCGAGCGGCC
hBAD-S118A-for	GCGAGCTCCGGAGGATGGCTGACGAGTTTGTGGACTC
hBAD-S118A-rev	GAGTCCACAAACTCGTCAGCCATCCTCCGGAGCTCGC
hBAD-S124A-for	GAGTGACGAGTTTGTGGACGCCTTTAAGAAGGGACTTCCTCG
hBAD-S124A-rev	CGAGGAAGTCCCTTCTTAAAGGCGTCCACAAACTCGTCACTC
hBAD-S134A-for	GACTTCCTCGCCCGAAGGCCGCGGGCACAGCAACGC
hBAD-S134A-rev	GCGTTGCTGTGCCCGCGGCCTTCGGGCGAGGAAGTC
hBAD-S157A-for	CCAGTCCTGGTGGGATGCGAACTTGGGCAGGGGAAGC
hBAD-S157A-rev	GCTTCCCCTGCCCAAGTTCGCATCCCACCAGGACTGG

2.1.9. siRNAs for RNA Interference

Name	*Target*	*Sequence*
siBAD-CDS	hBAD, coding sequence (CDS)	5’-ACGAGTTTGTGGACTCCTTTA-3’
siBAD-UTR	hBAD, 3’UTR	5’-TCACTACCAAATGTTAATAAA-
siLuci	Luciferase	5’-AACUUACGCUGAGUACUUCGA-3’

2.1.10. Cell Lines and Bacterial Strains

Cell lines	*Source*
HEK-293	ATCC #CRL-1573
HeLa 229	ATCC #CCL-2.1
NIH3T3	ATCC #CRL-1658
Sf9	PTA-3099
A375	ATCC #CRL-1619
SK-MEL-28	ATCC #HTB-72
DX3	Daniela Haug (University of Würzburg, Germany)
MEL-Juso	Daniela Haug (University of Würzburg, Germany)
PC3	Joachim Fensterle (Æterna Zentaris, Germany)
HCT 116	Joachim Fensterle (Æterna Zentaris, Germany)

Bacterial strains	***Source***
Escherichia coli (*E. coli*) DH5α	Bethesda Research Laboratories. Optimized for DNA transformation and replication

2.2. Solutions and Buffers

LB-Medium (Luria/Miller)

The ready-to-use LB-medium powder was purchases from Roth (Ingredients: 10 g/l Bacto-tryptone, 5 g/l Yeast extract, and 10 g/l NaCl pH 7.0). Disperse 25 g of ready-to-use powder in 1 l of deionized water. Swirl to mix and sterilize by autoclaving at 121°C for 15 min. Cool to ca. 47°C and add filter sterilized antibiotic if required.

LB-Agar (Luria/Bertani)

The ready-to-use LB-agar powder was obtained from Roth (Ingredients: 10 g/l Bacto-tryptone, 5 g/l Yeast extract, 10 g/l NaCl, and 15 g/l Agar pH 7.0). Disperse 40 g of ready-to-use powder in 1 l of deionized water. Swirl to mix and sterilize by autoclaving at 121°C for 15 min. Cool to ca. 47°C and add filter sterilized antibiotic if required. Pour into Petri dishes, allow to set and dry the surface prior to inoculation.

TB-Buffer

	final concentration
PIPES	10 mM
$CaCl_2$	15 mM
KCl	250 mM

Adjust pH to 6.7 with KOH and add 2.7 g $MnCl_2$ (55 mM, final concentration). Sterilize the solution by filtering and store at 4°C.

5 × HF-Buffer

The 5 × HF-buffer was obtained together with *Phusion* DNA polymerase from Finnzymes. It contains 7.5 mM $MgCl_2$, which supplies 1.5 mM $MgCl_2$ in final reaction conditions.

10 × TBE-Buffer

The *Rotiphorese* ready-to-use 10 × TBE-buffer was obtained from Roth. It contains 1 M Tris-Borat (pH 8.3) and 20 mM EDTA in deionized water.

6 × DNA Gel Loading Buffer

	final concentration
Sucrose	40% (w/v)
Bromphenol Blue	0.25% (w/v)
Xylene cyanol	0.25% (w/v)

10 × T4 DNA Ligase Buffer

The buffer was obtained together with T4 DNA ligase enzyme from New England BioLabs. (Ingredients: 500 mM Tris-HCl, pH 7.5, 100 mM $MgCl_2$, 100 mM DTT, 10 mM ATP, and 250 µg/ml BSA)

10 × PfuTurbo DNA Polymerase Reaction Buffer

The buffer was obtained together with *PfuTurbo* DNA polymerase from Stratagene. (Ingredients: 200 mM Tris-HCl (pH 8.8), 20 mM $MgSO_4$, 100 mM KCl, 100 mM $(NH_4)_2SO_4$, 1% Triton X-100, and 1 mg/ml nuclease-free BSA)

1 × MC Lysis Buffer

	final concentration
Tris-HCl, pH 8.0	50 mM
NaCl	137 mM
Sodium pyrophosphate	10 mM
β-Glycerophosphate	25 mM
EDTA	2 mM
EGTA	2 mM
Glycerol	10% (v/v)
β-Mercaptoethanol	0.1% (v/v)
NaF	25 mM

The buffer was aliquoted in 50 ml samples and stored at –20°C. Following reagents were added before use:

	final concentration
Sodium orthovanadate	1 mM
Antipain	10 µg/ml
Aprotinin	10 µg/ml
Leupeptin	1 µg/ml
Pepstatin	1.4 µg/ml
PMSF	200 µg/ml

NP-40	desired concentration

IC Lysis Buffer

	final concentration
Tris-HCl, pH 7.6	25 mM
NaCl	150 mM
Sodium pyrophosphate	10 mM
β-Glycerophosphate	25 mM
NaF	25 mM
Glycerol	10%

Following reagents were added before use:

	final concentration
Sodium orthovanadate	1 mM
Antipain	10 µg/ml
Aprotinin	10 µg/ml
Leupeptin	1 µg/ml
Pepstatin	1.4 µg/ml
PMSF	200 µg/ml
NP-40	desired concentration

PBS Buffer

The phosphate buffered saline (PBS) Ready-Mixed Powder was obtained from BioAtlas. Ready-mixed PBS powder was dissolved in distilled water. On dilution, the resultant PBS will have final concentrations: 137 mM NaCl, 10 mM Phosphate, pH 7.4, and 2.7 mM KCl.

5 × SDS-Loading Buffer

	final concentration
Tris-HCl, pH 6.8	70 mM
β-Mercaptoethanol	5% (v/v)
Glycerol	40% (v/v)
SDS	3% (w/v)
Bromphenol Blue	0.05% (w/v)

SDS-PAGE Buffer

The ready-to-use *Rotiphorese* 10 × SDS-PAGE buffer was obtained from Roth. It contains 1.92 M glycine, 0.25 M Tris, and 1% (w/v) SDS.

SD Buffer I

	final concentration
Tris, pH 10.4	25 mM
Methanol	10% (v/v)

SD Buffer II

	final concentration
Tris, pH 10.4	300 mM
Methanol	10% (v/v)

SD Buffer III

	final concentration
Tris, pH 9.4	25 mM
Glycine	40 mM
Methanol	10% (v/v)

10 × TBST Buffer

	final concentration
Tris-HCl, pH 7.6	400 mM
NaCl	2.75 M
Tween 20	1%

Prior to use, 10 x TBST buffer was dissolved to 1 x TBST buffer with distilled water.

ECL Solution I

	final concentration
Tris-HCl, pH 8.5	0.1 M
Luminol	2.5 mM
Coumaric acid	0.4 mM

ECL Solution II

	final concentration
Tris-HCl , pH 8.5	0.1 M
Hydrogen peroxide	0.019%
ddH_2O	

Stripping Buffer

	final concentration
Tris-HCl, pH 6.7	62.5 mM
SDS	2% (w/v)

Before use, 345 µl β-mercaptoethanol per 50 ml buffer was added.

10 × Kinase Buffer

	final concentration
HEPES, pH 7.4	250 mM
NaCl	1.5 M
β-Glycerophosphate	250 mM

GST Elution Buffer

	final concentration
Tris-HCl, pH 7.6	25 mM
Glycerol	10%
Glutathione	20 mM

IC Transfection Buffer

	final concentration
HEPES, pH 7.1	25 mM
NaCl	140 mM
$CaCl_2$	125 mM
(filter sterilized)	

Biosensor Buffer

	final concentration
HEPES, pH 7.4	10 mM
NaCl	150 mM
NP-40	0.01%

2.3. Methods

2.3.1. Microbiological Methods

2.3.1.1. Preparation of Chemocompetent Bacteria ($CaCl_2$ Method)

Bacteria were streaked on a LB-Agar plate and incubated for 24 h in 37°C. The next day, 10–12 colonies were picked, inoculated in 250 ml SOB-medium (2 l Erlenmeyer flask), and left to grow at 18°C shaking (180 rpm) until OD_{600} of 0.6 was reached. Then the culture was cooled down on ice for at least 10 min. The following procedures were carried out at 4°C in pre-cooled sterile tubes. The cells were transferred into 50 ml tubes and harvested in a centrifuge (Megafuge 1.0) at 1900 g for 10 min. The supernatant was discarded. The bacterial pellets were resuspended thoroughly in 80 ml ice cold TB-buffer and incubated on ice for 10 min. Then the cells were harvested as before and the bacterial pellets were resuspended carefully in 20 ml ice cold TB-buffer. The bacteria suspension was supplemented with 1.4 ml DMSO (7%, finale concentration) and left on ice for 10 min. The suspension was aliquoted in 100 to 200 µl samples, shock-frozen, and stored at –80°C.

2.3.1.2. Transformation of Chemocompetent Bacteria

Chemocompetent bacteria were thawed on ice for 20 min. A maximum of 20 ng ligated DNA or purified plasmid DNA were added to 100 µl cells in a pre-cooled 1.5 ml microfuge tube. The bacteria were mixed carefully and kept on ice for 30 min. Then the bacteria were heat-shocked at 42°C for 45 sec and 750 µl pre-warmed antibiotic-free LB-medium was added. The cells were aerate at 37°C for 1 h. Selection of transformed bacteria was done by plating the hole bacterial suspension on antibiotic containing LB-agar plates. Only bacteria that have taken up a plasmid containing an antibiotic resistance cassette can grow on the LB-agar plates. Single colonies were expanded in LB-medium and used for DNA preparation.

2.3.2. Molecular Biological Methods

2.3.2.1. Amplification of DNA by PCR

The polymerase chain reaction (PCR) is a method for an oligonucleotide primer directed enzymatic amplification of a specific DNA sequence. This technique is capable of amplifying a sequence up to 106-fold from ng amounts of template DNA within a large background of irrelevant sequences (e.g. from total genomic DNA). A prerequisite for amplifying a sequence through PCR is to know unique sequences flanking the DNA segment of interest, so that applicable oligonucleotides can be designed. The PCR product is amplified from the DNA template using a heat-stable DNA polymerase and an automated thermal cycler to put the reaction through cycles of denaturation, annealing of primers and polymerization.

Recommendations for Choosing Oligonucleotide Primers

The first primer is complementary to the sense DNA strand upstream and the second primer is complementary to the antisense strand downstream of the sequence to be amplified. Both primers should be 20–30 bp long and ideally contain a sequence with a relatively balanced GC vs. AT content (e.g. 45–55% GC) and no long stretches of any one base. Caution should also be taken that the two oligonucleotides of the primer pair do not contain complementary structures >2 bp to avoid "primer dimer" formation resulting from annealing of the two primers (especially at their 3'-ends). The melting temperature (Tm) of flanking primers should not differ by more than 5°C. Therefore, the GC content and length must be chosen accordingly. It can be calculated using the following formula:

$Tm = 69.3 + 41 \times (nC + nG) / S – 650 / S$

nC, number of cytosine nucleotides in the primer

nG, number of guanine nucleotides in the primer

S, number of all nucleotides in the primer

Procedure for Polymerase Chain Reaction

The PCR reaction was performed in volume of 50 µl. The following components were mixed on ice:

	for 50 µl reaction volume	*final concentration*
Sterile ddH_2O	29 µl	
Reaction buffer (5 × HF-buffer)	10 µl	1 ×
dNTPs (2 mM)	5 µl	200 µM
Primer 1 (10 pmol/l)	2.5 µl	0.5 µM
Primer 2 (10 pmol/l)	2.5µ	0.5 µM
Plasmid DNA (10 ng/l)	0.5 µl	0.1 ng/µl
Phusion DNA polymerase (2 U/l)	0.5 µl	0.02 U/µl

Cycling Conditions

The PCR machine must be programmed for the specific reaction conditions desired. Each cycle in the polymerase chain reaction involves three steps (denaturation, primer annealing, polymerization), and the products are amplified by performing many cycles one after the other with the help of the automated thermal cycler.

Initial denaturation step:

The initial denaturation was done at 98°C for 30 sec.

Denaturation step:

The denaturation was done at 98°C for 10 sec.

Primer annealing step:

The primers longer than 20 nucleotides were annealed for 30 sec at a Tm +3°C. For primers shorter than 20 nucleotides an annealing temperature equal to the Tm was used. If nonspecific PCR products were obtained, the first 5 cycles were performed at the annealing temperature equal to the Tm or Tm +3°C, whereas the remaining cycles were done at the temperature of 68°C.

Extending step:

The extending step was performed at 72°C. The extension time of 15 sec per 1 kb was used.

Number of cycles:

The number of PCR cycles depends on the amount of template DNA in the reaction mix and on the expected yield of the PCR product. As the initial quantity of template DNA used in this work was high, 16 cycles were sufficient.

Final extending step:

After the last cycle, the samples were incubated at 72°C for 7 min to fill-in the protruding ends of newly synthesized PCR products. After amplification, the products were separated accordingly to size by agarose gel electrophoresis and were directly visualized after staining with ethidium bromide.

2.3.2.2. Agarose Gel Electrophoresis of DNA

Agarose gel electrophoresis is a method for separating and visualizing DNA fragments. The fragments are separated by charge and size by forcing them to move through an agarose gel matrix, which is subjected to an electric field. The electric field is generated by applying potential (voltage) across an electrolytic solution (buffer). To pour a gel, 1 g agarose powder was mixed with 100 ml electrophoresis buffer (TBE-buffer) to obtain a final concentration of 1% and heated in a microwave oven until completely melted. After cooling the solution to about 60°C, ethidium bromide was added (0.5 g/ml, final concentration) to facilitate visualization of DNA after electrophoresis. Then the solution was poured into a casting tray containing a sample comb and allowed to solidify at room temperature. After the gel has solidified, the comb was removed. The gel, still in its plastic tray, was inserted horizontally into the electrophoresis chamber and covered with TBE-buffer. Samples, containing DNA mixed with 6 × DNA gel loading buffer, were filled into the sample wells. DNA electrophoresis was performed at 120 V until adequate separation of DNA fragments has occurred. The DNA fragments were visualized under UV-light.

2.3.2.3. Isolation of DNA Fragments from an Agarose Gel

DNA fragments were isolated from agarose gel using the *QIAquick* gel extraction kit according to the manufacturer's protocol.

2.3.2.4. Purification of DNA Fragments

DNA fragments were purified using *QIAquick* PCR purification kit according to the manufacturer's protocol.

2.3.2.5. Digestion of DNA with Restriction Endonucleases

The following components were mixed in a 1.5 ml microfuge tube on ice:

	for 20 µl
Nuclease-free ddH_2O	16 µl
10 × Recommended buffer for restriction enzyme	2 µl
Substrate DNA (in ddH_2O)	1 µl (~ 1 g)
Restriction enzyme	0.2–0.5 µl (2–5 U)

The restriction reaction was incubated at the optimum temperature for 1–16 h.

2.3.2.6. DNA Ligation

The ligation reaction was performed in a total volume of 20 µl. The plasmid and/or DNA fragment was prepared by cutting it with suitable restriction enzymes, which was followed by purification. To ligate an insert DNA molecule into a plasmid a 3:1 molar ratio of insert to vector was used.

Following components were mixed in a 1.5 ml microfuge tube on ice:

	for 20µ l
Nuclease-free ddH_2O	add to 16 µl
10 × T4 DNA ligase buffer	2 µl
Purified linearized vector (in ddH_2O)	25 ng
Purified linearized insert (in ddH_2O)	75 ng
T4 DNA ligase (400 U/µl)	2 µl (800 U)

The reaction was incubated at RT for 2 h or at 16°C overnight. To inactivate the enzyme the mixture was heated at 65°C for 10 min.

2.3.2.7. Purification of Plasmid DNA

Plasmid DNA was purified by using the *QIAprep* spin miniprep kit, the *QIAGEN plasmid midi kit* or the *QIAGEN plasmid maxi kit* according to the manufacturer's protocols.

2.3.2.8. Determination of DNA Concentration and Quality

The quality as well as the concentration of a DNA sample was determined by a Spectrophotometer (NanoDrop NP-1000, Peqlab) according to the manufacturer`s instruction.

2.3.2.9. Site-Directed Mutagenesis

Site-specific mutations were introduced using the *QuikChange* sitedirected mutagenesis kit (Stratagene) according to the operating manual.

2.3.3. Biochemical Methods

2.3.3.1. Preparation of Cell Lysates

Preparation of cell lysates was performed on ice.

Lysis of Adherent Mammalian Cells

Cells were washed twice with PBS buffer (2 ml for 35 mm diameter Petri dish), scraped off in ice cold AC lysis buffer (1 ml for 10 cm diameter Petri dish) containing 1% NP-40, transferred into an microtube and lysed by rotating at 4°C for 45 min. The lysate were used for Western blotting.

Lysis of Sf9 Insect Cells

Baculovirus-infected Sf9 cells were transferred into 15 ml tubes, pelleted at 200 g (*Megafuge 1.0R*) for 2 min and washed with 3 ml PBS buffer. The pelleted cells were resuspended in 1 ml PBS and transferred into 1.5 ml microfuge tubes. The cell suspension was centrifuged at 200 g for 3 min and the supernatant was discarded. The cell pellet was resuspended in 1 ml IC lysis buffer containing 0.75% NP-40 and incubated at 4°C for 45 min with gentle rotation. Every 5 min, the cell suspension was mixed by vortexing for few seconds. The cell lysate was then clarified by centrifuging at 21,000 g for 10 min at 4°C. The supernatant was transferred into a clean microfuge tube, and the pellet containing cell nuclei and membranes was discarded. The lysate was used for protein purification.

2.3.3.2. Determination of Protein Concentration (Bradford Assay)

1 ml of Bradford reagent (ready-to-use Coomassie Blue G-250 based reagent, Pierce) was mixed with 10 µl of the protein solution (cell lysate). After 5 min of incubation, the extinction was measured at 595 nm versus respective controls in a photometer. Absolute values were determined by correlation to known amounts of BSA.

2.3.3.3. Sodium Dodecyl Sulfate Polyacrylamide Gel Electrophoresis (SDS-PAGE)

Proteins can be easily separated on the basis of mass by electrophoresis in a polyacrylamide gel under denaturing conditions. Proteins in lysate or eluate samples were denaturated in 4 × SDS-loading buffer and then heated at 100°C for 7 min. SDS is an anionic detergent that disrupts nearly all non-covalent interactions in native proteins. β-Mercaptoethanol is also included in the sample buffer to reduce disulfide bonds. The SDS complexes with the denatured proteins were electrophoresed in a polyacrylamide gel. Vertical gels are set in between two glass plates with an internal thickness of 0.8-1.5 mm between the two plates. In this chamber, the acrylamide mix was poured and left to polymerize for at least 30 min at RT. The gels are composed of two layers: a 6–15% separating gel

(pH 8.8) that separates the proteins according to size and a lower percentage (5%) stacking gel (pH 6.8) that insures the proteins simultaneous entry into the separating gel at the same height.

	for 50 ml separating gel	*for 10 ml stacking gel*
ddH_2O	26.5-11.4 ml	3.09 ml
30% Acrylamide mix	10-25 ml	1.7 ml
1.5 M Tris-HCl, pH 8.8	12.5 ml	-
250 mM Tris pH 6.8	-	5 ml
10% SDS	0.5 ml	0.1 ml
10% APS	0.5 ml	0.1 ml
TEMED	0.04-0.02 ml	0.01 ml

The separating gel was poured in between two glass plates, leaving a space of about 1cm plus the length of the teeth of the comb. 1-Butanol was added to the surface of the gel to exclude air. After the separating gel was polymerized, the 1-butanol was removed. The stacking gel was poured on top of the separating gel, the comb inserted and allowed to polymerize. The samples were loaded into the wells of the gel and electrophoresis buffer (SDS-PAGE buffer) was added to the chamber. A cover was then placed over the gel chamber and 160 V was applied.

2.3.3.4. Immunoblotting

Proteins were separated using gel electrophoresis under denaturing conditions. In order to make the proteins accessible to antibody detection, they were moved from within the gel onto a membrane made of nitrocellulose using a semidry electroblotter. The gel was removed from its glass cassette and any stacking gel was trimmed away. The gel was immersed in SD buffer 3 for 15 min. The nitrocellulose membrane was equilibrated in SD buffer I for at least 5 min. Two pieces of filter paper soaked in SD buffer II were placed in the center of the anode electrode plate. One piece of filter paper soaked in SD buffer I were placed on top of the first two sheets. The nitrocellulose membrane was placed on top of the filter papers. The gel was placed on top of the membrane. Three pieces of filter paper soaked in SD buffer 3 were placed on top of the membrane. To ensure an even transfer, air bubbles between layers were removed by carefully rolling a pipette or stirring rod over the surface of each layer in the stack.

The protein transfer was performed at 2.5 mA/cm^2 for 2 h. For immunodetection, the membrane was incubated in TBST buffer and 5% milk and 1% BSA (unless otherwise indicated) for 1 h at RT or overnight at 4°C on a shaker. Then the membrane was washed three times with TBST buffer by vigorous shaking, each time for 5 min. The first antibody was diluted in TBST buffer (unless otherwise indicated) and added to the membrane. The membrane was incubated with the first antibody overnight at 4°C on a shaker. After incubation, the membrane was washed again three times with

TBST buffer by vigorous shaking, each time for 5 min. The appropriate peroxidase-conjugated secondary antibody was dilute in TBST buffer (or according to manufacturers' instructions) and added to the membrane. The membrane was incubated with the secondary antibody at RT for 1 h and washed three times with TBST buffer by vigorous shaking, each time for 5 min. This step was followed by the standard enhanced chemiluminescence reaction (ECL system).The membrane was incubated in a 1:1 mixture of ECL solutions I and II. This reaction is based on a peroxidase-catalyzed oxidation of luminol, which leads to the emission of light photons that can be detected on X-ray film.

2.3.3.5. Immunoblot Stripping

After the enhanced chemiluminescence reaction, the membrane was washed with TBST buffer for 5 min by vigorous shaking and subsequently incubated in stripping buffer for 1 h at 60°C. Every 20 min the membrane was vigorously shaken for 5 sec. Then the membrane was washed three times with TBST buffer by vigorous shaking, each time for 10 min. The membrane was then reprobed as described above.

2.3.3.6. Kinase Activity Assay

To measure activity of purified RAF kinases as well as the RAF kinase activity in crude cellular extracts, the ability of these kinases to phosphorylate substrates such as MEK or BAD was analyzed. In respect of MEK, the phosphorylation signal was amplified by detection of its unique substrate ERK. The kinase reaction was performed in a total volume of 50 µl. The reaction mixture for the kinase activity assay was prepared on ice as indicated below:

	for 50 µl
ddH_2O	add to 50 µl
10 x kinase buffer	5 µl
$MgCl_2$ (1 M)	0.5 µl
DTT (100 mM)	0.5 µl
ATP (10 mM)	5 µl
Na_3VO_4 (100 mM)	0.5 µl
Purified RAF kinase or cell lysate	1–10 µl
Purified recombinant MEK and ERK2	
(1.5 µg/µl, respectively)	3 and 2 µl, respectively
or	
Purified recombinant BAD (1 µg/µl)	8 µl

The appropriate amount of the reaction mixture was added to the RAF kinase sample, still on ice, mixed well and transferred to the thermoshaker for microfuge tubes. The reaction mixture was incubated at 30°C for 30 min at 700 rpm. The assay was terminated by adding 20 µl 4 × SDS-loading

buffer. The kinase reaction was monitored by Western blotting analysis with a monoclonal anti-phospho-ERK1/2 antibody that recognizes phosphorylated ERK.

2.3.3.7. Purification of Proteins

GST-hBAD, GST-hBADΔN131, GST-14-3-3 and GST-Bcl-X_L were expressed in *E. coli* using pGEX-2T vector and purified by glutathione-Sepharose affinity chromatography as described (Hekman *et al.* 2006). 14-3-3 proteins and Bcl-X_L were released from GST by thrombin cleavage. Expression and purification of RAF kinases, PAK1, Akt/PKB, 14-3-3 proteins and Bcl-X_L from Sf9 insect cells were performed as described previously (Fischer *et al.* 2009; Hekman *et al.* 2006; Hekman *et al.* 2002; Hekman *et al.* 2004). For expression and purification of phosphorylated His-hBAD, Sf9 cells were infected with baculoviruses at the multiplicity of infection of 5 and incubated shaking for 48 h at 27°C in the dark. The Sf9 cell pellet (2×10^8 cells) was lysed in 10 ml lysis buffer containing 50 mM sodium phosphate, pH 8.0, 150 mM NaCl, 10 mM sodium pyrophosphate, 25 mM NaF, 25 mM β-glycerophosphate, 10% glycerol, 0.5% NP-40 and a cocktail of standard protease inhibitors for 30 min with gentle rotation at 4°C. The cell lysate was centrifuged at 27,000 g for 30 min at 4°C. The supernatant (10 ml, containing His-hBAD) was incubated with 0.5 ml Ni^{2+}-nitrilotriacetic acid-agarose beads for 2 h at 4°C with rotation. After incubation, beads were washed 3 times with lysis buffer containing 0.2% NP-40, 300 mM NaCl and 20 mM imidazole and hBAD was eluted with an imidazole step gradient. For lipid bilayer experiments, GST-hBAD was ancillary purified by ion exchange chromatography using an ÄKTA-System (GE Healthcare). The purity of the proteins was evaluated by SDS-PAGE and staining with Coomassie Blue. For some approaches, phosphorylated His-hBAD was separated from the non-phosphorylated fraction by incubation with recombinant GST-14-3-3ζ on glutathione-Sepharose beads (300 µl) for 40 min at room temperature. After washing with 10 mM Hepes, pH 7.4, 150 mM NaCl and 0.01% NP-40, the phosphorylated hBAD fraction was released from the complex by 1% Empigen.

2.3.4. Biophysical Methods

2.3.4.1. Surface Plasmon Resonance (SPR) Technique

Biosensor measurements presented in this work were carried out either on a BIAcore-X or BIAcore-J system at 25°C using Pioneer L1 sensor chip (Biacore AB, Uppsala, Sweden). To monitor interaction between two protein components, usually GST- and his-tagged purified components were used. For that purpose, the biosensor chip CM5 was first loaded with an anti-GST antibody using covalent derivatization. Purified and GST-tagged protein was injected in BIAsensor buffer (10 mM HEPES, pH 7.4, 150 mM NaCl, and 0.01% NP-40) at a flow rate of 10 µl/min. Next, the purified his-tagged interacting partner was injected at increasing concentrations. The values for unspecific binding measured in the reference cell were subtracted. To measure the competition between the binding of a full length protein and peptides to the same ligand, the GST-tagged ligand was first captured to the

anti-GST antibody. Next, the purified protein was injected in the absence and presence of increasing concentrations of the peptide and the competition between the full length protein and the peptide of interest for binding was monitored.

To determine the interaction between different BAD segments in the presence of lipid vesicles, large unilamellar vesicles consisting of 47% phosphatidylcholine, 28% phosphatidylethanolamine, 9% phosphatidylserine, 9% phosphatidylinositol, and 7% cardiolipin were prepared. Therefore, a LiposoFast extrusion apparatus (Avestin Inc., Canada) was used as described (Hekman *et al.* 2006). To this end, the surface of the Pioneer L1 sensor chips was first cleaned with 20 mM CHAPS followed by the injection of mitochondrial liposomes (0.4 mM lipid concentration) at a flow rate of 10 µl/min in 10 mM Hepes, pH 7.4, 150 mM NaCl, and 0.1 mM DTT which resulted in a deposition of approximately 5-6000 RU. Next, proteins were immobilized at a flow rate of 10 µl/min resulting in approximately 1000-2000 RU of bound protein. Following injection of the analytes, the association-dissociation curves were monitored. To monitor the dissociation of Bcl-X_L/GST-BAD complex induced by BAD phosphorylation, the biosensor chip was treated with active C-RAF in the presence of 0.5 mM ATP. The modified biosensor buffer contained 5 mM $MgCl_2$ and 0.5 mM DTT. The working temperature was set to 30°C. At the end of the binding assays, the sensor chip surface was regenerated by injection of 20 mM CHAPS.

The evaluation of kinetic parameters was performed by non-linear fitting of binding data using the BiaEvaluation 2.1 software. The apparent association (k_a) and dissociation rates constant (k_d) were evaluated from the differential binding curves (Fc2-Fc1) assuming a A+B=AB association type for the protein-protein interaction. The affinity constant K_D was calculated from the equation $K_D = k_d/k_a$.

2.3.4.2. Mass Spectrometry Analysis of BAD Phosphorylation

Purified His-hBAD samples (about 100 pmol of each) were applied to SDS-PAGE. Proteins were visualized by Coomassie Blue staining applying the method of Neuhoff *et al*. (Neuhoff *et al.* 1988). In-gel reduction, acetamidation, tryptic and/or GluC digestion were done according to Wilm *et al.* (Wilm *et al.* 1996). After elution of the peptides, solutions were desalted using Millipore C18 ZipTip according to the manufacturer's instructions. ESI-MS was performed on a Bruker APEX II FT-ICR mass spectrometer (Bruker Daltonic GmbH Bremen) equipped with an Apollo-Nano-ESI ion source in positive ion mode.

To determine the exact positions of phosphates within the peptides, the nano-LC-MS/MS analysis was carried out as follows: purified hBAD samples were separated by SDS-PAGE, protein bands were excised, washed, and in-gel digested as described (Reinders *et al.* 2007). Afterwards, generated peptides were extracted using 15 µL 0.1% TFA and samples were analyzed by nano-LC-MS/MS on an LTQ Orbitrap XL mass analyzer (Thermo Scientific, Dreieich, Germany) coupled to an Ultimate 3000 (Dionex, Amsterdam, The Netherlands) using multistage activation as described (Zahedi *et al.* 2008).

To this end, peptides were preconcentrated on a PepMap trapping column (100 µm ID, 5 µm particle size, 100 Å pore size, 1 cm length, Dionex) and separated on a PepMap nano-LC column (75 µm ID, 3 µm particle size, 100 Å pore size, 15 cm length, Dionex) at a flow rate of 270 nl/min, using a gradient ranging from 5-50% of 86% acetonitrile and 0.1% formic acid. Raw data were transformed into mgf format using extract_msn.exe as part of the Bioworks package and generated peak lists were searched against an SGD database with concatenated standard protein and BAD sequences (6319 entries) using Mascot 2.2. The following search parameters were used: trypsin as protease with a maximum of one missed cleavage site, 10 ppm mass tolerance for MS, 0.5 Da for MS/MS, oxidation of Met (+15.99 Da), and phosphorylation of Ser/Thr/Tyr (+79.96 Da) as variable modifications, and ^{13}C was set to one. All identified phosphopeptides were manually validated to correct for potentially false phosphorylation site assignments.

2.3.4.3. Circular Dichroism

Circular Dichroism (CD) measurements were carried out using peptide solutions ranging in concentration from 0.1 to 0.2 mg/ml, in 20 mM sodium phosphate buffer, pH 8.0, at 25°C, in the presence or absence of 50 µM lipid micelles and/or 1 mM CHAPS. Some samples were supplemented with 30% of TFE. Samples containing lipids were sonicated for 5 min prior to analysis. Measurements were taken using an Jasco J-810 Circular Dichroism spectrophotometer using Jasco *Spectra Manager* data processing software.

2.3.4.4. NMR Spectrometry

NMR measurements were taken at 298 K on a BrukerAvance 600 MHz spectrometer. For that purpose, peptides were dissolved in H_2O containing 10% D_2O in the concentration range between 0.5 and 2 mM.

2.3.4.5. Lipid Bilayer Experiments

The channel-forming ability of proteins was assessed in artificial lipid bilayer membranes using a teflon chamber as described previously (Benz 1994; Benz *et al.* 1992). Briefly, to form the membranes a 1% (w/v) solution of diphytanoylphosphatidylcholine (DiphPC) (Avanti Polar Lipids) in n-decane was used. Purified hBAD peptides (phosphorylated and non-phosphotylated), purified hBAD proteins (phosphorylated and non-phosphotylated) or Bcl-X_L were injected alone or combined into the 1 M KCl buffer in both compartments of the chamber and the single-channel conductance was measured after application of a fixed membrane potential. To test the effects of 14-3-3 proteins on pore-forming abilities of hBAD, purified heterodimeric 14-3-3 proteins (14-3-3ζ/14-3-3ε) were incubated with phosphorylated hBAD for 30 min at RT prior to channel formation. To examine the geometry of channels, the single channel conductances *G* were measured in the presence of different sized nonelectrolytes at a concentration of 20% (w/v) in the bathing solution.

2.3.5. Cell Biology Methods

2.3.5.1. Cultivation and Passaging of Eukaryotic Cells

Cultivation and Passaging of Mammalian Adherent Cells

HeLa 229, HEK-293, MEL-Juso, DX3, SK-MEL-28, A375 and NIH3T3 cells were cultivated in DMEM (Invitrogen) supplemented with 10% fetal calf serum, 2 mM L-glutamine, and 100 units/ml penicillin/streptomycin. For the cell lines PC3 and HCT 116, we used RPMI (Invitrogen) and Mc Coy´s 5a medium (Invitrogen), respectively, that were supplemented with 10% fetal bovine serum, 2 mM L-glutamine, and 100 units/ml penicillin/streptomycin. All cells were stored in humidified air with 5% CO_2 at 37°C. For passaging, cells were washed once with PBS after removing the medium and 2 ml trypsin/EDTA solution was added. After an incubation of maximal 5 min at 37°C cells were detached from culture plates via throbbing and trypsin was inactivated by addition of serum-containing media. An appropriate volume of cell suspension was then aliquoted into freshly prepared T-flasks with media.

Cultivation and Passaging of Insect Cells

Sf9 insect cells grow well in suspension or monolayer culture. They exhibit a doubling time of approximately 20 h at 27°C. They require 10% FCS in an appropriate medium and constant temperature but they do not require CO_2, since their growth media are buffered at a pH of approximately 6.2. As Sf9 cells adhere relatively loosely to tissue culture vessels, they can be conveniently subcultured without the use of trypsin. Sf9 cells of monolayer culture are normally subcultured two or three times per week. Therefore, resuspended cells are diluted 4- to 8-fold in fresh medium. The insect cells do not become contact-inhibited. Thus, they should be subcultured at 90% confluency or below.

For protein expression, Sf9 cells were grown in suspension. The cells were seeded at density of approximately 2.5×10^5 cells per ml in to a total volume of 250 ml of complete medium in a 1000 ml spinner flask. Subsequently, the cells were incubated at 27°C with constant stirring at 50–60 rpm until the cell density reaches approximately 2×10^6 cells/ml. Then the cells were subcultured by removing 200 ml of the suspension and replacement of 200 ml of fresh complete medium, reaching a cell density of approximately 0.4×10^6 cells/ml.

2.3.5.2. Cell Counting

Trypsinized cells were counted by using a hemocytometer (Bürker´s cell counting chamber). To distinguish living and dead cells, Trypan blue staining was used. Trypan blue is excluded from viable cells, so the blue cells are dead ones, and the white colored cells are alive. A small amount of cell suspension was diluted 2:1 with Trypan blue and incubated for 5 min.

2.3.5.3. Freezing, Long-Term Storage and Thawing of Cells

For long-term storage, eukaryotic cells were frozen down in their appropriate medium containing 10% DMSO and 20% serum. Trypsinized cells were harvested by centrifuging at 200 × g for 10 min at RT. The cell pellet was resuspended in the freezing medium to achieve a final concentration of 2-4 × 10^6 cells/ml and 1 ml of this cell suspension was aliquoted into each cryovial. Before transferring into liquid nitrogen, the cells were at first incubated at -20°C for 2 h followed by overnight incubation at -80°C. For thawing, cells were hand warmed or placed in a 37°C water bath, until all ice clusters were melted. Then 1 ml serum was added to the cryovial and the cell suspension was transferred into the 15 ml tube. The cells were pelleted at ca. 200 × g for 10 min at RT. After removal of supernatant cells were carefully resuspended in their appropriate medium and taken into general tissue culture.

2.3.5.4. Transfection of Mammalian Cells

Mammalian cells were seeded at 3 x 10^5 cells/well in a 6-well plate and grown for 24 h before transfection by jetPEI (Polyplus). 16 h post-transfection, some preparations were washed with PBS buffer and cultivated for the indicated time in medium supplemented with 0.1-0,3% serum with or without addition of specific kinase inhibitors. The specific kinase inhibitors PD98059, U0126, PD0325901, CI1040, Wortmannin, LY294002, and BAY 43-9006 were dissolved in DMSO. Forskolin and isobutylmethylxanthine (IBMX) were also dissolved in DMSO whearas H-89 was dissolved in ethanol.

Prior to harvest, cells were washed once with PBS and lysed by the direct addition of *SDS loading buffer* or in *MC lysis buffer* containing 1% Nonidet P-40.

2.3.5.5. Infection of Insect Cells

Transfection of Insect Cells with Baculovirus DNA using Calcium Phosphate

Approximately 1 × 10^6 Sf9 cells were seeded (from a long-phase culture) per 35 mm tissue culture dish in 2 ml of complete medium and allowed to attach to the surface for 1 h at 27°C. Subsequentliy, the medium was aspirated and replaced with 1 ml fresh medium. 200 ng linearized baculovirus DNA and 2 µg recombinant transfer vector were diluted in 1ml of the *IC transfection buffer*. The mixture was added drop-wise to the cells wile swirling to the medium in the dish. The plate was incubated 5 h at 27°C without shaking. After this incubation, the medium was aspirated and the cells were washed with 2 ml of complete medium. Finally, 2 ml of complete medium were added to the cells and the cells were incubated at 27°C for 4–5 days without shaking. Subsequently, the medium from the plate was transferred to a sterile centrifuge tube and centrifuged at 1000 g for 5 min to clarify the virus-containing supernatant fluid. The resultant virus stock was stored at 4°C prior to plaque assay or amplification.

Plaque Assay

A suspension culture of Sf9 cells was grown to a density of at most 3×10^6. This culture was diluted to a density of 5-6 $\times 10^5$. 2 ml of this cell suspension were transferred into each well of a 6-well culture dish. The cells were left to settle to bottom of the plate for 1 h at RT. Subsequently, the monolayers were observed under the inverted microscope to confirm cell attachment and 50% confluence. Meanwhile, an eight-log serial dilution of the harvested viral supernatant was produced by sequentially diluting 0.5 ml of the previous dilution in 4.5 ml of complete medium. Eight tubes containing each of a 10^{-1} to 10^{-8} dilution of the original virus stock were prepared. The supernatant from each well was removed and immediately replaced with 1 ml of the respective virus dilution. The plate was incubated for 1 h at RT. 30 ml of the complete medium (incubated at 40°C in a water bath before use) and 10 ml of a 4% liquid agarose gel (incubated at 70°C in a water bath before use) were mixed in a bottle. The virus liquid was removed from the wells and replaced with 2 ml of the diluted agarose. The plates were incubated at RT for 10 to 20 min to allow gel to harden. Then the plates were incubated at 27°C in a humidified incubator for 4 to 10 days. Recombinant virus produces milky/gray plaques of slight contrast. The plates were monitored daily until the number of plaques counted did not change for two consecutive days. To stain the plates, an overlay agarose solution was prepared: 1/100 volume of the 1% Neutral Red solution was added to the molten agarose (e.g. 100 µl Neutral Red to 10 ml agarose). 1 ml of the overlay agarose was then added to each well and the plate was incubated at 27°C for at least 4 h. The titer (plaque forming unit (pfu)/ml) was calculated by the following formula:

Pfu/ml (of original stock) = number of plaques per ml of inoculum × $(\text{dilution factor})^{-1}$

Preparation of Clonal Virus Stocks

In wells containing just a few plaques, well-isolated ones were marked by circling with a pen on the underside of the plate. About 10 of the marked plaques were picked by pushing a Pasteur pipette through the agarose into the plaque, and gently sucking an agarose plug into the pipette tip. Each plug was transferred into 1 ml of complete medium in a separate microcentrifuge tube. The medium was vortexed gently and left overnight at 4°C to elute the virus particle from the agarose. Subsequently, 35 mm wells were seeded with 5×10^5 Sf9 cells in 2 ml of complete medium. The cells were incubated for 1 h at 27°C to allow the cells to settle and attach. Afterwards, the medium was aspirated and 100 µl eluted virus suspension was added to the middle of the dish. After incubation of the cells for 1 h at R 1 ml of complete medium was added. The cells were incubated at 27°C for 3–4 days. Thereafer, the medium was transferred to the sterile centrifuge tube and centrifuged at 100 g for 5 min to clarify the virus containing supernatant fluid. The resultant virus stock was stored at 4°C prior to plaque assay or amplification. Expression of the desired recombinant protein was confirmed by Western blotting analysis of the cell lysate.

Estimation of Viral Titre by Cell-Lysis Assay

Sf9 cells were harvested from exponentially growing culture, sedimented at 1000 g for 5 min at RT and resuspended gently at a density of 0.25×10^6 cells/ml in complete medium. A sample of viral stock was serially diluted in sterile cryovials, making dilutions (200 µl volume) in complete medium from 10^{-1} to 10^{-10}. One volume of cell suspension was added to each virus dilution and mixed gently. Triplicate 10 µl aliquots of each mixture were added to a well of a *Nunc HLA* plate resulting in approx. 50% confluency after setting. To maintain humidity within the plate, medium was added to the empty wells or a drop (100 µl) in each corner. The lid of the plate was replaced and the plate was placed in a sealed humid box inside of a 27°C incubator. The cells were incubated at 27°C until no further increase in cell lysis was observed (approximately 6 days). At the end of the experiment, the viral titre was approximated using the following approach: Consider the situation where there is lysis in all wells of dilution $10^{-(x-1)}$, but not in all of 10^{-x}. For this to occur, there must be less than 1 virus particle in 10 µl of the 10^{-x} dilution, but more than 0.1 particles. Correspondingly, there must be less than 1×10^x virions in 10 µl of the mixture of original virus stock plus cell suspension, but more than $1 \times 10^{(x-1)}$. It follows, that there are less than 2×10^x particles in 10 µl of the original virus stock, and more than $2 \times 10^{(x-1)}$. Therefore, the titre lies between $2 \times 10^{(x+1)}$ and $2 \times 10^{(x+2)}$ virus particles/ml.

Amplification and Storage of Recombinant Baculovirus

Virus containing supernatant fluid was transferred to sterile tubes. The fluid was clarified by centrifugation at 1000 *g* for 5 min at RT. The clarified medium was transferred to fresh tubes and the titre was determined. To amplify the virus, a monolayer exponential culture of Sf9 cells was infected at a ratio of infective virion to Sf9 cells (MOI) of 0.01–0.1. The virus was harvested after 72–120 h. This resulted in an at least 100-fold amplification of the virion. The virus was stored at 4°C in the dark. To estimate the viral inoculum required the following formula was used:

Inoculum required (ml) = (total number of cells) × (MOI in pfu/ml) / (viral titer of inoculum in pfu/ml).

2.3.5.6. siRNA Transfection

The function of cellular proteins can be investigated by the delivery of small interfering RNAs (siRNAs) into cells, which then leads to the degradation of respective complementary mRNA transcripts (Elbashir *et al.* 2001). In order to deplete host cells of specific proteins, siRNA transfection was performed with Lipofectamine 2000. One day before transfection, cells were seeded into 12-well plates to gain 70% confluency. 20 pmol siRNAs were incubated in 200 µl OptiMEM transfection medium containing 2 µl Lipofectamine 2000 for 25 min at RT before dropwise addition to each well. For cotransfecting plasmid DNA and siRNA, 20 pmol siRNA as well as 400 ng plasmid DNA were incubated in 200 µl OptiMEM transfection medium containing 3 µl Lipofectamine for 25 min at RT before dropwise addition to each well.

3 h post transfection, 600 µl fresh cell cultivation medium was added to each well. Two days after

transfection, cells were harvested for analyses as indicated.

2.3.5.7. Cell Survival Assay

To examine cell survival, cells were transiently transfected in triplicates. 16 h post-transfection, cells were washed twice with PBS and grown for additional 30 h in medium supplemented with 0.1% serum. Subsequently, cell viability was assessed by Trypan blue staining.

2.3.5.8. Colony Yield Assay

NIH 3T3 cells were transfected with the indicated plasmids. One day after transfection, cells were splitted and around 50 cells of each set of transfection were seeded in 6 cm dishes. Colony assays were performed in triplicates by scoring number of colonies (consisting of at least 20 cells) in the dishes grown for 14-18 days with appropriate antibiotic selection (450 μg/ml neomycin and 6 μg/ml puromycin, Calbiochem). To visualize the growing colonies, cells were washed with PBS, fixed with methanol and adjacent stained with Giemsa dye.

2.3.5.9. Analysis of Cell Proliferation and Growth Inhibition

To monitor cell proliferation, HEK-293 and HeLa cells were transiently transfected in triplicates. 16 h post-transfection, cells were washed twice with PBS and grown in medium supplemented with 0.3% serum. SK-MEL-28, A375, PC3, HCT 116, MEL-Juso and DX3 cells were incubated with and without the indicated kinase inhibitors or transfected with the named siRNAs for 48 h. Cell proliferation and growth inhibition were analyzed by photographing and counting of the cells as well as by counting living cells by use of Trypan blue in a hemicytometer at different time points (2, 3 and 6 days following transfection). To visualize cell proliferation, mitochondria of viable cells were stained by MitoTracker Deep Red according to manufacturer's instructions and fluorescence intensity was measured at 633 nm excitation and 670/30 nm emission by the Typhoon 9200 imager.

3. Manuscripts

3.1. Identification of Novel *in vivo* Phosphorylation Sites of the Human Pro-Apoptotic Protein BAD: Pore-Forming Activity of BAD is Regulated by Phosphorylation

BAD is a pro-apoptotic member of Bcl-2 family proteins that is regulated by phosphorylation in response to survival factors. Although much attention has been devoted to the identification of phosphorylation sites in murine BAD, little data are available with respect to phosphorylation of human BAD protein. Using mass spectrometry we identified here besides the established phosphorylation sites at serines 75, 99 and 118 several novel *in vivo* phosphorylation sites within human BAD (serines 25, 32/34, 97 and 124). Furthermore, we investigated the quantitative contribution of BAD targeting kinases in phosphorylating serine residues 75, 99 and 118. Our results indicate that RAF kinases represent, besides PKA, PAK and Akt/PKB, *in vivo* BAD phosphorylating kinases. RAF-induced phosphorylation of BAD was reduced to control levels using the RAF-inhibitor BAY 43-9006. This phosphorylation was not prevented by MEK inhibitors. Consistently, expression of constitutively active RAF suppressed apoptosis induced by BAD and the inhibition of colony formation caused by BAD could be prevented by RAF. In addition, using surface plasmon resonance technique we analyzed the direct consequences of BAD phosphorylation by RAF with respect to association with 14-3-3 and Bcl-2/Bcl-X_L proteins. Phosphorylation of BAD by active RAF promotes 14-3-3 protein association, in which the phosphoserine 99 represented the major binding site. Finally, we show here that BAD forms channels in planar bilayer membranes *in vitro*. This pore-forming capacity was dependent on phosphorylation status and interaction with 14-3-3 proteins. Collectively, our findings provide new insights into the regulation of BAD function by phosphorylation.

3.1.1. Introduction

Apoptosis is a genetically programmed, morphologically distinct form of cell death that can be triggered by a variety of physiological and pathological stimuli (Danial and Korsmeyer 2004; Letai 2006; Reed *et al.* 2004). This form of cellular suicide is widely observed in nature and is not only essential for embryogenesis, immune responses and tissue homeostasis, but is also involved in diseases such as tumor development and progression. Bcl-2 family proteins play a pivotal role in controlling programmed cell death. The major function of these proteins is to directly modulate outer mitochondrial membrane permeability and thereby regulate the release of apoptogenic factors from the intermembrane space into the cytoplasm (for recent review see (Youle and Strasser 2008)). On the

basis of various structural and functional characteristics, the Bcl-2 family of proteins is divided into three subfamilies, including proteins which either inhibit (e.g. Bcl-2, Bcl-X_L or Bcl-w) or promote programmed cell death (e.g. Bax, Bak or Bok) (Adams and Cory 1998; Gross *et al.* 1999). A second sub-class of pro-apoptotic Bcl-2 family members, the BH3-only proteins, comprises BAD, Bik, Bmf, Hrk, Noxa, tBid, Bim and Puma (Youle and Strasser 2008). BH3-only proteins share sequence homology only at the BH3 domain. The amphipathic helix formed by the BH3 domain (and neighboring residues) associates with a hydrophobic groove of the anti-apoptotic Bcl-2 family members (Fesik 2000; Petros *et al.* 2004). Originally, truncated Bid (tBid) has been reported to interact with Bak and Bax (Wei *et al.* 2000) suggesting that some BH3-only proteins promote apoptosis *via* at least two different mechanisms: inactivating Bcl-2-like proteins by direct binding and/or by inducing modification of Bax-like molecules. BAD (Bcl-2 associated death promoter, Bcl-2 antagonist of cell death) was described to promote apoptosis by forming heterodimers with the pro-survival proteins Bcl-2 and Bcl-X_L, thus, preventing them from binding with Bax (Yang *et al.* 1995). More recently, two major models have been suggested, how BH3-only proteins may induce apoptosis. In the *direct model*, all BH3-only proteins promote cell death by directly binding and inactivating their specific anti-death Bcl-2 protein partner (Galonek and Hardwick 2006; Willis *et al.* 2007). In this model the relative killing potency of different BH3-only proteins is based on their affinities for anti-apoptotic proteins. Thus, the activation of Bax/Bak would be mediated through their release from anti-apoptotic counterparts. Contrary to this model, Kim *et al.* (2006) provided support for an alternative *hierarchy model*, in which BH3-only proteins are divided into two distinct subsets. According to this model, the *inactivator* BH3-only proteins, like BAD, Noxa and some others, respond directly to survival factors resulting in phosphorylation, 14-3-3 binding and suppression of the pro-apoptotic function. In the absence of growth factors, these proteins engage specifically their preferred anti-apoptotic Bcl-2 proteins. The targeted Bcl-2 proteins then release the other subset of BH3-only proteins designated the *activators* (tBid, Bim and Puma) that in turn bind to and activate Bak and Bax.

Non-phosphorylated BAD associated with Bcl-2/Bcl-X_L is found at the outer mitochondrial membrane. Phosphorylation of specific serine residues, Ser-112 and Ser-136 of mouse BAD (mBAD) or the corresponding phosphorylation sites Ser-75 and Ser-99 of human BAD (hBAD), results in association with 14-3-3 proteins and subsequent relocation of BAD (Hekman *et al.* 2006; Zha *et al.* 1996). Phosphorylation of mBAD at Ser-155 (Ser-118 of hBAD) within its BH3-domain disrupts the association with Bcl-2 or Bcl-X_L promoting cell survival (Datta *et al.* 2000). Therefore, the phosphorylation status of BAD at these serine residues reflects a checkpoint for cell death or survival. Although the C-RAF kinase was the first reported BAD kinase (Wang *et al.* 1996), its target sites were not clearly defined. However, there is a growing body of evidence for direct participation of RAF in regulation of apoptosis *via* BAD (Jin *et al.* 2005; Panka *et al.* 2006). In addition, Kebache *et al.* (Kebache *et al.* 2007) reported recently that the interaction between adaptor protein Grb10 and C-RAF is essential for BAD-mediated cell survival. On the other hand, numerous reports suggest that PKA

(Harada *et al.* 1999), Akt/PKB (Datta *et al.* 1997), PAK (Gnesutta *et al.* 2001; Jin *et al.* 2005; Schurmann *et al.* 2000), Cdc2 (Konishi *et al.* 2002), RSK (She *et al.* 2002; Shimamura *et al.* 2000), CK2 (Klumpp *et al.* 2004) and PIM kinases (Macdonald *et al.* 2006) are involved in BAD phosphorylation as well. The involvement of JNK in BAD phosphorylation is controversially discussed. Whereas Donovan *et al.* (Donovan *et al.* 2002) reported that JNK phosphorylates mBAD at serine 128, Zhang *et al.* (Zhang *et al.* 2005) claimed that JNK is not a BAD-serine-128 kinase. On the other hand, it has been shown that JNK is able to suppress IL-3 withdrawal-induced apoptosis *via* phosphorylation of mBAD at threonine 201 (Yu *et al.* 2004). Thus, taken together, with respect to regulation of mBAD by phosphorylation, five serine phosphorylation sites (at positions 112, 128, 136, 155 and 170) and two threonines (117 and 201) have been identified so far. Intriguingly, only few data are available regarding the role of phosphorylation in regulation of hBAD protein, although significant structural differences between these two BAD proteins exist.

During apoptosis, some members of the Bcl-2 family of proteins such as Bax or Bak have been shown to induce permeabilization of the outer mitochondrial membrane, allowing proteins in the mitochondrial intermembrane space to escape into the cytosol where they can initiate caspase activation and cell death (for review see (Antignani and Youle 2006; Zamzami and Kroemer 2003)). Despite intensive investigation, the mechanism whereby Bak and Bax induce outer membrane permeability remains controversial (Antignani and Youle 2006). Based on crystal structure (Muchmore *et al.* 1996), it became evident that Bcl-X_L has a pronounced similarity to the translocation domain of diphtheria toxin (Choe *et al.* 1992), a domain that can form pores in artificial lipid bilayers. This discovery provoked the predominant view, that upon commitment to apoptosis, the pro-apoptotic proteins Bak and Bax also form pores in the outer mitochondrial membrane (Martinou and Green 2001). As expected from the structural considerations, Bcl-X_L was found to form channels in synthetic lipid membranes (Minn *et al.* 1997). Since then, other Bcl-2 family members like Bcl-2, Bax and the BH3-only protein Bid have been reported to have channel-forming ability. These pores can be divided into two different types: proteinaceous channels of defined size and ion specificity (Antonsson *et al.* 1997; Minn *et al.* 1997; Schendel *et al.* 1999; Schendel *et al.* 1997; Schlesinger *et al.* 1997) and large lipidic pores that allow free diffusion of 2 megadalton macromolecules (Basanez *et al.* 1999; Kuwana *et al.* 2002). With respect to the BH3-only protein BAD, no pore forming abilities have been reported so far, although human BAD has been found to possess *per se* high affinity for negatively charged phospholipids and liposomes mimicking mitochondrial membranes (Hekman *et al.* 2006).

The RAF kinases (A-, B- and C-RAF) play a central role in the conserved Ras-RAF-MEK-ERK signaling cascade and mediate cellular responses induced by growth factors (Daum *et al.* 1994; Rapp *et al.* 2006; Wellbrock *et al.* 2004). Direct involvement of C-RAF in inhibition of pro-apoptotic properties of BAD established a link between signal transduction and apoptosis control (Rapp *et al.* 2004; Troppmair and Rapp 2003). However, the early works did not identify the exact RAF

phosphorylation sites on BAD (Wang *et al.* 1996). Here we demonstrate that hBAD serves as a substrate of RAF isoforms. With respect to hBAD phosphorylation by PKA, Akt/PKB and PAK1 *in vivo*, we observed different specificity compared to RAF kinases. hBAD phosphorylation by RAF was accompanied by reduced apoptosis in HEK293 and NIH 3T3 cells. Furthermore, we show that *in vitro* phosphorylation of hBAD by RAF at serines 75, 99 and 118 regulates the binding of 14-3-3 proteins and association with Bcl-2 and Bcl-X_L. By use of mass spectrometry we detected several novel *in vivo* phosphorylation sites of hBAD in addition to the established phosphorylation sites serine 75, 99 and 118. Finally, we show here that hBAD forms channels in planar bilayer membranes *in vitro*. This pore-forming capacity was dependent on phosphorylation status and interaction with 14-3-3 proteins.

3.1.2. Experimental Procedures

Cell culture, transfection and immunoblotting – HEK-293 cells and NIH 3T3 cells were cultivated in DMEM supplemented with 10% FCS (fetal calf serum; heat inactivated at 56 °C for 45 min), 2 mM L-glutamine and 100 units/ml penicillin/streptomycin at 37 °C in humidified air with 5% CO_2. U0126 (Promega), PD98059 (Promega), BAY 43-9006, Forskolin (Alexis), IBMX (Sigma), CI1040 (Axon Medchem), Wortmannin (Santa Cruz) and LY294002 (Promega) were dissolved in DMSO (Sigma), whereas H-89 (Sigma) was dissolved in ethanol. NIH 3T3 fibroblasts were seeded at 2×10^5 cells/well of a 6-well plate and grown for 24 h before transfection by lipofectamine (Invitrogen). HEK293 cells were seeded at 7.5×10^5 cells/well on a 6-well plate and grown for 24 h before transfecting them with expression plasmids by the calcium phosphate method (Chen and Okayama 1987). 16 h post transfection, cells were washed twice with PBS (phosphate buffered saline) and cultivated for indicated time in medium supplemented with 0.3% serum to avoid activity of endogenous kinases. Cells were washed once in PBS and equal amounts of cells were lysed by direct addition of Laemmli buffer or in NP-40 buffer (10 mM Hepes, pH 7.5, 142.5 mM KCl, 5 mM $MgCl_2$, 1 mM EGTA and 0.2% NP-40 supplemented with a cocktail of standard protease inhibitors). Protein concentration was determined by Bradford method. SDS-PAGE and immunoblotting were performed as described previously (Hekman *et al.* 2006). The following primary antibodies were used: monoclonal anti-phospho-ERK antibody (#9106, Cell Signaling Technology), phosphospecific antibodies against mBAD phosphoserines 112, 155 (#9295 and #9297, Cell Signaling Technology) and phosphoserine 136 (44-524Z, Biosource), polyclonal anti-actin (A2066, Sigma) polyclonal anti-Akt/PKB (#9272, Cell Signaling Technology), polyclonal anti-BAD antibody (sc-943 and sc-8044, Santa Cruz), anti-PAK antibody (sc-881, Santa Cruz), anti-B-RAF antibody (sc-166, Santa Cruz), anti-PKA antibody (sc-903, Santa Cruz) and pan-RAF antibody (30K, MSZ).

Cell survival assay – For the analysis of cell survival, HEK-293 cells were transiently transfected in triplicates. 16 h post transfection, cells were washed twice with PBS and grown for 30 h in medium supplemented with 0.3% serum. Cell viability was assessed by staining cells in Trypan blue (Sigma).

Colony yield assay – NIH 3T3 cells were transfected with the indicated plasmids using Lipofectamine. The day after transfection cells were splitted and around 50 cells of each set of transfection had been seeded in 6 cm dishes. Colony assays were performed in triplicate by scoring number of colonies (consisting of at least 20 cells) in the dishes grown for 14-18 days with appropriate antibiotic selection (450 μg/ml neomycin and 6 μg/ml puromycin, Calbiochem). To visualize the growing colonies, cells were washed once with PBS, fixed with methanol and stained with Giemsa dye (Sigma).

DNA expression plasmids – Human BAD cDNA (kind gift of John Reed, La Jolla, California) and cDNAs mutated at serine 75 (S75A), serine 99 (S99A), serine 118 (S118A), serines 75/99 (S75A/S99A) and serines 75/99/118 (S75A/S99A/S118A) were cloned into pGEX-4T-1 (Pharmacia). Deletion mutants of hBAD were PCR-amplified, with primer overhangs containing restriction sites and cloned into GST fusion vector pGEX-TT cleaved with the appropriate enzymes. Site-directed mutagenesis has been performed by using QuikChange (Stratagene). To generate N-terminal His-tagged hBAD, the cDNA was released by *EcoRI*/*NotI* from pGEX-4T-1 and ligated in the *EcoRI*/*NotI* sites of pFastBac H1 (Invitrogen). Human Bcl-X_L (John Reed, La Jolla, California) was isolated from pcDNA3 using *EcoRI* and ligated with blunt-ends in pFastBac-GST linearized by *StuI*. PAK1 constructs were from Jonathan Chernoff (Philadelphia, Pennsylvania). Akt/PKB plasmids were kindly provided by Jakob Troppmair (Innsbruck, Austria). pGEX-Bcl-2 was kindly donated by John Reed (La Jolla, California).

Purification of kinases, BAD, Bcl-X_L and 14-3-3 proteins – Expression and purification of RAF kinases, PAK1, Akt/PKB, 14-3-3 proteins and Bcl-X_L from Sf9 insect cells were performed as previously described (Fischer *et al.* 2009; Hekman *et al.* 2006; Hekman *et al.* 2002; Hekman *et al.* 2004). For purification of phosphorylated His-hBAD, Sf9 cells were infected with baculoviruses at the multiplicity of infection of 5 and incubated for 48 h at 27°C. The Sf9 cell pellet (2×10^8 cells) was lysed in 10 ml lysis buffer containing 50 mM sodium phosphate, pH 8.0, 150 mM NaCl, 10 mM Na-pyrophosphate, 25 mM β-glycerophosphate, 25 mM NaF, 10% glycerol, 0.5% NP-40 and a cocktail of standard proteinase inhibitors for 30 min with gentle rotation at 4°C. The lysate was centrifuged at 27,000 g for 30 min at 4°C. The supernatant (10 ml) containing His-hBAD was incubated with 0.5 ml Ni^{2+}-nitrilotriacetic acid-agarose for 2 h at 4°C with rotation. After incubation, the beads were washed 3 times with lysis buffer containing 0.2% NP-40, 300 mM NaCl and 20 mM imidazole and hBAD was eluted with an imidazole step gradient. GST-tagged 14-3-3 proteins and GST-hBAD were expressed in *E. coli* using pGEX-2T vector (Pharmacia) and purified by glutathione-Sepharose affinity chromatography. For lipid bilayer experiments, GST-hBAD was additionally purified by ion exchange chromatography using an ÄKTA-System (GE Healthcare). 14-3-3 proteins were released by thrombin (Sigma) cleavage using standard protocols. The purity of the proteins was assessed by SDS-PAGE and staining with Coomassie Blue. To enrich and separate phosphorylated His-hBAD from the non-

phosphorylated fraction, His-hBAD purified from Sf9 cells (0.5 mg) was incubated with 0.5 mg of recombinant GST-14-3-3ζ on glutathione-Sepharose beads (300 µl) for 40 min at room temperature. After excessive washing with 10 mM Hepes, pH 7.4, 150 mM NaCl and 0.01% NP-40, the phosphorylated hBAD fraction was released from the complex by 1% Empigen (Calbiochem).

Kinase activity assay – Human GST-BAD was incubated with purified preparations of RAF kinases, PKA, Akt/PKB or PAK1 in 50 mM Hepes buffer, pH 7.6 in the presence of 10 mM $MgCl_2$, 1 mM DTT and 500 µM ATP. The mixture was incubated at 30°C for 30 min and the reaction was terminated by addition of Laemmli buffer. The proteins were separated by SDS-PAGE and transferred to nitrocellulose membranes. The extent of BAD phosphorylation at serine 75, 99 and 118 was detected by phosphospecific antibodies. To inhibit kinase activity *in vitro*, purified kinases were pre-incubated with BAY 43-9006 or H-89 at room temperature for 30 min.

Mass spectrometry analysis of BAD phosphorylation – Purified His-hBAD samples (about 100 pmol of each) were applied to SDS-PAGE. Proteins were visualized by Coomassie Blue staining applying the method of Neuhoff *et al*. (Neuhoff *et al.* 1988). In-gel reduction, acetamidation, tryptic and/or GluC digestion were done according to Wilm *et al.* (Wilm *et al.* 1996). After elution of the peptides, solutions were desalted using Millipore C18 ZipTip according to the manufacturer's instructions. ESI-MS was performed on a Bruker APEX II FT-ICR mass spectrometer (Bruker Daltonic GmbH Bremen) equipped with an Apollo-Nano-ESI ion source in positive ion mode.

To determine the exact positions of phosphates within the peptides, the nano-LC-MS/MS analysis was carried out as follows: purified hBAD samples were separated by SDS-PAGE, protein bands were excised, washed, and in-gel digested as described previously (Reinders *et al.* 2007). Afterwards, generated peptides were extracted using 15 µL 0.1% TFA and samples were analyzed by nano-LC-MS/MS on an LTQ Orbitrap XL mass analyzer (Thermo Scientific, Dreieich, Germany) coupled to an Ultimate 3000 (Dionex, Amsterdam, The Netherlands) using multistage activation as described previously (Zahedi *et al.* 2008). To this end, peptides were preconcentrated on a PepMap trapping column (100 µm ID, 5 µm particle size, 100 Å pore size, 1 cm length, Dionex) and separated on a PepMap nano-LC column (75 µm ID, 3 µm particle size, 100 Å pore size, 15 cm length, Dionex) at a flow rate of 270 nl/min, using a gradient ranging from 5-50% of 86% acetonitrile and 0.1% formic acid. Raw data were transformed into mgf format using extract_msn.exe as part of the Bioworks package and generated peak lists were searched against an SGD database with concatenated standard protein and BAD sequences (6319 entries) using Mascot 2.2. The following search parameters were used: trypsin as protease with a maximum of one missed cleavage site, 10 ppm mass tolerance for MS, 0.5 Da for MS/MS, oxidation of Met (+15.99 Da) and phosphorylation of Ser/Thr/Tyr (+79.96 Da) as variable modifications, and ^{13}C set to one. All identified phosphopeptides were manually validated to correct for potentially false phosphorylation site assignments.

Lipid bilayer experiments – The channel-forming ability of proteins was assessed in artificial lipid bilayer membranes using a teflon chamber as described previously (Benz 1994; Benz *et al.* 1992). Briefly, to form the membranes a 1% (w/v) solution of diphytanoylphosphatidylcholine (DiphPC) (Avanti Polar Lipids) in *n*-decane was used. Purified hBAD proteins (phosphorylated and non-phosphotylated) or Bcl-X_L were added to the KCl buffer in both compartments of the chamber and the single-channel conductance of the pores was measured after application of a fixed membrane potential. To test the effects of 14-3-3 proteins on pore-forming abilities of hBAD, purified heterodimeric 14-3-3 protein (14-3-3ζ/14-3-3ε) were incubated with phosphorylated form of BAD for 30 min at room temperature prior to channel formation. Samples were applied on both sides of the DiphPC membrane in KCl buffer and single-channel formation was measured.

Biosensor measurements – The biosensor measurements were carried out either on BIAcore-X or BIAcore-J system (Biacore AB, Uppsala, Sweden) at 25°C. The biosensor chip CM5 was loaded with anti-GST antibody using covalent derivatization according to the manufacturer's instructions. Purified and GST-tagged proteins (GST-BAD wt and substitution mutants) were immobilized in biosensor buffer (10 mM Hepes, pH 7.4, 150 mM NaCl and 0.05% NP-40) at a flow rate of 10 µl/min, which resulted in a deposition of approximately 1000 response units (RU). Next, the purified analytes (14-3-3ζ or Bcl-X_L) were injected at indicated concentrations. The values for unspecific binding measured in the reference cell were subtracted. To monitor the dissociation of Bcl-X_L/GST-BAD complex induced by BAD phosphorylation the biosensor chip was treated with active C-RAF in the presence of 0.5 mM ATP. The modified biosensor buffer contained 5 mM $MgCl_2$ and 0.5 mM DTT. The working temperature was set to 30°C. The evaluation of kinetic parameters was performed by non-linear fitting of binding data using the BiaEvaluation 2.1 analysis software. The apparent association (k_a) and dissociation rates constant (k_d) were evaluated from the differential binding curves (Fc2-Fc1) assuming a A+B=AB association type for the protein-protein interaction. The dissociation constant K_D was calculated from the equation $K_D = k_d/k_a$.

3.1.3. Results

Detection of novel in vivo phosphorylation sites of human BAD by mass spectrometry – Besides the highly conserved murine BAD phosphorylation sites at serines 112, 136 and 155 (corresponding to serine 75, 99 and 118 in human BAD) that are crucial for 14-3-3 binding and interaction with Bcl-2/Bcl-X_L, four other murine phosphorylation sites (positioned at serines 128 and 170 and threonines 117 and 201) have been reported (for ref. see Introduction). Although human BAD compared to murine BAD shows striking differences in the length of its amino acid sequence (168 *versus* 204 residues) and in the number and locations of putative phosphorylation sites no systematic analysis of *in vivo* phosphorylation of this pro-apoptotic protein has been performed.

As phosphospecific antibodies directed against the putative 14-3-3 binding sites (serine 75 and 99) and docking segment of Bcl-2/Bcl-X_L proteins (surrounding serine 118) are available, we examined first the phosphorylation status at these established positions. As shown in Fig. 8A, all three of these sites were detectable in purified hBAD by use of phosphospecific antibodies, indicating that a fraction of hBAD expressed in Sf9 cells is associated with 14-3-3 proteins and decoupled from Bcl-2/Bcl-X_L proteins. Such a complex is predicted to be excluded from mitochondria and, consequently, to act in an anti-apoptotic manner (Zha *et al.* 1996). To analyze the complete phosphorylation status of human BAD, we performed a detailed mass spectrometry analysis of the protein purified from Sf9 cells. For that purpose, we digested purified hBAD by trypsine and/or GluC and the selective detection of phosphopeptides was carried out by both ESI-MS and nano-LC-MS/MS technique. Two independent measurements provided almost 89% coverage of the entire protein sequence. The combined results obtained for hBAD phosphorylation are summarized in Fig. 8B and Table 2 revealing several novel *in*

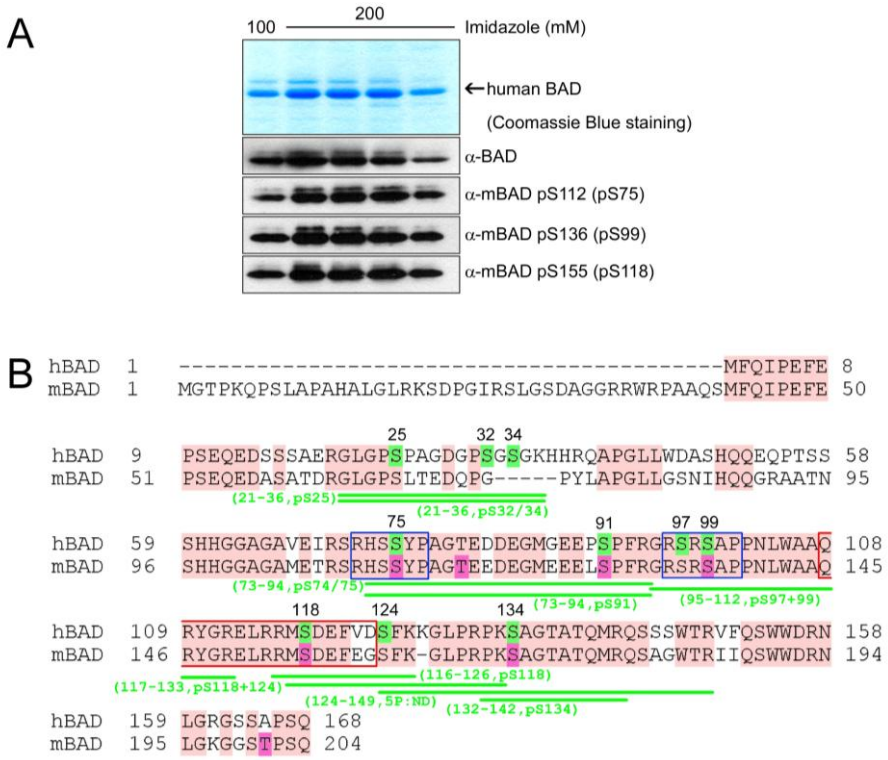

Figure 8: Analysis of *in vivo* phosphorylation of purified human BAD protein.
A, purification of human BAD from Sf9 insect cells. The upper panel shows Coomassie Blue staining after SDS-PAGE of human BAD obtained by elution from nickel-agarose beads by 100 and 200 mM imidazole, respectively. The phosphorylation of serines 75, 99, and 118 was verified by use of phosphospecific antibodies. B, sequence alignment of human and murine BAD protein and mass spectrometry analysis of phosphopeptides obtained by tryptic and GluC digestion of hBAD. For detailed list of identified phosphopeptides see also Table 2. The putative phosphorylation sites of human BAD are highlighted in green, and their positions within the sequence are indicated by numbers. The published phosphorylation sites of murine BAD are highlighted in magenta. The conserved regions between human and murine BAD are shown in pink. The putative 14-3-3 binding sites are indicated by blue rectangles and the conserved BH3 domain by a red rectangle.

vivo phosphorylation sites. To compare the mass spectrometry results obtained for human BAD with the known phosphorylation sites in murine BAD, we aligned the amino acid sequences of both BAD proteins (Fig. 8B). Remarkably, with exception of two novel phosphorylation sites localized closely to the N-terminus (serines 25 and 32/34), most of the phosphorylated peptides obtained by mass spectrometry were localized in the C-terminal half of the protein. The last 20 residues at the very C-terminal sequence bear no phosphate molecules, whereby it should be noted that human BAD does not possess threonine 201that was found to be phosphorylated in murine BAD.

Two N-terminal phosphorylation sites were identified within the tryptic peptide 21-36 and the positions of the phosphates (25 and 32/34) were verified *via* fragmentation analysis using nano-LC-MS/MS approach (see Table 2). Next, we identified a peptide corresponding to hBAD (73-94) sequence carrying one phosphate. The fragmentation analysis of this peptide did not provide unambiguous result: it suggested phosphorylation of either serine 74 or 75. We propose, however, that this phosphate could be ascribed to phosphoserine 75, as the phosphospecific antibody directed against the homologous site in mBAD identified also the hBAD protein (Fig. 8A). Interestingly, fragmentation analysis of the tryptic peptide 71-94 revealed phosphorylation at serine 91 but not at serine 75. As the homologous serine in murine BAD (serine 128) has been reported to be phosphorylated we can conclude that this serine in front of the putative 14-3-3 binding region may also play a regulatory role in human BAD signaling. The next two peptides (peptide 97-109 and 99-109) carrying one phosphate, respectively, cover the sequence of the putative 14-3-3 binding domain that has been described to be phosphorylated at serine 99. The antibody directed against the analogous site in mouse recognized the position Ser-99 within the purified hBAD protein (Fig. 8A). In accordance with this, the fragmentation analysis identified phosphoserine 99 within the tryptic peptide 99-109. Surprisingly, the peptide 97-109 carried the phosphate molecule at serine 97 revealing a novel phosphorylation site in hBAD. Of note, we identified also a peptide comprising the segment between residues 95 and 112 in which both serines (in positions 97 and 99) were phosphorylated (Table 2). This finding suggests a novel regulatory mechanism regarding 14-3-3 binding to their association partners.

The next two peptides (peptide 116-126 and 117-126) carrying one phosphate, respectively, comprise the C-terminal part of BH3 domain of BAD where the serine 118 (corresponding to serine 155 in mBAD) is located. The phosphorylation of this residue regulates the interaction of BAD with Bcl-2/Bcl-X_L proteins. The fragmentation analysis localized a phosphate molecule at serine 118 within both peptides. This finding documents that a fraction of BAD expressed in Sf9 cells does not appear associated with the anti-apoptotic proteins Bcl-2/Bcl-XL. Importantly, the peptide 117-133 revealed two phosphorylation sites (serine 118 and 124). Because the number of phosphates within the peptide 117-133 corresponds to the number of phosphorylation possibilities, we conclude that besides the well-characterized serine 118, serine 124 represents a novel regulatory site in hBAD. Phosphorylation

of serine 124 may be of particular importance due to its vicinity to the lipid binding domain of human BAD comprising the FKK motif that is located in the close proximity to this serine (see Fig. 18).

The alignment of human and murine BAD reveals that both BAD proteins contain the conserved segment RPK**S**AG that represents an appropriate consensus sequence for some kinases. The phosphorylation of murine BAD at serine 170 within this segment has been previously reported (Dramsi *et al.* 2002). Our MS analysis revealed two tryptic peptides (132-142 and 134-143) carrying one phosphate each. This phosphorylation site was ascribed unambiguously to the serine 134 which is homologous to murine serine 170. Finally, we detected a peptide that was cleaved by GluC and trypsin carrying five phosphates (Fig. 8B and Table 2). This peptide has been ascribed to the C-terminal BAD region located between residues 128 and 149. However, this sequence stretch bears up to eight possible phosphorylation sites. Unfortunately, we were not successful in specifying the exact positions of all of the phosphates detected by MS analysis within this fragment. Nevertheless, the phosphorylation of serines 124 and 134 is probable, since it has been detected within several peptides listed in Table 2.

Taken together, we present here for the first time a detailed analysis of human BAD phosphorylation. We confirm several phosphorylation sites that are common to both human and murine BAD and identified in addition a number of novel phosphorylation sites that are specific for human BAD. These novel sites may be involved in regulation of 14-3-3 binding and membrane anchoring of BAD.

Human BAD is a direct substrate of RAF kinases – Next, we investigated whether RAF kinases are directly involved in phosphorylation of human BAD *in vivo*. It was previously shown that C-RAF phosphorylates hBAD (Wang *et al.* 1996). In these preliminary reports, the precise sites of RAF-mediated BAD phosphorylation have not been determined. More recent reports support the view that C-RAF participates in BAD phosphorylation either in conjunction with PAK (Jin *et al.* 2005) or the adaptor protein Grb10 (Kebache *et al.* 2007). The role of other RAF isoforms (A- and B-RAF) has not been evaluated in this context. Particularly, the quantitative contribution of the RAF kinases in phosphorylating serine residues 112, 136 and 155 and the direct comparison of RAF isoforms with other BAD targeting kinases has not been performed so far.

Table 2: Human BAD phosphopeptides obtained by trypsin and/or GluC digestion. The putative phosphorylation sites and the number of the phosphates detected in each of the peptides by mass spectrometry are indicated.

hBAD Peptides	Amino acid sequence	Phosphates/ Peptide	Phosphorylation site(s)
21-36	GLGP**pS**PAGDGPSGSGK	1	Ser25
21-36	GLGPSPAGDGP**S**G**S**GK	1	Ser32 or Ser34
73-94	H**SS**YPAGTEDDEGMGEEPSPFR	1	Ser74 or Ser75
71-94	SRHSSYPAGTEDDEGMGEEP**pS**PFR	1	Ser91
73-94	HSSYPAGTEDDEGMGEEP**pS**PFR	1	Ser91
95-112	GR**pS**R**pS**APPNLWAAQRYGR	2	Ser97 and Ser99
97-109	**pS**RSAPPNLWAAQR	1	Ser97
97-109	SR**pS**APPNLWAAQR	1	Ser99
99-109	**pS**APPNLWAAQR	1	Ser99
116-126	RM**pS**DEFVDSFK	1	Ser118
117-126	M**pS**DEFVDSFK	1	Ser118
117-133	M**pS**DEFVD**pS**FKKGLPRPK	2	Ser118 and Ser124
132-142	PK**pS**AGTATQMR	1	Ser134
134-142	**pS**AGTATQMR	1	Ser134
124-149	SFKKGLPRPKSAGTATQMRQSSSWTR	5	ND

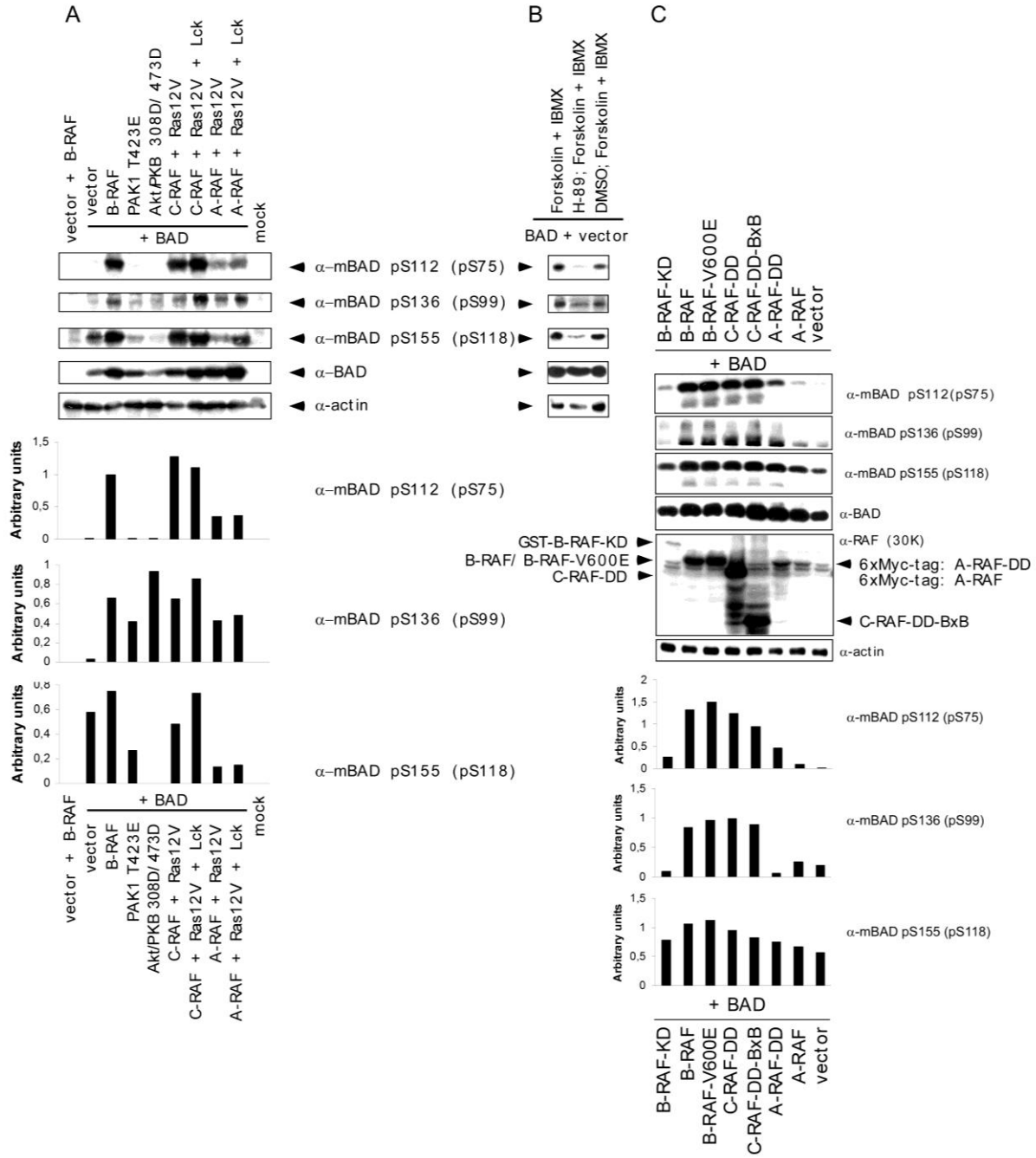

Figure 9: Comparative analysis of hBAD phosphorylation in HEK-293 cells by PKA, Akt/PKB, PAK1, and RAF kinases.

HEK-293 cells were transiently transfected with the indicated expression vectors. A, C- and A-RAF kinases were activated in cells by co-transfecting Ras12V and Lck. In the case of Akt/PKB and PAK1, activating mutants (T308D/S473D and T423E, respectively) were used. In B endogenous PKA was stimulated for 30 min with 25 μM Forskolin and 500 μM IBMX. Pre-treatment with 10 μM H-89 for 30 min prevented PKA activity. In C B-RAF-WT and various constitutively active mutants of RAF kinases (B-RAF-V600E; C-RAF-Y340D/Y341D, termed as C-RAF-DD; truncated C-RAF lacking N-terminal regulatory domains: BxB wt and BxB-DD) were transfected. As a negative control kinase-dead B-RAF (B-RAF-K483A) mutant was chosen. 16 h post transfection, cells were cultivated for additional 30 h in medium supplemented with 0.3% serum. Total cell lysates were separated on a 15% SDS polyacrylamide gel, blotted onto nitrocellulose membrane and phosphorylation of human BAD at serine 75, 99 and 118 as well as BAD expression was analyzed. Endogenous actin was used as a loading control. Presence of different RAF proteins was verified with anti pan-RAF antibody. Representative blots from A and C were quantified by optical densitometry. These experiments were repeated three times with the same results.

In order to address these open issues, we monitored the phosphorylation pattern on critical serine residues (serine 75, 99 and 118 of human BAD) by different RAF isoforms *in vivo* and *in vitro* and performed a comparative analysis involving other BAD phosphorylating kinases such as PAK, PKA and/or Akt/PKB. Due to the fact that the sensitivity of the phosphospecific BAD antibodies is too low to analyze phosphorylation status of endogenous BAD in HEK293, NIH 3T3 or HeLa cells, we decided to overexpress hBAD. Analyzing co-transfected HEK-293 cells we found that the exogenous BAD has been efficiently phosphorylated at the critical positions not only by active PAK1 and Akt/PKB mutants (PAK1-T423E and Akt/PKB-T308D/S473D) but also in the presence of activated RAF isoforms (Fig. 9A).

In the absence of RAF kinases Ras12V and Lck did not lead to significant phosphorylation of hBAD (data not shown). To exclude the participation of kinases other than RAF in BAD phosphorylation that may have been activated by overexpression of Ras12V and Lck, we co-expressed BAD with a variety of constitutively active A-, B- and C-RAF mutants (Fig. 9C). While inactive B-RAF-K483M (KD) or un-stimulated A- and C-RAF failed to phosphorylate BAD significantly, mutants of RAF kinases with elevated kinase activity revealed the same phosphorylation pattern as presented in Fig. 9A. Similar results were obtained by stimulating endogenous PKA with Forskolin in combination with isobutylmethylxanthine (Fig. 9B). Quantification of the results obtained by phosphospecific antibodies directed against serine 75, 99, and 118 revealed that active PAK1 and Akt/PKB were most efficient in the phosphorylation of the putative 14-3-3 binding site of BAD localized at the serine 99 (see *bar graph* in Fig. 9A). Compared with these data, the activated or constitutively active forms of RAF kinases were more efficient in phosphorylation of serines 75 and 118. To investigate, whether these results are HEK-293 cell specific, we co-transfected also NIH 3T3 and HeLa cells with BAD and activated forms of RAF, PAK1 and Akt/PKB. The results obtained with these cell lines were consistent among all three cell lines (data not shown). In contrast to *in vivo* data, more efficient phosphorylation of recombinant GST-BAD by activated PAK1 or Akt/PKB was observed using the intact cell lysates comprising the over-expressed active kinases from the experiment described in Fig. 9A (Fig. 10). Whereas cell lysate containing activated PAK1 was able to phosphorylate recombinant GST-BAD to low levels at serine 75, 99 and to a higher extent at serine 118, activated Akt/PKB again showed efficient phosphorylation of BAD predominantly at serine 99 and more weakly at serine 118 and 75 (Fig. 10). These *in vitro* data are in accordance with findings published earlier (Datta *et al.* 1997; Schurmann *et al.* 2000; Tang *et al.* 2000). BAD phosphorylation by RAF kinases exhibited consistent data *in vivo* and *in vitro*.

To demonstrate that BAD is a direct substrate of RAF kinases, several inhibitors were applied to exclude the possible influence of endogenous kinases. Importantly, we observed no reduction of BAD phosphorylation after treatment of HEK-293 cells co-transfected with hBAD and B-RAF using three different MEK inhibitors (U0126, PD98059 and CI1040) or the PI3K inhibitors Wortmannin and LY294002 (Fig. 11, A and B). An involvement of autocrine loops could be excluded, since treatment with Suramin, an inhibitor blocking the activation of growth factor receptors at the plasma membrane through interference with receptor-ligand binding (Hosang 1985; Huang *et al.* 1990), did not prevent phosphorylation of BAD by B-RAF (Fig. 11C). Importantly, the RAF kinase inhibitor BAY 43-9006 reduced BAD phosphorylation at all three serine residues already at 1 μM (Fig. 11D). The results presented here (using RAF and MEK inhibitors) are in accordance with data published by Jin *et al.* (Jin *et al.* 2005). Finally, the PKA inhibitor H-89 reduced considerably the phosphorylation degree at all three sites (Fig. 9B).

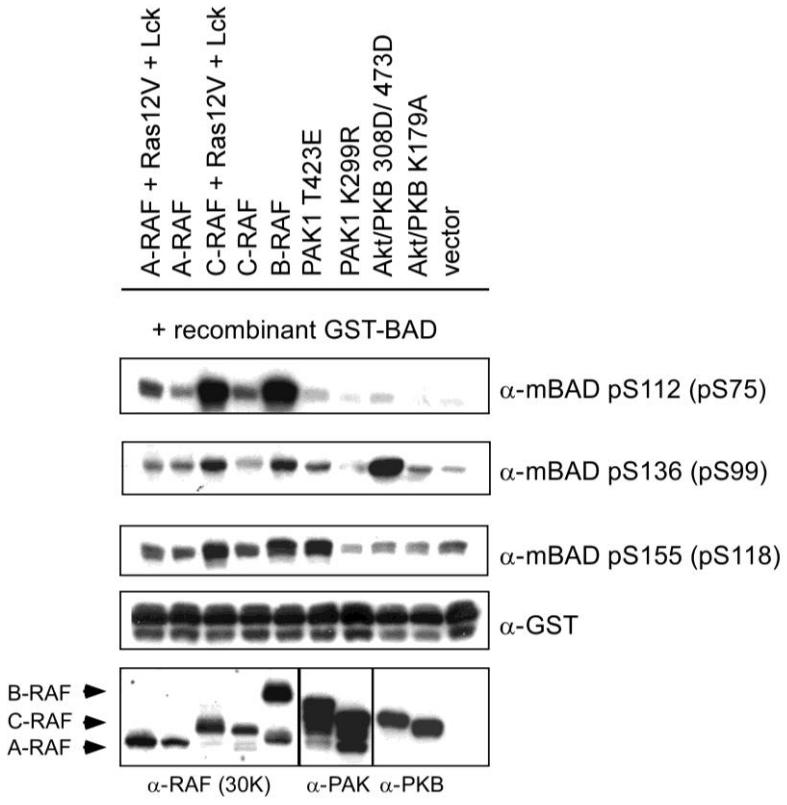

Figure 10: *In vitro* phosphorylation of recombinant GST-BAD by kinases overexpressed in HEK-293 cells. HEK-293 cells were transiently transfected with the indicated plasmids. Inactive mutants of PAK1 and Akt/PKB (K299R and K179A, respectively) were used as negative controls. 16 h post transfection, cells were cultivated for additional 30 h in medium supplemented with 0.3% serum. Afterwards cells were washed once in PBS and lysed by direct addition of NP-40 buffer. For kinase assay, 35 μg of the protein lysates containing the desired kinases were mixed with 1 μg recombinant GST-BAD (purified from *E. coli*) in kinase buffer. Proteins were separated on a 12% SDS polyacrylamide gel and blotted. Phosphorylation of BAD was visualized with phosphospecific BAD antibodies. Expression levels of RAF kinases, PAK1 and Akt/PKB are shown in the lower panels. This experiment was repeated three times with the same results.

In vitro phosphorylation of BAD by purified B- and C-RAF kinases – To further explore whether BAD is a direct substrate of RAF, we analyzed phosphorylation of recombinant BAD by purified RAF kinases *in vitro*. For C-RAF, we tested several activated forms including constitutively active C-RAF (C-RAF-Y340D/Y341D, termed C-RAF-DD), highly activated C-RAF (co-expressed in the presence of Ras12V and Lck, called here C-RAF-R/L) and truncated C-RAF lacking N-terminal regulatory domains (BxB wt and BxB-DD). In experiments with B-RAF, the wild-type (wt) kinase was chosen because of its high basal activity compared to A- and C-RAF wt. As illustrated in Fig. 12A, all active RAF preparations phosphorylated hBAD at Ser-75 and Ser-118. Only C-RAF-R/L additionally phosphorylated BAD at Ser-99. Of note, kinase dead mutants of C- and B-RAF (C-RAF-K375M and B-RAF-K483M) failed to phosphorylate hBAD *in vitro* (Fig., 12, A and B). In the presence of Akt/PKB, we observed phosphorylation at Ser-75, -99 and -118, whereas Ser-118 was the main target

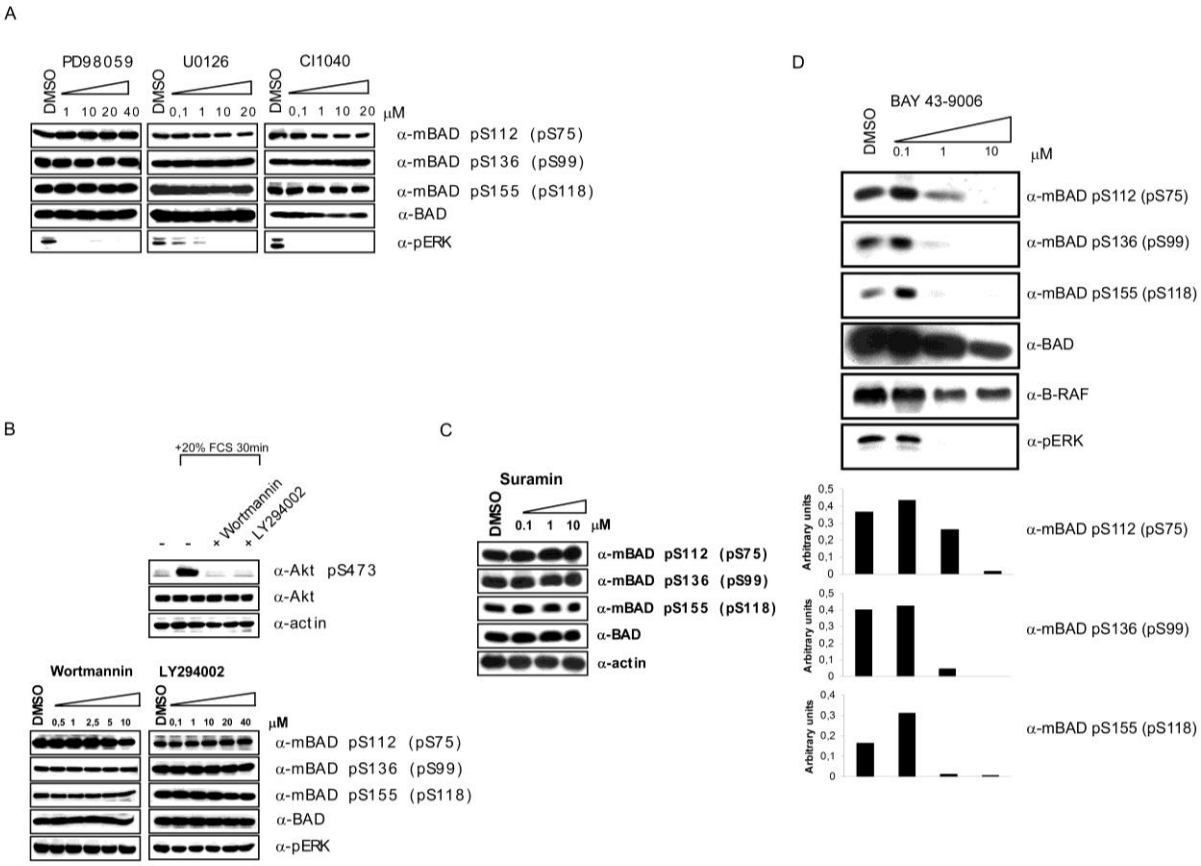

Figure 11: Kinase inhibitors indicate direct involvement of RAF kinases in BAD phosphorylation.
HEK-293 cells were transiently transfected with BAD and B-RAF expression vectors. 16 h post transfection cells were cultivated in medium supplemented with 0.3% serum. During that time cells were additionally treated with various concentrations of MEK inhibitors PD98059, U0126 and CI1040 (A), with PI3K inhibitors Wortmannin and LY294002 (B), Suramin (C) and RAF inhibitor (BAY 43-9006) (D) for 22 h respectively. Phosphorylation of BAD was detected with phospho-specific BAD antibodies. The efficiency of the PI3K inhibitors has been verified by abolishment of Akt-S473 phosphorylation in stimulated HEK-293 cells (B). Treatment with RAF inhibitor BAY 43-9006 prevented both BAD and ERK phosphorylation in a concentration-dependent manner. These experiments were repeated three times with the same results.

of PKA. PAK phosphorylated Ser-75 and Ser-118 (Fig. 12C). In accordance with *in vivo* data obtained by use of RAF inhibitor BAY 43-9006, we also observed *in vitro* effective inhibition of RAF-mediated hBAD phosphorylation by BAY 43-9006 (Fig. 12B).

BAD phosphorylation by RAF promotes survival of mammalian cells – BAD protein has to be phosphorylated in order to neutralize its pro-apoptotic properties (Danial and Korsmeyer 2004; Green and Kroemer 2005). To demonstrate that active RAF prevents BAD-mediated apoptosis we performed different cell survival assays using HEK-293 and NIH 3T3 cells. HEK-293 cells were transiently transfected with the indicated expression plasmids and starved for 30 hours in medium supplemented with 0.3% serum. Number of apoptotic cells was determined by Trypan blue exclusion (Fig. 13A). As demonstrated in Fig. 13A, BAD-induced apoptosis was effectively inhibited by B-RAF overexpression. About 24% of BAD overexpressing cells were apoptotic, whereas co-expression of B-RAF reduced the percentage of apoptotic cells to a level comparable to control cells. Under starvation conditions, substitution mutants of human BAD, S75A, S118A or S75A/S118A, induce apoptosis to the same extend as it was observed for wild type. However, in contrast to co-expression with BAD-WT, B-RAF did not inhibit BAD-mediated apoptosis, when it was co-expressed with BAD-S75A, BAD-S118A or BAD-S75A/S118A mutants (Fig. 13B). Of importance, expression of the kinase dead form of B-RAF did not prevent the BAD-induced apoptosis of the cells as well (Fig. 13A).

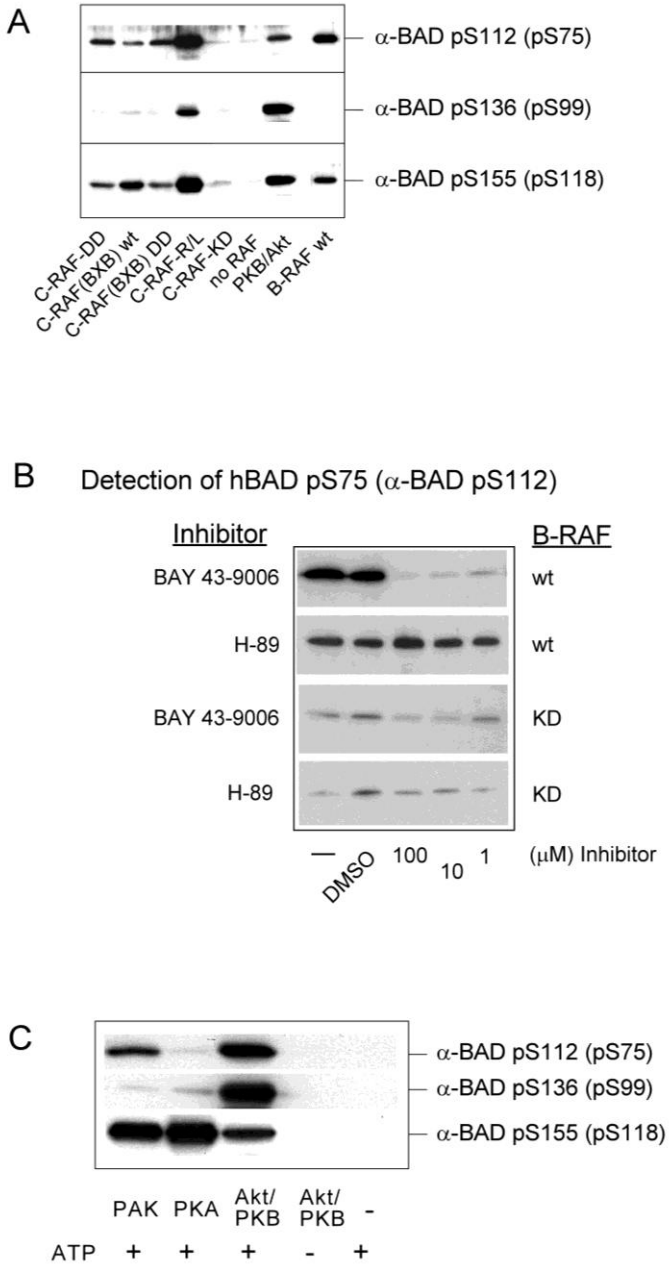

Figure 12: *In vitro* phosphorylation of recombinant GST-BAD by purified PKA, PAK1, Akt/PKB and RAF kinases.

A, B and C, phosphorylation of non-phosphorylated BAD purified from *E. coli* was carried out as described in Experimental Procedures. Recombinant GST-BAD (20 pmol) was phosphorylated by purified B- and C-RAF and corresponding RAF mutants (2 pmol each) as indicated, catalytic subunit of PKA, constitutively active Akt/PKB or PAK1 (4 pmol each). B, whereas the RAF inhibitor BAY 43-9006 prevented BAD phosphorylation in the concentration range between 1 and 100 µM, the PKA inhibitor H-89 had no effect on BAD phosphorylation demonstrating that purified B-RAF was not associated with PKA. Following SDS-PAGE and immunoblotting, BAD phosphorylation was visualized by phosphospecific antibodies directed against phosphoserines 112, 136 and 155 of mouse BAD (corresponding to phosphoserines 75, 99 and 118 of human BAD). These experiments were repeated five times with comparable results.

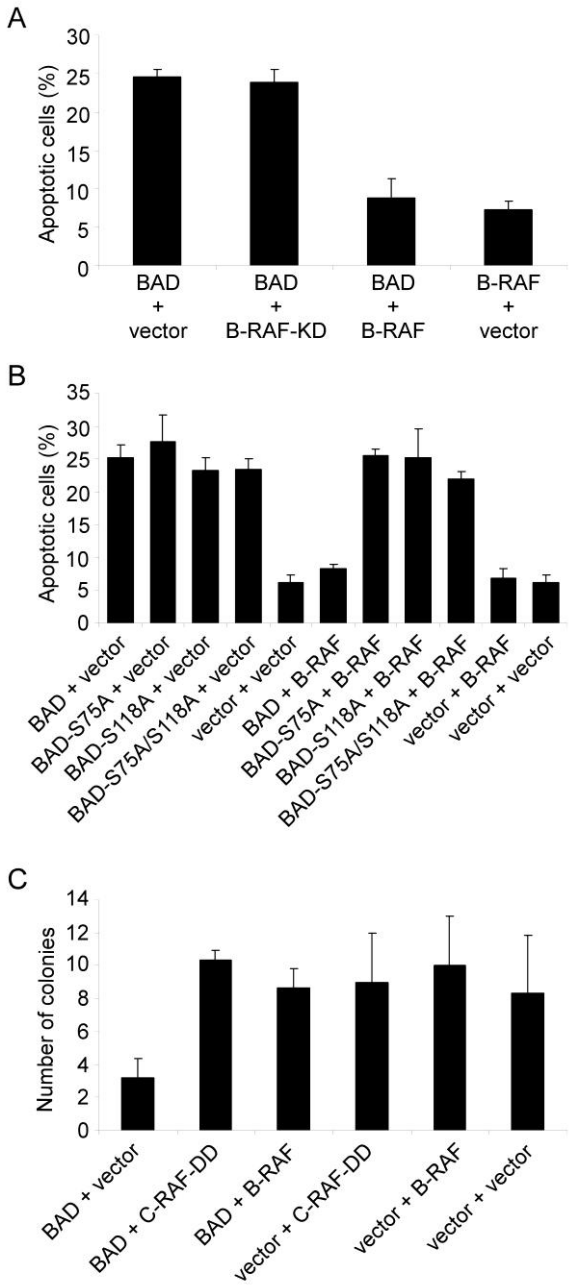

Figure 13: Expression of B- and C-RAF delays BAD-mediated apoptotic death of HEK-293 cells following growth factor removal.
A and B, HEK-293 cells were transiently transfected in triplicates with the indicated expression vectors (ratio 1:1). 16 h post transfection, cells were cultivated for additional 30 h in medium supplemented with 0.3% serum. Cell viability was assessed by Trypan blue staining. Mean values and standard deviations are shown. Experiment was repeated twice. C, colony formation assay shows reproductive survival of triplicate cultures of NIH 3T3 cells stably expressing either empty vectors, BAD alone, BAD in combination with B-RAF or activated C-RAF (C-RAF-DD) as well as B-RAF and C-RAF-DD alone. BAD phosphorylation by RAF protected cells from apoptosis and led to an increased number of colonies.

In order to corroborate the importance of B- and C-RAF-mediated BAD phosphorylation for the survival of mammalian cells, we additionally performed colony yield assays (Fig. 13C). BAD overexpressing cells seeded at low density in Petri dishes have difficulties to form clonogenic colonies, clear evidence that they are not protected against its pro-apoptotic activity. On the other hand, co-expression with active B- or C-RAF is expected to improve colony yields. In our experimental set we generated stable expression of the transfected DNA by double selection with different antibiotics. As a result, we found that the number of colonies formed by control cells and cells continuously expressing BAD in combination with C-RAF-DD or B-RAF was at least three times higher compared to cells expressing BAD only (Fig. 13C).

The associations of BAD with 14-3-3 proteins and Bcl-2/Bcl-X_L is affected by RAF kinases – Following pro-survival signaling BAD becomes phosphorylated, which enables complex formation with 14-3-3 proteins. To analyze the putative 14-3-3 binding site(s) of hBAD, particularly with respect to phosphorylation by RAF, purified hBAD and its mutants (S75A, S99A, S118A, S75A/S99A and S75A/S99A/S118A) have been treated in an *in vitro* kinase assay with active C-RAF-R/L as described in the legend to Fig. 12A. The real time association with 14-3-3 proteins has been performed by use of BIAcore technique. For that purpose, phosphorylated GST-BAD samples were captured on a chip surface and interactions with purified 14-3-3ζ were monitored. In contrast to S75A and S118A mutants, no 14-3-3ζ binding was observed for BAD-S99A mutant, indicating that the domain surrounding pS99 represents the major 14-3-3 binding site. The double mutant (S75A/S99A) and the triple mutant (S75A/S99A/S118A) did not interact with 14-3-3 as well (Fig. 14). GST-BAD wt revealed highest 14-3-3 binding efficiency indicating that a further binding site may enhance or stabilize this association. These data suggest that *in vivo* interaction of BAD with active C-RAF may result in 14-3-3 association and depletion of the BAD/14-3-3 complex from mitochondrial membranes.

Table 3: Association of BAD with Bcl-2 and Bcl-X_L. Purified full-length Bcl-2 and Bcl-X_L were immobilized on the Biosensor chip (approximately 1200 RU) that was coated with anti-GST antibody. His-BAD was injected in the concentration range between 40-320 nM.

	kd (s^{-1})	**ka** ($M^{-1}s^{-1}$)	**KD** (nM)
Bcl-2	$1.96\times10^{-4} \pm 4.02\times10^{-6}$	$9.06\times10^{4} \pm 1.38\times10^{3}$	**2.16**
Bcl-X_L	$7.82\times10^{-5} \pm 3.55\times10^{-6}$	$1.27\times10^{5} \pm 1.53\times10^{3}$	**0.62**

Next, we examined in more detail the interaction between BAD and Bcl-2 or Bcl-X_L, respectively. In a direct comparison of association-dissociation kinetics (Table 3), we have measured that Bcl-X_L/BAD complex (K_D=0.65 nM) was more stable than Bcl-2/BAD (K_D=2.16 nM). Notably, similar values have been reported for interaction between Bcl-X_L and synthetic peptide representing BH3 domain of BAD (Petros *et al.* 2001). In contrast, the affinity of BAD-BH3 peptide to Bcl-2 was much lower (K_D=15 nM) indicating that the binding parameters using full-length proteins may differ considerably from those using peptide samples (Petros *et al.* 2001). Due to the higher binding affinity, we used in the following experiments Bcl-X_L as a binding partner of BAD.

To investigate the relevance of phosphorylation of hBAD with respect to Bcl-X_L association, we first phosphorylated hBAD (purified from *E. coli*) *in vitro* with various kinases such as PKA, Akt/PKB, B-RAF and C-RAF-R/L. Next, the phosphorylated hBAD samples were immobilized on the Biosensor chip and interactions with Bcl-X_L were monitored. As depicted in Fig. 15A, phosphorylation by C-RAF-R/L, B-RAF and Akt/PKB led to ~25% decrease in Bcl-X_L association. Incubation with PKA resulted in ~50% reduction. This result is in agreement with earlier reports, suggesting that PKA phosphorylates BAD preferentially at serine 155 (Datta *et al.* 2000; Virdee *et al.* 2000).

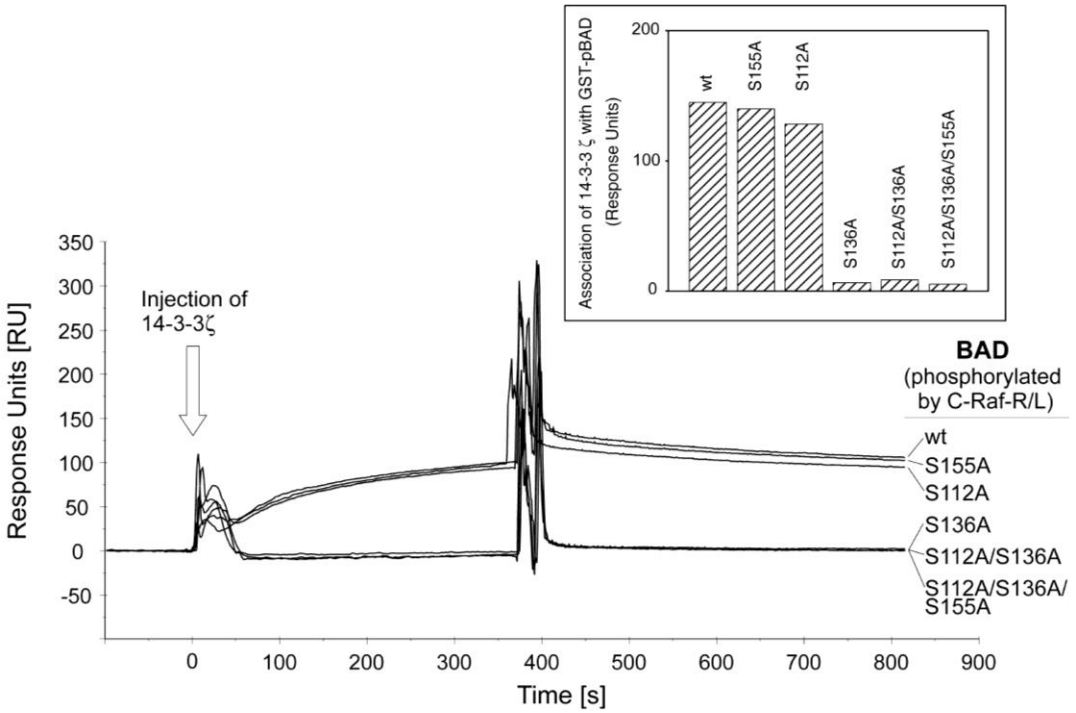

Figure 14: Phosphorylation of BAD wt and BAD mutants by C-RAF promotes association with 14-3-3 proteins.
Interactions of BAD with 14-3-3ζ were monitored by SPR technique. GST-BAD samples (200 pmol) were phosphorylated by highly activated C-RAF-R/L (10 pmol) as described in Experimental Procedures. Approximately 1000 RU of phosphorylated BAD were captured onto anti-GST chip. 14-3-3ζ (200 nM) was injected and the association-dissociation curves were monitored. For better understanding we used here (and in Fig. 15) the mouse nomenclature.

Finally, we asked whether RAF-mediated phosphorylation of BAD reported above is able to trigger the dissociation of the pre-existing Bcl-X_L/BAD complex. For that purpose, different complexes of Bcl-X_L with the following hBAD variants were used (see inset of Fig. 15B): BAD wt, mutated BAD-S75A/S99A and truncated BAD(ΔN102) consisting of the C-terminal fragment harboring the BH3 domain. We used BAD(ΔN102) because it lacks phosphorylation sites S75 and S99 that are involved in 14-3-3 binding. The complexes were formed on the surface of the biosensor chip (Fig. 15B). To monitor the effect of hBAD phosphorylation by RAF, C-RAF-R/L was injected in the presence of ATP. Whereas the complex with wild type BAD dissociated readily, the complex with the C-terminal part of BAD(ΔN102) remained stable. The double mutant (S75A/S99A) dissociated slowly, indicating that phosphorylation sites other than S75A and S99A are involved (Fig. 15B). From these experiments we conclude that RAF kinases do not only prevent the formation of the complex between BAD and Bcl-X_L, but also possess the ability to mediate the disruption of existing BAD/Bcl-X_L complexes.

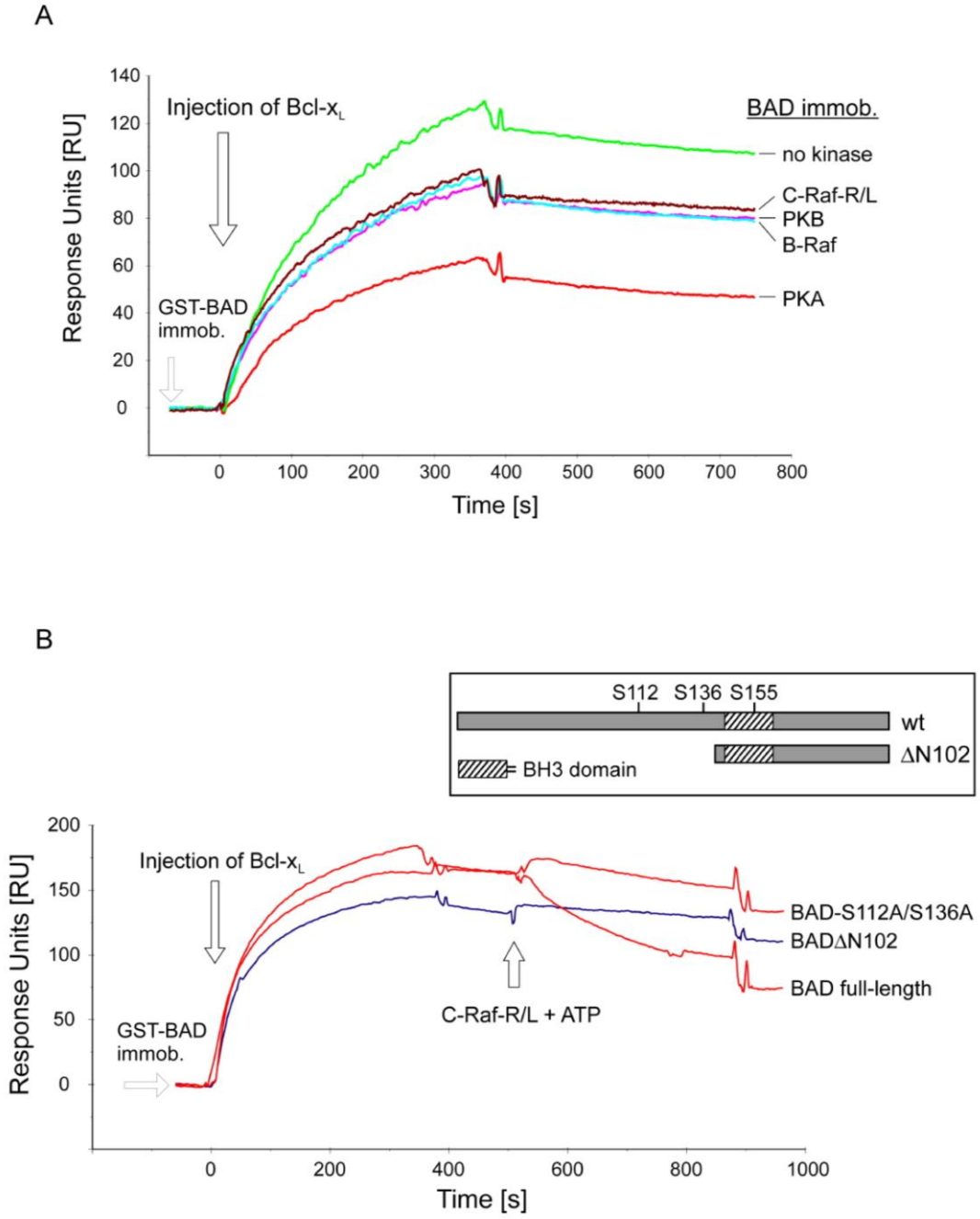

Figure 15: Phosphorylation of recombinant BAD inhibits complex formation between BAD and Bcl-X_L and disrupts pre-existing complex.
A, Purified GST-BAD (200 pmol) was phosphorylated by purified and active B- and C-RAF, Akt/PKB and PKA (20 pmol each) as described in Experimental Procedures. Association of phosphorylated BAD with full-length Bcl-X_L was monitored using SPR technique. Approximately 800 RU of GST-BAD phosphorylated with respective kinases were immobilized by anti-GST coated surface. Bcl-X_L (200 nM) was injected and the association-dissociation curves were monitored. B, Approximately 1000 RU of GST-tagged BAD wt, BAD-S75A/S99A (here termed as BAD-S112A/S136A) and BAD(ΔN102) were immobilized and Bcl-X_L (200 nM) was injected. After saturation, the formed complexes were treated with C-RAF-R/L in the presence of ATP. The structure of BAD samples used in this assay is illustrated in the inset.

Channel-forming activity of human BAD in planar lipid bilayers is influenced by phosphorylation and 14-3-3 proteins – Most Bcl-2 family proteins contain a C-terminal hydrophobic transmembrane domain, indicating that these proteins may exist as integral membrane proteins (del Mar Martinez-Senac *et al.* 2001; del Mar Martinez-Senac *et al.* 2000; Martinez-Senac Mdel *et al.* 2002). Some of them, including pro- and anti-apoptotic members as well as BH3-only protein Bid, show the ability to form pores in lipid bilayers (Antonsson *et al.* 1997; Basanez *et al.* 1999; Kuwana *et al.* 2002; Minn *et al.* 1997; Schendel *et al.* 1999; Schendel *et al.* 1997; Schlesinger *et al.* 1997).

Regarding the BH3-only protein BAD, Hekman *et al.* (Hekman *et al.* 2006) reported pronounced lipophilic properties and identified two lipid binding regions (LBD1 and LBD2) in hBAD. Therefore,

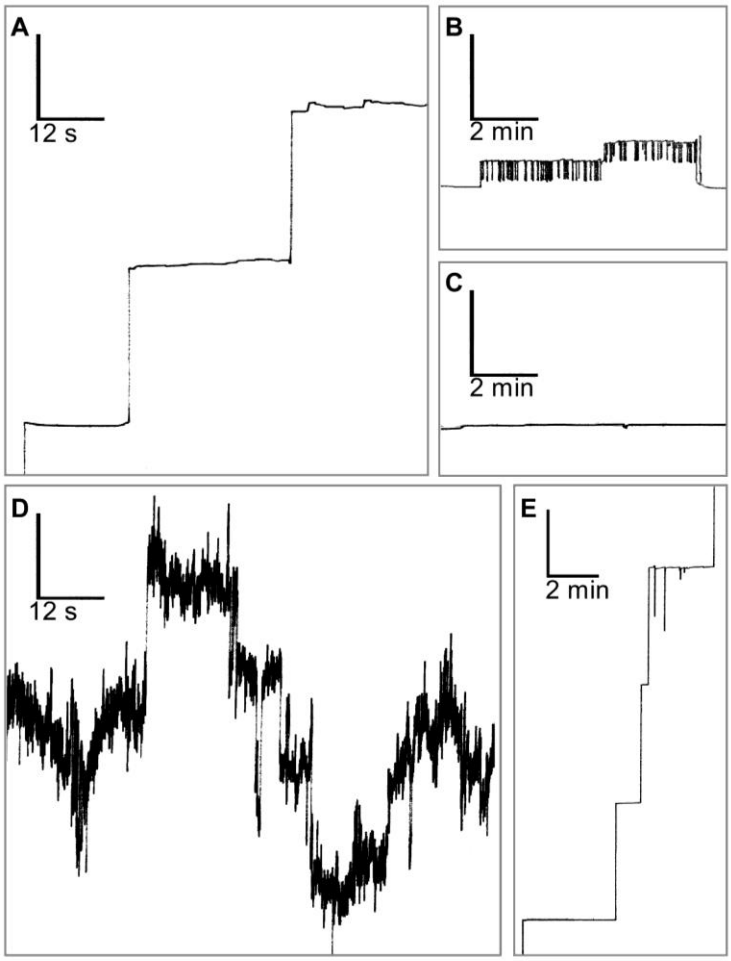

Figure 16: Channel-forming activity of hBAD. Single-channel recordings of purified hBAD or Bcl-X_L (30 ng/ml, respectively) in a DiphPC membrane were monitored.
The aqueous phase contained 1 M KCl. The temperature was 20°C and the applied voltage 20 mV. Phosphorylated hBAD forms large permanent open pores (A) as well as small channels that show a flickering behavior between a closed and an open state (B). Non-phosphorylated hBAD has no pore-forming ability (C). Preincubation of phosphorylated hBAD with the 14-3-3ζ/14-3-3ε heterodimer (1:2, mol/mol) for 30 min at 22°C resulted in a disruption of hBAD´s assembly into the lipid membrane and caused removal or closing of existing BAD channels (D). 14-3-3 proteins alone had no measurable effect on the lipid bilayer (data not shown). E, Bcl-X_L was used as a positive control. Vertical bars indicate conductance of 2.5 nS. DiphPC, diphytanoylphosphatidylcholine. These measurements were repeated three times with the same results.

we supposed that BAD, like several other Bcl-2 family members, may possess channel-forming ability. To test this issue, we investigated whether human BAD is able to form pores in artificial lipid bilayers. Here we used a planar bilayer configuration, where two teflon chambers are separated by a septum having a small (800 µm diameter) aperture in which the membrane bilayer is formed (Benz 1994; Benz *et al.* 1992). This or similar configurations are commonly used for the characterization of channels formed by Bcl-2 family proteins, mitochondrial porins or bacterial toxins (Antonsson *et al.* 1997; Le Mellay *et al.* 2002; Manich *et al.* 2008; Minn *et al.* 1997; Schendel *et al.* 1999; Schendel *et al.* 1998; Schendel *et al.* 1997; Schlesinger *et al.* 1997). It has been previously shown, that Bcl-X_L forms channels in synthetic lipid membranes (Minn *et al.* 1997). Thus, we applied this measurement as a positive control (Fig. 16E). For the measurements with hBAD, we used two different preparations that differ in their phosphorylation states. Beside the complete dephosphorylated protein (produced and purified from *E. coli*), we utilized hBAD expressed in Sf9 cells that was also analyzed by mass spectrometry and was shown here to be phosphorylated at several serine residues (Fig. 8). In the case of dephosphorylated hBAD, we did not detect any pore formation (Fig. 16C). In contrast, approximately 7 min after injection of phosphorylated hBAD into both chambers, step-like current fluctuations representing channel openings to various discrete conductance states were observed. These channels can be classified in two groups: small channels that show a flickering behavior between a closed and an open state (Fig. 16B) and larger permanent open pores (Fig. 16A). The small flickering pores had a single-channel conductance of about 500 pS. The large permanent open pores occur to a lesser frequency and showed single-channel conductance states of about 0.75 and 3.75 nS. Two histograms of the probability P(G) for the occurrence of specific conductivity states for 91 (Fig. 17A) and 341 (Fig. 17B) single-conductance events that were observed within the same experiment with phosphorylated hBAD are shown in Fig. 17. It has been reported that phosphorylation of serines 112 and 136 of mBAD (corresponding to serines 75 and 99 of hBAD) leads to cytoplasmic sequestration by 14-3-3 proteins (Zha *et al.* 1996). To test the functional consequence of this interaction with respect to hBAD pore-forming abilities, phosphorylated hBAD was pre-incubated with heterodimeric 14-3-3 protein (14-3-3ζ/14-3-3ε) before analyzing the channel activity. The consequence was a disruption of hBAD´s assembly into the lipid membrane. Furthermore, 14-3-3 proteins cause removal or closing of existing BAD channels (Fig. 16D). 14-3-3 proteins alone had no measurable effect on the lipid bilayer (data not shown).

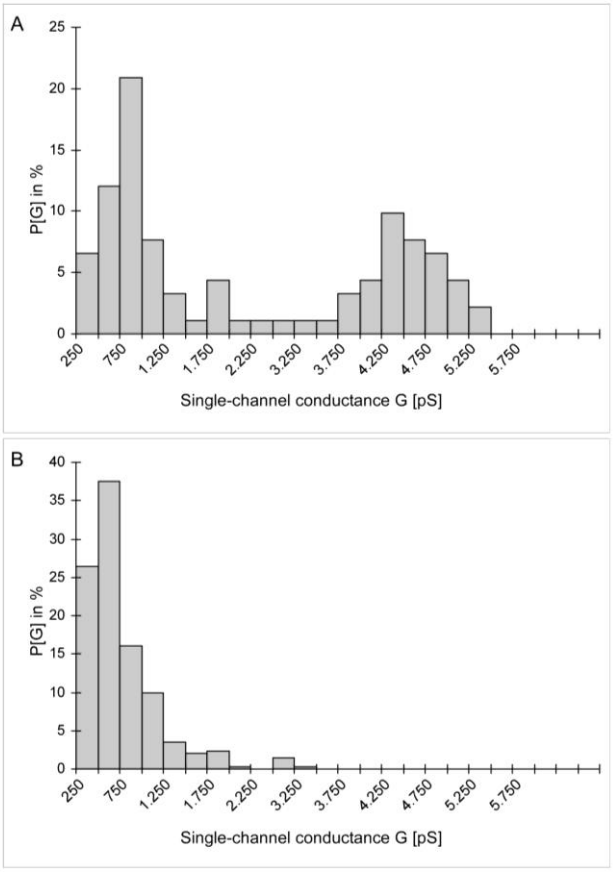

Figure 17: Histogram of the probability for the occurrence of a given conductivity unit.
The histogram was observed with membranes formed using 1% DiphPC in the presence of 30 ng phosphorylated hBAD. P(G) is the probability that a given conductance increment G is observed in the single-channel experiments. It was calculated by dividing the number of fluctuations with a given conductance increment by the total number of conductance fluctuations. A, shows large and permanent open pores (91 single-channel events were integrated). B, displays small channels that show a flickering behavior between a closed and an open state (341 single-channel events were considered). DiphPC, diphytanoylphosphatidylcholine.

3.1.4. Discussion

The phosphorylation of BAD provides an important connection between cell survival signaling and the apoptotic death machinery. A current model of BAD function implicates phosphorylation of at least three serine residues (using mouse nomenclature these are serine 112, 136 and 155). The consequence of phosphorylation of thee sites is complex formation of BAD with 14-3-3 proteins and removal of pro-survival Bcl-2 members at the outer mitochondrial membrane. Besides these highly conserved phosphorylation domains, four other phosphorylation sites of murine BAD (positioned at serine 128 and 170 and threonine 117 and 201) have been identified. Remarkably, although much attention has been devoted to the phosphorylation-mediated regulation of murine BAD function, with some exceptions the regulation of human BAD by phosphorylation has so far not been investigated. Therefore, we performed a systematic analysis of *in vivo* phosphorylation sites in human BAD by combined use of phosphospecific antibodies and mass spectrometry.

MS analysis of human BAD phosphorylation and identification of novel in vivo phosphorylation sites – As shown in Fig. 8A phosphorylation of all three highly conserved serines in purified hBAD were detectable by use of phosphospecific antibodies indicating that a fraction of human BAD expressed in Sf9 cells is associated with 14-3-3 proteins. Such a complex is predicted to be cytosolic or relocated to lipid rafts and not to be associated with Bcl-2/Bcl-X_L proteins (Hekman *et al.* 2006; Zha *et al.* 1996). To investigate, whether hBAD is phosphorylated on more than the three established phosphorylation sites (serines 75, 99 and 118), the purified hBAD samples were analyzed by both ESI-MS and nano-LC-MS/MS technique. The results obtained by MS analysis revealed numerous novel phosphorylation sites (Fig. 8B and Table 2). Interestingly, with exception of serine 25 and 32/34 most of the phosphorylated peptides are clustered within a 75 amino acid stretch comprising also the BH3-like domain. In contrast, the last 20 residues at the very C-terminal sequence bear no phosphate molecules.

Three peptides (peptide 95-112, 97-109 and 99-109) carrying one or two phosphates, comprise the sequence of the putative 14-3-3 binding domain RSR**S**^{99}AP. By use of phosphospecific antibodies, the serine 99 has been found to be phosphorylated in the hBAD sample (see Fig. 8A). Surprisingly, in addition to serine 99, the peptide 95-112 was phosphorylated also at serine 97, indicating a novel regulatory mechanism regarding association of 14-3-3 proteins with BAD. Possibly, the phosphorylation of the second serine in the position 97 within the 14-3-3 binding motif (R**S**^{97}RSAP) inhibits the association of BAD with 14-3-3 proteins. Similar accumulation of phosphates has been observed within the C-terminal 14-3-3 binding motif of A-RAF kinase (R**S**^{580}A**S**^{582}EP) where both serines 580 and 582 were found to be phosphorylated (Baljuls *et al.* 2008). We have proposed that the multiple phosphorylation of the C-terminal 14-3-3 binding region in A-RAF may be one of the reasons for the relative low activity of this RAF isoform. On the other hand, perturbations within the internal 14-3-3 binding domain of C-RAF (RST**S**^{259}TP) have been reported to be a reason for severe cardio-facio-cutaneous disorders called Noonan and LEOPARD syndrome (Pandit *et al.* 2007; Razzaque *et al.* 2007). Displacement of the serine 259 by phenyl alanine abolished the autoinhibitory mechanism of C-RAF resulting in a permanent active kinase form. In conclusion, we suggest that phosphorylation of the serine in position –2 relative to the obligatory phosphorylated serine within the 14-3-3 binding motif (e.g. serine 99 in hBAD) is sufficient to displace 14-3-3 from BAD. In this scenario previous dephosphorylation of the crucial serine within the 14-3-3 binding domain would be dispensable.

The binding motif surrounding serine 75 (RHS**S**^{75}YP) fulfils criteria for a typical 14-3-3 binding site as well (Aitken 2002). In human BAD, phosphorylation of serine 75 has been detected by use of phosphospecific antibody (see Fig. 8A). Also the fragmentation of the tryptic peptide 73-94 suggests phosphorylation of this residue (see Table 2). However, binding data presented in Fig. 14 obtained by mutated BAD proteins do not support a significant contribution of this domain for association of 14-3-3 proteins. We propose that phosphorylated serine 75 is functioning as a gatekeeper for the association

to dimeric 14-3-3 molecules. In other words, the heterodimeric 14-3-3 proteins may occupy both functional 14-3-3 binding sites, with a region surrounding serine 99 representing the high affinity binding site. Besides displacement of 14-3-3 protein from the internal binding site, also other functions of the phosphoserine 75 should be taken into account. Indeed, Fueller *et al.* (Fueller *et al.* 2008) reported recently that the transient phosphorylation of serine 75 in hBAD protein mediated by the activated catalytic domain of C-RAF promotes poly-ubiquitylation of hBAD and increases the turn-over of this protein by proteosomal degradation. The alignment of the amino acid sequences of several mammalian BAD proteins reveals two PEST regions, which constitute a marker for proteins that undergo proteosomal degradation. Interestingly, one of these PEST regions overlap with the 14-3-3 binding domain surrounding phosphoserine 75, thus, indicating a competition between 14-3-3 binding and the ubiquitylation machinery.

Four other phosphopeptides (114-127, 116-126, 117-126 and 117-133) carrying either one or two phosphates, partially cover the BH3 domain where the serine 118 (corresponding to serine 155 in mBAD) is located. Phosphorylation of this residue regulates the interaction of BAD with Bcl-2/Bcl-X_L proteins. Importantly, within the peptide 117-133 two phosphates were detected (see Fig. 8B and Table 2). Because the number of phosphates within the peptide 117-133 corresponds to the number of phosphorylation possibilities, both serine residues (serine 118 and 124) within this peptide appear to be phosphorylated *in vivo*. Thus, we propose that besides the well-characterized serine 118, the serine 124 represents a novel phosphorylation site in hBAD possibly regulating the interaction with membrane lipids. In our previous attempts to characterize the translocation of BAD to mitochondria, we made an unexpected observation that BAD associates with the same efficiency with non-treated and protein-depleted mitochondria (Hekman *et al.* 2006). By use of plasmon resonance-based measurements, two lipid-binding domains (termed LBD1 and LBD2) were identified in C-terminal region of human BAD. While LBD2 overlaps with helix-5 localized at the very C-terminus, LBD1

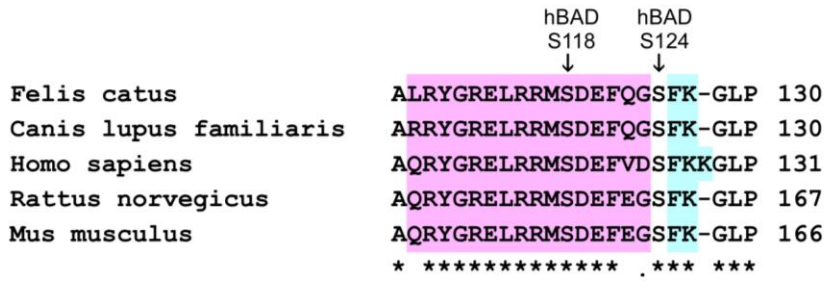

Figure 18: Amino acid sequences of BAD fragment surrounding BH3 domain from different mammalian species.
Amino acid sequences were aligned using the ClustalW algorithm (http://www.ebi.ac.uk/Tools/clustalw2/index.html). The BH3 domain is highlighted in pink and the vicinal FKK/FK regions are in turquoise. This alignment reveals that in contrast to the highly conserved BH3 domain, the neighboring FKK lipid binding motif exists only in humans.

encompasses the C-terminal half of BH3 helix. The LBD1 segment covers also the short FKK motif that has been shown to be necessary for lipid binding of hBAD because mutations within this motif led to dysfunction of BAD and reduced significantly the association with liposomes (Hekman *et al.* 2006). Therefore, we suggest that the phosphorylation of serine 124 may be of regulatory importance due to its close proximity to the FKK motif (S^{124}-FKK^{127}). It is reasonable to speculate that the negative charge of the phosphate molecule may serve to neutralize the influence of the positively charged lysines 126 and 127, with the consequence of reduced affinity of BAD for certain membrane lipids or membrane lipid micro domains. Importantly, the proposed regulation of BAD function by phosphorylation of serine 124 seems to be unique for human BAD protein since most of the mammalian homologues do not contain the complete FKK motif (see also the sequence alignment of several mammalian species illustrated in Fig. 18).

Finally, we detected a peptide carrying five phosphates overlapping partially with the peptide 117-133 (see Fig. 8B). This peptide has been ascribed to the C-terminal BAD region located between residues 128 and 149. At present, we cannot definitively specify the exact positions of all of the phosphates found by MS analysis. Nevertheless, the phosphorylation of serine 124 is very probable since it has already been detected within the peptide 117-133. Also the phosphorylation of murine BAD at the serine 170 (corresponding to serine 134 in hBAD) has been previously reported (Dramsi *et al.* 2002). As the alignment of human and murine BAD shows that both BAD proteins contain the conserved segment RPK$S^{134/170}$AG, it appears probable that this position is phosphorylated in both proteins. Indeed, two other phosphopeptides (132-142 and 134-142) confirmed this assumption. Nevertheless, the role of multiple phosphorylations at the C-terminal end of the BAD protein remains unclear. Such an accumulation of negative charged residues may support the 14-3-3 depletion of BAD from mitochondria.

Inhibition of BAD-mediated apoptosis by RAF kinases – The pro-apoptotic protein BAD has been reported to be a substrate for a broad spectrum of kinases. Here, we demonstrate that BAD is phosphorylated *in vivo* and *in vitro* by RAF kinases as well. However, the role of RAF kinases in BAD phosphorylation is still controversially discussed (Harada *et al.* 1999; Jin *et al.* 2005; Kebache *et al.* 2007; Zha *et al.* 1996). B-RAF has so far not been considered as a BAD phosphorylating kinase. Our results here indicate that RAF kinases (particularly B- and C-RAF) play an active role in BAD phosphorylation and regulation of apoptosis. Due to quality limitations of the phosphospecific BAD antibodies it was almost impossible to analyze the phosphorylation status of endogenous BAD in cell lines like HEK-293, NIH 3T3 or HeLa. To avoid immunoprecipitation experiments where phosphorylated BAD fractions are highly enriched *in vitro*, we decided to perform forced expression experiments. An advantage of this method is that it allows direct testing of RAF kinases, Akt/PKB or PAK1 on BAD phosphorylation and avoids broad activation of effector kinases that normally occurs after stimulation with growth factors like EGF or PDGF.

It has been previously demonstrated that active C-RAF is involved in BAD phosphorylation (Wang *et al.* 1996). However, the exact position of BAD phosphorylation by RAF has not been elucidated. Here we resolved BAD phosphorylation mediated by all three RAF kinases and compared it with data obtained by PKA, Akt/PKB and PAK1. *In vitro* experiments are in accordance with previously published reports (Datta *et al.* 2000; Harada *et al.* 1999; Schurmann *et al.* 2000) that PKA, Akt/PKB and PAK1 phosphorylate BAD to different extents at serines 75, 99 and 118 (Fig. 10 and 12). Under the same conditions, B-RAF phosphorylated BAD predominantly at Ser-75 and Ser-118, whereas highly active C-RAF-R/L phosphorylated BAD at all of these positions (Fig. 12). In contrast, *in vivo* experiments show that RAF kinases and PKA possess the ability to phosphorylate BAD at all three crucial serines (75, 99 and 118) whereas Akt/PKB and PAK1 were more efficient in phosphorylation of the serine 99 that is involved in association of 14-3-3 proteins (Fig. 9). These findings indicate that besides kinase specificity intracellular localization may be important for substrate recognition.

Blocking of autocrine loops by Suramin, e.g. NF-κB pathway or stress kinase cascades (Fig. 11) to downregulate BAD phosphorylation suggests that these pathways do not play an essential role in BAD regulation. Cultivating cells with three different MEK inhibitors (U0126, PD98059 and CI1040) we observed no differences in BAD phosphorylation in the presence of B-RAF (Fig. 11). In contrast, cells grown in the presence of RAF inhibitor BAY 43-9006 or PKA inhibitor H-89 showed significant reduction of BAD phosphorylation *in vivo* and *in vitro*, suggesting that RAF kinases and PKA are involved directly in suppression of BAD-mediated apoptosis. Although BAY 43-9006 was initially developed as a RAF kinase inhibitor, it can additionally target the MAP kinase p38, several tyrosine kinases including VEGFR-2, Flt-3 and c-Kit but none of the reported BAD kinases (Fabian *et al.* 2005; Wilhelm *et al.* 2004). Importantly, Jin *et al.* (Jin *et al.* 2005) showed, in accordance with our results, that C-RAF/PAK-mediated BAD phosphorylation could be effectively inhibited *in vivo* in the presence of 2 μM RAF inhibitor BAY 43-9006. In contrast, the use of MEK inhibitor PD98059 (20 μM) did not prevent BAD phosphorylation. Also consistently with our data it has been shown by using the same cell line that Akt/PKB phosphorylates BAD efficiently at serine 136 (Datta *et al.* 1997). Collectively, we compare here in the same experiment BAD phosphorylation by RAF and other kinases and show that Akt/PKB and PAK1 phosphorylate BAD with different specificity compared to RAF and PKA. Furthermore, we demonstrated that BAD-induced apoptosis can be inhibited by B- and C-RAF and showed that this inhibition is dependent on the phosphorylation of serines 75 and 118 of hBAD (Fig. 13).

Based on data presented here, we suggest that *in vivo* phosphorylation of BAD by RAF kinases represents an important pathway in the phosphorylation of BAD domains, that are involved either in 14-3-3 protein association or mediate coupling/decoupling of BAD with Bcl-2 and Bcl-X_L proteins. To corroborate these findings we performed binding studies with purified components by use of BIAcore

technique. In Fig. 14, we demonstrate that *in vitro* phosphorylation of BAD by activated C-RAF promotes association of BAD with 14-3-3ζ. We used 14-3-3ζ, since of the seven 14-3-3 isoforms analyzed this isoform bound phosphorylated BAD most efficiently (Hekman *et al.* 2006). While serines 75 and 118 are essentially not required for 14-3-3 binding, the domain surrounding serine 99 represents the preferential 14-3-3 binding site. However, a second binding site may enhance or stabilize this association. Quantitative interactions of BAD with truncated Bcl-2 and Bcl-X_L had previously been investigated only using peptide samples derived from BH3 domain of BAD (Chen *et al.* 2005; Petros *et al.* 2001). Consistent with these data we detected a preference for the interaction between BAD and full length Bcl-X_L suggesting that Bcl-X_L is the preferential binding partner of BAD (Table 3).

C-RAF has been found to colocalize with mitochondria markers, indicating a high proportion of C-RAF located at mitochondria (Galmiche *et al.* 2008). The presence of activated C-RAF at mitochondria is also supported by the contribution of Jin *et al.* (Jin *et al.* 2005) who demonstrated that PAK mediates C-RAF activation and its subsequent translocation to the mitochondria. At present, we cannot completely exclude the possibility that RAF kinases and PKA act simultaneously or synergistically, as it has been reported that C-RAF and PKA form a complex *in vivo* (Dumaz and Marais 2003). However, the C-RAF/PKA complex was found to be stable only in non-stimulated cells. It is possible that Akt/PKB and C-RAF also act as a complex *in vivo.* In this scenario, C-RAF would phosphorylate mBAD mainly at serines 112 and 155 and Akt/PKB might be responsible for Ser-136 phosphorylation. These combined phosphorylations would enable effective association of 14-3-3 with BAD and separation from the BAD/Bcl-X_L. She *et al.* (She *et al.* 2005) proposed that BAD might represent the convergence point of the RAF- and the PI3K/Akt kinase pathway. According to this report, BAD protein acts as a switch that integrates the anti-apoptotic effects of the EGFR/MAPK and PI3K/Akt pathways (as detected in MDA-468 cancer cells). This model is further supported by the observation that BAD can associate with PKB and B-RAF in conjunction with the co-chaperone BAG-1 on the mitochondrial level (Gotz *et al.* 2005).

Pore-forming activity of human BAD is regulated by phosphorylation and 14-3-3 Proteins – Within the Bcl-2 family of proteins Bcl-X_L, Bcl-2, Bax, Bak and the BH3-only protein Bid have been reported to possess channel-forming ability in artificial lipid bilayers (Antonsson *et al.* 1997; Minn *et al.* 1997; Schendel *et al.* 1999; Schendel *et al.* 1997; Schlesinger *et al.* 1997). In addition, it was observed by confocal and electron microscopy that Bak and Bax coalesce during apoptosis into large clusters on the surface of mitochondria (Karbowski *et al.* 2002). Here we present biophysical evidence that the pro-apoptotic BH3-only protein BAD forms channels in artificial membranes. To form pores such proteins must contain helices that are long enough to span the membrane bilayer and these helices must be largely devoid of charged residues (Schendel *et al.* 1998). As an average lipid bilayer has a hydrophobic cross-section of ≈30 Å (Montal and Mueller 1972), the α-helix needs to be ≈20

residues long in order to span a membrane bilayer and to be able to participate in channel formation (Schendel *et al.* 1998). A helix probability plot of human BAD exhibited a C-terminal region of about 20 residues with a high probability of a helical structure and only two charged residues (Hekman *et al.* 2006). This region is surrounded by positively charged residues, which may additionally facilitate the association of the protein with membranes. Although one helix is insufficient to form a channel, some molecules could come together, each contributing their hydrophobic helix to create a pore. Furthermore, in the vicinity of this putative C-terminal helix a second lipid binding domain in human BAD comprising the FKK motif has been identified (Hekman *et al.* 2006).

We show here that human BAD is able to form ion channels, which exhibit multiple conductance states with complex opening kinetics. Similar properties have been also reported for other Bcl-2 family members including Bcl-X_L, Bcl-2, Bax and Bid (Antonsson *et al.* 1997; Dejean *et al.* 2006; Minn *et al.* 1997; Schendel *et al.* 1997; Schlesinger *et al.* 1997). The presence of three different channel activities with progressively greater conductances (≈500 pS, ≈750 pS and ≈3750 pS) but occurring with progressively lesser frequency raises the possibility of step-wise oligomerization of BAD protein molecules in planar bilayers. The BAX channel progresses within 2-4 min of its initial appearance (Schlesinger *et al.* 1997). This includes an early low-conducting channel, followed by a transition phase with multiple sub-conductance levels and finally achieves an apparently stable ohmic pore of large conductance. Our findings that the lower conductive hBAD channels are flickering between a closed and an open state and the higher conductive hBAD channels persist open raises the question of what factors may control opening and closing of hBAD channels *in vivo*. Although it was demonstrated, that phosphorylation of BAD does not affect membrane binding (Hekman *et al.* 2006) dephosphorylated hBAD fails to form discrete channels in lipid bilayers. Possibly, some specific phosphorylation patterns of hBAD are responsible for the formation of particular conductance states. Furthermore, we observed that 14-3-3 proteins disrupt hBAD´s assembly into the lipid membrane and that 14-3-3 is able to remove or close existing hBAD channels. Based on these data we propose that the formation of hBAD pores is a reversible process that is regulated by phosphorylation and 14-3-3 proteins. This fits well to the suggested model that BAD is a membrane associated protein that has the hallmarks of a receptor rather than a ligand which shuttles in a phosphorylation-dependent manner between mitochondria and other membranes with 14-3-3 as a key regulator of this relocation (Hekman *et al.* 2006). Additionally, our results emphasize that phosphorylation alone is insufficient to release BAD from membranes, because the depletion process depends on 14-3-3 proteins. *In vivo*, the formation of hBAD pores may also be affected by other proteins that have been reported to interact with BAD. Two candidates are Akt/PKB and B-RAF that were demonstrated to co-immunoprecipitate with BAD (Gotz *et al.* 2005). It is possible that these kinases affect hBAD´s pore-forming ability beside their BAD phosphorylating activity. Another open issue is the putative influence of other pore-forming members of the Bcl-2 family of proteins, like Bcl-2 and Bcl-X_L that have been shown to interact with BAD (Minn *et al.* 1997; Schendel *et al.* 1997; Yang *et al.* 1995). Do they merely shut off

their own and hBAD´s pore-forming activity by heterodimerization or do they alternatively form counteracting pores? Our preliminary data suggest that Bcl-X_L does not abolish pore formation of hBAD (data not shown). Similar observations were reported with respect to the effects of Bax on the pore-forming ability of Bcl-2. Although it was recently demonstrated that Bax interacts preferentially with the membrane-inserted form of Bcl-2 (Dlugosz *et al.* 2006), it was reported that Bax does not merely abrogate pore formation of Bcl-2 (Schendel *et al.* 1997). These authors suggested that Bcl-2 allows the transport across membranes in a direction that is cytoprotective, whereas Bax does the opposite. Bcl-X_L and hBAD may also be involved in controlling such a homeostasis. In this regard it should be mentioned that hBAD forms pores in its phosphorylated and non-apoptotic state. Therefore it is possible that it cooperates with anti-apoptotic proteins instead of counteracting them.

Results presented here raised the question, what could be the physiological role of BAD channels? BAD has been found to localize at the outer mitochondrial membrane and cholesterol rich rafts at the plasma membrane (Fleischer *et al.* 2004; Hekman *et al.* 2006). Therefore, the ion-conducting BAD channels could contribute to the regulation of the mitochondrial permeability transition (Zoratti and Szabo 1995), a process that has been suggested to be critical in apoptosis (Zamzami *et al.* 1996; Zamzami *et al.* 1996). Recently, it was demonstrated that BAD targets the permeability transition pore and sensitizes it to Ca^{2+} in a phosphorylation dependent manner (Roy *et al.* 2009). It is also possible that hBAD conducts other molecules than ions, such as cytochrome c or further apoptogenic factors. Also Bax was originally described to form ion-conducting channels (Schlesinger *et al.* 1997), whereas cell-free studies on isolated mitochondria demonstrated that it can accelerate the release of cytochrome c (Jurgensmeier *et al.* 1998). Another function of BAD channels could be to influence metabolic processes apart from apoptosis. It was already suggested that mitochondrial ion channels such as those regulated by Bcl-2 family members may control the export of metabolites including ATP under normal physiological conditions (Gottlieb *et al.* 2002; Jonas *et al.* 2003; Vander Heiden and Thompson 1999). An example for a Bcl-2 family member that may regulate a non-apoptotic process by the formation of pores is the naturally occurring proteolytic cleavage fragment of Bcl-X_L (Bcl-X_S). There is evidence that during hypoxia Bcl-X_S results in the formation of large conductance channels (Jonas *et al.* 2004), which contribute to the run-down of synaptic transmission in the squid presynaptic terminal (Jonas *et al.* 2005).

Other interesting aspects that could unravel the function of pore-formation by Bcl-2 proteins are observations that link apoptosis to mitochondrial morphogenesis. Bax/Bak were found to colocalize with mitochondrial fission sites and dynamin family GTPases, Drp1 and Mfn2 (Karbowski *et al.* 2002). Additionally, it was found that during apoptosis close in time to Bax translocation and cytochrome c release, mitochondria fragment into small units (Frank *et al.* 2001). This indicates that cytochrome c release may occur through Bax-modified mitochondrial scission machinery. It is also feasible that the insertion of hBAD into membranes is of greater importance to its function as adaptor

or docking protein than for pore formation, as it has been suggested for Bcl-2, Bax and Bcl-X_L (Schendel *et al.* 1998).

Concluding remarks – Generally, BH3-only proteins are proposed to function as sentinels of the cellular health status. Data presented by She *et al.* (She *et al.* 2005) indicate that BAD might represent the convergence point of the RAF- and the PI3K/Akt kinase pathway. According to this report, BAD protein acts as a switch integrating the anti-apoptotic effects of the central mitogenic and PI3K/Akt pathways. This model is further supported by the observation that BAD can associate with both PKB and RAF kinases at the mitochondrial level. Data presented here suggest also that there is interplay between RAF- and the PKB-pathway and that BAD can function as a node of these two signaling pathways. Thus, C-RAF might coordinate the assembly, recruitment and possibly the activity of other kinases resulting in the correct signaling output. Identification of novel hBAD phosphorylation sites indicates another type of regulation for human BAD compared to murine (and some other mammalian) BAD proteins. The finding that human BAD exhibits pore-forming activities opens new insights into the regulation of apoptotic mechanisms mediated by Bcl-2 family of proteins.

3.1.5. Acknowledgements

We thank Barbara Bauer, Nadine Schubert and Elke Maier for excellent technical assistance. This work was supported by the DFG (Grant SFB 487, project C3). The financial support by the Ministerium für Innovation, Wissenschaft, Forschung und Technologie des Landes Nordrhein-Westfalen and by the Bundesministerium für Bildung und Forschung is gratefully acknowledged.

3.2. Can BAD Pores be Good? New Insights from Examining BAD as a Target of RAF Kinases

RAF kinases work from a number of localizations within the cell such as mitochondria, endosomes, cytoplasm/cytoskeleton and the plasma membrane. BAD is a pro-apoptotic member of the Bcl-2 family of proteins that has been described to be targeted directly by RAF. We show here that RAF not only neutralizes BADs pro-apoptotic activity but activates it for a new function as a pore. These geometric pores are permeable for ions and many other signaling molecules and may function in a positive feedback loop to support mitogenic cascade signaling and transformation.

3.2.1. Introduction

RAF kinases are serine/threonine kinases (Mark and Rapp 1984; Moelling *et al.* 1984). They regulate the highly conserved Ras-RAF-MEK-ERK cascade that mediates transduction of extracellular mitogenic signals through activated Ras GTPases to a MAP kinase module (reviewed in Daum *et al.* 1994). This cascade coordinates diverse cellular processes important for development including proliferation, survival, metabolism, migration and senescence. Deregulation on the other hand is frequently found in tumors (www.sanger.ac.uk/genetics/CGP/) (Yeang *et al.* 2008).

C-RAF, the first isoform of the RAF kinase family, was discovered by retrovirus transduction experiments that led to isolation of the acutely transforming virus carrying the *v-raf* oncogene (3611-MSV) (Rapp *et al.* 1983). *v-mil* was independently isolated from the chicken carcinoma virus MH2 in a related retrovirally transduced sequence, (Jansen *et al.* 1983) that additionally carried the oncogene *v-myc*. The cooperation between RAF/Mil and MYC led to the identification of MYC as an apoptosis inducer and RAF as a survival kinase (Blasi *et al.* 1985; Cleveland *et al.* 1986; Principato *et al.* 1990; Principato *et al.* 1988; Rapp 1994; Rapp *et al.* 1985; Rapp *et al.* 1985; Rapp *et al.* 2009; Sutrave *et al.* 1984) As in the case of MYC (Eisenman 2001) RAF kinases belong to a family that includes A- B- and C-RAF. Team work between these enzymes refines RAF signaling by targeting the mitogenic cascade to different subcellular compartments (Rapp *et al.* 2006). Recently, the B-RAF isoform shaped up as an important player of cancer development. This is underlined by the observation that a single amino-acid exchange in B-RAF represents one of the most commonly found mutations in several types of cancer (the valine to glutamic acid exchange in position 600) (Davies *et al.* 2002). The isoforms of RAF kinases are ubiquitously expressed within an organism, but they differ in their expression levels (Storm *et al.* 1990). Specialized functions of each isoform are reflected in differential regulation of RAF kinase activity (Wellbrock *et al.* 2004) and varying phenotypes of RAF knockout mice (Pritchard *et al.* 1996; Wojnowski *et al.* 2000; Wojnowski *et al.* 1997). Embryos of C-RAF$^{-/-}$ as well as B-RAF$^{-/-}$ mice die early in development, whereas A-RAF$^{-/-}$ animals are viable

although they display neurological and intestinal abnormalities (Pritchard *et al.* 1996). B-RAF$^{-/-}$ embryos exhibit overall growth retardation and increased apoptosis in endothelial tissues resulting in death from vascular hemorrhage between day 10.5 and 12.5 (Wojnowski *et al.* 1997). The knockout of C-RAF in mice leads to disturbed development of the placenta and embryonic organs, in particular of the liver and the hematopoietic compartment (Huser *et al.* 2001; Mikula *et al.* 2001; Wojnowski *et al.* 2000). Embryonic lethality occurred in midgestation and may be due to a high apoptosis rate in the liver (Huser *et al.* 2001; Mikula *et al.* 2001) that is also observed in cell culture experiments (Zhong *et al.* 2001).

Growth factor regulation of RAF kinases is highly complex and still not completely elucidated. The regulation comprises binding by active Ras at the membrane, phosphorylations and heterodimer formation with other proteins. There is also evidence for control of the RAF kinases at the protein level (Dogan *et al.* 2008; Schulte *et al.* 1996; Stancato *et al.* 1997) and through microRNAs (http://microrna.sanger.ac.uk/). The existence of four Ras (H-RAS, N-RAS, K-RASa, K-RASb), three RAF, two MEK (MEK1 and MEK2) and two ERK (ERK1 and ERK2) isoforms introduces additional complexity. Therefore, the signaling output must be strongly regulated by the assembly of different complexes in a temporal and spatial fashion (Kyriakis 2007). To enable the formation of the right complex for the respective stimulation, components of the RAF cascade associate with different scaffold proteins, such as KSR (kinase suppressor of Ras), CNK (connector enhancer of KSR), MP-1 (MEK-Partner 1) and SUR-8 (suppressor of Ras-8) to form a functional cascade (Claperon and Therrien 2007; Morrison and Davis 2003). MP1, for instance, selectively interacts with MEK1 and ERK1 and facilitates their activation, but it does not to bind to MEK2 and ERK2 (Schaeffer *et al.* 1998). The pseudokinase KSR shares high homology to RAF kinases and associates with the same binding partners as RAF, like 14-3-3, Hsp90 and Cdc37 (Claperon and Therrien 2007), which facilitates the interaction to each other. Furthermore, mouse KSR was shown to interact constitutively with MEK and in a Ras dependent manner with RAF and ERK. KSR localizes in the cytoplasm of quiescent cells (Morrison 2001) and becomes recruited to the cell membrane upon specific dephosphorylation of an internal 14-3-3 binding site (Morrison 2001; Muller *et al.* 2001). These results demonstrate that these scaffold proteins not only localize and stabilize the Ras-activated RAF-MEK-ERK module to the plasma membrane but also coordinate interactions between the individual components of the pathway and regulate their activation (Raabe and Rapp 2002). By restricting interactions between the different components of the cascade, scaffold proteins increase the efficiency of signaling and maintain fidelity (Raabe and Rapp 2002). So, although the precise molecular mechanisms leading to activation of the RAF-MEK-ERK module are still not completely understood, compartmentalization of signaling complexes by scaffold proteins might be one way to ensure proper cellular responses to different extracellular stimuli (Raabe and Rapp 2002).

Important targets of the RAF pathway that were described to be highly involved in apoptosis control are proteins of the Bcl-2 family. The RAF-ERK module may directly phosphorylate the anti-apoptotic protein Bcl-2 and thereby enhance its apoptosis suppressing properties (Deng *et al.* 2000). Moreover pro-apoptotic Bcl-2 proteins, like BIM and BAD are targets of the RAF pathway. The phosphorylation of these proteins results in an inactivation of their pro-apoptotic properties. The phosphorylation of BIM can lead to the degradation of the protein (Ewings *et al.* 2007; Ley *et al.* 2003; Luciano *et al.* 2003). The phosphorylation of BAD results in its sequestration into the cytosol (Scheid *et al.* 1999; Zha *et al.* 1996). Analogous to BIM, phosphorylation via C-RAF can also promote BAD polyubiquitylation resulting in an increase of the turn-over of this protein through proteasomal degradation (Fueller *et al.* 2008). Recently, our group showed that BAD binds to lipids with high affinities, predominantly to negatively charged phospholipids and cholesterol-rich liposomes (Hekman *et al.* 2006). These data led to a model in which BAD shuttles in a phosphorylation-dependent manner between mitochondria and other membranes and where 14-3-3 is a key regulator of this relocation. Furthermore, we identified that in its phosphorylated, non-apoptotic state, BAD forms ion conductive channels in planar bilayer membranes (Polzien *et al.* 2009) (Fig. 19). These observations indicate that beside its pro-apoptotic activity, BAD exhibits a vital function under survival conditions.

3.2.2. Material and Methods

Plasmid construction – Human BAD (hBAD) cDNA (kind gift of John Reed, La Jolla, California) was cloned into pGEX-4T-1 (Pharmacia). To generate N-terminal His-tagged hBAD, the cDNA was released by *EcoRI*/*NotI* from pGEX-4T-1 and ligated in the *EcoRI*/*NotI* sites of pFastBac H1 (Invitrogen).

Purification of human BAD protein – For purification of phosphorylated His-hBAD, Sf9 cells were infected with baculoviruses at the multiplicity of infection of 5 and incubated for 48 hr at 27°C. The Sf9 cell pellet (2×10^8 cells) was lysed in 10 ml lysis buffer containing 50 mM sodium phosphate, pH 8.0, 150 mM NaCl, 10 mM Na-pyrophosphate, 25 mM ß-glycerophosphate, 25 mM NaF, 10% glycerol, 0.5% NP-40 and a cocktail of standard proteinase inhibitors for 30 min with gentle rotation at 4°C. The lysate was centrifuged at 27000 g for 30 min at 4°C. The supernatant (10 ml) containing His-hBAD was incubated with 0.5 ml Ni^{2+}-nitrilotriacetic acidagarose for 2 hr at 4°C with rotation. After incubation, the beads were washed 3 times with lysis buffer containing 0.2% NP-40, 300 mM NaCl and 20 mM imidazole and hBAD was eluted with an imidazole step gradient.

Lipid bilayer experiments – The channel forming by human BAD was assessed in artificial lipid bilayer membranes using a teflon chamber as described previously (Benz 1994; Benz *et al.* 1992). Briefly, to form the membranes a 1% (w/v) solution of diphytanoyl phosphatidylcholine (DiphPC) (Avanti Polar Lipids) in n-decane was used. Purified hBAD was applied on both sides of the DiphPC

membrane in 1 M KCl buffer and single channel formation was measured after application of a fixed membrane potential. The single channel conductances *G* were expressed as conductance steps in the presence of the corresponding nonelectrolyte at a concentration of 20% (w/v) in the bathing solution.

3.2.3. Results and Discussion

RAF kinases localize to mitochondria and control mitochondrial associated processes – In collaboration with the Reed lab, we detected for the first time a RAF-isoform at the mitochondrial level (Wang *et al.* 1996) (Fig. 19). In this study, we showed that a stably expressed active C-RAF localizes to mitochondria upon overexpression of the anti-apoptotic protein Bcl-2. These observations provoked other studies that confirmed the localization of C-RAF at mitochondria in cancer and normal tissues (Alavi *et al.* 2003; Cornelis *et al.* 2005; Majewski *et al.* 1999; Peruzzi *et al.* 2001; Salomoni *et al.* 1998). However, the underlying mechanisms of the mitochondrial recruitment of RAF kinases are still not entirely resolved. Some reports suggest phosphorylation of one residue on C-RAF, Ser-338, via the p21-activated kinase (PAK), as a prerequisite for the localization to mitochondria and conferring a protective effect to apoptosis (Jin *et al.* 2005). Other studies suggest this phosphorylation as an activation marker (Mason *et al.* 1999) and not involved in mitochondrial binding (Galmiche *et al.* 2008). There is also evidence that C-RAF recognizes some components of the mitochondrial membrane that promote the recruitment to mitochondria as C-RAF interacts with certain lipids (Hekman *et al.* 2002) and proteins (Wang *et al.* 1996). RAF-binding partners that are established on the mitochondrial level, are prohibitin (Rajalingam *et al.* 2005), the voltage dependent anion channel (VDAC) (Le Mellay *et al.* 2002), members of the small Ras GTPases (Bivona *et al.* 2006; Wolfman *et al.* 2006) and other molecules involved in signaling processes like Grb10 (Nantel *et al.* 1999). Beside C- RAF, there are also indications that B-RAF might be present at the mitochondrial level (Gotz *et al.* 2005; Wiese *et al.* 2001). B-RAF might be localized to mitochondria through recruitment by C-RAF, since heterodimer formation is a common feature for RAF kinases (Garnett *et al.* 2005; Rushworth *et al.* 2006; Weber *et al.* 2001). Concerning A-RAF a controversial study describes that, via interacting with the transport machinery of mitochondria, A-RAF could localize inside this organelle (Yuryev *et al.* 2000).

Recently, our group identified that the local activation of C-RAF on mitochondria is sufficient to initiate an intense mitochondrial remodeling, creating small spherical elements clustered around the nucleus (Galmiche *et al.* 2008). The reason could be that C-RAF intervenes with the mitochondrial fission and fusion, two highly regulated processes (Chan 2006; Lackner *et al.* 2009). The clustering of small units of cellular compartments in the cell center, as it was seen for mitochondria upon C-RAF activation, is also observed in the process of cell division to ensure the appropriate sequestration and inheritance of organelles. Components of the RAF pathway are involved in this regulation for other organelles, like the Golgi-apparatus and endosomes (Shaul and Seger 2006; Teis *et al.* 2006). Therefore, the effect of active C-RAF on mitochondria could establish a comparable regulation.

Changes in mitochondrial distribution display well-known features observed in various cancer cells (Alirol and Martinou 2006). Keeping in mind the fact that cancer cells have a reduced susceptibility to apoptosis the mitochondrial remodeling might represent a further mode in establishing and/or maintaining cancerous properties.

A variety of key events in apoptosis take place at the mitochondrial level (Green and Reed 1998). As mentioned before, C-RAF exhibits intrinsic binding to mitochondria (Galmiche *et al.* 2008). These results are in agreement with the observation that the RAF cascade is one of the signaling pathways that inactivate the apoptotic machinery upon growth factor stimulation (Cleveland *et al.* 1994; Letai 2006). The constitutive activation of the RAF-cascade increases the survival rate, even in the absence of growth factors (Cleveland *et al.* 1994; von Gise *et al.* 2001). The importance of the RAF pathway in the mediation of pro-survival and anti-apoptotic effects was also demonstrated in knock-out

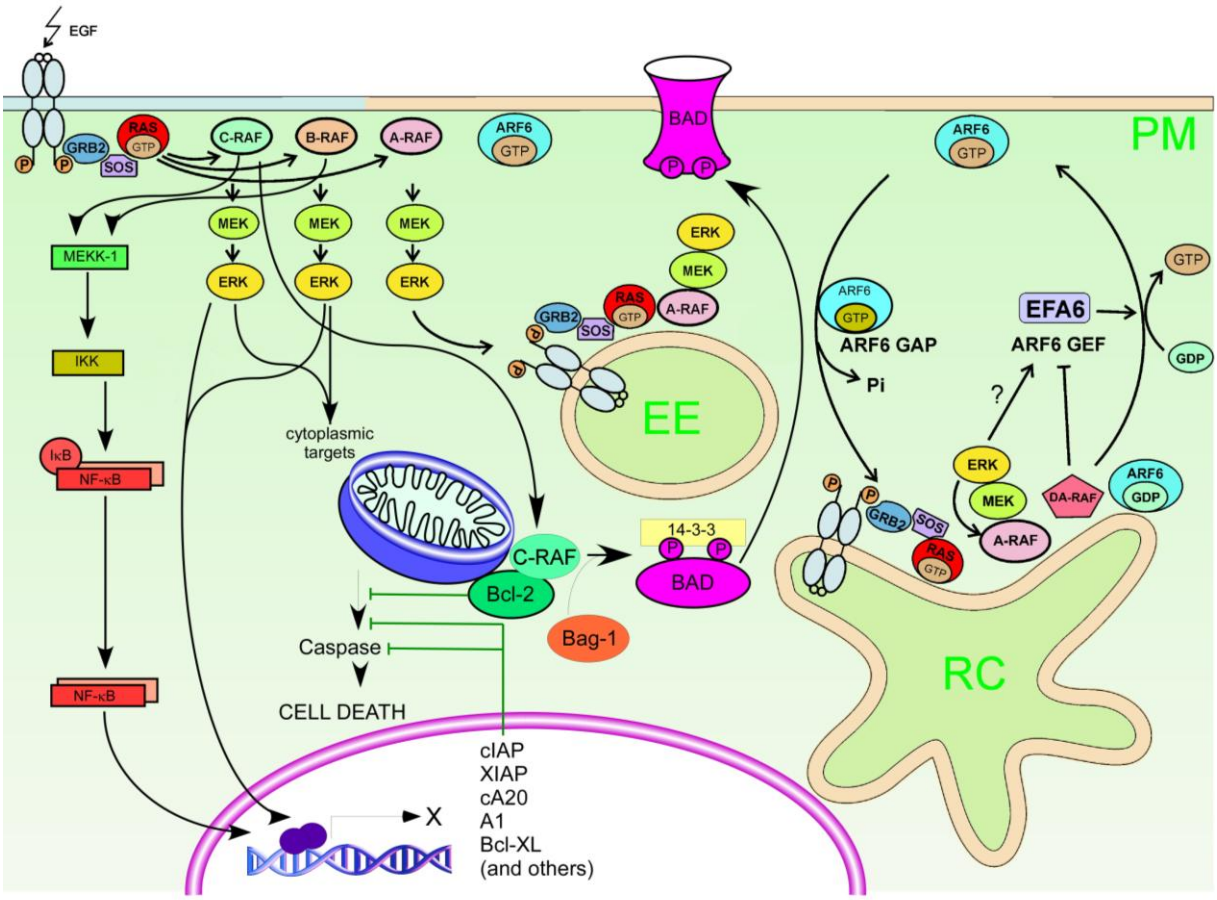

Figure 19: The RAF isoforms display individual localizations and specific functions.
The activation of a receptor tyrosine kinase (here EGF receptor) results in RAS-mediated activation of RAF kinases. A-RAF signals on endosomes and leads to ARF6 activation. Endosome signaling is inhibited by a negative feedback loop through DA-RAF witch blocks ERK activation in this compartment. B- and C-RAF target substrates at various localizations including cytoplasm and mitochondria and provoke cell growth, differentiation, proliferation and survival by multiple mechanisms. These mechanisms include direct activation or neutralization of apoptosis related proteins and transcriptional control of a number of genes. See the main text for details. EE, early endosomes; RC, recycling compartment; PM, plasma membrane ((Nekhoroshkova *et al.* 2009), highly modified).

experiments since knock-out mice exhibit an enhanced apoptosis rate as described in a previous chapter. C-RAF was shown to modulate cell survival on several levels (Chen *et al.* 2001; O'Neill *et al.* 2004; Piazzolla *et al.* 2005; Wang *et al.* 1998). The mechanisms include a direct regulation of the proteins that are important for apoptosis as well as the transcriptional regulation of such proteins (Fig. 19). As mentioned above, the RAF pathway also targets proteins of the Bcl-2 family that control apoptosis via several mechanisms. BAD is a member of that family that was shown to be targeted directly by RAF kinases (Polzien *et al.* 2009).

Furthermore, in the publication in hand we present new insights of BAD regulation that indicate opposed functions of BAD in dependence of its phosphorylation state. We will go into more detail on this topic in a later chapter.

The RAF cascade also intervenes with the progression of apoptosis downstream of mitochondria. ERK-mediated phosphorylation of the initiator caspase-9 blocks its activity and thereby disrupts the execution of apoptosis (Allan *et al.* 2003). Furthermore, C-RAF does not only rely on its kinase activity to counteract apoptosis. Through its binding, C-RAF can modulate the activity of crucial apoptosis regulating kinases, like apoptosis stimulating kinase 1 (ASK1) (Wang *et al.* 2001) or the mammalian sterile20-like kinase (MST2) (O'Neill *et al.* 2004). Additionally, activation of the RAF cascade affects the transcriptional regulation of various genes (Fig. 19). The ERK kinase is able to shuttle inside the nucleus where it regulates several transcription factors directly by phosphorylation (Treisman 1996). Two important target transcription factor families are Ets and AP-1(Bruder *et al.* 1992). Thereby the RAF pathway suppresses apoptosis induction through the direct transcriptional regulation of pro- and anti-apoptotic proteins (Shinjyo *et al.* 2001; Townsend *et al.* 1998). Furthermore, through the activation of the kinase MEKK1, the RAF pathway can also activate NF-κB, another transcription factor central in cell survival and transformation (Baumann *et al.* 2000). Of importance, the RAF cascade transcriptionally regulates also members of the inhibitor of apoptosis proteins (IAP) (Gotz *et al.* 2005; Pahl 1999; Wang *et al.* 1998) (Fig. 19). The first discovered proteins of the IAP family are the baculovirus IAPs Cp-IAP and Op-IAP that were identified based on their ability to complement the cell death inhibitor p35 in mutant viruses and directly inhibit caspases of the host (Clem *et al.* 1991; Clem and Miller 1994; Crook *et al.* 1993). Afterwards a multitude of related proteins have been described in virtually all eukaryotes and it was shown that IAPs are able to inhibit the caspases of many organisms including nematodes, flies and mammals. IAPs can be considered as major modulator of caspase activity which target the enzymes directly in a selective manner. The human IAPs, XIAP, cIAP-1, cIAP-2 and survivin, for example, have been shown to bind and potently inhibit selectively caspases 3,7 and 9 (Deveraux *et al.* 1997; Roy *et al.* 1997), but not caspases 6, 10 or 8. Interestingly, IAP family proteins also contribute to signal transduction (Chu *et al.* 1997; Wang *et al.* 1998). Furthermore, we identified that XIAP binds strongly to C-RAF and promotes the ubiquitylation of C-RAF (Dogan *et al.* 2008). In addition, XIAP

or c-IAP-1/2 knockdown cells show enhanced cell migration in a C-RAF-dependent manner (for review see Rajalingam *et al.*, in prep.)

Further targets of the RAF pathway are polycomb group proteins (Voncken *et al.* 2005) and histones (Dyson *et al.* 2005). This indicates the contribution of RAF kinases in the epigenetic control of transcription. In summary, RAF kinases have been shown to localize on mitochondria and intensely interfere with various mitochondrial associated mechanisms including the subcellular distribution of this organelle and apoptosis control.

RAF kinases localize to the cytoskeleton and interfere with cellular metabolism and reorganization – We discussed in a previous chapter that C-RAF directly provokes movement of mitochondria. Intracellular transport of mitochondria and other cellular organelles uses the cytoskeleton as "railroads" (Boldogh and Pon 2007; Frederick and Shaw 2007). Indeed, C-RAF was shown to interfere with the organization of the cytoskeleton (Kerkhoff *et al.* 2002; Khosravi-Far *et al.* 1995; Lovric *et al.* 1998; Mavria *et al.* 2006; Prendergast *et al.* 1995; Qiu *et al.* 1995; Qiu *et al.* 1995; Roux *et al.* 1997).

A cytosolic/cytoskeletal localization of RAF kinases is also a prerequisite for the interaction with cytosolic proteins. A-RAF was shown to bind the cytosolic glycolytic isoenzyme M2-PK thereby increasing its activity (Le Mellay *et al.* 2002). This is in accordance with the finding that introduction of an activated version of C-RAF into NIH3T3 cells is sufficient to increase the content of glycolytic metabolites (Le Mellay *et al.* 2002). So the RAF pathway also affects the metabolism of cells. In cancer, cells often exhibit a modified metabolic state, which is commonly called the "Warburg effect". These cells use glycolysis as major energy supply route rather than the oxidative phosphorylation of mitochondria even in the presence of O_2 (Gottlieb and Tomlinson 2005). Therefore the involvement of RAF kinases in metabolic processes could provide an additional step to facilitate cell transformation.

In the last years it emerged that the actin organization and the intracellular transport are functionally linked. One example is the involvement of the Spir actin organizer in vesicle transport processes (Kerkhoff *et al.* 2001). Therefore it is not surprising, that RAF kinases also play a role in endocytosis control as described in the next chapter.

A-RAF localizes to endosomes and highly interferes with the execution of endocytosis – Endocytosis is a process essential for many aspects of cellular life, including receptor internalization and recycling. Recently, our group identified a role of A-RAF regulated ERK signaling in membrane trafficking (Nekhoroshkova *et al.* 2009). In this study, we ascertained A-RAF to accumulate at punctate cortical structures that are known to contain proteins associated with early steps of endocytosis (Nekhoroshkova *et al.* 2009; Pelkmans *et al.* 2005). Additionally, a C-terminally truncated version of A-RAF, AR149, that is nearly identical with inhibitory A-RAF splice variant DA-RAF2 (Yokoyama *et al.* 2007) was discovered in this work (Nekhoroshkova *et al.* 2009;

Yokoyama *et al.* 2007). AR149 was demonstrated to be targeted to tubular endosomes where it colocalizes with the endocytosis regulator ARF6. Furthermore, the results obtained suggest that endocytosis regulation involves feedback regulation by DA-RAF2. Additionally, this work shows that activity of A-RAF kinase in the mitogenic cascade on endosomes is a prerequisite for the shuttling of Tfn-positive endosomes to the pericentriolar region (Nekhoroshkova *et al.* 2009). A model of the role of A-RAF in endocytosis control in illustrated in Fig. 19 Previous reports demonstrated that A-RAF participates in regulation of caveolae/raft-mediated endocytosis by stabilizing the caveolar coat (Pelkmans *et al.* 2005; Pelkmans and Zerial 2005). These results are reinforced by several reports that demonstrate crosstalk between endocytosis and signal transduction (Polo and Di Fiore 2006; Rapp *et al.* 2003) like the finding that scaffold protein KSR1 localizes to endosomes as well (Robertson *et al.* 2006).

RAF target BAD forms geometric pores at the plasma membrane upon phosphorylation – BAD is a pro-apoptotic Bcl-2 family protein that is regulated by phosphorylation in response to survival factors. The Bcl-2 family of proteins is divided into subfamilies, including proteins which either inhibit or promote programmed cell death (Adams and Cory 2001; Gross *et al.* 1999). BAD belongs to a sub-class of pro-apoptotic Bcl-2 family proteins, the BH3-only proteins, which share sequence homology only at their BH3 domain (Youle and Strasser 2008). C-RAF was the first reported BAD kinase (Wang *et al.* 1996), a finding that provided first evidence for a link between signal transduction and the intrinsic apoptosis machinery. There is a growing body of evidence for a direct participation of RAF kinases in the regulation of apoptosis via BAD (Jin *et al.* 2005; Panka *et al.* 2006; Polzien *et al.* 2009). Non-phosphorylated BAD associates with Bcl-2/Bcl-XL and localizes to the outer mitochondrial membrane. Phosphorylation of murine BAD at Ser-155 (Ser-118 of human BAD) disrupts the association with Bcl-2 or Bcl-XL and promotes cell survival (Datta *et al.* 2000). Whereas the current view suggests that BAD exerts its pro-apoptotic function solely by displacing and thereby activating "activator" BH3-only proteins it has to be considered that phosphorylated BAD may actively contribute to survival preservation in cells. Recently, our group identified that human BAD forms channels in planar bilayer membranes in vitro (Polzien *et al.* 2009). BAD forms these pores only in its phosphorylated and for 14-3-3 proteins accessible form. In this state, BAD is located at cholesterol-rich domains (rafts) of the plasma membrane (Hekman *et al.* 2006). We identified that human BAD contains at least nine phosphorylation sites (Polzien *et al.* 2009). So whether phosphorylation of BAD leads to proteasomal degradation of BAD (Fueller *et al.* 2008) or gives the protein a second life as a pore depends presumably on the phosphorylation signature of BAD. Here we show that these BAD pores are not only permeable for ions but also for non-charged molecules. Furthermore, we identified that BAD pores posses a funnel-shaped geometry with a water lumen diameter of 1 nm which can conduct substances up to a molecular weight of 200 Da.

To evaluate the inner structure of the water lumen of BAD channels we used a method based on the determination of channel filling by different nonelectrolyte molecules (NE) (Krasilnikov *et al.* 1998). NEs can give results concerning the size of the ion channel entrance as well as the presence and apparent localization of structural constrictions inside an ion channel water lumen. This method has been used in various studies to determine the size and geometry of proteinous single ion channels (Krasilnikov *et al.* 1998; Nablo *et al.* 2008).

According to our previously published data (Polzien *et al.* 2009), the conductance of the largest channel formed by human BAD is 3.75 nS, in symmetrical 1 M KCl (Table 4). We measured the conductance of the BAD channel in the presence of different NEs. The NEs applied ranging from the highly permeating ethylene glycol up to impermeate NE molecules with large hydrodynamic radii (Table 4 and Fig. 20A). In the presence of different small NEs the single channel conductances decrease to a different extend, as evidenced in Table 4 and Fig. 20A. By contrast, large impermeate NEs like PEG3000 produces no effect on the single channel conductance at all (Table 4, Fig. 20A). For a better understanding of the measurements one can use the filling (*F*) witch is given by:

$$F = [(g_0 - g_i)/g_i]/[\chi_0 - \chi_i)/\chi_i] \qquad (1)$$

Where g_0 is the single channel conductance in the presence of an impermeate NE or the single channel conductance in a solution without NEs; gi is the single channel conductance in the presence of a solution containing 20% (w/v) of an NE with access to the channel interior; χ_0 is the conductivity of the solution without NEs or the conductivity of the virtual volume free of NEs in a solution with NEs; and χ_i is the conductivity of the solution containing 20% (w/v) of a given NE (for further information see (Krasilnikov *et al.* 1998).

Table 4: Single-channel conductances of human BAD in the presence of different nonelectrolytes in the bath solution. *Mr* = molecular mass; *r* = hydrodynamic radius; χ= conductivity of the solution, 24,5°C for measurements of χ

Nonelectrolyte	***Mr* (*g/mol*)**	***r* (*nm*)**	***G* (*pS*)**	**χ (*mS x cm*$^{-1}$)**
none	none	0	3750	110,3
Ethylene glycol	62	0,26	3500	57,2
Glycerol	92	0,31	3250	49,1
PEG200	200	0,5	3000	46,1
PEG300	300	0,6	2500	45,5
PEG400	400	0,7	2250	46,4
PEG600	600	0,8	1750	54,1
PEG1000	1000	0,94	1250	49,5
PEG2000	2000	1,22	1500	62,4

PEG3000	3000	1,44	3750	48,9
PEG4000	4000	1,92	3750	61,39

Assuming the filling of the channel by the two smallest NEs, namely ethylene glycol and glycerol, is close to the maximum possible level, allowing calculation of the filling in terms of percentage (*F%*) as follows:

$$F\% = 2F_i /(F_1 + F_2) \text{ x } 100\% \quad (2)$$

where F_i is the filling in the presence of a given NE and F_1 and F_2 represent filling in the presence of ethylene glycol and glycerol in the bathing solutions, respectively.

The geometrical parameters of the BAD channel can be derived from out data by comparing two possible structures for an ion channel pore, cylindrical and funnel-shaped. Then for an ideal cylindrical structure all permeant NEs should fill the channel to the same maximum extent. This fact will hold up to the point where the radius of a particular NE becomes equal to the radius of the channel. After this point, we expect a sharp decrease in the extent of filling. Hence for an ideal cylindrical structure the NE used in this study should behave as two distinct groups; one which will fill the channel completely and another that will not fill the channel at all. By the same reasoning, for a funnel-like structure we expect to find several NEs able to completely fill the channel, given that the hydrodynamic sizes of the molecules are smaller than the size of the narrowest part of the channel (Fig. 20, B and C; hydrodynamic radii ≤ 0,5 nm). On the other hand, when the hydrodynamic size of the NE molecules becomes larger than the size of the largest entrance of the channel, the NEs will not fill the channel at all (Fig. 20, B and C; hydrodynamic radii ≥ 1,44 nm) and intermediate-sized NE will fill the channel to an extent inversely related to their sizes (Fig. 20, B and C; hydrodynamic radii = 0,5 - 1,44 nm) (for more details see (Krasilnikov *et al.* 1998)). The theoretical considerations for a funnel-shaped channel agree with the results obtained for the BAD pore indicating that the BAD channel has a funnel-like structure as illustrated in Fig. 20 C.

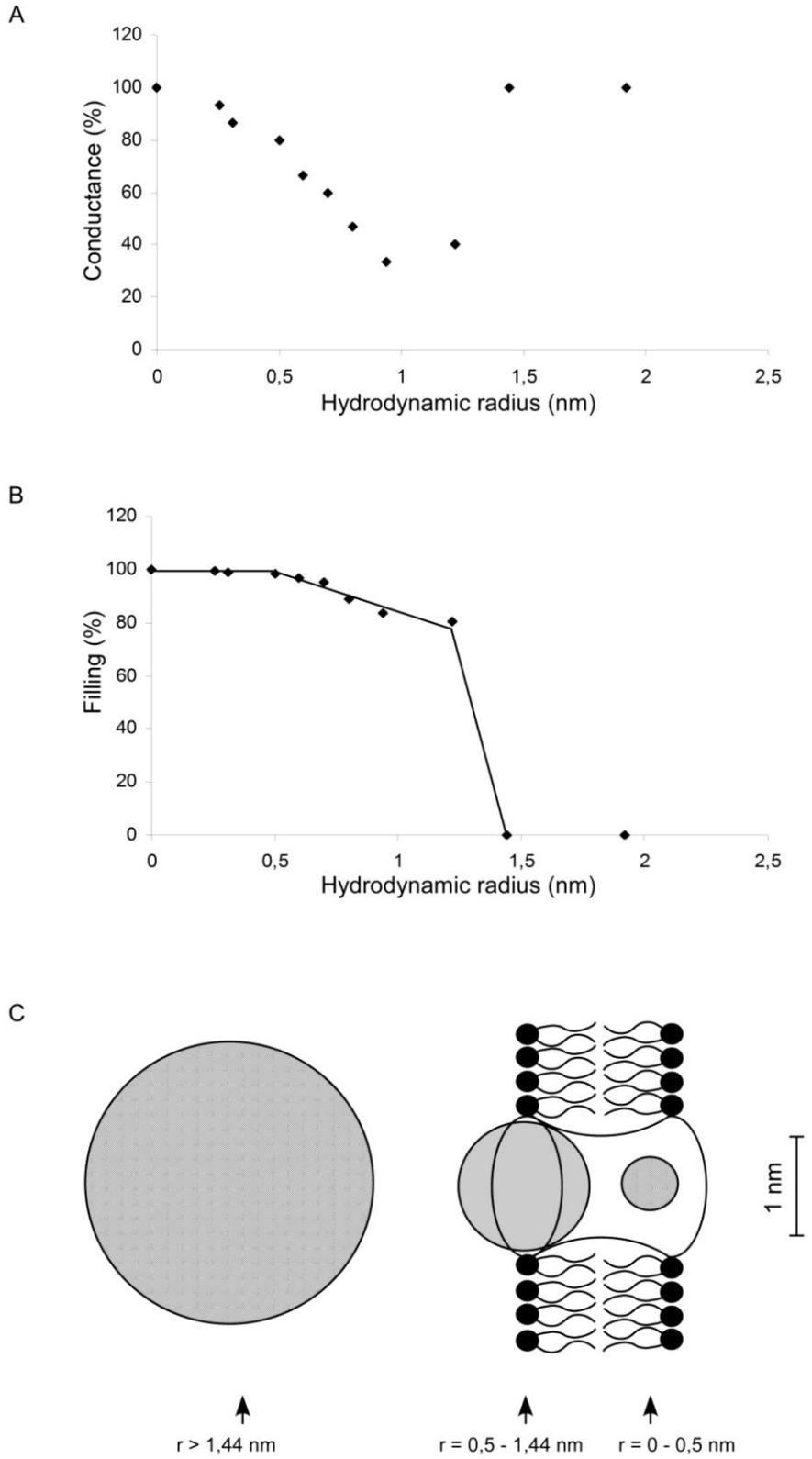

Figure 20: Determination of the geometry of BAD channels with the aid of nonelectrolytes (NEs).
Single-channel conductances of human BAD protein were recorded in the presence of different sized NEs. The aqueous phase contained 20% of the respective NE in 1 M KCl. The temperature was 20°C and the applied voltage 20 mV. Single channel conductance (A) and channel filling (B) depend of the hydrodynamic radii of the nonelectrolytes added to both sides of the bilayer. C, Model of the geometry of BAD channels. See the main text for details. Hydrodynamic radii of NEs were taken from Table 4.

What could be the physiological role of BAD pores at the plasma membrane? The finding that BAD channels conduct ions as well as non-charged molecules entails a broad spectrum of potential functions. For instance, BAD pores could act as ion channels and contribute to the regulation of various cellular processes. Ca^{2+} for instance, is regulating the mitogenic cascade at multiple positions (Ren *et al.* 2008). The BAD pores conduct molecules up to 200 Da, so they are permeable for many signaling molecules beside ions like nitric oxide, glutamate, γ-aminobutyric acid (GABA) and histamine and may contribute to positive feedback loops. In its pore forming phosphorylation status, BAD was found to be located at rafts of the plasma membrane (Hekman *et al.* 2006). Rafts and caveolae (which can be considered as a subclass of rafts (Anderson 1998; Smart *et al.* 1999)) play an important role for the interactions of a number of signaling molecules. Several signaling associated proteins such as heterotrimeric and small G-proteins, Src kinases, eNOS, Shc, Nck MAPK and RAF kinases have been found to be attached to the rafts/caveolae microdomains (Hekman *et al.* 2002). So it is feasible that BAD pores and RAF kinases cooperate in signaling processes in rafts of the plasma membrane. The close proximity between BAD and RAF kinases at the plasma membrane might also be a hint for a contribution of BAD pores in the mechanism of endocytosis. Indeed, BAD has been shown to play a role in cellular membrane trafficking. Beside its contribution to glucose metabolism, the regulation of autophagy displays a further non-apoptotic function of BAD (Danial *et al.* 2003; Maiuri *et al.* 2007).

Another aspect to discuss in this respect is the observation that phosphorylation of Ser-170 of murine BAD (corresponding to Ser-134 of human BAD) has a proliferative effect under non-starvation conditions (Dramsi *et al.* 2002). To express human BAD protein, we used Sf9 insect cells. We recently published that Sf9 cells phosphorylate human BAD at multiple sites, including Ser-134 (Polzien *et al.* 2009). Therefore it is also feasible, that the BAD pores contribute to cell cycle progression and thereby facilitate oncogenic transformation. Keeping in mind that BAD is a relatively weak inducer of apoptosis one should consider if the primary function of BAD is associated with non-apoptotic processes. Although the function of BAD channels is incompletely understood at this point, we suggest that BAD phosphorylation by the survival kinase C-RAF switches its function from Bcl-2/Bcl-X_L blocker to a transformation facilitating pore.

3.2.4. Acknowledgements

We thank Elke Maier for excellent technical assistance.

3.3. Pore-Forming Activity of BAD is Regulated by Specific Phosphorylation and Structural Transitions of the C-Terminal Part

Background: **BAD protein (Bcl-2 antagonist of cell death) belongs to the BH3-only subfamily of proapoptotic proteins and is proposed to function as the sentinel of the cellular health status. Physiological activity of BAD is regulated by phosphorylation, association with 14-3-3 proteins, binding to membrane lipids and pore-formation. Since the functional role of the BAD C-terminal part has not been considered so far, we have investigated here the interplay of the structure and function of this region.**

Methods: **The structure of the regulatory C-terminal part of human BAD was analyzed by CD spectroscopy. The channel forming activity of full-length BAD and BAD peptides was carried out by lipid bilayer measurements. Interactions between proteins and peptides were monitored by the surface plasmon resonance technique.**

Results: **In aqueous solution, C-terminal part of BAD exhibits a well-ordered structure and stable conformation. In a lipid environment, the helical propensity considerably increases. The interaction of the C-terminal segment of BAD with the isolated BH3 domain results in the formation of permanently open pores whereby the phosphorylation of serine 118 within the BH3 domain is necessary for effective pore-formation. In contrast, phosphorylation of serine 99 in combination with 14-3-3 association suppresses formation of channels.**

Conclusions: **C-terminal part of BAD controls BAD function by structural transitions, lipid binding and phosphorylation. Conformational changes of this region upon membrane interaction in conjunction with phosphorylation of the BH3 domain suggest a novel mechanism for regulation of BAD.**

General Significance: **Multiple signaling pathways mediate inhibition and activation of cell death via BAD.**

3.3.1. Introduction

Apoptosis or programmed cell death is an evolutionary widely conserved suicidal process by which multicellular organisms remove or replace undesirable cells and it is essential for normal embryonic development. This form of coordinated cell death is widely observed in nature and is not only critical for proper execution of developmental processes, immune responses, and tissue homeostasis but disruptions of this process also have far-reaching effects causing diseases such as tumor development and autoimmune disorders (Danial and Korsmeyer 2004; Reed *et al.* 2004; Wang and Youle 2009).

Mitochondria constitute a convergence point in apoptosis progression. Proteins of the Bcl-2 family

are crucial regulators of the onset of apoptosis at the level of mitochondria (Wang and Youle 2009; Youle and Strasser 2008). There, apoptosis proceeds through a complex interplay between anti- and pro-apoptotic proteins of Bcl-2 proteins. However, the exact modes and the mechanisms of the pathways involved in this process are still not completely understood (Youle and Strasser 2008). In addition, several proteins of the Bcl-2 family contribute to the regulation of various other physiological processes beyond regulation of apoptosis, such as autophagy, mitochondrial respiration and glucose metabolism (Danial 2008). All Bcl-2 proteins contain at least one of the four so-called Bcl-2 homology domains: BH1-BH4. Several Bcl-2 family proteins contain a carboxy-terminal membrane anchor that may be involved in their binding to plasma- or different intracellular membranes. On the basis of various structural and functional characteristics, the Bcl-2 family of proteins is divided into three subfamilies, including proteins which either inhibit (e.g. Bcl-2, Bcl-X_L or Bcl-w) or promote programmed cell death (e.g. Bax, Bak or Bok) (Adams and Cory 1998; Gross *et al.* 1999; Youle and Strasser 2008).

A second sub-class of pro-apoptotic Bcl-2 family members, the BH3-only proteins, comprises BAD, Bik, Bmf, Hrk, Noxa, tBid, Bim and Puma (Youle and Strasser 2008). BH3-only proteins share sequence homology only at the BH3 domain. The amphipathic helix formed by the BH3 domain (and flanking residues) associates with a hydrophobic groove of several members of the Bcl-2 family proteins (Fesik 2000; Petros *et al.* 2004).

BAD (Bcl-2 associated death promoter, Bcl-2 antagonist of cell death) was originally described to promote apoptosis by forming heterodimers with the pro-survival proteins Bcl-2 and Bcl-X_L, thus, preventing them from binding to Bax (Yang *et al.* 1995). Phosphorylation plays a crucial role in regulation of BAD function and modulates the association with other proteins as well as its subcellular localization. In the non-phosphorylated state BAD associates with Bcl-2 or Bcl-X_L via its BH3 domain and localizes to mitochondria, representing the active state of BAD. Phosphorylation of specific serine residues, Ser-112 and Ser-136 of murine BAD (mBAD) or the corresponding phosphorylation sites Ser-75 and Ser-99 of human BAD (hBAD), results in association with 14-3-3 proteins and subsequent relocation of BAD (Hekman *et al.* 2006; Zha *et al.* 1996). Supporting data of Ayllon *et al*. (Ayllon *et al.* 2002) who showed that BAD segregation from the lipid rafts at the plasma membrane is implicated in the regulation of apoptosis, we provided evidence that the BAD/14-3-3-complex possesses high affinity for cholesterol-rich membranes (lipid rafts) indicating a 14-3-3 driven shuttling of BAD between cholesterol-rich and mitochondrial membranes (Hekman *et al.* 2006). Phosphorylation of mBAD at Ser-155 (Ser-118 of hBAD) within its BH3-domain disrupts the association with Bcl-2 or Bcl-X_L promoting cell survival (Datta *et al.* 2000). Therefore, the phosphorylation status of BAD at these serine residues reflects a checkpoint for cell death or survival.

Several members of the Bcl-2 family were shown to form pores in lipid bilayers (Antignani and Youle 2006; Antonsson *et al.* 1997; Basanez *et al.* 1999; Kuwana *et al.* 2002; Minn *et al.* 1997;

Schendel *et al.* 1999; Schendel *et al.* 1997; Schlesinger *et al.* 1997; Zamzami and Kroemer 2003). However, it has not been clarified yet whether this pore-formation is an apoptosis- or survival-associated event, since this process was observed for both pro- and anti-apoptotic proteins. Keeping in mind that Bcl-2 proteins were demonstrated to be involved in the regulation of other events than apoptosis (Danial 2008), one cannot exclude a vital function for channel-formation. Recently, we identified BAD also as a pore-forming Bcl-2 protein (Polzien *et al.* 2009; Polzien *et al.* 2009). Its pore-forming capacity was dependent on phosphorylation and interaction with 14-3-3 proteins. Although the amino acid sequence of human BAD does not reveal a typical C-terminal transmembrane domain, we found that BAD binds to model membranes with high affinity, predominantly to negative charged phospholipids and cholesterol-rich membranes (Hekman *et al.* 2006). Two lipid binding domains (LBD1 and LBD2) with different binding preferences were identified, both located in the C-terminal part of the hBAD protein.

To elucidate the origin of the extraordinarily high affinity of the C-terminal part of BAD for membrane lipids we studied in this report the secondary structure of a 32-residue peptide corresponding to the C-terminus of the proapoptotic protein BAD and containing the lipid binding domain 2 (LBD2) (see Fig. 21). Our results obtained by use of CD spectroscopy indicate a well-defined structure for this region that undergoes structural transitions in the presence of artificial membranes. Importantly, the interaction of the C-terminal part of hBAD with the phosphorylated BH3 region proved to be sufficient for formation of open pores in lipid bilayers. Similar to full-length BAD association with 14-3-3 proteins suppresses channel formation. The binding studies performed with the C-terminus and peptides comprising the BH3 domain of hBAD allow us to conclude that an intermolecular bridge between these two moieties could be established.

Figure 21: Amino acid sequence of human BAD protein and peptides covering the BH3 domain, the 14-3-3 binding motif surrounding serine 99 and the C-terminal part of the protein.
The BH3 domain is shown in *blue* and the putative lipid binding domains (LBD1 and LBD2) are indicated by *yellow* and *green rectangles,* respectively. The sequences of Peptide1, -2 and -3 are depicted in *bold* and the regulatory serines 99 and 118 are highlighted in *magenta*.

3.3.2. Materials and Methods

Materials – Benzamidine, leupeptin, aprotinin, phenylmethylsulfonyl fluoride, Nonidet P-40, CHAPS and trifluoroethanol (TFE) were obtained from Sigma. Glutathione-Sepharose was purchased from Amersham Biosciences and Ni^{2+}-nitrilotriacetic acid-agarose was from Qiagen. The phospholipids (phosphatidylcholine, phosphatidylethanolamine, phosphatidylserine, phosphatidylinositol and cardiolipin), sphingomyelin and asolectin (soybean lipid extract) were from Sigma. All synthetic peptides used in this study were purified by high pressure liquid chromatography, and the sequences were verified by mass spectrometry analysis. The purity of the preparations was greater than 90%. The sequences of the peptides used are shown in Fig. 21.

DNA expression plasmids and purification of proteins – The purification of hBAD was carried out as published (Polzien *et al.* 2009). GST-hBAD, GST-hBADΔN131, GST-14-3-3 zeta and GST-Bcl-X_L were expressed in *E. coli* using pGEX-2T vector and purified by glutathione-Sepharose affinity chromatography as described (Hekman *et al.* 2006). Bcl-X_L was released by thrombin cleavage. His-tagged 14-3-3 zeta was purified from *E. coli* by Ni^{2+}-agarose (Quiagen) affinity chromatography according to the manufactur´s protocol.

Circular dichroism – CD analyses were conducted at 20°C using peptide solutions ranging in concentration from 0.1 to 0.2 mg/ml in the presence or absence of unilamellar asolectin vesicles (50 µM total lipid concentration) and/or 1 mM CHAPS. Some samples were measured in the presence of 30% TFE. Samples containing lipids were sonicated for 5 min prior to analysis. Each measurement was carried out in buffer containing 20 mM sodium phosphate, pH 8.0. CD spectra were registered in a 1 mm cuvette employing a J-810 spectropolarimeter (Jasco) at wavelength from 260 to 185 nm with a data pitch of 1 nm and a scan speed of 20 nm/min using standard sensitivity. The band width was 2 nm and response was 1 sec.

NMR spectroscopy – One dimensional ^{1}H-NMR spectra were recorded on a Bruker Avance 800 MHz NMR spectrometer using a sample temperature of 298 K. Peptides (concentration 0.5 - 2 mM) were dissolved in H_2O (pH 3) containing 10% D_2O for field/frequency lock.

Lipid bilayer (black lipid) experiments – The channel-forming ability of proteins was assessed in artificial lipid bilayer membranes using a teflon chamber as described previously (Benz 1994; Benz *et al.* 1992). Briefly, to form the membranes a 1% (w/v) solution of diphytanoylphosphatidylcholine (DiphPC) (Avanti Polar Lipids) in n-decane was used. Purified full-length hBAD as well as different hBAD peptides (phosphorylated and non-phosphorylated, 100 nM each) were added alone or combined to the KCl buffer in both compartments of the chamber and the single-channel conductance of the pores was measured after application of a fixed membrane potential. To test the effects of 14-3-3 proteins on pore-forming abilities of hBAD peptides, purified 14-3-3 proteins were incubated with peptides (1.4:1, mol/mol) for 30 min at room temperature prior to channel formation.

Preparation of model membranes and biosensor measurements – Unilamellar vesicles were prepared by extrusion method using a LiposoFast extrusion apparatus (Avestin Inc., Canada) as described (Hekman *et al.* 2006). To determine quantitatively the interaction between different BAD segments (in the presence of lipid vesicles mimicking mitochondrial membranes) and association of BAD with Bcl-X_L or 14-3-3 proteins (in solution) the surface plasmon resonance (SPR) technique was applied. The biosensor measurements were carried out either on BIAcore-X or BIAcore-J machines (Biacore AB, Uppsala, Sweden) at 25°C. The interactions of C-terminal BAD segment (GST-BADΔN131) with peptides corresponding to BH3 region in the presence of model membranes was monitored using Pioneer L1 sensor chip (Biacore AB, Uppsala, Sweden). To this end, the surface of the sensor chips was first cleaned with 20 mM CHAPS followed by the injection of mitochondrial liposomes consisting of 47% phosphatidylcholine, 28% phosphatidylethanolamine, 9% phosphatidylserine, 9% phosphatidylinositol and 7% cardiolipin (0.4 mM total lipid concentration) at a flow rate of 10 µl/ min in 10 mM Hepes, pH 7.4, 150 mM NaCl and 0.1 mM DTT which resulted in a deposition of approximately 6000 RU. Next, purified GST-BADΔN131 (200 nM) was applied to the captured liposomes at a flow rate of 10 µl/min resulting in approximately 2000 RU of bound protein. To detect the interaction of phosphorylated and non-phosphorylated forms of BH3 domain with the C-terminal part of BAD the corresponding peptides (1000 nM) were injected at a flow rate of 10 µl/min and the association-dissociation curves were monitored. At the end of the binding assay, the sensor chip surface was regenerated by injection of 20 mM CHAPS. Inhibition of GST-BAD binding to Bcl-X_L by BH3 peptides was monitored by use of CM5 biosensor chip as described (Hekman *et al.* 2006). Briefly, the biosensor chip CM5 was loaded with anti-GST antibody using covalent derivatization according to the manufacturer's instructions. Purified GST-tagged hBAD wt was immobilized in biosensor buffer (10 mM Hepes, pH 7.4, 150 mM NaCl, and 0.05% Nonidet P-40) at a flow rate of 10 µl/min resulting in approximately 800 RU of bound protein. Next, the purified analyte Bcl-X_L was injected in the presence and absence of BH3 peptides as indicated in Fig. 24. The evaluation of kinetic parameters was performed by non-linear fitting of binding data using the BiaEvaluation 2.1 software. The apparent association (k_a) and dissociation rates constant (k_d) were evaluated from the differential binding curves (Fc2-Fc1) assuming a A+B=AB association type for the protein-protein interaction. The affinity constant K_D was calculated from the equation $K_D = k_d/k_a$.

3.3.3. Results

To analyze structure and function of BAD regulatory C-terminal part bearing BH3 domain, lipid binding motifs and several other regulatory sites we used in this study CD spectroscopy, black lipid experiments and biosensor measurements.

Membrane interaction leads to redistribution of the secondary structure of the C-terminal part of human BAD – To study the secondary structure of the C-terminal part of hBAD protein by means of CD spectroscopy, synthetic peptides (referred here as Peptide1 and Peptide3, see also Fig. 21)

covering regulatory BH3 domain as well as lipid binding domains LBD1 and LBD2 (Hekman *et al.* 2006) were used. The synthetic peptides were either non-phosphorylated (Peptide1 and Peptide3) or selectively phosphorylated at position 118 (Peptide1-pS118). As previously reported, the secondary structure of hydrophobic regions can be stabilized by addition of model membranes (del Mar Martinez-Senac *et al.* 2001; del Mar Martinez-Senac *et al.* 2000; Martinez-Senac Mdel *et al.* 2002). Therefore, we carried out the CD measurements also in the presence of liposomes. To avoid putative interference of lipid vesicles with the assay we used also micellar lipid samples that were prepared by sonication of a mixture consisting of unilamellar liposomes and detergents exhibiting high CMC values such as CHAPS.

Table 5: Secondary structure of peptides corresponding to BH3 domain (Peptide1/Peptide1-pS118) and C-terminal part (Peptide3) of human BAD. CD spectra were obtained as described in Experimental Procedures. Measurements were performed in aqueous solution, with and without addition of liposomes and/or lipid-CHAPS micelles. The secondary structural elements were calculated using the Jasco secondary structure prediction software included with the spectropolarimeter.

Peptide	Liposomes	CHAPS	α-helix	β-sheet	turn	random
Peptide1	-	-	7.2%	47.9%	5.7%	39.2%
Peptide1	+	-	26.1%	8.1%	22.5%	43.4%
Peptide1	+	+	23.2%	30.3%	6.0%	40.6%
Peptide1-pS118	-	-	0.0%	51.9%	4.7%	43.4%
Peptide1-pS118	+	-	1.0%	51.7%	3.4%	43.9%
Peptide1-pS118	+	+	0.1%	49.0%	0.0%	50.9%
Peptide3	-	-	3.4%	47.6%	6.3%	42.7%
Peptide3	+	-	14.6%	36.4%	12.9%	36.1%
Peptide3	+	+	24.1%	21.5%	10.3%	44.1%

The CD data presented in Fig. 22 and Table 5 were acquired using a 0.2 mg/ml aqueous (buffer) solution of Peptide1, Peptide1-pS118 and Peptide3. To investigate the influence of lipid environment on the secondary structure measurements were taken also in the presence of liposomes or lipid-CHAPS micelles as indicated in Table 5. The results obtained by CD measurements indicate clearly a structural transition depending on immediate environment. The CD spectrum of the C-terminal peptide comprising the last 32 residues of hBAD revealed in aqueous solution a predominance of an extended β-sheet structure (while 48% of β-sheet structure was detected only 3% helical structure was present). Surprisingly, upon addition of liposomes or lipid-CHAPS micelles the extent of α-helical structure significantly increased (up to 24%) whereas the percentage of β-sheet structure dropped down to a value of 21%. Further addition of TFE did not change significantly the helix propensity (data not shown). Regarding CD spectra of phosphorylated (Peptide1-pS118) and non-phosphorylated Peptide1 we observed dual effects. In the case of non-phosphorylated BH3 peptide the formation of helical structures was strongly stimulated following the addition of model membranes (up to 26%). Unexpectedly, the phosphorylated BH3 peptide (Peptide1-pS118) behaved completely different. It did

not reveal any helical structures, even upon addition of lipid vesicles (Table 5). Instead, high proportion of β-sheet structure (approx. 50%) was detected in both aqueous and lipid environment (Fig. 22 and Table 5). Thus, taken together, results presented here illustrate that the introduction of phosphate molecule in position serine 118 within the BH3 domain dramatically changes the secondary structure of this segment. This result might explain the *in vivo* observation that BAD dissociates rapidly from its coupling partner Bcl-X_L upon phosphorylation of serine 118 (see also (Petros *et al.* 2000; Petros *et al.* 2004)). In addition, data presented here document that the C-terminus of hBAD possesses an ordered secondary β-structure in aqueous solution that adopts partly helical disposition upon interaction with lipid membranes. These observations are in agreement with our previous data (Hekman *et al.* 2006) and support the existence of distinct lipid binding domains within the C-terminal part of hBAD.

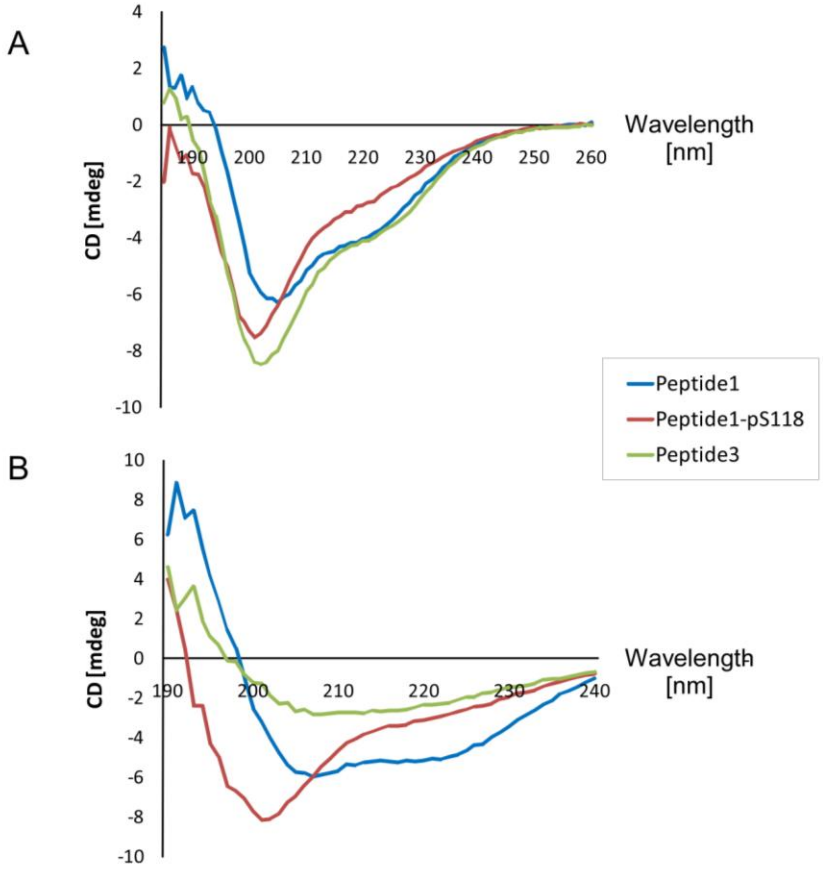

Figure 22: Circular dichroism spectra of peptides corresponding to BH3 domain (Peptide1/Peptide1-pS118) and C-terminal part (Peptide3) of human BAD.
Spectra were obtained as described in Experimental Procedures. A and B, CD spectra of Peptide1, Peptide1-pS118 and Peptide3 in aqueous solution without (A) and with addition of lipid-CHAPS micelles (B). All three peptides exhibited high structural stability in a temperature range between 20 and 95°C (data not shown). Each graph shows the average of 5 spectra without smoothing. [nm] means wavelength in nm.

C-terminal region of hBAD protein possesses per se and in conjunction with BH3 domain the ability of pore-formation within model membranes – Recently, we reported that hBAD forms channels in planar bilayer membranes (Polzien *et al.* 2009). As both lipid binding domains of hBAD (LBD1 and LBD2) are localized at the C-terminal region, we reasoned that this part of the protein may be responsible for channel formation. To test this issue, we investigated whether the Peptides1, -2 and -3 (see Fig. 21) are able to form pores in artificial lipid bilayers comparable to full-length hBAD (Fig. 23C). Toward this end, we performed the lipid bilayer measurements (black lipid) as described (Polzien *et al.* 2009). Surprisingly, following injection of the hBAD C-terminal peptide (Peptide3) into the teflon chambers (Benz 1994; Benz *et al.* 1992) current fluctuations representing channel openings were observed. The channels formed by this BAD fragment exhibited a flickering behavior between a closed and an open state (Fig. 23B). Injection of peptides covering the phosphorylated and non-phosphorylated BH3 domain provoked larger and more stable pores (Fig. 23A). The peptide representing the phosphorylated BH3 domain led to more solid channels than its non-phosphorylated counterpart, indicating different structural compositions of the formed pores (Fig. 23A, compare Peptide1-pS118 with Peptide1). More importantly, the combination of these peptides with the BAD C-terminus (Peptide3) led to opposite effects. While the combination of the Peptide3 and peptides with the phosphorylated BH3 domain resulted in large, fast accumulating and permanent open pores (Fig. 23A), the physical contact between the Peptide3 and peptides comprising the non-phosphorylated BH3 domain completely abolished the formation of channels (Fig 23A).

These results are in accordance with data obtained with the full-length hBAD protein, demonstrating that only the phosphorylated protein was able to form pores (Fig. 23C and (Polzien *et al.* 2009)). Thus, data presented here allow the conclusion that specific phosphorylation in position serine 118 within the BH3 domain contributes to intermolecular interactions facilitating channel formation. The opposite results using phosphorylated and non-phosphorylated BH3 domains are also supported by NMR spectroscopy. ^{1}H-NMR spectra of the BH3 peptides used for pore-formation experiments show changes in the amide and aromatic proton region upon phosphorylation of S118 (data not shown).

Figure 23 (right): Channel-forming activity of hBAD peptides comprising the BH3 domain (with and without the 14-3-3 binding motif surrounding serine 99) and the C-terminal segment of the protein.
Single-channel formation of the indicated peptides (see also Fig. 21) was monitored in a diphytanoylphosphatidylcholine membrane. The aqueous phase contained 1 M KCl. The temperature was 20°C, and the applied voltage was 20 mV. Pore formation of the hBAD Peptide1, -2 and -3 are shown in A, B and D. For direct comparison of the hBAD peptides with the full-length hBAD regarding their channel-forming ability also the effects monitored with full-length protein are also shown (C). Whereas combination of non-phosphorylated Peptide1 and Peptide2 with Peptide3 resulted in complete abolishment of pore-formation activity (A and D), phosphorylation of serine 118 led to the formation of fast accumulating, large and permanently open pores (A and D). Depending on phosphorylation in position serine 99, the treatment of the Peptide2 with 14-3-3 zeta caused total disruption of the pores (D), similar to effects monitored with full-length hBAD (C). Notably, the addition of 14-3-3 proteins to the combination of Peptide2-pS118 and Peptide3 did not influence the rapid formation of the pores (D). The vertical bars indicate conductance of 2 nanosiemens, the horizontal bars indicate time of 12 seconds. These measurements were repeated three times with the same results.

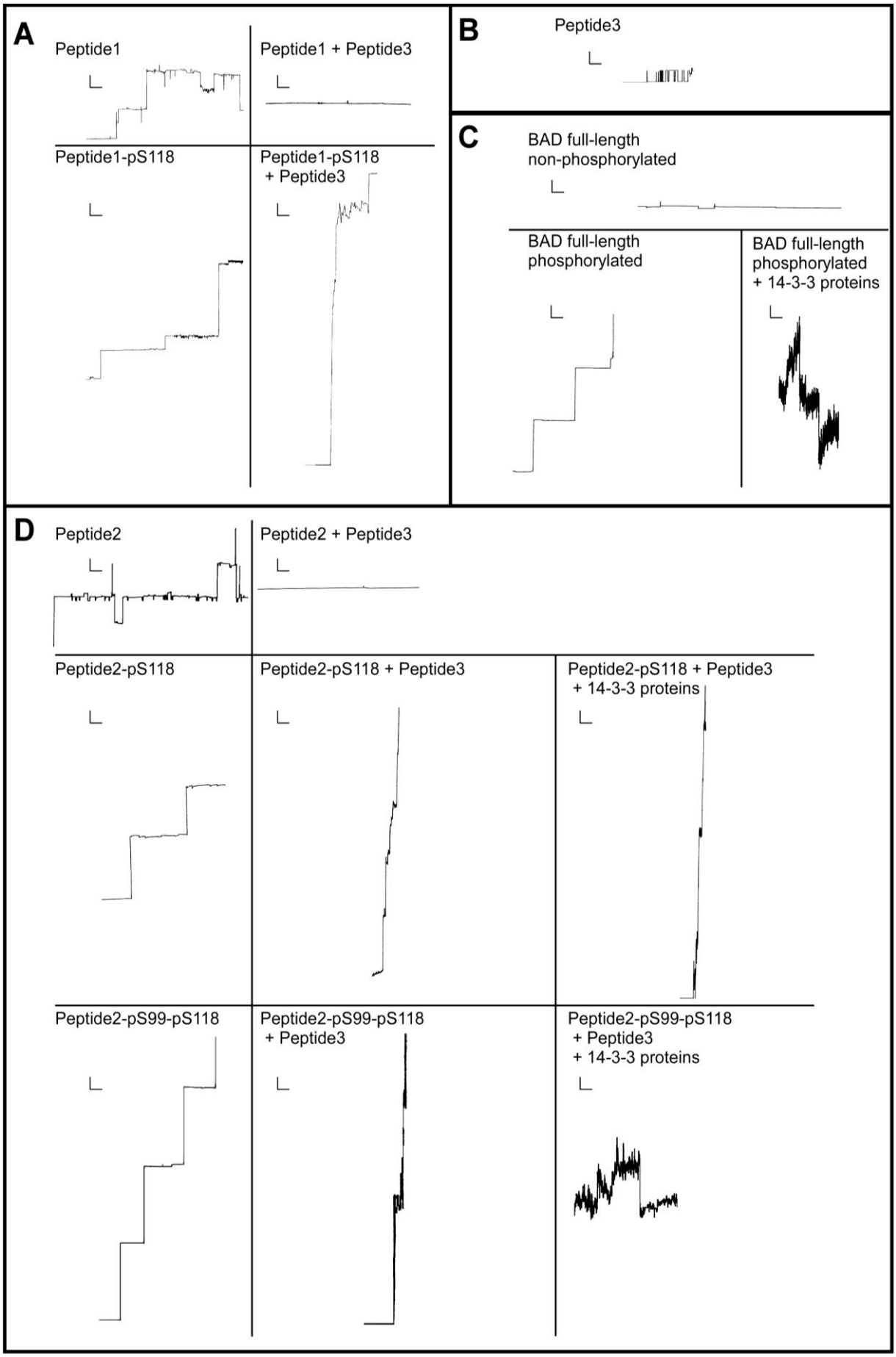
A
Peptide1
Peptide1 + Peptide3
Peptide1-pS118
Peptide1-pS118
+ Peptide3
B
Peptide3
C
BAD full-length
non-phosphorylated
BAD full-length
phosphorylated
BAD full-length
phosphorylated
+ 14-3-3 proteins
D
Peptide2
Peptide2 + Peptide3
Peptide2-pS118
Peptide2-pS118 + Peptide3
Peptide2-pS118 + Peptide3
+ 14-3-3 proteins
Peptide2-pS99-pS118
Peptide2-pS99-pS118
+ Peptide3
Peptide2-pS99-pS118
+ Peptide3
+ 14-3-3 proteins

Next, we investigated whether association with 14-3-3 proteins disrupts the pore-formation monitored with peptides corresponding to the BH3 domain and C-terminus as previously observed with full-length BAD protein (Fig. 23C and (Polzien *et al.* 2009)). To this end, we used prolonged BH3 peptides containing the 14-3-3 binding motif surrounding the serine 99 (Peptide2, Peptide2-pS118 and Peptide2-pS99-pS118, see also Fig. 21). Without addition of 14-3-3 proteins, peptides

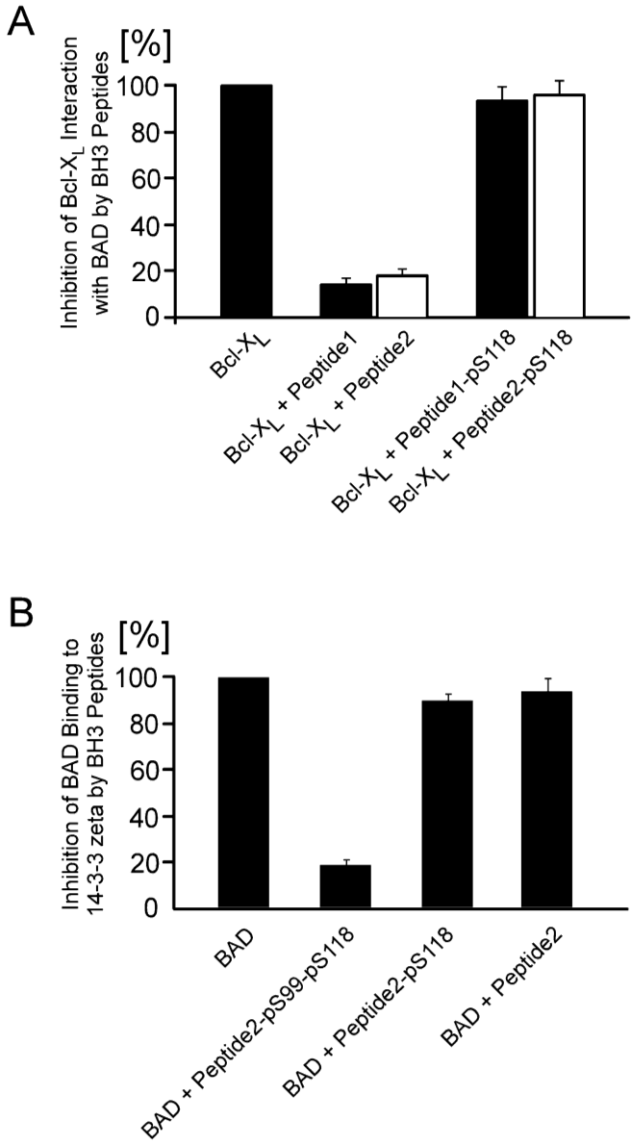

Figure 24: Functionality of the synthetic hBAD peptides used in this study.
A, the non-phosphorylated Peptide1 and -2 inhibit the interaction between BAD and Bcl-X_L. The interaction between purified GST-BAD and Bcl-X_L was monitored by SPR technique as described in Experimental Procedures. To this end, GST-BAD was captured by anti-GST antibody and Bcl-X_L was injected in the absence and presence of BH3 peptides (2 μM) as indicated. B, inhibition of the BAD interaction with 14-3-3 proteins by Petide2-pS99/pS118. The interaction between GST-14-3-3 zeta and his-tagged hBAD was monitored using SPR technique essentially as described (Hekman *et al.* 2006). For that purpose, GST-14-3-3 zeta was captured by anti-GST antibody and purified hBAD was applied in the absence and presence of BH3 peptides (10 μM) as indicated. Due to phosphorylation at serine 99 within the 14-3-3 binding motif (RSRS^{99}AP) only the Peptide2-pS99/pS118 displayed inhibitory potency. In both assays control peptides (phosphorylated and non-phosphorylated) did not show any effect (data not shown).

comprising the non-phosphorylated and phosphorylated 14-3-3 binding site (Peptide2, Peptide2-pS118 and Peptide2-pSer-99-pS118) behaved in the same manner as their shorter counterparts (Fig. 23D).

Of note, effective binding of 14-3-3 dimers to its client proteins can be achieved only in the case that the 14-3-3 binding motif becomes phosphorylated (for review see (Aitken *et al.* 2002)). Indeed, in the presence of phosphoserine 99, 14-3-3 proteins disrupt pore-formation in the same way as they did with phosphorylated full-length hBAD (compare Fig. 23C and D). These effects were observed in the presence (Fig. 23D) and absence (data not shown) of Peptide3. Importantly, pore-formation was not affected by 14-3-3 proteins in the case that serine 99 was not phosphorylated (Fig. 23D).

In general, the most effective pore formation was achieved by use of equimolar concentrations between C-terminal and BH3 peptides indicating primarily intramolecular contact points within the BAD protein. Change of buffer compositions did not influence the channel formation (data not shown). These data, in summary, suggest that phosphorylation of serine 99 alone (that is a prerequisite for 14-3-3 binding) would not prevent the putative pore-formation of BAD *in vivo*. Apparently, only a rapid complex formation between 14-3-3 proteins and BAD (possibly resulting in BAD depletion from mitochondria) would terminate the process.

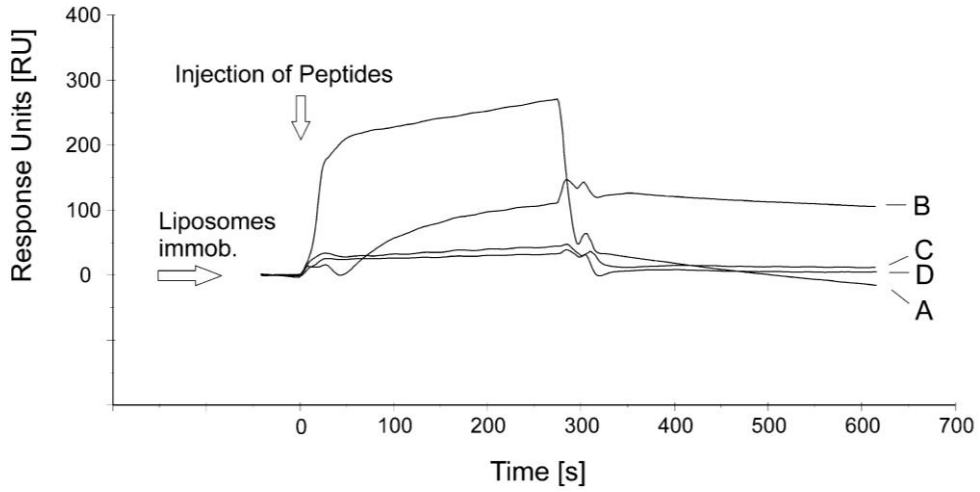

Figure 25: Differential interaction between BH3 peptides (Peptide1 and Peptide1-pS118) and C-terminal part of hBAD in lipid environment.
The interaction between these two segments of hBAD was monitored by SPR technique using Pioneer L1 sensor chip as described in Experimental Procedures. First, liposomes mimicking mitochondrial lipids were injected, resulting in a deposition of approximately 6000 RU. Next, purified GST-BADΔN131 (200 nM) that represents the C-terminal part of hBAD was applied to the captured liposomes leading to approximately 2000 RU of bound protein (not shown in the diagram). To detect the interaction of phosphorylated and non-phosphorylated forms of BH3 domain (Peptide1 and Peptide1-pS118, A and B, respectively) with the C-terminal part of BAD the corresponding peptides (1000 nM) were injected and the association-dissociation curves were monitored. Control measurements (C and D) were performed in the absence of GST-BADΔN131. Of note, BH3 peptides containing the LBD1 possess poor affinity for mitochondrial membranes. Instead, as previously documented (Hekman *et al.* 2006) hBAD missing the LBD2 associates preferentially with cholesterol-rich membranes (rafts like liposomes).
Due to the continuous slow dissociation of GST-BADΔN131 from liposomes the baseline in A and B (contrary to C and D) does not appear to be horizontal. Analogous results were obtained with Peptide2 and Peptide2-pS118 in combination with GST-BADΔN131 (data not shown).

The functional efficiency of the BH3 peptides used for pore-formation experiments has been validated by SPR technique. In the first assay (Fig. 24A) we took advantage of the ability of the phosphorylated BH3 domain to inhibit the interaction between BAD and Bcl-X_L protein. Binding between purified GST-BAD and Bcl-X_L was monitored essentially as described (Polzien *et al.* 2009). For that purpose, GST-tagged BAD was captured by immobilized anti-GST antibody and Bcl-X_L was injected in the absence and presence of phosphorylated and non-phosphorylated BH3 peptides. As demonstrated in Fig. 24A the non-phosphorylated BH3 peptides inhibited almost quantitatively the association of BAD with Bcl-X_L. In contrast, the BH3 fragments phosphorylated at serine 118 did not significantly affect the interaction between BAD and Bcl-X_L (Fig. 24A). To test the functionality of the Peptide2 regarding its association with 14-3-3 proteins, we used an indirect assay as well. To this end, the ability of Peptide2-pS99-pS118, Peptide2-pS118 and non-phosphorylated Peptide2 to inhibit the interaction between GST-14-3-3 zeta and full-length hBAD was utilized. As shown in Fig. 24B only the Peptide2 carrying phosphate in position serine 99 exhibited inhibitory potency in this regard.

Differential interaction between the C-terminal part of hBAD and BH3 peptides supports the effects monitored by pore-formation experiments – To elucidate the reason for diametrically opposed effects obtained by interaction of the C-terminal part of hBAD with phosphorylated and non-phosphorylated BH3 peptides with respect to pore-formation we investigated the mode of binding between these fragments in the presence of model membranes. Toward this end, we performed quantitative binding studies using SPR technique. Purified GST-BADΔN131 protein representing the C-terminal part of hBAD was used as the coupling partner for BH3 domain peptides. As previously reported BADΔN131 associated effectively with liposomes mimicking the lipid composition of mitochondrial membranes (Hekman *et al.* 2006). On the other hand, in accordance with published data (Hekman *et al.* 2006) the BH3 peptides (Peptide1 and Peptide1-pS118) did not exhibit significant binding to mitochondrial liposomes (Fig. 25). Instead, as previously stated, the BH3 domain containing the lipid binding domain 1 (LBD1) associates preferentially with cholesterol-rich membranes (Hekman *et al.* 2006). Thus, the use of experimental conditions applied here allowed detection of putative interaction between C-terminal part and BH3 region. As depicted in Fig. 25 we observed association of both BH3 peptides with BADΔN131 fragment, however, with essential differences regarding their kinetic parameters. While the non-phosphorylated BH3 peptide revealed a fast association with BADΔN131 and rapid dissociation resulting in a K_D value of 242 nM, the phosphorylated BH3 peptide (Peptide1-pS118) exhibited a slower association to BADΔN131. However, due to the very slow dissociation a high affinity binding with a K_D value of 11 nM could be calculated. Thus, these data may explain the finding that only the phosphorylated BH3 domain possessed the ability of pore-formation.

3.3.4. Discussion

Due to the fact that the amino acid sequence of BAD does not allow an exact prediction for the existence of a C-terminal transmembrane domain, most of the studies dealing with BAD function did not take into consideration that lipophilic properties of BAD may also play a role in its function. Our studies dealing with interaction of BAD with model membranes revealed that BAD possesses high affinity for particular negatively charged phospholipids and raft microdomains (Hekman *et al.* 2006). Two lipid binding domains (termed LBD1 and LBD2, respectively), both located at the C-terminal part of the protein, were identified. Moreover, the functional studies showed that BAD mutants compromised in lipid binding confer resistance to apoptosis. The functional importance of lipid binding of BAD is additionally underlined by the observation that hBAD forms channels in lipid bilayers (Polzien *et al.* 2009). To define a precise connection between pore-forming activity and structure of BAD, we analyzed in this study the secondary structure of the C-terminal part of hBAD including the putative helix region located within the conserved BH3 domain. Regarding the secondary structure of hBAD contradictory data exist. While Yang (Yang 2009) predicted seven α-helices for hBAD, Hinds *et al.* (2007) provided evidence that BH3-only proteins such as Bim, Bmf and BAD are intrinsically unstructured in the absence of binding partners. The results presented here demonstrate that the C-terminal part of hBAD reveals dynamic structural elements conditioned by its immediate environment. In principle, our data presented here are not contradictory to the results reported by Hinds *et al.* (2007). However, it is difficult to make a correlation between our data and results published in Hinds *et al.* (2007) because they used for their NMR measurements a BAD construct missing the C-terminal part. Nevertheless, these authors showed that BAD undergoes localized conformational changes upon binding to Bcl-2 targets. Contrary to this study, we observed in solution (i.e. in the absence of lipid vesicles) a high degree of β-sheet elements within the BH3 and C-terminal fragment. In the presence of liposomes or lipid micelles we detected dramatic changes of the secondary structure. As summarized in Table 1 the helix and β-sheet propensity was considerably increased in the presence of liposomes or lipid micelles. This holds for C-terminal segment of BAD and non-phosphorylated BH3 domain. Surprisingly, phosphorylation of serine 118 within the BH3 domain strongly reduces the formation of α-helical structures. The consequence of the phosphate introduction in this position was a complete abolishment of helical structure, as documented by CD measurements performed in absence or presence of lipids (Table 5). Considering these observations and keeping in mind that the BAD lipid binding domains are localized within the C-terminal part of the protein, we hypothesized that the elements responsible for pore-forming activity of BAD may be located within the Peptides1 and -3 that cover the C-terminal part and the BH3 region (see also Fig. 21). Indeed, the measurements regarding channel-forming ability using these peptides confirmed this assumption. Moreover, as shown in Fig. 23 our data demonstrates that only the interaction of the C-terminal Peptide3 with peptides covering the phosphorylated form of BH3 domain (Peptide1-pS118, Peptide2-pS118 and Peptide2-pS99-pS118) allows the formation of large, fast accumulating and

permanently open pores. In lipid environment BAD C-terminus as well as the phosphorylated BH3 domain exhibits a high proportion of β-sheet structure (Peptide3 and Peptide1-pS118, Table 5). Accordingly, only the combination of peptides that display a high amount of β-sheet structure in lipid environment were shown to possess pore-forming activity. This observation indicates that BAD pores might be composed of β-barrels similar to VDAC channels as reported by Hiller *et al*. (Hiller *et al.* 2008). Notably, in the absence of the BAD C-terminus, the non-phosphorylated BH3 domain (Peptide1) was also able to form channels. In contrast to the phosphorylated BH3 domain, this peptide showed a high proportion of α-helical structures in lipid environment (Table 5). Consequently, it assembled to less stable pores than its phosphorylated counterpart (Fig. 23). Therefore, pores formed by the non-phosphorylated BH3 domain seem to possess another secondary structure, probably consisting of α-helices.

Leber *et al.* (2007) recently discussed an *embedding together model* that emphasizes the importance of the interaction of Bcl-2 family proteins with and within membranes. Additionally, the model proposes that interactions between pro- and antiapoptotic Bcl-2 proteins are governed by membrane-dependent conformational changes. Our results regarding conformational changes of the C-terminal part of hBAD dependent on the presence of membranes and the fact that translocation of Bcl-X_L to the mitochondrial membrane occurs by complex formation with BAD (Jeong *et al.* 2004) are consistent with the *embedded together model*.

Together, we show here that the C-terminal part of hBAD (comprising BH3 domain and C-terminus) is *per se* sufficient to form ion channels. We identified phosphorylation of serine 118 within the BH3 domain to be essential for the formation of pores in the presence of the C-terminus. Furthermore, we disclosed that serine 99 serves an important role in controlling pore-formation via interaction of 14-3-3 proteins.

What could be the physiological function of BAD channels? Dephosphorylated BAD was found to be localized at mitochondria (Hekman *et al.* 2006; Wang and Youle 2009). Therefore, BAD pores could possibly play a role in the regulation of the mitochondrial permeability transition (Zoratti and Szabo 1995), a process that has been identified to be important in apoptosis (Zamzami *et al.* 1996; Zamzami *et al.* 1996). Indeed, it was discovered that BAD targets the permeability transition pore and furthermore, sensitizes it to Ca^{2+} in a phosphorylation dependent manner (Roy *et al.* 2009). A relevant aspect regarding the function of pores formed by Bcl-2 proteins is the observation that both pro- and anti-apoptotic Bcl-2 proteins exhibit pore-forming activity. Concerning the putative interplay between pores formed by different Bcl-2 proteins it was reported that in combination pro-apoptotic Bax does not abrogate pore-formation of anti-apoptotic Bcl-2 (Schendel *et al.* 1997). The authors suggested that Bcl-2 channels allow the transport across membranes in a direction that is cytoprotective, whereas the channels of Bax do the opposite. hBAD pores may also be involved in the control of such homeostasis. In this regard, it should be emphasized that hBAD forms channels in its phosphorylated

and non-apoptotic state. Therefore, it is likely that hBAD pores cooperate with anti-apoptotic proteins instead of counteracting them. It was also suggested that mitochondrial channels such as those regulated by proteins of the Bcl-2 family may control the export of mitochondrial metabolites like ATP under non-apoptotic conditions (Gottlieb *et al.* 2002; Jonas *et al.* 2003; Vander Heiden and Thompson 1999). Notably, results presented here show that the pore-forming BH3 domain of BAD has no binding affinity to mitochondrial membranes indicating that BAD channels may be located also at membranes other than mitochondria (Fig. 25). Indeed, as shown previously a high proportion of BAD was found to be localized at the cholesterol-rich microdomains (rafts) of the plasma membrane (Ayllon *et al.* 2002; Fleischer *et al.* 2004; Garcia *et al.* 2003; Hekman *et al.* 2006). Rafts play an important role for the interactions of a several signaling molecules (Hekman *et al.* 2002; Simons and Toomre 2000). In a previous study, we identified that ions as well as non-charged molecules with sizes of up to 200 Da can enter the BAD channel (Polzien *et al.* 2009). Therefore, hBAD pores might be permeable for many signaling molecules beside ions like γ-aminobutyric acid (GABA), nitric oxide or histamine. So it is feasible that BAD pores contribute to signaling processes in rafts of the plasma membrane.

A previous model of BAD inactivation proposed sequential phosphorylation including phosphorylation of serine 118 and consequently disruption of the BAD/Bcl-X_L complex (Datta *et al.* 2000). This process may finally result in inactivation and depletion of BAD from mitochondria by complex formation with 14-3-3 proteins. The alternative mechanism proposed in this study implies that the phosphorylation of serine 118 does not necessarily lead to inactivation of BAD. In the case of selective phosphorylation in this position the formation of large pores at mitochondria may take place (Fig. 23). On the other hand, the translocation model, first presented by the group of Rebollo (Ayllon *et al.* 2002; Fleischer *et al.* 2004; Garcia *et al.* 2003) and extended by our results (Hekman *et al.* 2006; Rapp *et al.* 2007) involves recruitment of BAD to the lipid rafts. This process is regulated by growth factor stimulation and is dependent on phosphorylation of the 14-3-3 binding motif. In this model we have suggested (see also Fig. 38) that the BAD/14-3-3 complex is of transient nature. Due to its preferential affinity for cholesterol rich membranes (Hekman *et al.* 2006) the BAD/14-3-3 complex translocates readily to rafts, whereby dissociation of 14-3-3 occurs. Thus, the pore-formation of phosphorylated BAD protein would take place rather at rafts located at plasma membrane than mitochondria. Pore-formation data presented here (see Fig. 23) with doubly phosphorylated Peptide2 (Peptide2-pS99-pS118) supports strongly this pathway.

3.3.5. Concluding Remarks

The multifunctional role of the C-terminal part of the BAD protein and in particular its lipid binding properties have not yet been considered sufficiently. Based on our observations, we propose that only in the presence of membranes does a close interaction between the phosphorylated BH3 helix and the C-terminal part of hBAD take place. Furthermore, selective phosphorylation at serine 118

within the BH3 domain results in activation of BAD by induction of pore-formation. However, the signaling cascades that determine whether BAD becomes a sentinel or executioner protein is at the present time matter for speculation. The same holds for activation of Bak and Bax; the precise biochemical mechanisms that lead to translocation and pore-formation of Bak and Bax are not sufficiently understood.

3.3.6. Acknowledgements

This work was supported by Deutsche Forschungsgemeinschaft Grant SFB 487 (Projects C3, A5 and C7) and graduate college 1141 (GCWN). We thank Elke Maier for brilliant technical assistance, Prof. Dr. Thomas Müller (Julius-von-Sachs Institute for Biosciences, University of Würzburg) for fruitful discussions, Laura Goldberg (Lafayette College, NY, USA) for excellent cooperativeness and proof reading. Marco Albrecht (Biocenter, Department of Microbiology, University of Würzburg) was a great help in methods of electronic data processing.

3.4. BAD Contributes to RAF-Mediated Proliferation and Cooperates with B-RAF-V600E in Cancer Signaling

BAD (Bcl-2 antagonist of cell death) belongs to the pro-apoptotic BH3-only subfamily of Bcl-2 proteins. Physiological activity of BAD is highly controlled by phosphorylation. To further analyze the regulation of BAD function, we investigated the role of recently identified phosphorylation sites on BAD-mediated apoptosis. We found that in contrast to the N-terminal phosphorylation sites the serines 124 and 134 act in an anti-apoptotic manner since the replacement by alanine led to enhanced cell death. Our results further indicate that RAF kinases represent, besides PAK1, BAD serine 134 phosphorylating kinases. Importantly, in the presence of wild type BAD co-expression of survival kinases, such as RAF and PAK1 leads to a strongly increased proliferation, whereas substitution of serine 134 by alanine abolishes this process. Furthermore, we identified BAD serine 134 to be strongly involved in survival signaling of B-RAF-V600E containing tumor cells and found that phosphorylation of BAD at this residue is critical for efficient proliferation in these cells. Collectively, our findings provide new insights into the regulation of BAD function by phosphorylation and its role in cancer signaling.

3.4.1. Introduction

Apoptosis is a programmed cell death mechanism that regulates the destruction of cells. This is crucial for multicellular organisms in processes such as development and tissue homeostasis (Danial and Korsmeyer 2004; Reed *et al.* 2004; Wang and Youle 2009). Mitochondria constitute a convergence point in the process of apoptosis (Wang and Youle 2009; Youle and Strasser 2008). Crucial regulators of apoptosis at the level of mitochondria are the proteins of the Bcl-2 family that are characterized by the presence of Bcl-2 homology domains (BH1-BH4). The Bcl-2 family of proteins is divided into three subfamilies, including proteins which either inhibit (e.g. Bcl-X_L, Bcl-2 or Bcl-w) or promote (e.g. Bak, Bax or Bok) programmed cell death (Adams and Cory 1998; Gross *et al.* 1999; Youle and Strasser 2008). A second sub-class of pro-apoptotic Bcl-2 family members consists of the BH3-only proteins that share sequence homology only at the BH3 domain. This sub-class comprises BAD, Bmf, Bik, Noxa, Hrk, Bim, Bid, and Puma (Youle and Strasser 2008). A complex interplay between anti- and pro-apoptotic proteins of this family mediates induction and execution of programmed cell death. Surprisingly, several proteins of the Bcl-2 family shaped up as regulators of various physiological processes other than apoptosis, such as autophagy, mitochondrial respiration and the glucose metabolism (Danial 2008).

BAD (Bcl-2 associated death promoter, Bcl-2 antagonist of cell death) is a BH3-only protein that promotes apoptosis by forming heterodimers with the pro-survival proteins Bcl-2 and Bcl-X_L (Yang *et al.* 1995). Phosphorylation of specific serine residues, Ser-112 and Ser-136 of murine BAD (mBAD)

or the corresponding phosphorylation sites Ser-75 and Ser-99 of human BAD (hBAD) leads to complex formation with 14-3-3 proteins and subsequent relocation of BAD (Hekman *et al.* 2006; Zha *et al.* 1996). Phosphorylation of mBAD at Ser-155 (Ser-118 of hBAD) disrupts the association with Bcl-X_L or Bcl-2 provoking cell survival (Datta *et al.* 2000). Therefore, the phosphorylation status of BAD at specific serine residues reflects a checkpoint for cell death or survival. Numerous kinases were shown to phosphorylate BAD (Datta *et al.* 1997; Gnesutta *et al.* 2001; Harada *et al.* 1999; Jin *et al.* 2005; Klumpp *et al.* 2004; Konishi *et al.* 2002; Macdonald *et al.* 2006; Schurmann *et al.* 2000; She *et al.* 2002; Shimamura *et al.* 2000) including RAF kinases (Jin *et al.* 2005; Kebache *et al.* 2007; Panka *et al.* 2006; Polzien *et al.* 2009; Wang *et al.* 1996). Regarding RAF kinases, we demonstrated that B-RAF phosphorylates BAD in a direct manner leading to inhibition of BAD induced cell death (Polzien *et al.* 2009). This finding is of particular importance, since highly active B-RAF has been demonstrated to represent one of the crucial players in cancer development (Davies *et al.* 2002). In total, five serine phosphorylation sites (at positions 112, 128, 136, 155 and 170) and two threonines phosphorylation sites (117 and 201) have been reported so far for murine BAD. In human BAD we recently identified several novel *in vivo* phosphorylation sites (serines 25, 32/34, 97, 124, and 134) besides the established phosphorylation sites at Ser-75, Ser-99, and Ser-118 (Polzien *et al.* 2009).

In this study, we investigated the putative role of hBAD phosphorylation sites located at the N- and C-terminus and demonstrate that, contrary to the N-terminal part of hBAD, the residues serines 124 and 134 are directly involved in regulation of apoptosis. Additionally, our results indicate that RAF kinases represent, besides PAK1, *in vivo* BAD Ser-134 phosphorylating kinases. Furthermore, we demonstrated that phosphorylation of BAD Ser-134 by RAF kinases and PAK1 triggers cell proliferation and disclose that BAD cooperates with RAF in promoting proliferation in B-RAF mutant cancer cells.

3.4.2. Experimental Procedures

Reagents and antibodies – Benzamidine, leupeptin, aprotinin and Nonidet P-40 were obtained from Sigma. Glutathione-Sepharose was purchased from GE Healthcare and Ni^{2+}-nitrilotriacetic acid-agarose was from Qiagen. Monoclonal anti-phospho-ERK antibody (sc-7383), polyclonal anti-B-RAF antibody (sc-166), polyclonal anti-BAD antibodies (sc-943 and sc-8044), anti-Myc antibody (sc-40) and polyclonal anti-actin antibody (sc-1616) were from Santa Cruz Biotechnology (Santa Cruz, CA) and polyclonal anti-Akt/PKB antibody was from Cell Signaling Technology. Phosphospecific antibody directed against phosphoserine 134 of human BAD (or corresponding phosphoserine 170 in murine BAD) was from Abnova. Phosphospecific antibodies directed against phosphoserines 75 and 118 of human BAD (or corresponding phosphoserines 112 and 155 in murine BAD) were obtained from Cell Signaling Technology (#9296 and #9297, respectively). Horseradish peroxidase-conjugated polyclonal anti-rabbit and anti-mouse IgG were obtained from GE Healthcare.

Cell culture, transfection and immunoblotting – HEK-293 (ATCC #CRL-1573), HeLa 229 (ATCC #CCL-2.1), A375, SK-MEL-28, DX3 and MEL-Juso cells (kindly provided by Daniela Haug, University of Würzburg, Germany) were cultivated in DMEM supplemented with 10% fetal bovine serum (Biochrom), 2 mM L-glutamine, and 100 units/ml penicillin/ streptomycin at 37°C in humidified air with 5% CO_2. The cell lines PC3 and HCT 116 (kindly provided by Joachim Fensterle, Æterna Zentaris, Germany) were cultivated in RPMI and Mc Coy´s 5a medium, respectively, that were supplemented with 10% fetal bovine serum (Biochrom), 2 mM L-glutamine, and 100 units/ml penicillin/ streptomycin. Prior to transfection cells were seeded at 3 x 10^5 cells/well of a 6-well plate and grown for 24 h before transfection by jetPEI (Polyplus). 16 h post-transfection, cells were washed twice with phosphate-buffered saline (PBS) and cultivated for 22 h in medium supplemented with 0.1-0.3% serum. To investigate the putative involvement of different survival kinases, the following kinase inhibitors were used: U0126 (Promega), PD0325901, Wortmannin (Santa Cruz Biotechnology, Santa Cruz, CA) and Sorafenib (Bayer, Leverkusen). All inhibitors were dissolved in DMSO and used at indicated concentrations. After harvesting, the cells were washed once with PBS and than lysed in Nonidet P-40 buffer (50 mM Tris-HCl, pH 8.0, 137 mM NaCl, 2 mM EDTA, 2 mM EGTA, 10% (v/v) glycerol, 0.1% (v/v) β-mercaptoethanol, 25 mM β-glycerophosphate, 10 mM sodium pyrophosphate, 1 mM Na_3VO_4, 25 mM NaF, 1% Nonidet P-40, and a mixture of standard proteinase inhibitors). Protein concentration was determined by Bradford method. SDS-PAGE and immunoblotting were performed as described previously (Hekman *et al.* 2006).

siRNA transfection – One day prior to transfection, cells were seeded into 12-well plates to a confluency of 60%. Transfection of siRNAs targeting the coding sequence (5'-ACGAGTTTGTGGACTCCTTTA-3') or the 3'-UTR (5'-TCACTACCAAATGTTAATAAA-3') of BAD or luciferase as control (5'-AACUUACGCUGAGUACUUCGA-3') was performed with Lipofectamine 2000 reagent (Invitrogen) and Optimem medium (Gibco) with a final siRNA concentration of 100 nM. After 48 h, cells were harvested and used for Western blotting and monitoring of the number of viable cells by Trypan blue (Sigma) exclusion.

DNA expression plasmids and purification of proteins – The hBAD expression plasmid was generated as described (Polzien *et al.* 2009). Site-specific mutations of hBAD were introduced using QuikChange site-directed mutagenesis kit (Stratagene) according to the manufacturer's instructions. The accuracy of the BAD mutants was confirmed by DNA sequencing. PAK1 constructs were from Jonathan Chernoff (Philadelphia, PA). Akt/PKB plasmids were kindly provided by Jakob Troppmair (Innsbruck, Austria). Expression and purification of RAF kinases, PAK1 and Akt/PK from Sf9 insect cells were performed as previously described (Fischer *et al.* 2009; Hekman *et al.* 2002). GST-tagged hBAD was expressed in *E. coli* using pGEX-2T vector (GE Healthcare) and isolated by glutathione-Sepharose affinity chromatography. Further purification was achieved by ion exchange chromatography using an ÄKTA system (GE Healthcare). The purity of the proteins was assessed by

SDS-PAGE and Coomassie Blue staining (see also Fig. 29).

Cell survival assay – For the analysis of cell survival, cells were transiently transfected in triplicates. After 16 h, cells were washed twice with PBS and grown for 30 h in medium supplemented with 0.1% serum. Cell viability was assessed by staining cells with Trypan blue.

Analyzes of cell proliferation and growth inhibition – To monitor cell proliferation, HEK-293 and HeLa cells were transiently transfected in triplicates. 16 h post-transfection, cells were washed twice with PBS and grown in medium supplemented with 0.3% serum. SK-MEL-28, A375, PC-3, HCT 116, MEL-Juso and DX3 cells were incubated with and without the indicated kinase inhibitors or transfected with the named siRNAs for 48 h. Cell proliferation and growth inhibition were analyzed by photographing and counting of the cells as well as by counting living cells by use of Trypan blue in a hemicytometer at different time points (2, 3 and 6 days following transfection). To visualize cell proliferation, mitochondria of viable cells were stained by MitoTracker Deep Red FM (#M22425, Invitrogen) according to manufacturer's instructions and fluorescence intensity was measured at 633 nm excitation and 670/30 nm emission by the Typhoon 9200 imager (GE Healthcare).

Kinase activity measurements – Kinase activity of RAF-containing samples was monitored using recombinant MEK and ERK-2 as substrates. For that purpose, HeLa cell lysates (5 µg) or purified proteins (1 µg) were mixed with 0.5 mM ATP in 25 mM Hepes, pH 7.6, 150 mM NaCl, 25 mM β-glycerophosphate, 10 mM $MgCl_2$, 1 mM dithiothreitol, and 1 mM sodium vanadate buffer (50 µl final volume). Following addition of MEK and ERK-2 the reaction mixture was incubated for 30 min at 30°C. The incubation was terminated by addition of Laemmli sample buffer, and the proteins were separated by 10% SDS-PAGE and transferred to nitrocellulose membranes. The extent of ERK phosphorylation was determined with anti-phospho-ERK antibodies.

3.4.3. Results

In contrast to the N-terminal phosphorylation sites, Ser-124 and Ser-134 of hBAD contribute to apoptosis control – BAD function is regulated by phosphorylation at several residues in response to survival factors. Phosphorylation of mBAD at serines 112, 136 and 155 (corresponding to serines 75, 99 and 118 in hBAD) was a subject of numerous studies. In contrast, little is known about the function of the recently published phosphorylation sites (Polzien *et al.* 2009). As the function of the internal phosphoserines, regulating the interactions of BAD with 14-3-3 proteins, has been thoroughly investigated (Datta *et al.* 2000; Hekman *et al.* 2006; Masters *et al.* 2001; Subramanian *et al.* 2001; Zha *et al.* 1996; Zhang *et al.* 2005), we examined in this study the role of phosphorylation of serines located at the N- and C-terminal parts of hBAD. For that purpose, we analyzed the role of phosphorylation of serines 25, 32 and 34, located at the N-terminus as well as phosphorylation sites located at the C-terminal part of hBAD protein, i.e. serines 124 and 134 with respect to survival regulation (Fig. 26A). The functional role of these novel phosphorylation sites was assessed by site-

directed mutagenesis, where the serines of interest were replaced by alanine. The analysis of the pro-apoptotic function of hBAD and hBAD mutants was carried out in HeLa cells. The cells were transiently transfected with the indicated expression plasmids and starved for 30 h in medium supplemented with 0.1% serum. The number of apoptotic cells was determined by Trypan blue.

As displayed in Fig. 27A, the substitution of the N-terminal Ser-25, Ser-32 and Ser-34 by alanine did not result in significant changes of the pro-apoptotic activity of BAD. In contrast, the substitution of Ser-124 or Ser-134 by alanine led to enhanced cell death indicating that phosphorylation at these positions plays a pivotal role in the regulation of cell survival. In these experiments, BAD was expressed to the same levels (Fig. 27B). These results were also verified by PARP cleavage (data not shown).

Characterization of hBAD Ser-134 phosphorylation – The proapoptotic protein BAD has been reported to be a substrate for a wide spectrum of kinases (see references in (Polzien *et al.* 2009)). Recently, we and others demonstrated that mammalian RAF isoforms represent direct BAD-phosphorylating kinases (Jin *et al.* 2005; Kebache *et al.* 2007; Panka *et al.* 2006; Polzien *et al.* 2009; Wang *et al.* 1996). However, in our previous study (Polzien *et al.* 2009) we restricted our efforts to the regulatory serines 75, 99 and 118. In this study, we focused our efforts on characterization of human BAD serine 134 phosphorylation. To monitor the *in vivo* phosphorylation at this critical serine residue we co-expressed different RAF isoforms (B- and C-RAF) and performed a comparative analysis involving other BAD-phosphorylating kinases, such as PAK1 or Akt/PKB. By analyzing co-transfected HeLa cells we found that Ser-134 of hBAD becomes efficiently phosphorylated by B- and C-RAF and PAK1 (Fig. 28A). As the co-expression of active Akt/PKB caused relative low extents of

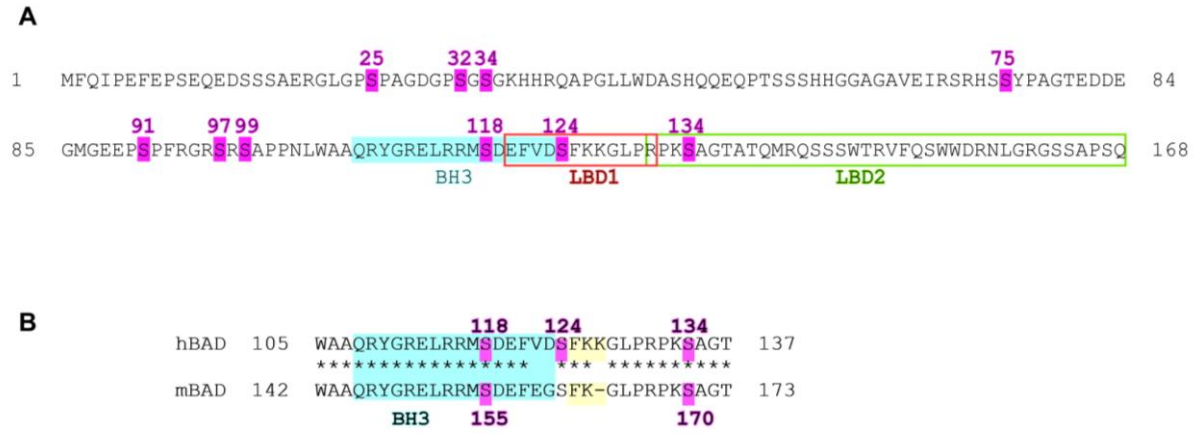

Figure 26: Amino acid sequence of human BAD protein (A) and of the BAD fragment surrounding the BH3 domain in human and mouse BAD (B).
Amino acid sequences were aligned using the ClustalW algorithm (www.ebi.ac.uk/Tools/clustalw2). All published phosphorylation sites are highlighted in *magenta*, and their positions within the sequence are indicated by *numbers*. The BH3 domain is shown in *blue* and the putative lipid binding domains (LBD1 and LBD2) are indicated by *orange* and *green rectangles*, respectively. In B, the FKK/FK regions vicinal to the BH3 domain are indicated in *yellow*.

Ser-134 phosphorylation (in the range of about 25% of the value obtained by RAF) we concluded that Akt/PKB is less involved in this process. To investigate whether the replacement of Ser-134 by alanine influences the phosphorylation of the survival sites Ser-75 and Ser-118 by B-RAF, we monitored also the extent of phosphorylation at these sites. As demonstrated in Fig. 28A (below) no difference was observed between S134A mutant and hBAD wild type. RAF kinases appear to be able to phosphorylate BAD serine 134 directly since two different MEK inhibitors (U0126 and PD0325901) did not affect the phosphorylation signal by RAF (Fig. 28C).

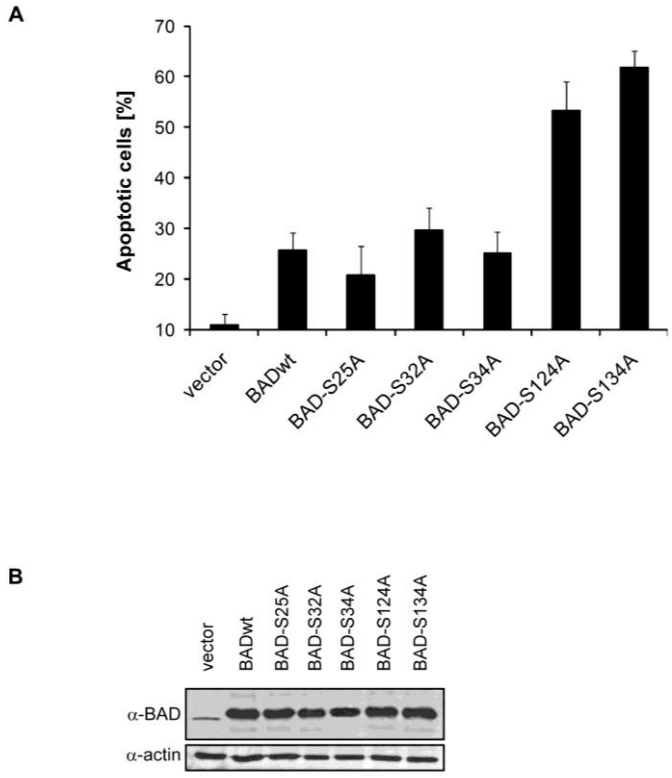

Figure 27: Serines 124 and 134 located at the C-terminal part of hBAD contribute to apoptosis control.
HeLa cells were transiently transfected with the indicated expression vectors. 16 h post-transfection, cells were cultivated for 30 h in medium supplemented with 0.1% serum. A, The extent of apoptotic cells was detected by Trypan blue staining. B, Expression levels of BAD wild type and BAD variants in transfected cell lysates were detected with an antibody directed against BAD. The experiments were repeated three times with the same results.

Figure 28 (right): Comparative analysis of hBAD phosphorylation by Akt/PKB, PAK1, and RAF kinases using anti-BAD-pS134 antibody.
HeLa cells were transiently transfected with the indicated expression vectors. In the case of Akt/PKB and PAK1, activating mutants (T308D/S473D and T423E, respectively) were used. 16 h post-transfection, cells were cultivated for 30 h in medium supplemented with 0.3% serum with (C) or without (A) of the indicated MEK inhibitors (10 µM). Total cell lysates were separated on a 15% SDS-polyacrylamide gel and blotted onto nitrocellulose membrane. Phosphorylation of human BAD at serine134 as well as BAD expression was analyzed. Phosphorylation degrees of the survival serines 75 and 118 are also included (see lower lines). The expression of different kinases was verified by use of specific antibodies. The phosphorylation degree of BAD at serine 134 by kinases shown in A was quantified by optical densitometry (B). In C, the efficiency of MEK inhibitors was analyzed by an antibody directed against phosphorylated ERK. These experiments were repeated three times with comparable results.

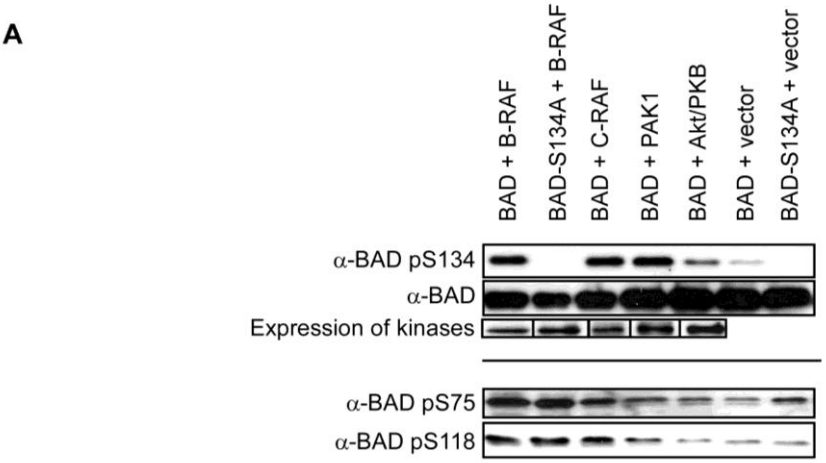
A
BAD + B-RAF
BAD-S134A + B-RAF
BAD + C-RAF
BAD + PAK1
BAD + Akt/PKB
BAD + vector
BAD-S134A + vector
α-BAD pS134
α-BAD
Expression of kinases
α-BAD pS75
α-BAD pS118

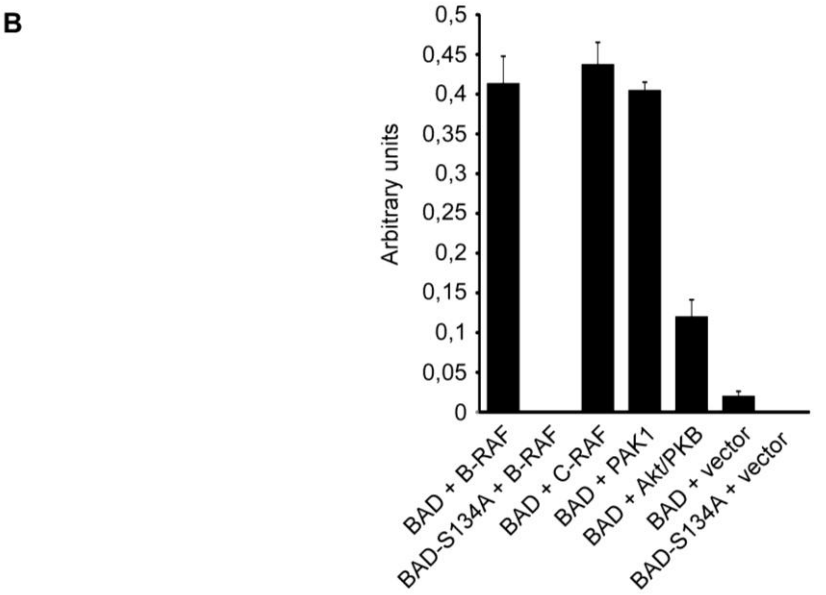
B
Arbitrary units
0,5
0,45
0,4
0,35
0,3
0,25
0,2
0,15
0,1
0,05
0
BAD + B-RAF
BAD-S134A + B-RAF
BAD + C-RAF
BAD + PAK1
BAD + Akt/PKB
BAD + vector
BAD-S134A + vector

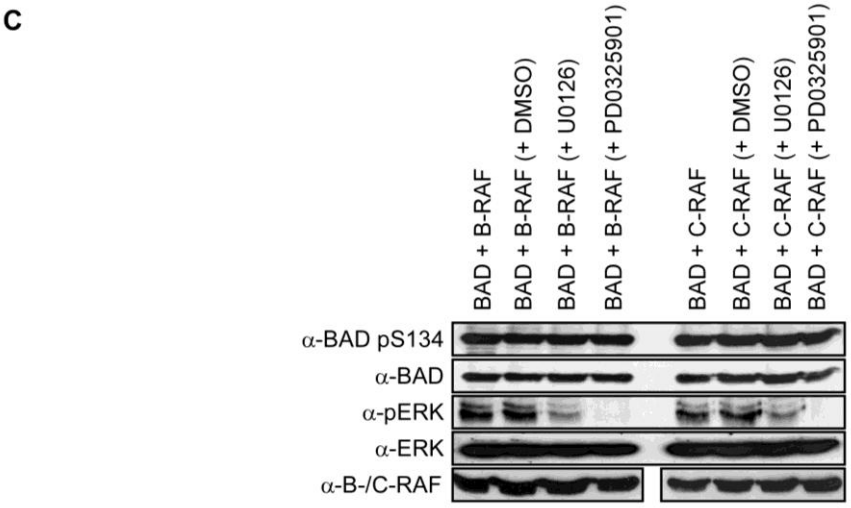
C
BAD + B-RAF
BAD + B-RAF (+ DMSO)
BAD + B-RAF (+ U0126)
BAD + B-RAF (+ PD0325901)
BAD + C-RAF
BAD + C-RAF (+ DMSO)
BAD + C-RAF (+ U0126)
BAD + C-RAF (+ PD0325901)
α-BAD pS134
α-BAD
α-pERK
α-ERK
α-B-/C-RAF

To monitor the direct phosphorylation of Ser-134 by the indicated kinases (Fig. 28), we investigated also the *in vitro* phosphorylation of hBAD by purified kinases (Fig. 29). To this end, non-phosphorylated hBAD has been purified from *E. coli* whereas RAF kinases, PAK1 and Akt/PKB were expressed and isolated from Sf9 insect cells. The purity of the isolated proteins was assessed by SDS-PAGE and Coomassie Blue staining (Fig. 29). The phosphorylating kinases PAK1, Akt/PKB and B-RAF provided similar results *in vivo* and *in vitro* (Fig. 28A and Fig. 29). In contrast, although C-RAF proved to be a potent *in vivo* Ser-134 phosphorylating kinase, *in vitro* it failed to phosphorylate this site significantly. The reason for this discrepancy could be explained by the ability of C-RAF to build an active heterodimeric complex with B-RAF (Garnett *et al.* 2005; Rushworth *et al.* 2006; Weber *et al.* 2001) *in vivo.*

As previously reported (Polzien *et al.* 2009) we demonstrated that co-expression of B-RAF (or activated C-RAF) inhibits BAD-mediated apoptosis following growth factor removal. These effects were ascribed to RAF-mediated phosphorylation of serine 75 and 118 in human BAD because the substitution of these residues by alanine led to increased apoptotic levels even in the presence of B-RAF (Polzien *et al.* 2009). In this study we investigated the putative impact of serine 134

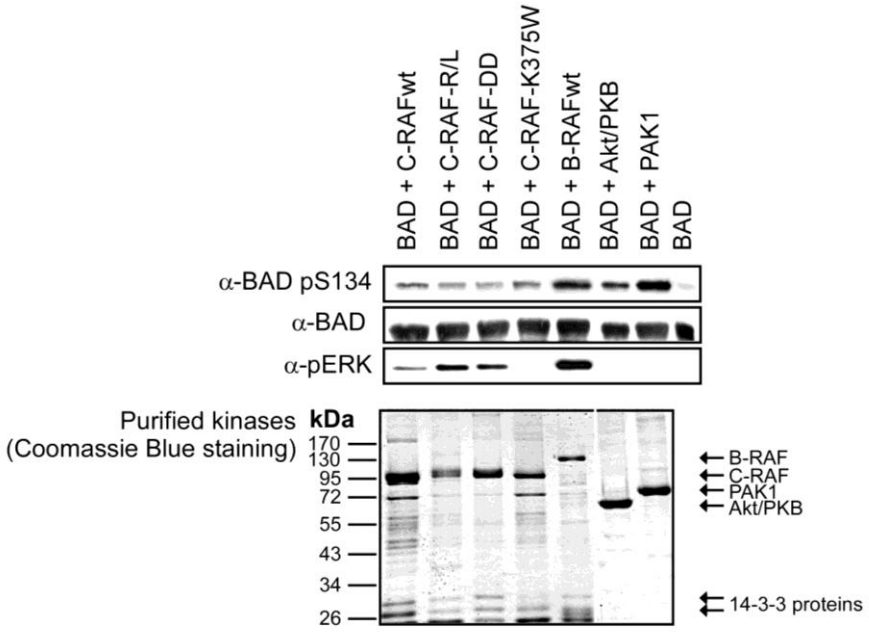

Figure 29: *In vitro* phosphorylation of recombinant BAD by purified PAK1, Akt/PKB, and RAF kinases. Purified GST-BAD (20 pmol) was incubated in the presence of RAF kinases, constitutively active PAK1 (T423E) and Akt/PKB (T308D/S473D) (2 pmol of each). The highly active C-RAF-R/L was co-expressed with Ras12V (R) and Lck (L). C-RAF-DD represents the active C-RAF mutant C-RAF-Y340D/Y341D and C-RAF (K375W) is a kinase inactive form. Following SDS-PAGE and immunoblotting, BAD phosphorylation was visualized by a phosphospecific antibody directed against BAD phosphoserine 134. The activity of RAF kinases was analyzed by an antibody directed against phosphorylated ERK. The kinases were expressed in Sf9 insect cells and purified either by glutathione-Sepharose (GST-tagged RAF kinases) or nickel chelate affinity chromatography (PAK1 and Akt/PKB) as described in Experimental Procedures. The purified proteins were visualized by Coomassie Blue staining (below). The RAF kinases shown are constitutively associated with 14-3-3 proteins (see arrows at approx. 30 kDa). The other co-purified proteins were recently identified as EF1, Cdc37, HSP40, HSP70 and HSP90 (not indicated in this illustration) (Fischer *et al.* 2009).

phosphorylation on apoptosis degree in the presence of active RAF, such as B-RAF.

As exhibited in Fig. 30A the single mutation of serine 134 to alanine does not influence the pro-apoptotic activity of BAD as much as observed in Fig. 27A. The reason of this effect might be, that BAD-induced apoptosis is regulated through an interplay between the serine residues 75, 118, and 134 that is controlled by B-RAF. In the presence of B-RAF, single mutation of serine 134 to alanine barely affects the pro-apoptotic activity of BAD because co-expression of B-RAF leads to increased

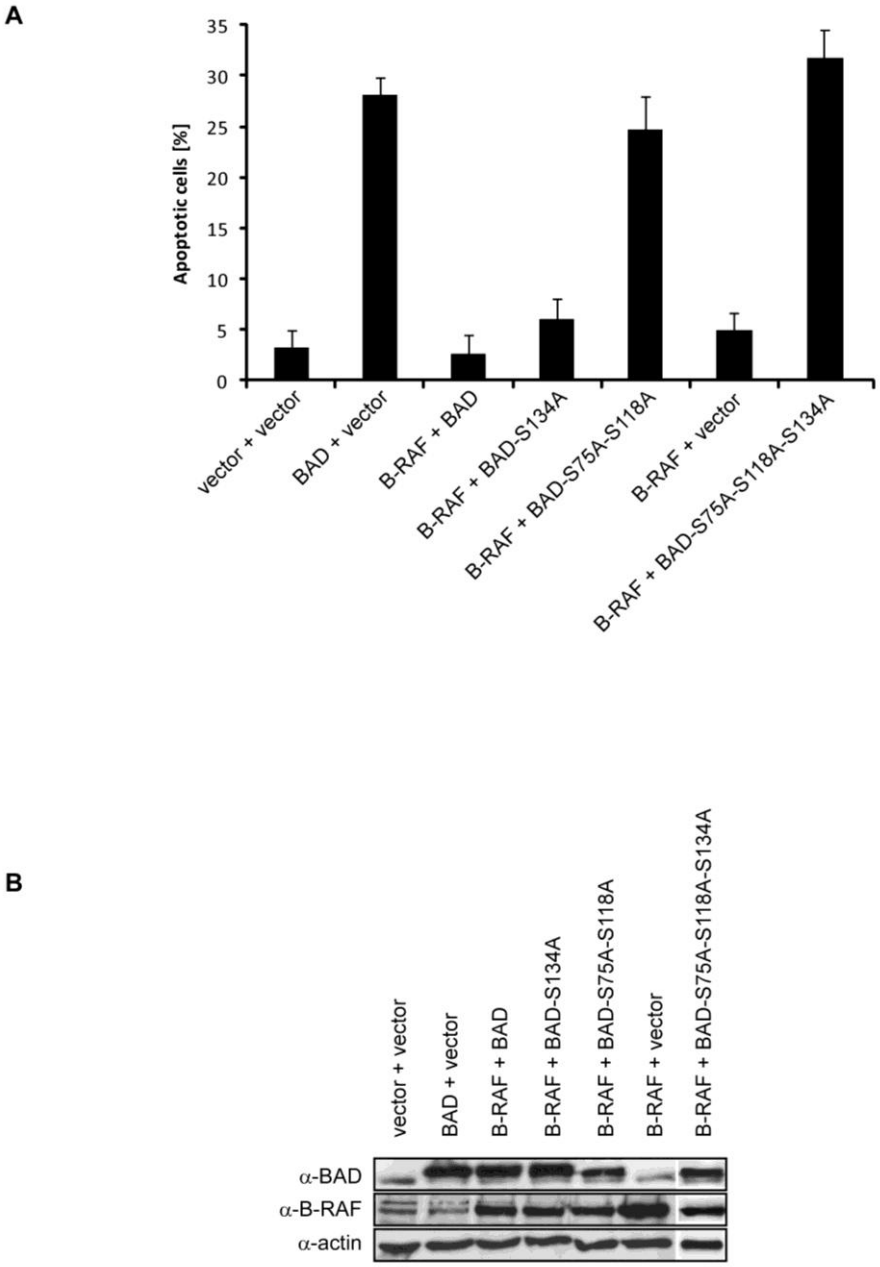

Figure 30: BAD-induced apoptosis is regulated by interplay between serines 75, 118, and 134.
HeLa cells were transiently transfected in triplicates with the expression vectors as indicated. 16 h post-transfection, cells were washed and grown in medium supplemented with 0.1% serum. A, The extent of apoptotic cells was detected by trypan blue staining. B, Expression levels of BAD constructs and B-RAF in transfected cell lysates were detected via specific antibodies.

phosphorylation of BAD serines 75 and 118 (Fig. 28A). In a previous report (Polzien *et al.* 2009) we demonstrated that B-RAF-mediated phosphorylation of BAD serines 75 and 118 leads to inhibition of BAD-induced apoptosis. Without co-expression of B-RAF, the phosphorylation levels of the regulatory serines 75 and 118 are low resulting in strong induction of apoptosis. The degree of apoptosis induction can even be strengthened by mutation of serine 134. This situation was simulated by using a triple BAD mutant (BAD-S75A-S118A-S134A) that resulted in intense induction of apoptosis, even in the presence of B-RAF (Fig. 30A). These results, together, indicate that residues 75 and 118 are crucial for regulation of BAD proapoptotic activity whereas serine 134 mediates the fine tuning of BAD induced apoptosis.

These observations, together, indicate that residues 75 and 118 are crucial for the regulation of BAD proapoptotic activity whereas serine 134 mediates the fine tuning of BAD induced apoptosis.

Phosphorylation of hBAD Ser-134 enhances cell proliferation – Data shown in Fig. 28 reveals that RAF kinases and PAK1 phosphorylate BAD at position serine 134. Since these survival kinases play a crucial role in several types of cancer, we analyzed here in more detail the role of BAD phosphorylation on cell proliferation. To this end, we co-expressed RAF kinases and PAK1 with wild type BAD or BAD-S134A mutant in HeLa cells and induced apoptosis through starvation conditions. Cell proliferation was analyzed by counting of living cells (Fig, 31A and C) as well as by staining of mitochondria of viable cells and detection of fluorescence intensity by a laser scanner (Fig. 31B and C).

Results obtained by both methods support the finding that RAF and PAK1 serve as phosphorylating kinases for hBAD serine 134. Surprisingly, proliferation activity of cells expressing RAF and PAK1 was considerably elevated in the presence of wild type hBAD (Fig. 31). On the other hand, in the presence of BAD-S134A mutant the degree of cell proliferation was reduced to control levels. The measured fluorescence intensities reflect the amount of viable cells since they correlate with counted cell numbers (Fig. 31C). The change of mitochondrial activity may play a minor role in this context.

Figure 31 (right): BAD stimulates RAF-mediated cell proliferation.
HEK-293 and HeLa cells were transiently transfected in triplicates with the expression vectors as indicated. 16 h post-transfection, cells were washed and grown in medium supplemented with 0.3% serum. A, Cell proliferation was analyzed by counting living cells by Trypan blue exclusion two days following transfection. B, To visualize cell proliferation, mitochondria of viable cells were stained by MitoTracker and fluorescence intensity of the wells was measured by Typhoon 9200 imager. C, Combination of results obtained in A and B. To show that the measured fluorescence intensities correlate with counted cell numbers the results presented in A and B were quantitatively compared. BAD constructs and kinases were expressed to comparable levels in each sample (data not shown). These experiments were repeated three times with comparable results.

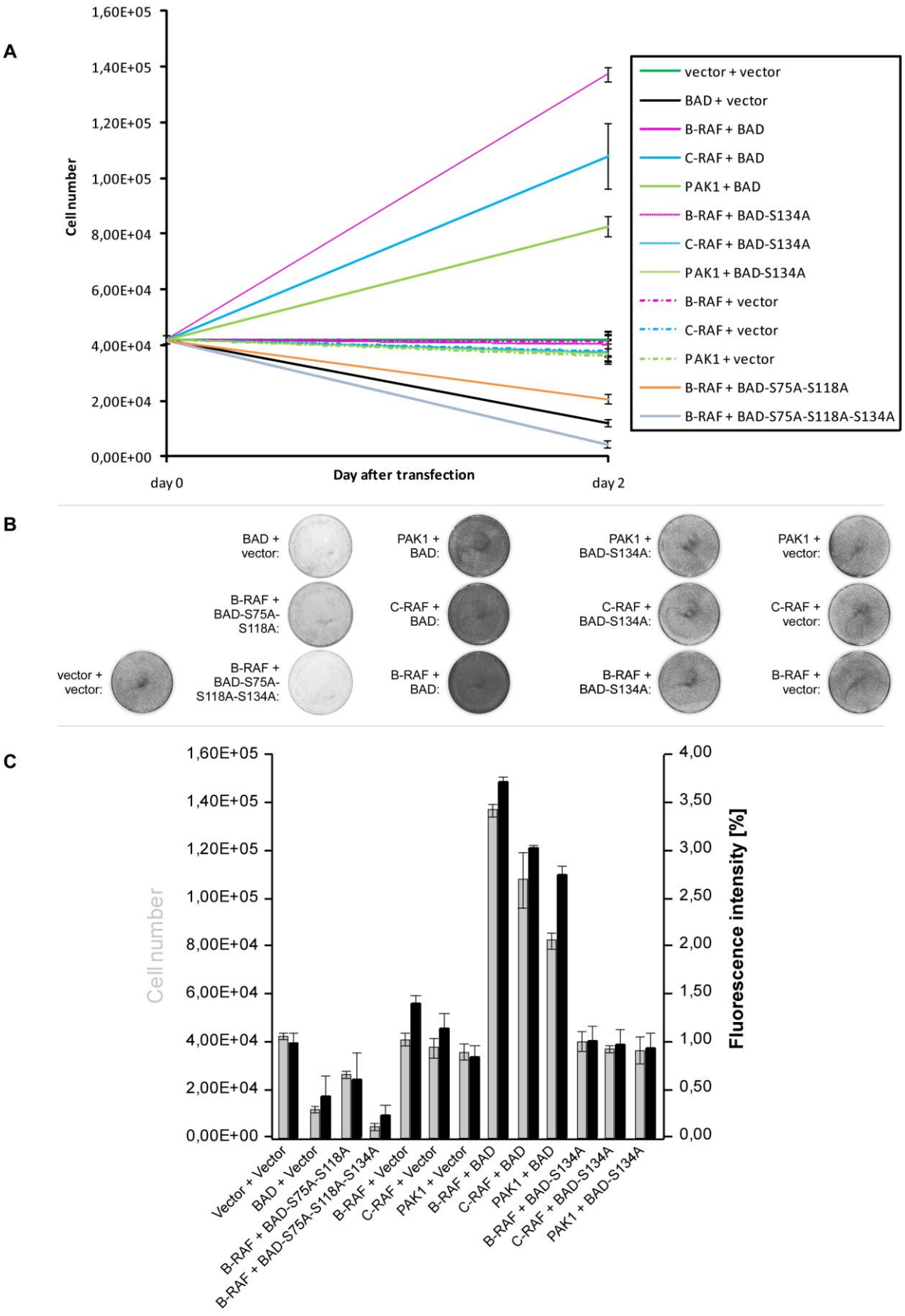
A
1,60E+05
1,40E+05
1,20E+05
1,00E+05
8,00E+04
6,00E+04
4,00E+04
2,00E+04
0,00E+00
Cell number
day 0
Day after transfection
day 2
vector + vector
BAD + vector
B-RAF + BAD
C-RAF + BAD
PAK1 + BAD
B-RAF + BAD-S134A
C-RAF + BAD-S134A
PAK1 + BAD-S134A
B-RAF + vector
C-RAF + vector
PAK1 + vector
B-RAF + BAD-S75A-S118A
B-RAF + BAD-S75A-S118A-S134A
B
vector + vector:
BAD + vector:
B-RAF + BAD-S75A-S118A:
B-RAF + BAD-S75A-S118A-S134A:
PAK1 + BAD:
C-RAF + BAD:
B-RAF + BAD:
PAK1 + BAD-S134A:
C-RAF + BAD-S134A:
B-RAF + BAD-S134A:
PAK1 + vector:
C-RAF + vector:
B-RAF + vector:
C
1,60E+05
1,40E+05
1,20E+05
1,00E+05
8,00E+04
6,00E+04
4,00E+04
2,00E+04
0,00E+00
Cell number
4,00
3,50
3,00
2,50
2,00
1,50
1,00
0,50
0,00
Fluorescence intensity [%]
Vector + Vector
BAD + Vector
B-RAF + BAD-S75A-S118A
B-RAF + BAD-S75A-S118A-S134A
B-RAF + Vector
C-RAF + Vector
PAK1 + Vector
B-RAF + BAD
C-RAF + BAD
PAK1 + BAD
B-RAF + BAD-S134A
C-RAF + BAD-S134A
PAK1 + BAD-S134A

Of note, the induction of cell proliferation by the co-expression of BAD with survival kinases is not only due to an inhibition of apoptosis as the percentage of apoptotic cells is similar to the vector control (Fig. 30A). These observations are not cell type specific since comparable results were obtained using HEK-293 cells (data not shown).

Taken together, we show here that serine134 has two functions during survival signaling. On the one hand this site controls intensity of BAD-mediated apoptosis and on the other hand it is involved in the regulation of proliferation.

Phosphorylation of BAD serine 134 plays an exclusive role in B-RAF mutant tumor cells – In experiments performed with cells containing wild type RAF or Ras we showed by overexpression that RAF kinases effectively phosphorylate BAD at position serine 134 whereas Akt/PKB caused relative low extents of Ser-134 phosphorylation (Fig. 28A). To test whether this observation is valid in naturally occurring tumor cells we investigated cancer cell lines possessing endogenously mutated RAF and Ras proteins. Two melanoma cell lines used in this study (A375 and SK-MEL-28) carry a valine-to-glutamic acid mutation at residue 600 of B-RAF (B-RAF-V600E) which leads to elevated RAF signaling in these cell lines (Davies *et al.* 2002) (see also Fig. 37). In contrast, the cell lines HCT 116, DX3 and MEL-Juso are known to harbor activating mutations within the *Ras* genes. Ras has been reported to activate a variety of cellular targets beside RAF, such as Ras-GDS, Tiam-1 and PI3K (for review see (Shaw and Cantley 2006)). Concerning driving tumorigenesis, one of the most probable targets of Ras is PI3K. This is known to activate the pro-survival Akt/PKB pathway (Amaravadi and Thompson 2005) (see also Fig. 37). As control we also used the tumor cell line PC3 that carries neither a RAF nor a Ras mutation. Surprisingly, the phosphorylation of BAD serine 134 was only observed in the cell lines containing B-RAF mutant (Fig. 32A). These results are in agreement with the experiments presented in Fig. 28A where we overexpressed RAF kinases and Akt/PKB in HeLa cells. The RAF Inhibitor Sorafenib (also known as BAY 43-9006 or Nexavar®) has been reported to decrease proliferation in B-RAF mutant tumor cells (Karasarides *et al.* 2004) (see also Fig. 32B). Interestingly, impaired proliferation goes along with a diminished phosphorylation of hBAD serine 134 in Sorafenib treated A375 and SK-MEL-28 cells (Fig. 32B and C). In contrast, the PI3K inhibitor Wortmannin had a minor effect on cell proliferation and phosphorylation of hBAD serine 134 (Fig. 32B and C). To investigate the putative synergistic effects between Sorafenib and Wortmannin, we also incubated the cells with both inhibitors together. Since Wortmannin barely impaired the effects of Sorafenib alone we could exclude the possibility that inhibition of PI3K leads to enhanced RAF signaling that would mask the effect of Wortmannin (Fig. 32B and C).

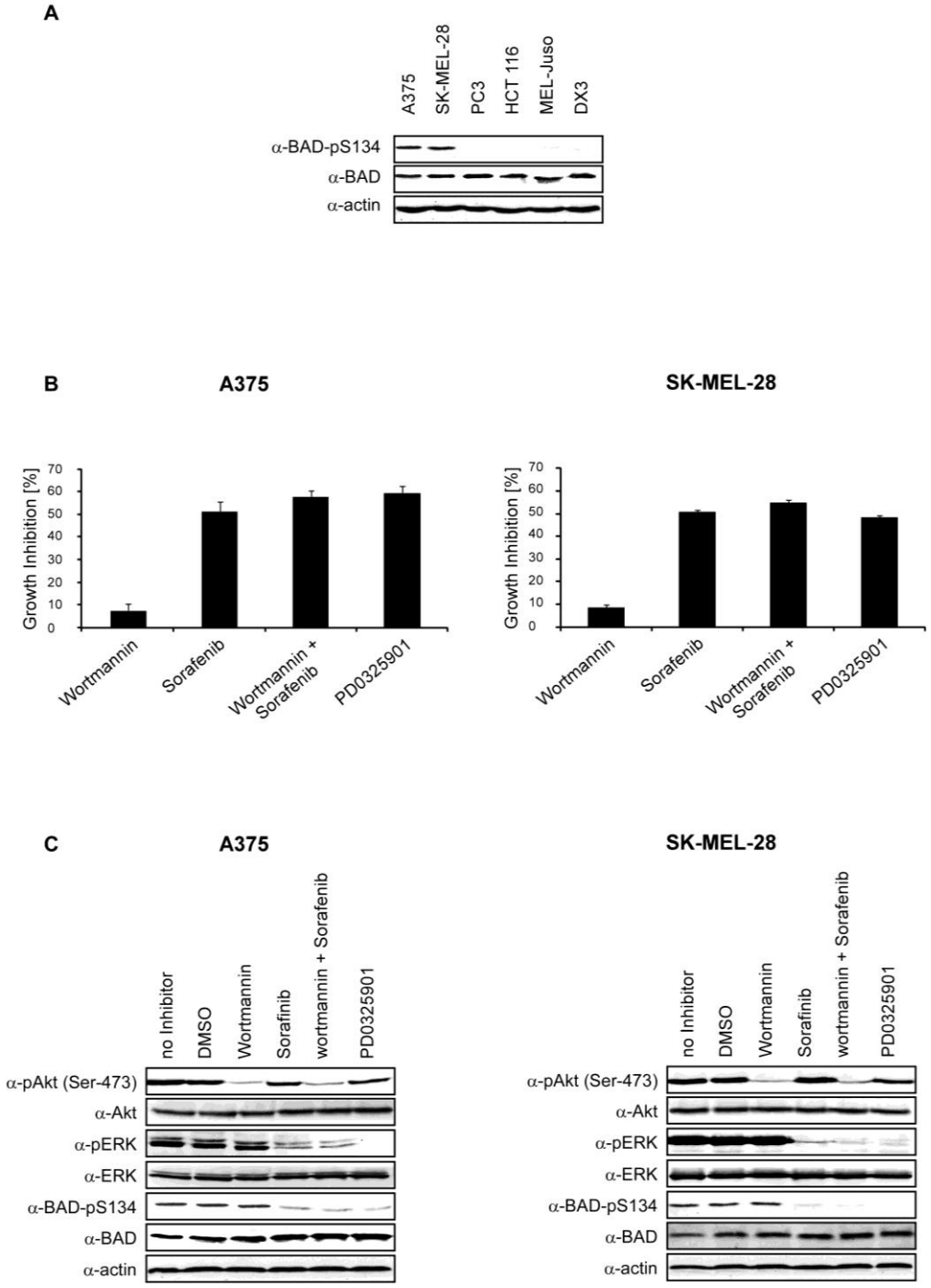

Figure 32: BAD serine 134 plays an exclusive role in B-RAF mutant tumor cells.
A, To monitor the phosphorylation degree of BAD at serine 134 in naturally occurring cancer cells, two cell lines that carry B-RAF-V600E mutant (A375 and SK-MEL-28), three cell lines that harbor activating mutations within the *RAS* genes (HCT 116, DX3 and MEL-Juso) and a control tumor cell line that carries neither RAF nor RAS mutation (PC3) were investigated. The amounts of the endogenous BAD protein, phosphorylation of BAD at serine 134 as well as endogenous actin were detected by immunoblotting. B and C, A375 and SK-MEL-28 cells were treated with the indicated kinase inhibitors and cell growth (B), expression levels of endogenous BAD and actin as well as phosphorylation of BAD serine 134 (C) were analyzed. The efficiency of the kinase inhibitors Wortmannin, Sorafenib or PD0325901 has been verified by change of Akt serine 473 and ERK phosphorylation, respectively.

Inhibition of MEK by PD0325901 affects proliferation and phosphorylation of hBAD serine 134 similar to inhibition of RAF by Sorafenib (Fig. 32B and C). This leads to the conclusion that although RAF kinases are potentially able to phosphorylate hBAD serine 134 directly (Fig. 28C), in naturally occurring tumor cell lines proliferation and phosphorylation of BAD serine 134 is apparently mediated through the RAF-MEK-ERK cascade. In agreement with published data (Boisvert-Adamo and Aplin 2008), inhibition of MEK or RAF leads to a slight increase of the whole amount of BAD protein (Fig. 32C), indicating a dual role of BAD in MAPK-mediated survival signaling. The efficiency of Wortmannin, Sorafenib or PD0325901 has been verified by change of Akt serine 473 and ERK phosphorylation, respectively. In cell lines containing mutated Ras, proliferation was more inhibited by Wortmannin than by Sorafenib or PD0325901 (Fig. 35). All three inhibitors barely caused inhibition of proliferation in cells containing neither a RAF nor Ras mutation (Fig. 35).

To analyze whether BAD directly contributes to cell proliferation in B-RAF mutant melanoma cells we used BAD-specific siRNA to downregulate the endogenous BAD protein (Fig. 33A). Compared to mock cells and control cells that were transfected with siRNA directed against luciferase, knock-down of BAD led to marked inhibition of proliferation in A375 and SK-MEL-28 cells (Fig. 33B).

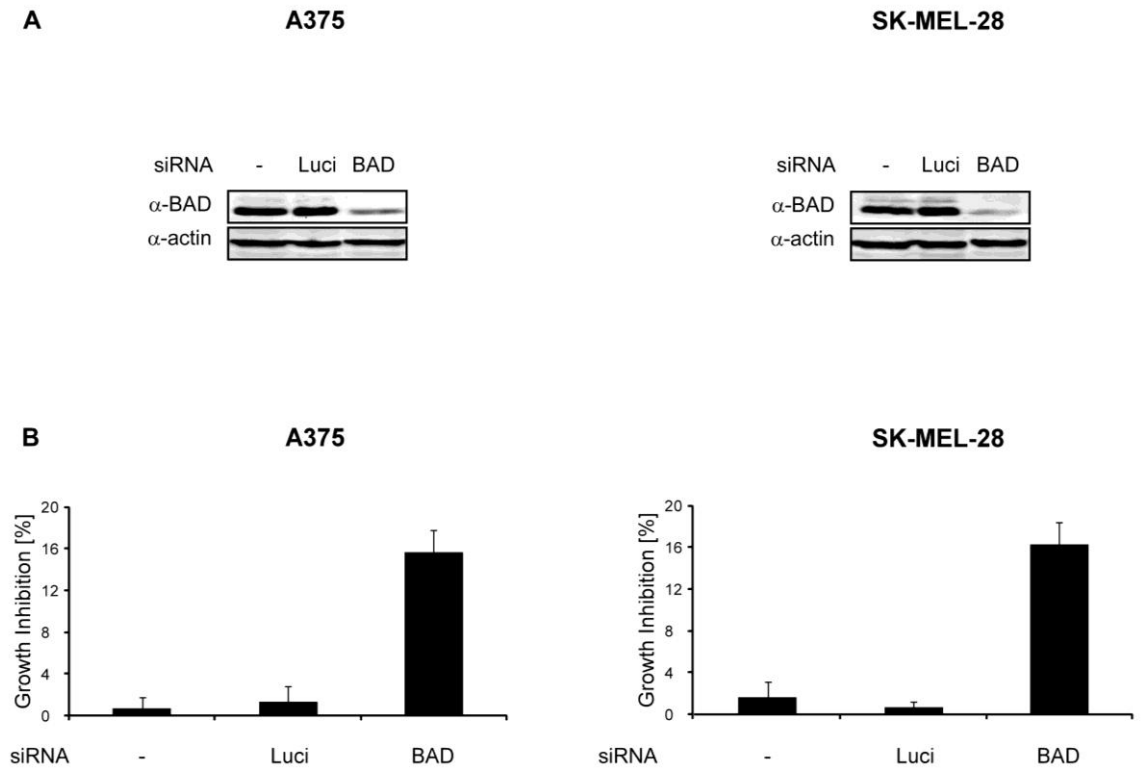

Figure 33: BAD is required for efficient proliferation in B-RAF mutant melanoma cells.
A375 and SK-MEL-28 cells were transfected with siRNAs against human BAD or luciferase as control. Two days post transfection knock-down of BAD at protein level (A) as well as the effect of BAD knock-down on cell growth (B) was analyzed. In A, actin levels show equal loading.

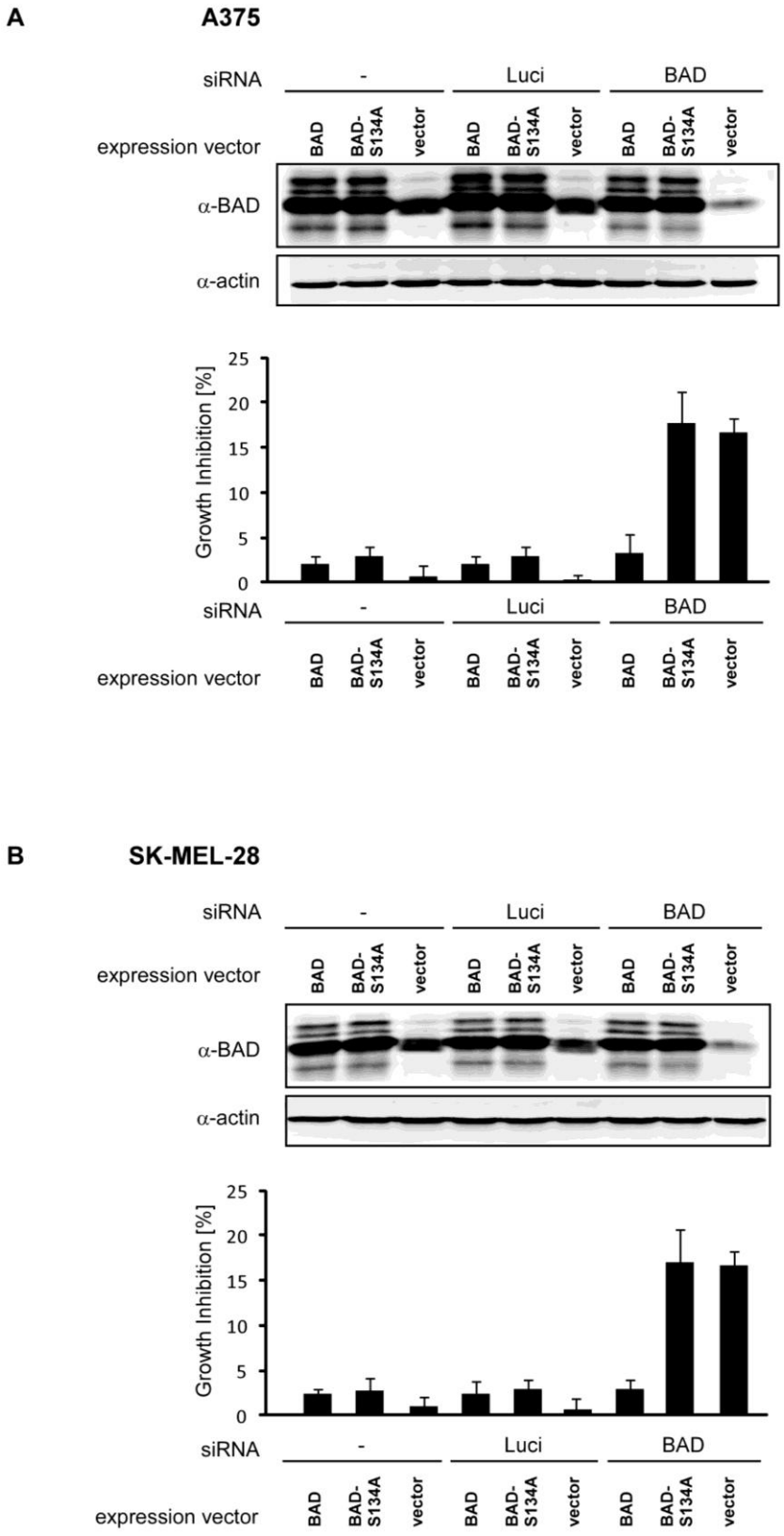

Figure 34: Phosphorylation of BAD at the position serine 134 is critical for B-RAF driven proliferation. A375 (A) and SK-MEL-28 (B) cells were co-transfected with siRNAs against the 3'-UTR of endogenous BAD (but not against exogenous BAD) or luciferase and the indicated expression vectors. Two days post transfection, knock-down of endogenous BAD and overexpression of BAD wild type as well as BAD-S134A mutant was monitored by immunoblotting. Actin levels show equal loading. The resulting growth inhibition is presented below (see *bar graph*).

This growth inhibition could be abrogated by overexpression of wild type BAD (Fig. 34). Importantly, overexpression of BAD serine 134 to alanine mutant was not able to rescue efficient proliferation upon knock-down of endogenous BAD. In cell lines containing mutated RAS and in cells containing neither a RAF nor RAS mutation, knock-down of BAD did not affect cell proliferation (Fig. 36).

3.4.4. Discussion

Post-translational modifications of BH3-only proteins, such as phosphorylation, proteolytic processing and lipid modifications emerged as regulatory elements that integrate extracellular survival signals with the apoptotic machinery. Regarding regulation of BAD function, phosphorylation plays perhaps the most important role among these post-translational events. Recently, using mass spectrometry we identified ten distinct phosphorylation sites within the human BAD protein ((Polzien *et al.* 2009), see also Fig. 26A). While some of these phosphoserines have been found to be located at

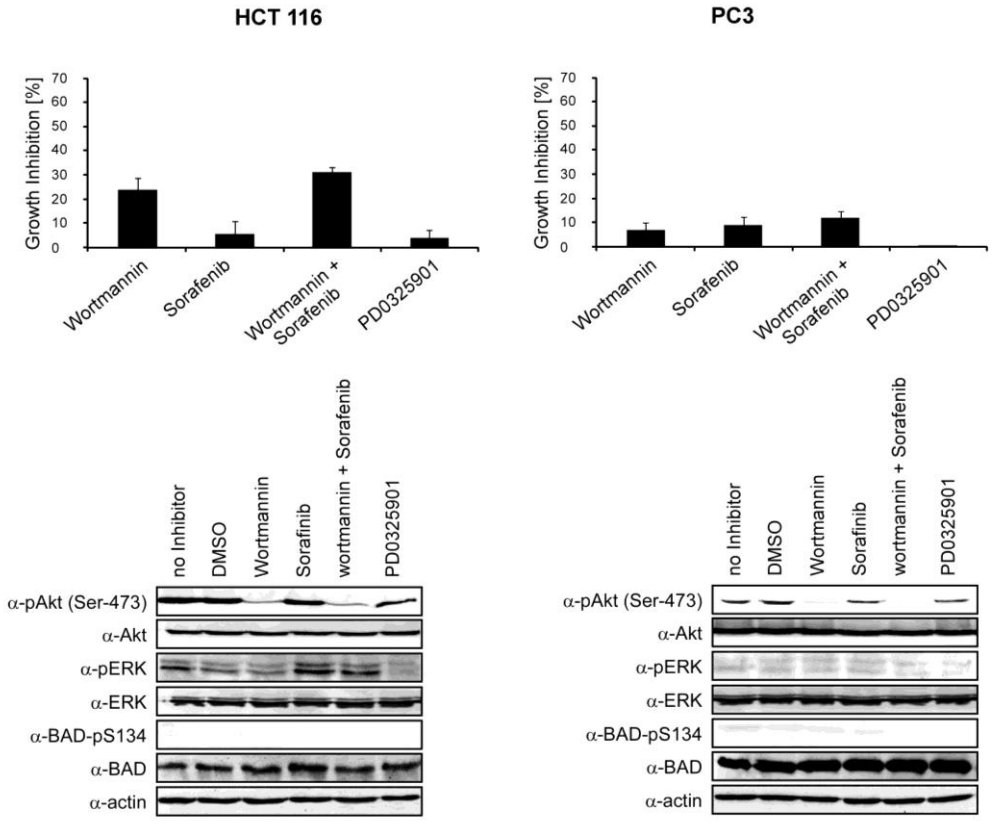

Figure 35: BAD serine 134 plays a minor role regarding cell growth in RAS mutant and B-RAF/RAS wild type tumor cells.
The tumor cell line HCT 116 that harbors mutated RAS and the tumor cell line PC3 that carries neither a RAF nor RAS mutation were treated with the indicated kinase inhibitors. Cell growth, expression levels of endogenous BAD, its phosphorylation at serine 134 and actin were analyzed. The efficiency of the kinase inhibitors Wortmannin, Sorafenib or PD0325901 has been verified by change of Akt serine 473 and ERK phosphorylation, respectively. Results obtained with RAS mutant tumor cell lines MEL-Juso and DX3 were analogous to results gained with HCT 116 cells (data not shown).

the N-terminus of hBAD (serines 25, 32 and 34) three other phosphorylation sites are positioned at the C-terminal part of the protein, i.e. serines 118, 124 and 134. The third group of hBAD phosphorylation sites (serines 75, 91, 97 and 99) are either directly or indirectly involved in binding of 14-3-3 proteins. As the function of the phosphoserines that regulate the interactions of BAD with 14-3-3 proteins has been thoroughly investigated so far (Datta *et al.* 2000; Hekman *et al.* 2006; Masters *et al.* 2001; Subramanian *et al.* 2001; Zha *et al.* 1996; Zhang *et al.* 2005), we examined in this study the role of serine phosphorylation at the N- and C-terminal parts of hBAD in more detail.

Substitution of Ser-124 and/or Ser-134 by alanine led to increase of apoptotic activity indicating that phosphorylation at these positions is actively involved in the control of apoptotic pathways (Fig. 27A). By contrast, substitution of N-terminal serines 25, 32 and 34 by alanine did not significantly

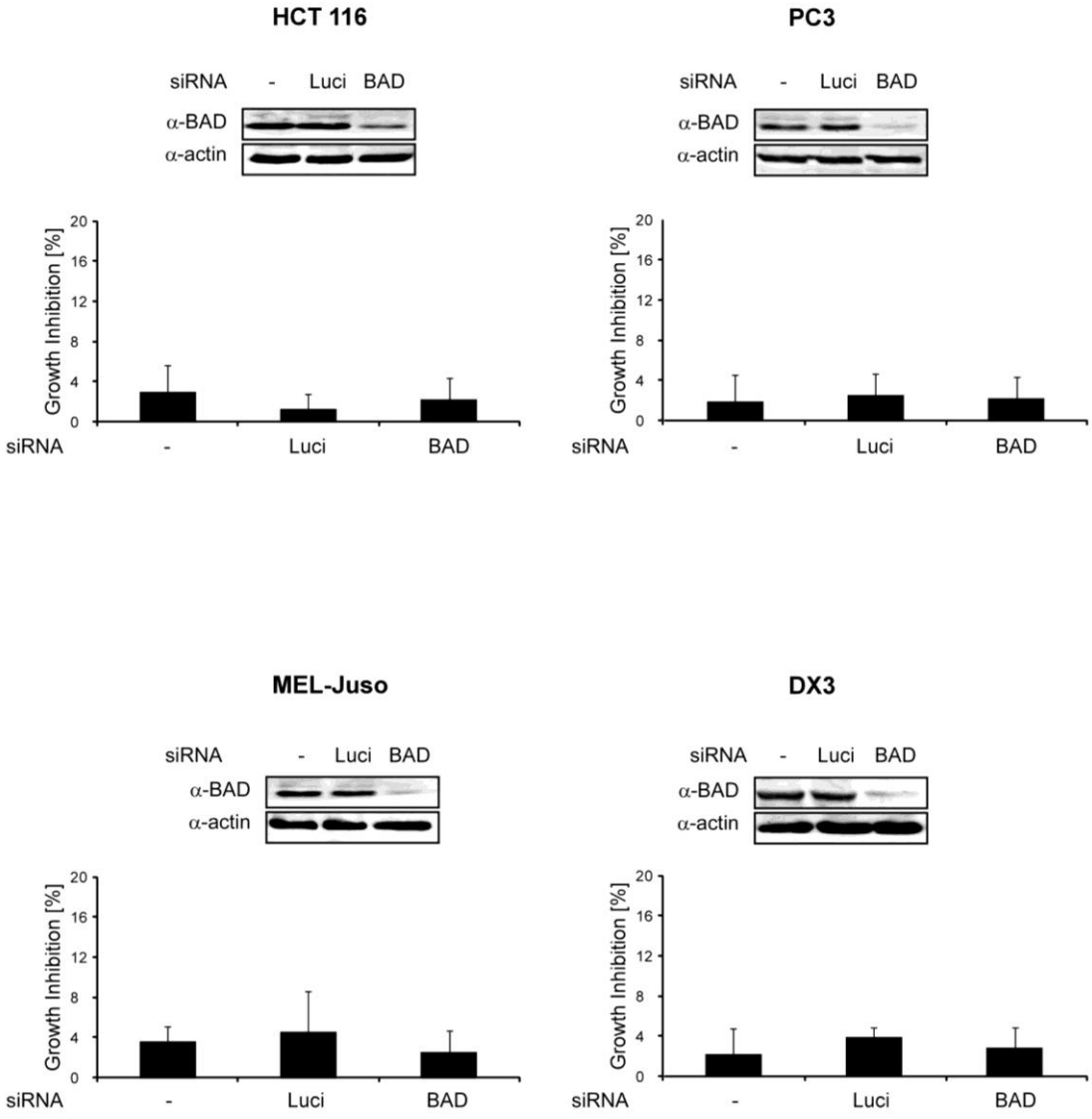

Figure 36: (right): BAD is not required for efficient proliferation in RAS mutant (HTC 116, MEL-Juso, and DX3) and B-RAF/RAS wild type (PC3) tumor cells.
The indicated tumor cell lines were transfected with siRNAs against BAD or luciferase. Two days post transfection, endogenous actin, knock-down of endogenous BAD at protein level (see inserts) as well as the effect of BAD knock-down on cell growth was monitored.

change the proapoptotic activities of BAD allowing the conclusion that the phosphorylation of the N-terminus does not play a decisive role in the regulation of cell survival. Although mutation of Ser-134 to alanine led to an increased apoptotic activity (Fig. 27A), in the presence of B-RAF this effect was less pronounced (Fig. 30A). This observation is in accordance with our previous results showing that B-RAF phosphorylates also serines 75 and 118 of human BAD, thereby inhibiting BAD mediated apoptosis (Polzien *et al.* 2009). Thus, the inhibition of hBAD-induced apoptosis by B-RAF could be realized mostly through phosphorylation of serines 75 and 118 whereas serine 134 mediates the fine tuning of BAD induced apoptosis.

In our previous attempts to characterize the translocation of BAD to mitochondria, we identified two lipid-binding domains (termed LBD1 and LBD2) within the C-terminal region of human BAD (Hekman *et al.* 2006). While LBD2 overlaps with helix-5 localized at the very C-terminus, LBD1 encompasses the C-terminal half of BH3 helix and covers also the short $S^{124}FKK^{127}$ region (Fig. 26A). Thus, due to its close proximity to the FKK motif it is feasible that the phosphorylation of Ser-124 may regulate BAD function by modulating the interaction of BAD with membrane lipids. However, the proposed regulation of BAD function by phosphorylation of Ser-124 seems to be unique for the human BAD protein since most of the mammalian homologues (e.g. murine BAD) do not contain the complete FKK motif (Fig. 26B). On the other hand, the alignment of human and murine BAD reveals that both BAD proteins contain the conserved segment $PRPKS^{134/170}AG$ comprising either Ser-134 in human or Ser-170 in murine BAD (Fig. 26B). Ser-170 has previously been identified as a BAD phosphorylation site in murine BAD (Dramsi *et al.* 2002). The recent availability of the phosphospecific antibodies against phosphoserine 134/170 allows the search for potential kinases that can phosphorylate Ser-134. Although the consensus sequence RXXS makes Akt/PKB probable as a potential phosphorylating kinase the two proline residues present in the motif PRPKSAG render this possibility unlikely. Indeed, co-expression of hBAD with Akt/PKB did not result in significant phosphorylation of Ser-134.

Instead, as shown in Fig. 28A we identified PAK1 and RAF as the most potent BAD-phosphorylating kinases under both, *in vivo* and *in vitro* conditions. Concerning PAK1 one should take into consideration that this kinase was described to phosphorylate BAD in an indirect manner targeting RAF as downstream effector kinase (Jin *et al.* 2005).

Intriguingly, our data display that co-expression of wild type BAD with RAF kinases and PAK1 strongly increases cell proliferation (Fig. 31) whereas BAD-S134A mutant abolishes this effect. As generally accepted the Ras-RAF-MEK-ERK pathway regulates cellular survival, differentiation and proliferation (Peyssonnaux and Eychene 2001; Rajalingam *et al.* 2007; Schreck and Rapp 2006; Wellbrock *et al.* 2004). Enhanced activation of this cascade, often caused through activating mutations in the composite proteins, is found in many tumors (Brose *et al.* 2002; Cohen *et al.* 2002). In human cancer, mutated RAF (mainly B-RAF) was identified in 60% of melanomas (Brose *et al.* 2002) and with lower incidence in papillary thyroid cancers (Cohen *et al.* 2003), colorectal carcinomas (Brose *et al.* 2002; Davies *et al.* 2002; Rajagopalan *et al.* 2002), and lung cancers (Brose *et al.* 2002). Ras mutations were found in about 15-30% of human cancers overall (Bos 1989; Brose *et al.* 2002; Pavey *et al.* 2004). Activating Ras and B-RAF mutations typically show mutual exclusivity in tumors (Brose *et al.* 2002; Davies *et al.* 2002; Gorden *et al.* 2003). Notably, although either mutated Ras or B-RAF is required for tumor development it was demonstrated that both mutations do not result in similar

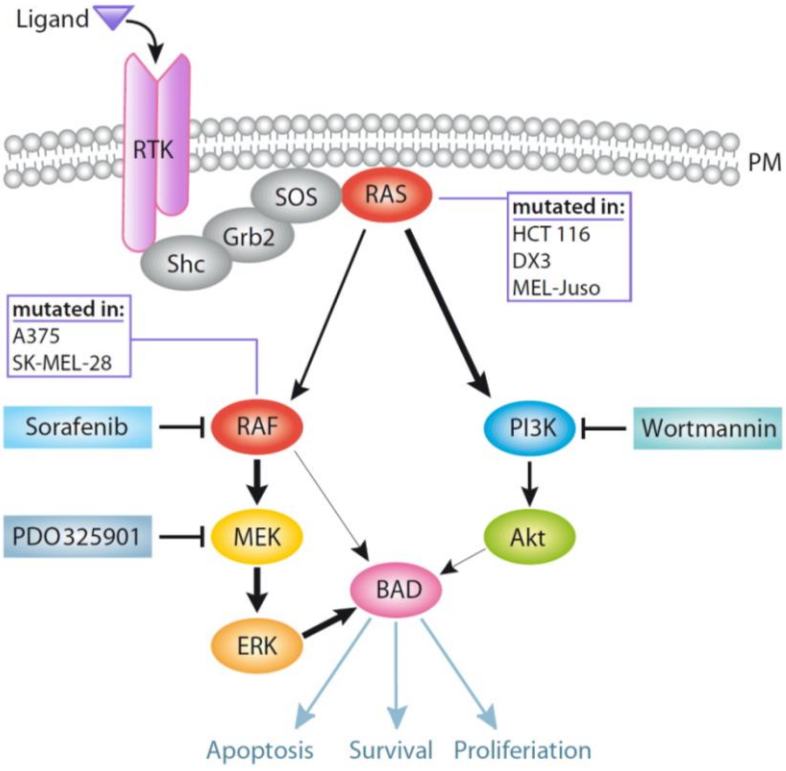

Figure 37: Schematic presentation of BAD serine 134 phosphorylation in RAF and Ras mutant tumor cells.
Stimulation of receptor tyrosine kinase (TRK) at the plasma membrane (PM) leads to activation of Ras GTPases and RAF kinases. The cell lines HCT 116, DX3 and MEL-Juso carry mutated *Ras* genes resulting in enhanced activation of the PI3K/Akt pathway. Although Akt was shown to be a BAD targeting kinase it has minor contribution in phosphorylating BAD at serine 134. The cell lines A375 and SK-MEL-28 harbor an activating mutation within B-RAF (V600E) that leads to elevated phosphorylation of BAD serine 134, mainly through the MEK-ERK cascade. The specific inhibitors of RAF, MEK and PI3K are highlighted in *blue boxes*. Phosphorylation of BAD at serine 134 affects efficiency of apoptosis and proliferation. Thick arrows indicate enhanced activation or phosphorylation. For more details see main text.

downstream effects (Cragg *et al.* 2008; Solit *et al.* 2006). In this study we disclose an additional parameter that is apparently involved in tumor progression. In this regard, we demonstrate that the phosphorylation of BAD serine 134 is increased in cell lines with elevated RAF activity but not in cells harboring a high Ras or Akt/PKB activity (Fig. 28A and Fig. 32A). Additionally, we found that in melanoma cells the phosphorylation of this site is preferentially realized through the RAF-MEK-ERK cascade (Fig. 32C) although RAF kinases are potentially able to phosphorylate this site directly (Fig. 28C). This result underlines the former observation that mutation of B-RAF leads to an exquisite dependency on MEK activity (Cragg *et al.* 2008; Solit *et al.* 2006) where the authors demonstrated that B-RAF mutant tumor cells are considerably more sensitive to MEK inhibition than either Ras mutant or B-RAF/RAS WT cells. These studies showed that only in B -RAF mutant cells MEK inhibition caused potent inhibition of proliferation (Cragg *et al.* 2008; Solit *et al.* 2006). The increased sensitivity to MEK inhibitors of B-RAF mutant cells was observed to be based on a different regulation of Bcl-2 proteins in these cell lines (Cragg *et al.* 2008). The aberrant regulation of Bcl-2 proteins in B-RAF mutant tumor cells may be realized by a specific mitochondrial localization of B-RAF-V600E compared to wild type B-RAF as recently reported (Lee *et al.* 2010). Concerning BAD phosphorylation, Eisenmann *et al*. demonstrated that the enhanced sensitivity to MEK inhibition is based on a melanoma-specific MAPK-mediated survival signaling (Eisenmann *et al.* 2003). In normal melanocytes BAD was shown to be phosphorylated at serines 75, 99 and 118, leading to insensitivity to MEK inhibition (Eisenmann *et al.* 2003). In contrast, in B-RAF mutant melanoma cells, BAD was only phosphorylated at serine 75. MEK inhibition resulted in dephosphorylation of this site and induction of apoptosis (Eisenmann *et al.* 2003). Another study linked resistance to anoikis in melanoma cells to phosphorylation of BAD serine 75 (Boisvert-Adamo and Aplin 2008). Accordingly, the MAPK dependent phosphorylation of BAD serine 75 seems to represent an important mechanism to escape from apoptosis, especially in melanoma cells. However, all former studies considered BAD to be only an inducer of apoptosis that is inactivated through phosphorylation, especially at serine 75. We demonstrate here for the first time that phosphorylation of serine 134 of hBAD is required for efficient proliferation in B-RAF-V600E containing tumor cells (Fig. 33 and 34). Serine 170 of murine BAD that corresponds to serine 134 of human BAD was previously connected to cell proliferation (Dramsi *et al.* 2002). However, one has to consider that the properties of murine BAD may differ from human BAD due to a large N-terminal extension. Additionally, in Dramsi et al. phosphorylation of serine 170 was mimicked by mutation of this residue to aspartic acid (Dramsi *et al.* 2002). Notably, in this study the kinases responsible for serine 134 phosphorylation as well as an involvement of this regulatory site in naturally occurring tumor cells has not been addressed. Here we disclose that BAD serine 134 is phosphorylated in a RAF-dependent manner and that BAD cooperates with RAF in promoting proliferation and therefore may play an active role during tumor development. The observation that MEK inhibition leads to a decrease in BAD serine 134 phosphorylation but to an increase in the amount of the whole BAD protein underlines the dual role of BAD. Under survival

conditions, BAD is phosphorylated at serine 134 and promotes proliferation in cells with elevated RAF activity. On the other hand, when entering apoptotic conditions, dephosphorylated BAD accumulates within the cell leading to complex formation with Bcl-2/X_L and induction of apoptosis. Thus, apoptosis and proliferation seem to be regulated through interplay between the phosphorylation sites serine 75, 118 and 134.

Conclusions – Results presented in this study open new insights regarding the function of BAD and are in accordance with studies pointing to alternative roles for BAD than apoptosis control (Danial *et al.* 2003). Furthermore, our findings showing that human BAD is actively involved in proliferation of B-RAF-V600E containing tumor cells may provide a new link between survival signaling and cancer development.

3.4.5. Acknowledgements

This work was supported by Deutsche Forschungsgemeinschaft Grant SFB 487 (Projects C3) and graduate college 1141 (GCWN). We thank Daniela Haug (University of Würzburg, Germany) and Joachim Fensterle (Æterna Zentaris, Germany) for providing cell lines and for fruitful discussions as well as Laura Goldberg (Lafayette College, NY, USA) for excellent cooperativeness and proof reading.

4. General Discussion

The phosphorylation of BAD provides an important connection between cell survival signaling and the apoptotic death machinery. A current model of BAD function implicates phosphorylation of at least three serine residues (using human nomenclature these are serine 75, 99, and 118). The immediate consequences of phosphorylation at these sites are complex formation of BAD with 14-3-3 proteins and dissociation of BAD from the pro-survival Bcl-2 family members. Besides these highly conserved serine residues, four other phosphorylation sites of murine BAD (positioned at serines 128 and 170 and threonines 117 and 201) have been identified. Remarkably, although much attention has been devoted to the phosphorylation-mediated regulation of mBAD function, with some exceptions the regulation of hBAD by phosphorylation has not been investigated yet. Therefore, we performed a systematic analysis of *in vivo* phosphorylation of hBAD protein by combined use of phosphospecific antibodies and mass spectrometry.

4.1. Identification of Novel hBAD *in vivo* Phosphorylation Sites by Mass Spectrometry

As presented in Fig. 8A, phosphorylation of all three highly conserved serines in purified hBAD were detectable by use of phosphospecific antibodies indicating that at least a fraction of hBAD expressed in Sf9 cells is associated with 14-3-3 proteins. To investigate, whether hBAD is phosphorylated at more than these three established phosphorylation sites (serines 75, 99 and 118), the purified hBAD samples were analyzed by both ESI-MS and nano-LC-MS/MS technique. The results obtained by MS analysis revealed numerous novel phosphorylation sites (Fig. 8B and Table 2). Interestingly, with exception of serine 25 and 32/34 most of the phosphorylated peptides are clustered within a 75 amino acid stretch that comprises also the BH3 domain. In contrast, the last 20 residues at the very C-terminal sequence bear no phosphate molecules.

Three peptides (peptide 95-112, 97-109 and 99-109) carrying one or two phosphates, include the sequence of the putative 14-3-3 binding domain RSR**S**^{99}AP. By use of phosphospecific antibodies, the serine 99 has been found to be phosphorylated in the hBAD sample (Fig. 8A). Surprisingly, in addition to serine 99, the peptide 95-112 was phosphorylated also at serine 97, indicating a novel regulatory mechanism regarding association of 14-3-3 proteins with hBAD. Possibly, the phosphorylation of the second serine in the position 97 within the 14-3-3 binding motif (R**S**^{97}RSAP) inhibits the association of hBAD with 14-3-3 proteins. Similar accumulation of phosphates has been observed within the C-terminal 14-3-3 binding motif of A-RAF kinase (R**S**^{580}A**S**^{582}EP) where both serines 580 and 582 were found to be phosphorylated (Baljuls *et al.* 2008). The authors proposed that the multiple phosphorylation of the C-terminal 14-3-3 binding region in A-RAF may be one of the reasons for the relative low activity of this RAF isoform. On the other hand, perturbations within the internal 14-3-3 binding domain of C-RAF (RST**S**^{259}TP) have been reported to be a reason for severe cardio-facio-cutaneous disorders called Noonan and LEOPARD syndrome (Pandit *et al.* 2007;

Razzaque *et al.* 2007). Displacement of the serine 259 by phenylalanine abolished the autoinhibitory mechanism of C-RAF resulting in a permanent active kinase form. In conclusion, we suggest that phosphorylation of the serine in position –2 relative to the obligatory phosphorylated serine within the 14-3-3 binding motif (e.g. serine 99 in hBAD) is sufficient to displace 14-3-3 from hBAD. In this scenario, previous dephosphorylation of the crucial serine within the 14-3-3 binding domain would be dispensable.

The binding motif surrounding serine 75 (RHS**S**^{75}YP) fulfills criteria for a typical 14-3-3 binding site as well (Aitken 2002). In hBAD, phosphorylation of serine 75 has been detected by use of phosphospecific antibody (see Fig. 8A). In addition, the fragmentation of the tryptic peptide 73-94 suggests phosphorylation of this residue (see Table 2). Fueller *et al.* (2008) reported recently that the transient phosphorylation of serine 75 in hBAD protein mediated by the activated catalytic domain of C-RAF promotes poly-ubiquitination of hBAD and increases the turn-over of this protein by proteosomal degradation. The alignment of the amino acid sequences of several mammalian BAD proteins reveals two PEST regions, which constitute a marker for proteins that undergo proteosomal degradation. Interestingly, one of these PEST regions overlaps with the 14-3-3 binding domain surrounding phosphoserine 75, thus, indicating a competition between 14-3-3 binding and the ubiquitination machinery.

Four other phosphopeptides (114-127, 116-126, 117-126 and 117-133) carrying either one or two phosphates, partially cover the BH3 domain where the serine 118 (corresponding to serine 155 in mBAD) is located. Phosphorylation of this residue regulates the interaction of BAD with Bcl-2/Bcl-X_L proteins. Importantly, within the peptide 117-133 two phosphates were detected (see Fig. 8B and Table 2). Because the number of phosphates within the peptide 117-133 corresponds to the number of phosphorylation possibilities, both serine residues (serine 118 and 124) within this peptide appear to be phosphorylated *in vivo*. Thus, we propose that besides the well-characterized serine 118, the serine 124 represents a novel phosphorylation site in hBAD.

Finally, we detected a peptide carrying five phosphates overlapping partially with the peptide 117-133 (Fig. 8B). This peptide has been ascribed to the C-terminal BAD region located between residues 128 and 149. At present, we cannot definitively specify the exact positions of all of the phosphates found by MS analysis. Nevertheless, the phosphorylation of serine 124 is very probable since it has already been detected within the peptide 117-133. In addition, the phosphorylation of murine BAD at the serine 170 (corresponding to serine 134 in hBAD) has been previously reported (Dramsi *et al.* 2002). As the alignment of human and murine BAD shows that both BAD proteins contain the conserved segment RPKS$^{134/170}$AG, it appears probable that this position is phosphorylated in both proteins. Indeed, two other phosphopeptides (132-142 and 134-142) confirmed this assumption. Nevertheless, the role of multiple phosphorylations at the C-terminal end of the hBAD protein remains

unclear. Such an accumulation of negative charged residues may support the depletion of hBAD from mitochondria.

4.2. Inhibition of hBAD-Induced Apoptosis by RAF Kinases

The pro-apoptotic protein BAD has been reported to be a substrate for a broad spectrum of kinases. Here we demonstrate that BAD is phosphorylated *in vivo* and *in vitro* by RAF kinases. Although it has been demonstrated previously that active C-RAF is involved in the phosphorylation of BAD (Wang *et al.* 1996) the role of RAF kinases in BAD phosphorylation is still controversially discussed (Harada *et al.* 1999; Jin *et al.* 2005; Kebache *et al.* 2007; Zha *et al.* 1996). Furthermore, the exact target sites of RAF within BAD protein have not been elucidated yet and B-RAF has so far not been considered as a BAD phosphorylating kinase. Our results indicate that RAF kinases (particularly B- and C-RAF) play an active role in BAD phosphorylation and regulation of apoptosis.

In the first part of this work, we investigated the role of RAF kinases in the phosphorylation of hBAD at the established phosphorylation sites Ser-75, 99, and 118. Therefore, we resolved BAD phosphorylation mediated by all three RAF kinases and compared it with data obtained by PKA, Akt/PKB and PAK1. *In vivo* experiments show that RAF kinases and PKA possess the ability to phosphorylate BAD at all three crucial serines (75, 99 and 118) whereas Akt/PKB and PAK1 were more efficient in phosphorylating the serine 99 that is involved in association of 14-3-3 proteins (Fig. 9). These findings indicate that besides kinase specificity intracellular localization may be important for substrate recognition.

Blocking of autocrine loops by Suramin, e.g. NF-κB pathway or stress kinase cascades (Fig. 11) to downregulate BAD phosphorylation, suggests that these pathways do not play an essential role in BAD regulation. By cultivating cells with three different MEK inhibitors (U0126, PD98059 and CI1040), we observed no differences in BAD phosphorylation in the presence of B-RAF (Fig. 11). In contrast, cells grown in the presence of RAF inhibitor Sorafenib (BAY 43-9006) or PKA inhibitor H-89 showed significant reduction of BAD phosphorylation, suggesting that RAF kinases and PKA are involved directly in suppression of BAD-mediated apoptosis (Figs. 9, 11 and 12). Although Sorafenib (BAY 43-9006) was initially developed as a RAF kinase inhibitor, it can additionally target the MAP kinase p38, several tyrosine kinases including VEGFR-2, Flt-3 and c-Kit but none of the reported BAD kinases (Fabian *et al.* 2005; Wilhelm *et al.* 2004). Importantly, Jin *et al.* (Jin *et al.* 2005) showed, in accordance with our results, that C-RAF/PAK-mediated BAD phosphorylation could be effectively inhibited *in vivo* in the presence of 2 μM RAF inhibitor Sorafenib (BAY 43-9006). In contrast, the use of MEK inhibitor PD98059 (20 μM) did not prevent BAD phosphorylation. Also consistently with our data, it has been shown by using the same cell line that Akt/PKB phosphorylates mBAD efficiently at serine 136 (Datta *et al.* 1997). Collectively, we compare here in the same experiment BAD phosphorylation by RAF and other kinases and show that Akt/PKB and PAK1

phosphorylate BAD with different specificity compared to RAF and PKA. Furthermore, we demonstrated that BAD-induced apoptosis can be inhibited by B- and C-RAF and showed that this inhibition is dependent on the phosphorylation of serines 75 and 118 of hBAD (Fig. 13).

Thus, based on data presented here, we suggest that *in vivo* phosphorylation of BAD by RAF kinases represents an important pathway in the phosphorylation of BAD domains, that are involved either in 14-3-3 protein association or mediate coupling/decoupling of BAD with Bcl-2 and Bcl-X_L proteins. To corroborate these findings we performed binding studies with purified components by use of BIAcore technique. In Fig. 14, we demonstrate that *in vitro* phosphorylation of BAD by activated C-RAF promotes association of BAD with 14-3-3ζ. We used 14-3-3ζ, since of the seven 14-3-3 isoforms analyzed this isoform bound phosphorylated BAD most efficiently (Hekman *et al.* 2006). While serines 75 and 118 are essentially not required for 14-3-3 binding, the domain surrounding serine 99 represents the preferential 14-3-3 binding site. However, a second binding site may enhance or stabilize this association.

C-RAF has been found to colocalize with mitochondria markers, indicating that a high proportion of C-RAF is located at mitochondria (Galmiche *et al.* 2008). The presence of activated C-RAF at mitochondria is also supported by the study of Jin *et al.* (2005) who demonstrated that PAK mediates C-RAF activation and its subsequent translocation to the mitochondria. At present, we cannot completely exclude the possibility that RAF kinases and PKA act simultaneously or synergistically, as it has been reported that C-RAF and PKA form a complex *in vivo* (Dumaz and Marais 2003). However, the C-RAF/PKA complex was found to be stable only in non-stimulated cells. It is possible that Akt/PKB and C-RAF also act as a complex *in vivo.* In this scenario, C-RAF would phosphorylate hBAD mainly at serines 75 and 118 and Akt/PKB might be responsible for serine 99 phosphorylation. These combined phosphorylations would enable effective association of 14-3-3 with BAD and separation from the BAD/Bcl-X_L complex. She *et al.* (2005) proposed that BAD might represent the convergence point of the RAF- and the PI3K/Akt kinase pathway. According to this report, BAD protein acts as a switch that integrates the anti-apoptotic effects of the EGFR/MAPK and PI3K/Akt pathways (as detected in MDA-468 cancer cells). This model is further supported by the observation that BAD can associate with PKB and B-RAF in conjunction with the co-chaperone BAG-1 at the mitochondrial level (Gotz *et al.* 2005).

4.3. Channel-Forming Activity of hBAD is Controlled by Phosphorylation and 14-3-3 Proteins

Within the Bcl-2 family of proteins Bcl-2, Bcl-X_L, Bak, Bax and the BH3-only protein Bid have been reported to possess channel-forming ability in artificial lipid bilayers (Antonsson *et al.* 1997; Minn *et al.* 1997; Schendel *et al.* 1999; Schendel *et al.* 1997; Schlesinger *et al.* 1997). In addition, it was observed by confocal and electron microscopy that Bak and Bax coalesce during apoptosis into large clusters on the surface of mitochondria (Karbowski *et al.* 2002). Here we present biophysical

evidence that the pro-apoptotic BH3-only protein BAD forms channels in artificial membranes (Fig. 16). Additionally, we could show that BAD pores possess a funnel-shaped geometry and that ions as well as non-charged molecules with molecular weights up to 200 Da can enter the BAD pore (Fig. 20). To form pores such proteins must contain helices that are long enough to span the membrane bilayer and these helices must be largely devoid of charged residues (Schendel *et al.* 1998). As an average lipid bilayer has a hydrophobic cross-section of ≈30 Å (Montal and Mueller 1972), the α-helix needs to be ≈20 residues long in order to span a membrane bilayer and to be able to participate in channel formation (Schendel *et al.* 1998). A helix probability plot of human BAD exhibited a C-terminal region of about 20 residues with a high probability of a helical structure and only two charged residues (Hekman *et al.* 2006). This region is surrounded by positively charged residues, which may additionally facilitate the association of the protein with membranes. Although one helix is insufficient to form a channel, some molecules could come together, each contributing their hydrophobic helix to create a pore. Furthermore, in the vicinity of this putative C-terminal helix a second lipid binding domain in human BAD comprising the FKK motif has been identified (Hekman *et al.* 2006).

We show here that hBAD is able to form channels which exhibit multiple conductance states with complex opening kinetics. Similar properties have also been reported for other Bcl-2 family members including Bcl-X_L, Bcl-2, Bax and Bid (Antonsson *et al.* 1997; Dejean *et al.* 2006; Minn *et al.* 1997; Schendel *et al.* 1997; Schlesinger *et al.* 1997). The presence of three different channel activities with progressively greater conductances (≈500 pS, ≈750 pS and ≈3750 pS), but occurring with progressively lesser frequency, raises the possibility of step-wise oligomerization of hBAD protein molecules in planar bilayers. The Bax channel progresses within 2-4 min of its initial appearance (Schlesinger *et al.* 1997). This includes an early low-conducting channel, followed by a transition phase with multiple sub-conductance levels and finally achieves an apparently stable ohmic pore of large conductance. Our findings that the lower conductive hBAD channels are flickering between a closed and an open state and the higher conductive hBAD channels persist open (Figs. 16A and B) raises the question of what factors may control opening and closing of hBAD channels *in vivo*. Although it was demonstrated, that phosphorylation of BAD does not affect the membrane binding significantly (Hekman *et al.* 2006), dephosphorylated hBAD fails to form discrete channels in lipid bilayers. Possibly, some specific phosphorylation sites of hBAD are responsible for the formation of particular conductance states. Furthermore, we observed that 14-3-3 proteins disrupt hBAD's assembly into the lipid membrane and that 14-3-3 is able to remove or close existing hBAD channels. Based on these data we propose that the formation of hBAD pores is a reversible process that is regulated by phosphorylation and 14-3-3 proteins. This fits well to the suggested model that BAD is a membrane associated protein that has the hallmarks of a receptor rather than a ligand which shuttles in a phosphorylation-dependent manner between mitochondria and other membranes with 14-3-3 as a key regulator of this relocation (Hekman *et al.* 2006).

4.4. Structural Transitions of the hBAD C-Terminus Regulate its Pore-Forming Activity

The amino acid sequence of BAD does not allow an exact prediction for the existence of a C-terminal transmembrane domain. Thus, a prediction of the sterical conformation of the BAD pore is quite difficult. However, two lipid binding domains (LBD1 and LBD2) have been identified at the BAD C-terminus (Hekman *et al.* 2006). Therefore, to define a precise connection between pore-forming activity and structure of BAD, we analyzed in this study the secondary structure of the C-terminal part of hBAD including the helix region located within the conserved BH3 domain. Previous data regarding the secondary structure of hBAD are contradictory. While Yang (2009) predicted seven α-helices for hBAD, Hinds *et al.* (2007) provided evidence that BH3-only proteins such as Bim, Bmf and BAD are intrinsically unstructured in the absence of binding partners. The results presented here demonstrate that the C-terminal part of hBAD reveals dynamic structural elements conditioned by its immediate environment (Fig. 22 and Table 5). In principle, the data presented here are not contradictory to the results reported by Hinds *et al.* (2007). However, it is difficult to make a correlation between our data and results published in Hinds *et al.* (2007) because they used for their NMR measurements a BAD construct missing the C-terminal part. Nevertheless, these authors showed that BAD undergoes localized conformational changes upon binding to Bcl-2 targets. Contrary to this study, we observed in solution (i.e. in the absence of lipid vesicles) a high degree of β-sheet elements within the BH3 domain and the C-terminal fragment (Fig. 22 and Table 5). In the presence of liposomes or lipid micelles, we detected dramatic changes of the secondary structure. As summarized in Table 5 the helix and β-sheet propensity was considerably increased in the presence of liposomes or lipid micelles. This holds for C-terminal segment of hBAD and non-phosphorylated BH3 domain. Surprisingly, phosphorylation of serine 118 within the BH3 domain strongly reduces the formation of α-helical structures. The consequence of the phosphate introduction in this position was a complete abolishment of helical structure, as documented by CD measurements performed in absence or presence of lipids (Fig. 22 and Table 5). Considering these observations and keeping in mind that the BAD lipid binding domains are localized within the C-terminal part of the protein, we hypothesized that the elements responsible for pore-forming activity of hBAD may be located within the Peptides1 and -3 that cover the C-terminal part and the BH3 region (see also Fig. 21). Indeed, the measurements regarding channel-forming ability using these peptides confirmed this assumption. Moreover, as shown in Fig. 23 our data demonstrate that only the interaction of the C-terminal Peptide3 with peptides covering the phosphorylated form of BH3 domain (Peptide1-pS118, Peptide2-pS118 and Peptide2-pS99-pS118) allows the formation of large, fast accumulating and permanently open pores. In lipid environment hBAD C-terminus as well as the phosphorylated BH3 domain exhibits a high proportion of β-sheet structure (Peptide3 and Peptide1-pS118, Table 5). Accordingly, only the combination of peptides that display a high amount of β-sheet structure in lipid environment were shown to possess pore-forming activity. This observation indicates that BAD pores might be

composed of β-barrels similar to VDAC channels as reported by Hiller *et al*. (2008). Notably, in the absence of the BAD C-terminus, the non-phosphorylated BH3 domain (Peptide1) was also able to form channels. In contrast to the phosphorylated BH3 domain, this peptide showed a high proportion of α-helical structures in lipid environment (see Table 5). Consequently, it assembled to less stable pores than its phosphorylated counterpart did (Fig. 23). Therefore, pores formed by the non-phosphorylated BH3 domain seem to possess another secondary structure, probably consisting of α-helices.

Leber *et al.* (2007) recently discussed an *embedding together model* that emphasizes the importance of the interaction of Bcl-2 family proteins with and within membranes. Additionally, the model proposes that interactions between pro- and anti-apoptotic Bcl-2 proteins are governed by membrane-dependent conformational changes. Our results regarding conformational changes of the C-terminal part of hBAD dependent on the presence of membranes and the fact that translocation of Bcl-X_L to the mitochondrial membrane occurs by complex formation with BAD (Jeong *et al.* 2004) are consistent with the *embedded together model*.

Together, we show in this work that the C-terminal part of hBAD (comprising BH3 domain and C-terminus) is *per se* sufficient to form ion channels. We identified phosphorylation of the RAF target site serine 118 within the BH3 domain to be essential for the formation of pores in the presence of the C-terminus. Furthermore, we disclosed that serine 99 plays an important role in controlling pore-formation via interacting with 14-3-3 proteins. Our results emphasize that phosphorylation alone is insufficient to release BAD from membranes, because the depletion process depends on 14-3-3 proteins. *In vivo*, the formation of hBAD pores may also be affected by other proteins that have been reported to interact with BAD. Two candidates are Akt/PKB and B-RAF that were demonstrated to co-immunoprecipitate with BAD (Gotz *et al.* 2005). It is possible that these kinases affect hBAD's pore-forming ability beside their BAD phosphorylating activity. Another open issue is the putative influence of other pore-forming members of the Bcl-2 family of proteins, like Bcl-2 and Bcl-X_L that have been shown to interact with BAD (Minn *et al.* 1997; Schendel *et al.* 1997; Yang *et al.* 1995). Do they merely shut off their own and hBAD's pore-forming activity by heterodimerization or do they alternatively form counteracting pores? Our preliminary data suggest that Bcl-X_L does not abolish pore formation of hBAD (data not shown). Similar observations were reported with respect to the effects of Bax on the pore-forming ability of Bcl-2. Although it was demonstrated that Bax interacts preferentially with the membrane-inserted form of Bcl-2 (Dlugosz *et al.* 2006), it was reported that Bax does not merely abrogate pore formation of Bcl-2 (Schendel *et al.* 1997). These authors suggested that Bcl-2 allows the transport across membranes in a direction that is cytoprotective, whereas Bax does the opposite. Bcl-X_L and hBAD may also be involved in controlling such a homeostasis. In this regard, it should be mentioned that hBAD forms pores in its phosphorylated and non-apoptotic state. Therefore, it is possible that it cooperates with anti-apoptotic proteins instead of counteracting them.

Results presented here raised the question: What could be the physiological role of hBAD channels? hBAD pores could act as ion channels and contribute to the regulation of various cellular processes. Ca^{2+} for instance, is regulating the mitogenic cascade at multiple positions (Ren *et al.* 2008). Concerning Ca^{2+} signaling, it was demonstrated that BAD targets the permeability transition pore (that has been suggested to be critical in apoptosis (Roy *et al.* 2009; Zamzami *et al.* 1996; Zamzami *et al.* 1996)) and sensitizes it to Ca^{2+} in a phosphorylation dependent manner (Roy *et al.* 2009). hBAD forms pores in its phosphorylated and non-apoptotic state. Therefore, BAD pores might play a role in processes that are not associated with apoptosis.

A previous model of BAD inactivation proposed sequential phosphorylation including phosphorylation of serine 118 and consequently disruption of the BAD/Bcl-X_L complex (Datta *et al.* 2000). This process may finally result in depletion of BAD from mitochondria by complex formation with 14-3-3 proteins and inhibition of apoptosis. In this study, we show that the phosphorylation of serine 118 does not only lead to inhibition of BAD-induced apoptosis. Phosphorylation at this position results in formation of open pores (see Fig. 23). The translocation model, first presented by the group of Rebollo (Ayllon *et al.* 2002; Fleischer *et al.* 2004; Garcia *et al.* 2003) and extended by our results (Hekman *et al.* 2006; Rapp *et al.* 2007) involves recruitment of BAD to the lipid rafts. This process is regulated by growth factor stimulation and is dependent on phosphorylation of the 14-3-3 binding motif. In this model, it was suggested that the BAD/14-3-3 complex is of transient nature (see also Fig. 38). Due to its preferential affinity for cholesterol rich membranes (Hekman *et al.* 2006) the BAD/14-3-3 complex translocates readily to rafts, whereby dissociation of 14-3-3 occurs. Thus, the pore-formation of phosphorylated BAD protein would take place rather at rafts located at plasma membrane than mitochondria. Pore-formation data presented here (see Fig. 23) with doubly phosphorylated Peptide2 (Peptide2-pS99-pS118) supports strongly this pathway.

Rafts and caveolae (which can be considered as a subclass of rafts (Anderson 1998; Smart *et al.* 1999)) play an important role for the interactions of a number of signaling molecules. Several signaling associated proteins such as heterotrimeric and small G-proteins, Src kinases, eNOS, Shc, Nck MAPK and RAF kinases have been found to be attached to the rafts/caveolae microdomains (Hekman *et al.* 2002). We showed in this work that formation of open pores requires phosphorylation of the RAF target site serine 118 (Fig. 23). Thus, it is feasible that hBAD pores and RAF kinases cooperate in signaling processes in rafts of the plasma membrane. We could demonstrate that ions as well as non-charged molecules up to 200 Da can enter the hBAD channel. Thus, BAD channels should be permeable for many signaling molecules and may contribute to positive feedback loops. The close proximity between hBAD and RAF kinases at the plasma membrane might also be a hint for a contribution of hBAD pores in the mechanism of endocytosis. Indeed, BAD has been shown to play a role in cellular membrane trafficking. Beside its contribution to glucose metabolism, the regulation of autophagy displays a further non-apoptotic function of BAD (Danial *et al.* 2003; Maiuri *et al.* 2007).

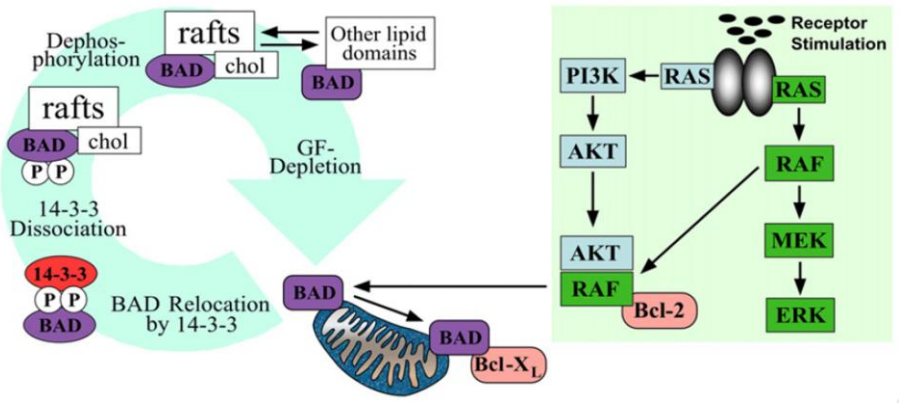

Figure 38: Model of BAD regulation involving phosphorylation by RAF and relocation mediated by 14-3-3 binding.
Phosphorylated BAD in complex with 14-3-3 proteins does not associate with mitochondrial membranes, but selectively binds to cholesterol rich (raft-like) membranes. Thus, the role of BAD as a receptor of Bcl-2 like proteins at the mitochondrial outer membrane is abolished. Figure adapted from Rapp *et al.*(2007).

4.5. Serine 134 of hBAD is Phosphorylated by RAF Kinases and Contributes to Apoptosis Control

Regarding regulation of hBAD function, phosphorylation plays perhaps the most important role among all post-translational events. Using mass spectrometry, we identified ten distinct phosphorylation sites within hBAD (Fig. 8B). While some of these phosphoserines have been found to be located at the N-terminus of hBAD (serines 25, 32 and 34) three other phosphorylation sites are positioned at the C-terminal part of the protein, i.e. serines 118, 124 and 134. The third group of hBAD phosphorylation sites consists of serines 75, 91, 97 and 99, that are either directly or indirectly involved in binding of 14-3-3 proteins. As the function of the phosphoserines that regulate the interactions of BAD with 14-3-3 proteins has been thoroughly investigated previously (Datta *et al.* 2000; Hekman *et al.* 2006; Masters *et al.* 2001; Subramanian *et al.* 2001; Zha *et al.* 1996; Zhang *et al.* 2005), we examined in this work the role of serine phosphorylation at the N- and C-terminal parts of hBAD in more detail. Substitution of Ser-124 or Ser-134 by alanine led to increase of apoptotic activity indicating that phosphorylation at these positions is actively involved in the control of apoptotic pathways (Fig. 27A). By contrast, substitution of N-terminal serines 25, 32 and 34 by alanine did not significantly change the pro-apoptotic activities of hBAD allowing the conclusion that the phosphorylation of the N-terminus does not play a decisive role in the regulation of cell survival. Although mutation of Ser-134 to alanine led to an increased apoptotic activity (Fig. 27A), in the presence of B-RAF this effect was less pronounced (Fig. 30A). This observation is in accordance with our previous results showing that B-RAF phosphorylates also serines 75 and 118 of human BAD, thereby inhibiting hBAD mediated apoptosis (Figs. 9-13). Thus, the inhibition of hBAD-induced apoptosis by B-RAF could be realized mostly through phosphorylation of serines 75 and 118 whereas serine 134 mediates the fine-tuning of BAD induced apoptosis.

Within BAD protein, the lipid binding domain LBD1 encompasses the C-terminal half of BH3 helix and covers the short $S^{124}FKK^{127}$ region (Fig. 26A). Thus, due to its close proximity to the FKK motif it is feasible that the phosphorylation of Ser-124 may regulate hBAD function by modulating the interaction of hBAD with membrane lipids. However, the proposed regulation of hBAD function by phosphorylation of Ser-124 seems to be unique for the human BAD protein since most of the mammalian homologues (e.g. murine BAD) do not contain the complete FKK motif (Fig. 26B). On the other hand, the alignment of human and murine BAD reveals that both BAD proteins contain the conserved segment $PRPKS^{134/170}AG$ comprising either Ser-134 in human or Ser-170 in murine BAD (Fig. 26B). Ser-170 has previously been identified as a BAD phosphorylation site in murine BAD (Dramsi *et al.* 2002). The recent availability of the phosphospecific antibodies against phosphoserine 134/170 allowed the search for potential kinases that can phosphorylate Ser-134. Although the consensus sequence RXXS makes Akt/PKB probable as a potential phosphorylating kinase the two proline residues present in the motif PRPKSAG render this possibility unlikely. Indeed, co-expression of hBAD with Akt/PKB did not result in significant phosphorylation of Ser-134. Instead, as shown in Figs. 28A and 29 we identified PAK1 and RAF as the most potent hBAD serine 134-phosphorylating kinases under both, *in vivo* and *in vitro* conditions. Concerning PAK1, one should take into consideration that this kinase was described to phosphorylate BAD in an indirect manner targeting RAF as downstream effector kinase (Jin *et al.* 2005).

4.6. BAD Contributes to RAF-Mediated Proliferation and Cooperates with B-RAF-V600E in Cancer Signaling

Unexpectedly, our data display that co-expression of RAF kinases and PAK1 with wild type BAD strongly increases cell proliferation whereas BAD-S134A mutant abolishes this effect (Fig. 31). As generally accepted the Ras-RAF-MEK-ERK pathway regulates cellular survival, differentiation and proliferation (Peyssonnaux and Eychene 2001; Rajalingam *et al.* 2007; Schreck and Rapp 2006; Wellbrock *et al.* 2004). Enhanced activation of this cascade, often caused through activating mutations in the composite proteins, is found in many tumors (Brose *et al.* 2002; Cohen *et al.* 2002). In human cancer, mutated RAF (mainly B-RAF) was identified in 60% of melanomas (Brose *et al.* 2002) and with lower incidence in papillary thyroid cancers (Cohen *et al.* 2003), colorectal carcinomas (Brose *et al.* 2002; Davies *et al.* 2002; Rajagopalan *et al.* 2002), and lung cancers (Brose *et al.* 2002). Ras mutations were found in about 15-30% of human cancers overall (Bos 1989; Brose *et al.* 2002; Pavey *et al.* 2004). Activating Ras and B-RAF mutations typically show mutual exclusivity in tumors (Brose *et al.* 2002; Davies *et al.* 2002; Gorden *et al.* 2003). Notably, although either mutated Ras or B-RAF is required for tumor development it was demonstrated that both mutations do not result in similar downstream effects (Cragg *et al.* 2008; Solit *et al.* 2006). In this work, we disclose an additional parameter that is apparently involved in tumor progression. In this regard, we demonstrate that the phosphorylation of hBAD serine 134 is increased in cell lines with elevated RAF activity but not in cells harboring a high Ras or Akt/PKB activity (Figs. 32A and 37). Additionally, we found that in

melanoma cells the phosphorylation of this site is preferentially realized through the RAF-MEK-ERK cascade (Fig. 32C) although RAF kinases are potentially able to phosphorylate this site directly (Fig. 28C). This result underlines the former observation that mutation of B-RAF leads to an exquisite dependency on MEK activity (Cragg *et al.* 2008; Solit *et al.* 2006) where the authors demonstrated that B-RAF mutant tumor cells are considerably more sensitive to MEK inhibition than either Ras mutant or B-RAF/Ras WT cells. These studies showed that only in B-RAF mutant cells MEK inhibition caused potent inhibition of proliferation (Cragg *et al.* 2008; Solit *et al.* 2006). The increased sensitivity to MEK inhibitors of B-RAF mutant cells was observed to be based at least in part on a different regulation of Bcl-2 proteins in these cell lines (Cragg *et al.* 2008). The aberrant regulation of Bcl-2 proteins in B-RAF mutant tumor cells may be realized by a specific mitochondrial localization of B-RAF-V600E compared to wild type B-RAF as recently reported (Lee *et al.* 2010). Concerning BAD phosphorylation, Eisenmann *et al*. (2003) demonstrated that the enhanced sensitivity to MEK inhibition is based on a melanoma-specific MAPK-mediated survival signaling. In normal melanocytes BAD was shown to be phosphorylated at serines 75, 99 and 118, leading to insensitivity to MEK inhibition (Eisenmann *et al.* 2003). In contrast, in B-RAF mutant melanoma cells, BAD was only phosphorylated at serine 75. MEK inhibition resulted in dephosphorylation of this site and induction of apoptosis (Eisenmann *et al.* 2003). Another study linked resistance to anoikis in melanoma cells to phosphorylation of BAD serine 75 (Boisvert-Adamo and Aplin 2008). Accordingly, the MAPK dependent phosphorylation of BAD serine 75 seems to represent an important mechanism to escape from apoptosis, especially in melanoma cells. However, all former studies considered BAD to be only an inducer of apoptosis that is inactivated through phosphorylation, especially at serine 75. We demonstrate here for the first time that phosphorylation of serine 134 of hBAD is required for efficient proliferation in B-RAF-V600E containing tumor cells (Figs. 33 and 34). Serine 170 of murine BAD that corresponds to serine 134 of human BAD was previously connected to cell proliferation (Dramsi *et al.* 2002). However, one has to consider that the properties of murine BAD may differ from human BAD due to a large N-terminal extension. Additionally, in Dramsi *et al*. (2002) phosphorylation of serine 170 was mimicked by mutation of this residue to aspartic acid. Notably, in this study the kinases responsible for serine 134 phosphorylation as well as an involvement of this regulatory site in naturally occurring tumor cells has not been addressed. Here we disclose that hBAD serine 134 is phosphorylated in a RAF-dependent manner and that hBAD cooperates with RAF in promoting proliferation and therefore may play an active role during tumor development. The observation that MEK inhibition leads to a decrease in BAD serine 134 phosphorylation but to an increase in the amount of total BAD protein underlines the dual role of BAD. Under survival conditions, BAD is phosphorylated at serine 134 and promotes proliferation in cells with elevated RAF activity. On the other hand, when entering apoptotic conditions, dephosphorylated BAD might accumulate within the cell leading to complex formation with Bcl-2/Bcl-X_L and induction of

apoptosis. Collectively, BAD-induced apoptosis and proliferation seem to be regulated through interplay between the phosphorylation sites serine 75, 118 and 134.

4.7. Concluding Remarks and Future Perspective

Generally, BH3-only proteins are proposed to function as sentinels of the cellular health status. Data presented in this work suggest that interplay between the RAF and the Akt/PKB pathway takes place and that BAD functions as a node of these two signaling pathways. Additionally, we identified that hBAD is phosphorylated *in vivo* at several sites and enclosed that RAF kinases are directly involved in this process integrating mitogenic survival signals into the apoptotic death machinery. The C-terminal part of hBAD plays a more important role than appreciated so far. We show here that phosphorylation of serines 124 and 134 at the C-terminal part of hBAD participates actively in the regulation of apoptosis. Furthermore, our results suggest a new mode of function of hBAD: In lipid environment, phosphorylation of the BH3 domain does not necessarily lead to inactivation of hBAD function but rather activates hBAD's pore-forming activity. Although we made the important observation that phosphorylation of hBAD at serine 134 controls proliferation in B-RAF-V600E containing tumor cells, a lot critical questions remain. At present, elucidation of the mechanisms underlying involvement of hBAD in cancer signaling is a high priority. Single nucleotide polymorphism (SNP) databases could provide a connection between aberrant hBAD phosphorylation and cancer development.

Under non-apoptotic conditions, pore-formation seems to be a mode of action of BAD. However, whether hBAD pores are significant regulators of cell fate is not elucidated yet. Does pore-formation play a role during cancer progression? Notably, results presented here show that the pore-forming (phosphorylated) BH3 domain of BAD has no binding affinity to mitochondrial membranes, indicating that BAD channels may be located at membranes other than mitochondrial. Indeed, a high proportion of BAD was found to localize to the cholesterol-rich microdomains (rafts) of the plasma membrane (Ayllon *et al.* 2002; Fleischer *et al.* 2004; Garcia *et al.* 2003; Hekman *et al.* 2006). Rafts play an important role for the interactions of various signaling molecules (Hekman *et al.* 2002; Simons and Toomre 2000). Several signaling associated proteins including RAF have been found to be attached to the raft microdomains. Importantly, we demonstrated that phosphorylation of the RAF target site serine 118 is a prerequisite for formation of open pores. Thus, it is feasible that, in rafts of the plasma membrane, hBAD pores and RAF cooperate in promoting proliferation. On the other hand, a proportion of endogenous and exogenous B-RAF-V600E, but not wild-type B-RAF, was detected in the mitochondrial fraction indicating that survival signaling mediated by B-RAF-V600E might take place in part at the mitochondrial level (Lee *et al.* 2010). Therefore, it is of prime importance to examine the location of hBAD within cancer cells, e.g. by use of cell fractionation or microscopy. Additionally, it remains questionable whether hBAD pores conduct ions or metabolites *in vivo*. To resolve this question, patch clamp measurements or specific staining methods should be applied.

What could be the molecular mechanism of BAD/RAF-induced proliferation? Does interplay between BAD and B-RAF-V600E influence RAF homo- or heterodimerization resulting in enhanced activity of mitogenic signaling and cell proliferation? In our view, another issue that still needs to be resolved is the identification of further interaction partners of BAD. Does phosphorylation of specific sites lead to association of distinct proteins that direct the cell to apoptosis or proliferation? Do cancer cells with elevated RAF signaling offer a specific set of BAD interaction partners? Mass spectrometry analyses might decipher these questions.

In contrast to the C-terminus, we showed that the hBAD N-terminal phosphorylation sites play minor role during apoptosis control. Therefore, it would be of interest to further investigate the function and regulation of these N-terminally located phosphorylation sites. BAD has been shown to be involved in various non-apoptotic processes, such as glucose metabolism and the regulation of autophagy (Danial *et al.* 2003; Maiuri *et al.* 2007). Thus, it would be reasonable to examine whether overexpression of serine to alanine or serine to glutamate mutants of the hBAD N-terminal phosphorylation sites affect these mechanisms. To identify kinases that contribute to the phosphorylation of these sites, a kinase-probability-software could be applied. Following co-expression of BAD with the putative kinases, the degree of phosphorylation should be analyzed via phosphospecific antibodies. Additionally, hBAD and the kinases could be co-expressed in the presence of specific kinase inhibitors to exclude the influence of endogenous kinases. Lipid bilayer (black lipid) experiments would provide more insight into the functional importance of all identified phosphorylation sites for pore-formation; therefore, purified serine to alanine mutants of hBAD could be used.

5. References

Adams, J. M. and Cory, S. (1998). "The Bcl-2 protein family: arbiters of cell survival." *Science* **281**(5381): 1322-1326.

Adams, J. M. and Cory, S. (2001). "Life-or-death decisions by the Bcl-2 protein family." *Trends Biochem Sci* **26**(1): 61-66.

Aitken, A. (2002). "Functional specificity in 14-3-3 isoform interactions through dimer formation and phosphorylation. Chromosome location of mammalian isoforms and variants." *Plant Mol Biol* **50**(6): 993-1010.

Aitken, A. (2006). "14-3-3 proteins: a historic overview." *Semin Cancer Biol* **16**(3): 162-172.

Aitken, A., Baxter, H., Dubois, T., Clokie, S., Mackie, S., Mitchell, K., Peden, A. and Zemlickova, E. (2002). "Specificity of 14-3-3 isoform dimer interactions and phosphorylation." *Biochem Soc Trans* **30**(4): 351-360.

Alavi, A., Hood, J. D., Frausto, R., Stupack, D. G. and Cheresh, D. A. (2003). "Role of Raf in vascular protection from distinct apoptotic stimuli." *Science* **301**(5629): 94-96.

Alirol, E. and Martinou, J. C. (2006). "Mitochondria and cancer: is there a morphological connection?" *Oncogene* **25**(34): 4706-4716.

Allan, L. A., Morrice, N., Brady, S., Magee, G., Pathak, S. and Clarke, P. R. (2003). "Inhibition of caspase-9 through phosphorylation at Thr 125 by ERK MAPK." *Nat Cell Biol* **5**(7): 647-654.

Amaravadi, R. and Thompson, C. B. (2005). "The survival kinases Akt and Pim as potential pharmacological targets." *J Clin Invest* **115**(10): 2618-2624.

Anderson, R. G. (1998). "The caveolae membrane system." *Annu Rev Biochem* **67**: 199-225.

Antignani, A. and Youle, R. J. (2006). "How do Bax and Bak lead to permeabilization of the outer mitochondrial membrane?" *Curr Opin Cell Biol* **18**(6): 685-689.

Antonsson, B., Conti, F., Ciavatta, A., Montessuit, S., Lewis, S., Martinou, I., Bernasconi, L., Bernard, A., Mermod, J. J., Mazzei, G., Maundrell, K., Gambale, F., Sadoul, R. and Martinou, J. C. (1997). "Inhibition of Bax channel-forming activity by Bcl-2." *Science* **277**(5324): 370-372.

Ayllon, V., Fleischer, A., Cayla, X., Garcia, A. and Rebollo, A. (2002). "Segregation of Bad from lipid rafts is implicated in the induction of apoptosis." *J Immunol* **168**(7): 3387-3393.

Baljuls, A., Schmitz, W., Mueller, T., Zahedi, R. P., Sickmann, A., Hekman, M. and Rapp, U. R. (2008). "Positive regulation of A-RAF by phosphorylation of isoform-specific hinge segment and identification of novel phosphorylation sites." *J Biol Chem* **283**(40): 27239-27254.

Barnhart, B. C., Alappat, E. C. and Peter, M. E. (2003). "The CD95 type I/type II model." *Semin Immunol* **15**(3): 185-193.

Basanez, G., Nechushtan, A., Drozhinin, O., Chanturiya, A., Choe, E., Tutt, S., Wood, K. A., Hsu, Y., Zimmerberg, J. and Youle, R. J. (1999). "Bax, but not Bcl-xL, decreases the lifetime of planar phospholipid bilayer membranes at subnanomolar concentrations." *Proc Natl Acad Sci U S A* **96**(10): 5492-5497.

Basu, S., Totty, N. F., Irwin, M. S., Sudol, M. and Downward, J. (2003). "Akt phosphorylates the Yes-associated protein, YAP, to induce interaction with 14-3-3 and attenuation of p73-mediated apoptosis." *Mol Cell* **11**(1): 11-23.

Baumann, B., Weber, C. K., Troppmair, J., Whiteside, S., Israel, A., Rapp, U. R. and Wirth, T. (2000). "Raf induces NF-kappaB by membrane shuttle kinase MEKK1, a signaling pathway critical for transformation." *Proc Natl Acad Sci U S A* **97**(9): 4615-4620.

Benz, R. (1994). "Permeation of hydrophilic solutes through mitochondrial outer membranes: review on mitochondrial porins." *Biochim Biophys Acta* **1197**(2): 167-196.

Benz, R., Maier, E., Thinnes, F. P., Gotz, H. and Hilschmann, N. (1992). "Studies on human porin. VII. The channel properties of the human B-lymphocyte membrane-derived "Porin 31HL" are similar to those of mitochondrial porins." *Biol Chem Hoppe Seyler* **373**(6): 295-303.

Berg, D., Holzmann, C. and Riess, O. (2003). "14-3-3 proteins in the nervous system." *Nat Rev Neurosci* **4**(9): 752-762.

Billen, L. P., Kokoski, C. L., Lovell, J. F., Leber, B. and Andrews, D. W. (2008). "Bcl-XL inhibits membrane permeabilization by competing with Bax." *PLoS Biol* **6**(6): e147.

Bivona, T. G., Quatela, S. E., Bodemann, B. O., Ahearn, I. M., Soskis, M. J., Mor, A., Miura, J., Wiener, H. H., Wright, L., Saba, S. G., Yim, D., Fein, A., Perez de Castro, I., Li, C., Thompson, C. B., Cox, A. D. and Philips, M. R. (2006). "PKC regulates a farnesyl-electrostatic switch on K-Ras that promotes its association with Bcl-XL on mitochondria and induces apoptosis." *Mol Cell* **21**(4): 481-493.

Blasi, E., Mathieson, B. J., Varesio, L., Cleveland, J. L., Borchert, P. A. and Rapp, U. R. (1985). "Selective immortalization of murine macrophages from fresh bone marrow by a raf/myc recombinant murine retrovirus." *Nature* **318**(6047): 667-670.

Boisvert-Adamo, K. and Aplin, A. E. (2008). "Mutant B-RAF mediates resistance to anoikis via Bad and Bim." *Oncogene* **27**(23): 3301-3312.

Boldogh, I. R. and Pon, L. A. (2007). "Mitochondria on the move." *Trends Cell Biol* **17**(10): 502-510.

Bos, J. L. (1989). "ras oncogenes in human cancer: a review." *Cancer Res* **49**(17): 4682-4689.

Bouillet, P., Metcalf, D., Huang, D. C., Tarlinton, D. M., Kay, T. W., Kontgen, F., Adams, J. M. and Strasser, A. (1999). "Proapoptotic Bcl-2 relative Bim required for certain apoptotic responses, leukocyte homeostasis, and to preclude autoimmunity." *Science* **286**(5445): 1735-1738.

Bouillet, P., Purton, J. F., Godfrey, D. I., Zhang, L. C., Coultas, L., Puthalakath, H., Pellegrini, M., Cory, S., Adams, J. M. and Strasser, A. (2002). "BH3-only Bcl-2 family member Bim is required for apoptosis of autoreactive thymocytes." *Nature* **415**(6874): 922-926.

Brimmell, M., Mendiola, R., Mangion, J. and Packham, G. (1998). "BAX frameshift mutations in cell lines derived from human haemopoietic malignancies are associated with resistance to apoptosis and microsatellite instability." *Oncogene* **16**(14): 1803-1812.

Brose, M. S., Volpe, P., Feldman, M., Kumar, M., Rishi, I., Gerrero, R., Einhorn, E., Herlyn, M., Minna, J., Nicholson, A., Roth, J. A., Albelda, S. M., Davies, H., Cox, C., Brignell, G., Stephens, P., Futreal, P. A., Wooster, R., Stratton, M. R. and Weber, B. L. (2002). "BRAF and RAS mutations in human lung cancer and melanoma." *Cancer Res* **62**(23): 6997-7000.

Bruder, J. T., Heidecker, G. and Rapp, U. R. (1992). "Serum-, TPA-, and Ras-induced expression from Ap-1/Ets-driven promoters requires Raf-1 kinase." *Genes Dev* **6**(4): 545-556.

Brunet, A., Bonni, A., Zigmond, M. J., Lin, M. Z., Juo, P., Hu, L. S., Anderson, M. J., Arden, K. C., Blenis, J. and Greenberg, M. E. (1999). "Akt promotes cell survival by phosphorylating and inhibiting a Forkhead transcription factor." *Cell* **96**(6): 857-868.

Cecconi, F., Alvarez-Bolado, G., Meyer, B. I., Roth, K. A. and Gruss, P. (1998). "Apaf1 (CED-4 homolog) regulates programmed cell death in mammalian development." *Cell* **94**(6): 727-737.

Chan, D. C. (2006). "Mitochondrial fusion and fission in mammals." *Annu Rev Cell Dev Biol* **22**: 79-99.

Chan, S. L. and Yu, V. C. (2004). "Proteins of the bcl-2 family in apoptosis signalling: from mechanistic insights to therapeutic opportunities." *Clin Exp Pharmacol Physiol* **31**(3): 119-128.

Chen, C. and Okayama, H. (1987). "High-efficiency transformation of mammalian cells by plasmid DNA." *Mol Cell Biol* **7**(8): 2745-2752.

Chen, J., Fujii, K., Zhang, L., Roberts, T. and Fu, H. (2001). "Raf-1 promotes cell survival by antagonizing apoptosis signal-regulating kinase 1 through a MEK-ERK independent mechanism." *Proc Natl Acad Sci U S A* **98**(14): 7783-7788.

Chen, L., Willis, S. N., Wei, A., Smith, B. J., Fletcher, J. I., Hinds, M. G., Colman, P. M., Day, C. L., Adams, J. M. and Huang, D. C. (2005). "Differential targeting of prosurvival Bcl-2 proteins by their BH3-only ligands allows complementary apoptotic function." *Mol Cell* **17**(3): 393-403.

Chiang, C. W., Harris, G., Ellig, C., Masters, S. C., Subramanian, R., Shenolikar, S., Wadzinski, B. E. and Yang, E. (2001). "Protein phosphatase 2A activates the proapoptotic function of BAD in interleukin- 3-dependent lymphoid cells by a mechanism requiring 14-3-3 dissociation." *Blood* **97**(5): 1289-1297.

Choe, S., Bennett, M. J., Fujii, G., Curmi, P. M., Kantardjieff, K. A., Collier, R. J. and Eisenberg, D. (1992). "The crystal structure of diphtheria toxin." *Nature* **357**(6375): 216-222.

Chong, H., Lee, J. and Guan, K. L. (2001). "Positive and negative regulation of Raf kinase activity and function by phosphorylation." *EMBO J* **20**(14): 3716-3727.

Chong, H., Vikis, H. G. and Guan, K. L. (2003). "Mechanisms of regulating the Raf kinase family." *Cell Signal* **15**(5): 463-469.

Chu, Z. L., McKinsey, T. A., Liu, L., Gentry, J. J., Malim, M. H. and Ballard, D. W. (1997). "Suppression of tumor necrosis factor-induced cell death by inhibitor of apoptosis c-IAP2 is under NF-kappaB control." *Proc Natl Acad Sci U S A* **94**(19): 10057-10062.

Claperon, A. and Therrien, M. (2007). "KSR and CNK: two scaffolds regulating RAS-mediated RAF activation." *Oncogene* **26**(22): 3143-3158.

Clark, G. J., Drugan, J. K., Rossman, K. L., Carpenter, J. W., Rogers-Graham, K., Fu, H., Der, C. J. and Campbell, S. L. (1997). "14-3-3 zeta negatively regulates raf-1 activity by interactions with the Raf-1 cysteine-rich domain." *J Biol Chem* **272**(34): 20990-20993.

Clem, R. J., Fechheimer, M. and Miller, L. K. (1991). "Prevention of apoptosis by a baculovirus gene during infection of insect cells." *Science* **254**(5036): 1388-1390.

Clem, R. J. and Miller, L. K. (1994). "Control of programmed cell death by the baculovirus genes p35 and iap." *Mol Cell Biol* **14**(8): 5212-5222.

Cleveland, J. L., Jansen, H. W., Bister, K., Fredrickson, T. N., Morse, H. C., 3rd, Ihle, J. N. and Rapp, U. R. (1986). "Interaction between Raf and Myc oncogenes in transformation in vivo and in vitro." *J Cell Biochem* **30**(3): 195-218.

Cleveland, J. L., Troppmair, J., Packham, G., Askew, D. S., Lloyd, P., Gonzalez-Garcia, M., Nunez, G., Ihle, J. N. and Rapp, U. R. (1994). "v-raf suppresses apoptosis and promotes growth of interleukin-3-dependent myeloid cells." *Oncogene* **9**(8): 2217-2226.

Cohen, C., Zavala-Pompa, A., Sequeira, J. H., Shoji, M., Sexton, D. G., Cotsonis, G., Cerimele, F., Govindarajan, B., Macaron, N. and Arbiser, J. L. (2002). "Mitogen-actived protein kinase activation is an early event in melanoma progression." *Clin Cancer Res* **8**(12): 3728-3733.

Cohen, Y., Xing, M., Mambo, E., Guo, Z., Wu, G., Trink, B., Beller, U., Westra, W. H., Ladenson, P. W. and Sidransky, D. (2003). "BRAF mutation in papillary thyroid carcinoma." *J Natl Cancer Inst* **95**(8): 625-627.

Conklin, D. S., Galaktionov, K. and Beach, D. (1995). "14-3-3 proteins associate with cdc25 phosphatases." *Proc Natl Acad Sci U S A* **92**(17): 7892-7896.

Cornelis, S., Bruynooghe, Y., Van Loo, G., Saelens, X., Vandenabeele, P. and Beyaert, R. (2005). "Apoptosis of hematopoietic cells induced by growth factor withdrawal is associated with caspase-9 mediated cleavage of Raf-1." *Oncogene* **24**(9): 1552-1562.

Cory, S. and Adams, J. M. (2002). "The Bcl2 family: regulators of the cellular life-or-death switch." *Nat Rev Cancer* **2**(9): 647-656.

Cragg, M. S., Jansen, E. S., Cook, M., Harris, C., Strasser, A. and Scott, C. L. (2008). "Treatment of B-RAF mutant human tumor cells with a MEK inhibitor requires Bim and is enhanced by a BH3 mimetic." *J Clin Invest* **118**(11): 3651-3659.

Crook, N. E., Clem, R. J. and Miller, L. K. (1993). "An apoptosis-inhibiting baculovirus gene with a zinc finger-like motif." *J Virol* **67**(4): 2168-2174.

Danial, N. N. (2008). "BAD: undertaker by night, candyman by day." *Oncogene* **27 Suppl 1**: S53-70.

Danial, N. N., Gramm, C. F., Scorrano, L., Zhang, C. Y., Krauss, S., Ranger, A. M., Datta, S. R., Greenberg, M. E., Licklider, L. J., Lowell, B. B., Gygi, S. P. and Korsmeyer, S. J. (2003). "BAD and glucokinase reside in a mitochondrial complex that integrates glycolysis and apoptosis." *Nature* **424**(6951): 952-956.

Danial, N. N. and Korsmeyer, S. J. (2004). "Cell death: critical control points." *Cell* **116**(2): 205-219.

Datta, S. R., Brunet, A. and Greenberg, M. E. (1999). "Cellular survival: a play in three Akts." *Genes Dev* **13**(22): 2905-2927.

Datta, S. R., Dudek, H., Tao, X., Masters, S., Fu, H., Gotoh, Y. and Greenberg, M. E. (1997). "Akt phosphorylation of BAD couples survival signals to the cell-intrinsic death machinery." *Cell* **91**(2): 231-241.

Datta, S. R., Katsov, A., Hu, L., Petros, A., Fesik, S. W., Yaffe, M. B. and Greenberg, M. E. (2000). "14-3-3 proteins and survival kinases cooperate to inactivate BAD by BH3 domain phosphorylation." *Mol Cell* **6**(1): 41-51.

Datta, S. R., Ranger, A. M., Lin, M. Z., Sturgill, J. F., Ma, Y. C., Cowan, C. W., Dikkes, P., Korsmeyer, S. J. and Greenberg, M. E. (2002). "Survival factor-mediated BAD phosphorylation raises the mitochondrial threshold for apoptosis." *Dev Cell* **3**(5): 631-643.

Daum, G., Eisenmann-Tappe, I., Fries, H. W., Troppmair, J. and Rapp, U. R. (1994). "The ins and outs of Raf kinases." *Trends Biochem Sci* **19**(11): 474-480.

Davies, H., Bignell, G. R., Cox, C., Stephens, P., Edkins, S., Clegg, S., Teague, J., Woffendin, H., Garnett, M. J., Bottomley, W., Davis, N., Dicks, E., Ewing, R., Floyd, Y., Gray, K., Hall, S., Hawes, R., Hughes, J., Kosmidou, V., Menzies, A., Mould, C., Parker, A., Stevens, C., Watt, S., Hooper, S., Wilson, R., Jayatilake, H., Gusterson, B. A., Cooper, C., Shipley, J., Hargrave, D., Pritchard-Jones, K., Maitland, N., Chenevix-Trench, G., Riggins, G. J., Bigner, D. D., Palmieri, G., Cossu, A., Flanagan, A., Nicholson, A., Ho, J. W., Leung, S. Y., Yuen, S. T., Weber, B. L., Seigler, H. F., Darrow, T. L., Paterson, H., Marais, R., Marshall, C. J., Wooster, R., Stratton, M. R. and Futreal, P. A. (2002). "Mutations of the BRAF gene in human cancer." *Nature* **417**(6892): 949-954.

Dejean, L. M., Martinez-Caballero, S. and Kinnally, K. W. (2006). "Is MAC the knife that cuts cytochrome c from mitochondria during apoptosis?" *Cell Death Differ* **13**(8): 1387-1395.

del Mar Martinez-Senac, M., Corbalan-Garcia, S. and Gomez-Fernandez, J. C. (2000). "Study of the secondary structure of the C-terminal domain of the antiapoptotic protein bcl-2 and its interaction with model membranes." *Biochemistry* **39**(26): 7744-7752.

del Mar Martinez-Senac, M., Corbalan-Garcia, S. and Gomez-Fernandez, J. C. (2001). "Conformation of the C-terminal domain of the pro-apoptotic protein Bax and mutants and its interaction with membranes." *Biochemistry* **40**(33): 9983-9992.

Deng, X., Ruvolo, P., Carr, B. and May, W. S., Jr. (2000). "Survival function of ERK1/2 as IL-3-activated, staurosporine-resistant Bcl2 kinases." *Proc Natl Acad Sci U S A* **97**(4): 1578-1583.

Deng, Y., Ren, X., Yang, L., Lin, Y. and Wu, X. (2003). "A JNK-dependent pathway is required for TNFalpha-induced apoptosis." *Cell* **115**(1): 61-70.

Deveraux, Q. L., Takahashi, R., Salvesen, G. S. and Reed, J. C. (1997). "X-linked IAP is a direct inhibitor of cell-death proteases." *Nature* **388**(6639): 300-304.

Dhillon, A. S. and Kolch, W. (2002). "Untying the regulation of the Raf-1 kinase." *Arch Biochem Biophys* **404**(1): 3-9.

Dlugosz, P. J., Billen, L. P., Annis, M. G., Zhu, W., Zhang, Z., Lin, J., Leber, B. and Andrews, D. W. (2006). "Bcl-2 changes conformation to inhibit Bax oligomerization." *EMBO J* **25**(11): 2287-2296.

Dogan, T., Harms, G. S., Hekman, M., Karreman, C., Oberoi, T. K., Alnemri, E. S., Rapp, U. R. and Rajalingam, K. (2008). "X-linked and cellular IAPs modulate the stability of C-RAF kinase and cell motility." *Nat Cell Biol* **10**(12): 1447-1455.

Domina, A. M., Vrana, J. A., Gregory, M. A., Hann, S. R. and Craig, R. W. (2004). "MCL1 is phosphorylated in the PEST region and stabilized upon ERK activation in viable cells, and at additional sites with cytotoxic okadaic acid or taxol." *Oncogene* **23**(31): 5301-5315.

Donovan, N., Becker, E. B., Konishi, Y. and Bonni, A. (2002). "JNK phosphorylation and activation of BAD couples the stress-activated signaling pathway to the cell death machinery." *J Biol Chem* **277**(43): 40944-40949.

Dougherty, M. K. and Morrison, D. K. (2004). "Unlocking the code of 14-3-3." *J Cell Sci* **117**(Pt 10): 1875-1884.

Dougherty, M. K., Muller, J., Ritt, D. A., Zhou, M., Zhou, X. Z., Copeland, T. D., Conrads, T. P., Veenstra, T. D., Lu, K. P. and Morrison, D. K. (2005). "Regulation of Raf-1 by direct feedback phosphorylation." *Mol Cell* **17**(2): 215-224.

Dramsi, S., Scheid, M. P., Maiti, A., Hojabrpour, P., Chen, X., Schubert, K., Goodlett, D. R., Aebersold, R. and Duronio, V. (2002). "Identification of a novel phosphorylation site, Ser-170, as a regulator of bad pro-apoptotic activity." *J Biol Chem* **277**(8): 6399-6405.

Du, C., Fang, M., Li, Y., Li, L. and Wang, X. (2000). "Smac, a mitochondrial protein that promotes cytochrome c-dependent caspase activation by eliminating IAP inhibition." *Cell* **102**(1): 33-42.

Dumaz, N. and Marais, R. (2003). "Protein kinase A blocks Raf-1 activity by stimulating 14-3-3 binding and blocking Raf-1 interaction with Ras." *J Biol Chem* **278**(32): 29819-29823.

Dyson, M. H., Thomson, S., Inagaki, M., Goto, H., Arthur, S. J., Nightingale, K., Iborra, F. J. and Mahadevan, L. C. (2005). "MAP kinase-mediated phosphorylation of distinct pools of histone H3 at S10 or S28 via mitogen- and stress-activated kinase 1/2." *J Cell Sci* **118**(Pt 10): 2247-2259.

Eisenman, R. N. (2001). "Deconstructing myc." *Genes Dev* **15**(16): 2023-2030.

Eisenmann, K. M., VanBrocklin, M. W., Staffend, N. A., Kitchen, S. M. and Koo, H. M. (2003). "Mitogen-activated protein kinase pathway-dependent tumor-specific survival signaling in melanoma cells through inactivation of the proapoptotic protein bad." *Cancer Res* **63**(23): 8330-8337.

Elbashir, S. M., Harborth, J., Lendeckel, W., Yalcin, A., Weber, K. and Tuschl, T. (2001). "Duplexes of 21-nucleotide RNAs mediate RNA interference in cultured mammalian cells." *Nature* **411**(6836): 494-498.

Ewings, K. E., Hadfield-Moorhouse, K., Wiggins, C. M., Wickenden, J. A., Balmanno, K., Gilley, R., Degenhardt, K., White, E. and Cook, S. J. (2007). "ERK1/2-dependent phosphorylation of BimEL promotes its rapid dissociation from Mcl-1 and Bcl-xL." *EMBO J* **26**(12): 2856-2867.

Fabian, M. A., Biggs, W. H., 3rd, Treiber, D. K., Atteridge, C. E., Azimioara, M. D., Benedetti, M. G., Carter, T. A., Ciceri, P., Edeen, P. T., Floyd, M., Ford, J. M., Galvin, M., Gerlach, J. L., Grotzfeld, R. M., Herrgard, S., Insko, D. E., Insko, M. A., Lai, A. G., Lelias, J. M., Mehta, S. A., Milanov, Z. V., Velasco, A. M., Wodicka, L. M., Patel, H. K., Zarrinkar, P. P. and Lockhart, D. J. (2005). "A small molecule-kinase interaction map for clinical kinase inhibitors." *Nat Biotechnol* **23**(3): 329-336.

Fantl, W. J., Muslin, A. J., Kikuchi, A., Martin, J. A., MacNicol, A. M., Gross, R. W. and Williams, L. T. (1994). "Activation of Raf-1 by 14-3-3 proteins." *Nature* **371**(6498): 612-614.

Fesik, S. W. (2000). "Insights into programmed cell death through structural biology." *Cell* **103**(2): 273-282.

Fischer, A., Baljuls, A., Reinders, J., Nekhoroshkova, E., Sibilski, C., Metz, R., Albert, S., Rajalingam, K., Hekman, M. and Rapp, U. R. (2009). "Regulation of RAF activity by 14-3-3 proteins: RAF kinases associate functionally with both homo- and heterodimeric forms of 14-3-3 proteins." *J Biol Chem* **284**(5): 3183-3194.

Fleischer, A., Ghadiri, A., Dessauge, F., Duhamel, M., Cayla, X., Garcia, A. and Rebollo, A. (2004). "Bad-dependent rafts alteration is a consequence of an early intracellular signal triggered by interleukin-4 deprivation." *Mol Cancer Res* **2**(12): 674-684.

Frank, S., Gaume, B., Bergmann-Leitner, E. S., Leitner, W. W., Robert, E. G., Catez, F., Smith, C. L. and Youle, R. J. (2001). "The role of dynamin-related protein 1, a mediator of mitochondrial fission, in apoptosis." *Dev Cell* **1**(4): 515-525.

Frederick, R. L. and Shaw, J. M. (2007). "Moving mitochondria: establishing distribution of an essential organelle." *Traffic* **8**(12): 1668-1675.

Freed, E., Symons, M., Macdonald, S. G., McCormick, F. and Ruggieri, R. (1994). "Binding of 14-3-3 proteins to the protein kinase Raf and effects on its activation." *Science* **265**(5179): 1713-1716.

Fu, H., Coburn, J. and Collier, R. J. (1993). "The eukaryotic host factor that activates exoenzyme S of Pseudomonas aeruginosa is a member of the 14-3-3 protein family." *Proc Natl Acad Sci U S A* **90**(6): 2320-2324.

Fu, H., Xia, K., Pallas, D. C., Cui, C., Conroy, K., Narsimhan, R. P., Mamon, H., Collier, R. J. and Roberts, T. M. (1994). "Interaction of the protein kinase Raf-1 with 14-3-3 proteins." *Science* **266**(5182): 126-129.

Fueller, J., Becker, M., Sienerth, A. R., Fischer, A., Hotz, C. and Galmiche, A. (2008). "C-RAF activation promotes BAD poly-ubiquitylation and turn-over by the proteasome." *Biochem Biophys Res Commun* **370**(4): 552-556.

Galmiche, A., Fueller, J., Santel, A., Krohne, G., Wittig, I., Doye, A., Rolando, M., Flatau, G., Lemichez, E. and Rapp, U. R. (2008). "Isoform-specific interaction of C-RAF with mitochondria." *J Biol Chem* **283**(21): 14857-14866.

Galonek, H. L. and Hardwick, J. M. (2006). "Upgrading the BCL-2 network." *Nat Cell Biol* **8**(12): 1317-1319.

Garcia, A., Cayla, X., Fleischer, A., Guergnon, J., Alvarez-Franco Canas, F., Rebollo, M. P., Roncal, F. and Rebollo, A. (2003). "Rafts: a simple way to control apoptosis by subcellular redistribution." *Biochimie* **85**(8): 727-731.

Gardino, A. K., Smerdon, S. J. and Yaffe, M. B. (2006). "Structural determinants of 14-3-3 binding specificities and regulation of subcellular localization of 14-3-3-ligand complexes: a comparison of the X-ray crystal structures of all human 14-3-3 isoforms." *Semin Cancer Biol* **16**(3): 173-182.

Garnett, M. J., Rana, S., Paterson, H., Barford, D. and Marais, R. (2005). "Wild-type and mutant B-RAF activate C-RAF through distinct mechanisms involving heterodimerization." *Mol Cell* **20**(6): 963-969.

Gnesutta, N., Qu, J. and Minden, A. (2001). "The serine/threonine kinase PAK4 prevents caspase activation and protects cells from apoptosis." *J Biol Chem* **276**(17): 14414-14419.

Gorden, A., Osman, I., Gai, W., He, D., Huang, W., Davidson, A., Houghton, A. N., Busam, K. and Polsky, D. (2003). "Analysis of BRAF and N-RAS mutations in metastatic melanoma tissues." *Cancer Res* **63**(14): 3955-3957.

Gottlieb, E., Armour, S. M. and Thompson, C. B. (2002). "Mitochondrial respiratory control is lost during growth factor deprivation." *Proc Natl Acad Sci U S A* **99**(20): 12801-12806.

Gottlieb, E. and Tomlinson, I. P. (2005). "Mitochondrial tumour suppressors: a genetic and biochemical update." *Nat Rev Cancer* **5**(11): 857-866.

Gotz, R., Wiese, S., Takayama, S., Camarero, G. C., Rossoll, W., Schweizer, U., Troppmair, J., Jablonka, S., Holtmann, B., Reed, J. C., Rapp, U. R. and Sendtner, M. (2005). "Bag1 is essential for differentiation and survival of hematopoietic and neuronal cells." *Nat Neurosci* **8**(9): 1169-1178.

Green, D. R. and Kroemer, G. (2005). "Pharmacological manipulation of cell death: clinical applications in sight?" *J Clin Invest* **115**(10): 2610-2617.

Green, D. R. and Reed, J. C. (1998). "Mitochondria and apoptosis." *Science* **281**(5381): 1309-1312.

Gross, A., McDonnell, J. M. and Korsmeyer, S. J. (1999). "BCL-2 family members and the mitochondria in apoptosis." *Genes Dev* **13**(15): 1899-1911.

Hagemann, C. (1999). Raf-Isoform spezifische Protein-Protein Wechselwirkungen, detektiert mit dem Hefe Two-Hybrid System. *Institut für Medizinische Zellforschung und Strahlenkunde*. Würzburg, University of Würzburg. **Doctoral degree**.

Hagemann, C. and Rapp, U. R. (1999). "Isotype-specific functions of Raf kinases." *Exp Cell Res* **253**(1): 34-46.

Hakem, R., Hakem, A., Duncan, G. S., Henderson, J. T., Woo, M., Soengas, M. S., Elia, A., de la Pompa, J. L., Kagi, D., Khoo, W., Potter, J., Yoshida, R., Kaufman, S. A., Lowe, S. W., Penninger, J. M. and Mak, T. W. (1998). "Differential requirement for caspase 9 in apoptotic pathways in vivo." *Cell* **94**(3): 339-352.

Harada, H., Becknell, B., Wilm, M., Mann, M., Huang, L. J., Taylor, S. S., Scott, J. D. and Korsmeyer, S. J. (1999). "Phosphorylation and inactivation of BAD by mitochondria-anchored protein kinase A." *Mol Cell* **3**(4): 413-422.

Hatzivassiliou, G., Song, K., Yen, I., Brandhuber, B. J., Anderson, D. J., Alvarado, R., Ludlam, M. J., Stokoe, D., Gloor, S. L., Vigers, G., Morales, T., Aliagas, I., Liu, B., Sideris, S., Hoeflich, K. P., Jaiswal, B. S., Seshagiri, S., Koeppen, H., Belvin, M., Friedman, L. S. and Malek, S. (2010). "RAF inhibitors prime wild-type RAF to activate the MAPK pathway and enhance growth." *Nature* **464**(7287): 431-435.

Heibein, J. A., Goping, I. S., Barry, M., Pinkoski, M. J., Shore, G. C., Green, D. R. and Bleackley, R. C. (2000). "Granzyme B-mediated cytochrome c release is regulated by the Bcl-2 family members bid and Bax." *J Exp Med* **192**(10): 1391-1402.

Heidorn, S. J., Milagre, C., Whittaker, S., Nourry, A., Niculescu-Duvas, I., Dhomen, N., Hussain, J., Reis-Filho, J. S., Springer, C. J., Pritchard, C. and Marais, R. (2010). "Kinase-dead BRAF and oncogenic RAS cooperate to drive tumor progression through CRAF." *Cell* **140**(2): 209-221.

Hekman, M., Albert, S., Galmiche, A., Rennefahrt, U. E., Fueller, J., Fischer, A., Puehringer, D., Wiese, S. and Rapp, U. R. (2006). "Reversible membrane interaction of BAD requires two C-terminal lipid binding domains in conjunction with 14-3-3 protein binding." *J Biol Chem* **281**(25): 17321-17336.

Hekman, M., Hamm, H., Villar, A. V., Bader, B., Kuhlmann, J., Nickel, J. and Rapp, U. R. (2002). "Associations of B- and C-Raf with cholesterol, phosphatidylserine, and lipid second messengers: preferential binding of Raf to artificial lipid rafts." *J Biol Chem* **277**(27): 24090-24102.

Hekman, M., Wiese, S., Metz, R., Albert, S., Troppmair, J., Nickel, J., Sendtner, M. and Rapp, U. R. (2004). "Dynamic changes in C-Raf phosphorylation and 14-3-3 protein binding in response to growth factor stimulation: differential roles of 14-3-3 protein binding sites." *J Biol Chem* **279**(14): 14074-14086.

Hermeking, H. (2003). "The 14-3-3 cancer connection." *Nat Rev Cancer* **3**(12): 931-943.

Hermeking, H. and Benzinger, A. (2006). "14-3-3 proteins in cell cycle regulation." *Semin Cancer Biol* **16**(3): 183-192.

Hiller, S., Garces, R. G., Malia, T. J., Orekhov, V. Y., Colombini, M. and Wagner, G. (2008). "Solution structure of the integral human membrane protein VDAC-1 in detergent micelles." *Science* **321**(5893): 1206-1210.

Hinds, M. G., Smits, C., Fredericks-Short, R., Risk, J. M., Bailey, M., Huang, D. C. and Day, C. L. (2007). "Bim, Bad and Bmf: intrinsically unstructured BH3-only proteins that undergo a localized conformational change upon binding to prosurvival Bcl-2 targets." *Cell Death Differ* **14**(1): 128-136.

Hong, J. H., Hwang, E. S., McManus, M. T., Amsterdam, A., Tian, Y., Kalmukova, R., Mueller, E., Benjamin, T., Spiegelman, B. M., Sharp, P. A., Hopkins, N. and Yaffe, M. B. (2005). "TAZ, a transcriptional modulator of mesenchymal stem cell differentiation." *Science* **309**(5737): 1074-1078.

Hosang, M. (1985). "Suramin binds to platelet-derived growth factor and inhibits its biological activity." *J Cell Biochem* **29**(3): 265-273.

Huang, D. C. and Strasser, A. (2000). "BH3-Only proteins-essential initiators of apoptotic cell death." *Cell* **103**(6): 839-842.

Huang, R. R., Dehaven, R. N., Cheung, A. H., Diehl, R. E., Dixon, R. A. and Strader, C. D. (1990). "Identification of allosteric antagonists of receptor-guanine nucleotide-binding protein interactions." *Mol Pharmacol* **37**(2): 304-310.

Huser, M., Luckett, J., Chiloeches, A., Mercer, K., Iwobi, M., Giblett, S., Sun, X. M., Brown, J., Marais, R. and Pritchard, C. (2001). "MEK kinase activity is not necessary for Raf-1 function." *EMBO J* **20**(8): 1940-1951.

Imaizumi, K., Morihara, T., Mori, Y., Katayama, T., Tsuda, M., Furuyama, T., Wanaka, A., Takeda, M. and Tohyama, M. (1999). "The cell death-promoting gene DP5, which interacts with the BCL2 family, is induced during neuronal apoptosis following exposure to amyloid beta protein." *J Biol Chem* **274**(12): 7975-7981.

Ionov, Y., Yamamoto, H., Krajewski, S., Reed, J. C. and Perucho, M. (2000). "Mutational inactivation of the proapoptotic gene BAX confers selective advantage during tumor clonal evolution." *Proc Natl Acad Sci U S A* **97**(20): 10872-10877.

Jansen, H. W., Patschinsky, T. and Bister, K. (1983). "Avian oncovirus MH2: molecular cloning of proviral DNA and structural analysis of viral RNA and protein." *J Virol* **48**(1): 61-73.

Jeong, S. Y., Gaume, B., Lee, Y. J., Hsu, Y. T., Ryu, S. W., Yoon, S. H. and Youle, R. J. (2004). "Bcl-x(L) sequesters its C-terminal membrane anchor in soluble, cytosolic homodimers." *EMBO J* **23**(10): 2146-2155.

Jin, S., Zhuo, Y., Guo, W. and Field, J. (2005). "p21-activated Kinase 1 (Pak1)-dependent phosphorylation of Raf-1 regulates its mitochondrial localization, phosphorylation of BAD, and Bcl-2 association." *J Biol Chem* **280**(26): 24698-24705.

Jonas, E. A., Hickman, J. A., Chachar, M., Polster, B. M., Brandt, T. A., Fannjiang, Y., Ivanovska, I., Basanez, G., Kinnally, K. W., Zimmerberg, J., Hardwick, J. M. and Kaczmarek, L. K. (2004). "Proapoptotic N-truncated BCL-xL protein activates endogenous mitochondrial channels in living synaptic terminals." *Proc Natl Acad Sci U S A* **101**(37): 13590-13595.

Jonas, E. A., Hickman, J. A., Hardwick, J. M. and Kaczmarek, L. K. (2005). "Exposure to hypoxia rapidly induces mitochondrial channel activity within a living synapse." *J Biol Chem* **280**(6): 4491-4497.

Jonas, E. A., Hoit, D., Hickman, J. A., Brandt, T. A., Polster, B. M., Fannjiang, Y., McCarthy, E., Montanez, M. K., Hardwick, J. M. and Kaczmarek, L. K. (2003). "Modulation of synaptic transmission by the BCL-2 family protein BCL-xL." *J Neurosci* **23**(23): 8423-8431.

Jost, P. J., Grabow, S., Gray, D., McKenzie, M. D., Nachbur, U., Huang, D. C., Bouillet, P., Thomas, H. E., Borner, C., Silke, J., Strasser, A. and Kaufmann, T. (2009). "XIAP discriminates between type I and type II FAS-induced apoptosis." *Nature* **460**(7258): 1035-1039.

Jurgensmeier, J. M., Xie, Z., Deveraux, Q., Ellerby, L., Bredesen, D. and Reed, J. C. (1998). "Bax directly induces release of cytochrome c from isolated mitochondria." *Proc Natl Acad Sci U S A* **95**(9): 4997-5002.

Karasarides, M., Chiloeches, A., Hayward, R., Niculescu-Duvaz, D., Scanlon, I., Friedlos, F., Ogilvie, L., Hedley, D., Martin, J., Marshall, C. J., Springer, C. J. and Marais, R. (2004). "B-RAF is a therapeutic target in melanoma." *Oncogene* **23**(37): 6292-6298.

Karbowski, M., Lee, Y. J., Gaume, B., Jeong, S. Y., Frank, S., Nechushtan, A., Santel, A., Fuller, M., Smith, C. L. and Youle, R. J. (2002). "Spatial and temporal association of Bax with mitochondrial fission sites, Drp1, and Mfn2 during apoptosis." *J Cell Biol* **159**(6): 931-938.

Kebache, S., Ash, J., Annis, M. G., Hagan, J., Huber, M., Hassard, J., Stewart, C. L., Whiteway, M. and Nantel, A. (2007). "Grb10 and active Raf-1 kinase promote Bad-dependent cell survival." *J Biol Chem* **282**(30): 21873-21883.

Kerkhoff, E., Leberfinger, C. B., Schmidt, G., Aktories, K. and Rapp, U. R. (2002). "Diverse effects of RacV12 on cell transformation by Raf: partial inhibition of morphological transformation versus deregulation of cell cycle control." *Biochim Biophys Acta* **1589**(2): 151-159.

Kerkhoff, E., Simpson, J. C., Leberfinger, C. B., Otto, I. M., Doerks, T., Bork, P., Rapp, U. R., Raabe, T. and Pepperkok, R. (2001). "The Spir actin organizers are involved in vesicle transport processes." *Curr Biol* **11**(24): 1963-1968.

Kerr, J. F., Wyllie, A. H. and Currie, A. R. (1972). "Apoptosis: a basic biological phenomenon with wide-ranging implications in tissue kinetics." *Br J Cancer* **26**(4): 239-257.

Khosravi-Far, R., Solski, P. A., Clark, G. J., Kinch, M. S. and Der, C. J. (1995). "Activation of Rac1, RhoA, and mitogen-activated protein kinases is required for Ras transformation." *Mol Cell Biol* **15**(11): 6443-6453.

Kim, H., Rafiuddin-Shah, M., Tu, H. C., Jeffers, J. R., Zambetti, G. P., Hsieh, J. J. and Cheng, E. H. (2006). "Hierarchical regulation of mitochondrion-dependent apoptosis by BCL-2 subfamilies." *Nat Cell Biol* **8**(12): 1348-1358.

Kimura, M. T., Irie, S., Shoji-Hoshino, S., Mukai, J., Nadano, D., Oshimura, M. and Sato, T. A. (2001). "14-3-3 is involved in p75 neurotrophin receptor-mediated signal transduction." *J Biol Chem* **276**(20): 17291-17300.

Klumpp, S., Maurer, A., Zhu, Y., Aichele, D., Pinna, L. A. and Krieglstein, J. (2004). "Protein kinase CK2 phosphorylates BAD at threonine-117." *Neurochem Int* **45**(5): 747-752.

Kockx, M. M., De Meyer, G. R., Buyssens, N., Knaapen, M. W., Bult, H. and Herman, A. G. (1998). "Cell composition, replication, and apoptosis in atherosclerotic plaques after 6 months of cholesterol withdrawal." *Circ Res* **83**(4): 378-387.

Kondo, S., Shinomura, Y., Miyazaki, Y., Kiyohara, T., Tsutsui, S., Kitamura, S., Nagasawa, Y., Nakahara, M., Kanayama, S. and Matsuzawa, Y. (2000). "Mutations of the bak gene in human gastric and colorectal cancers." *Cancer Res* **60**(16): 4328-4330.

Konishi, Y., Lehtinen, M., Donovan, N. and Bonni, A. (2002). "Cdc2 phosphorylation of BAD links the cell cycle to the cell death machinery." *Mol Cell* **9**(5): 1005-1016.

Krasilnikov, O. V., Da Cruz, J. B., Yuldasheva, L. N., Varanda, W. A. and Nogueira, R. A. (1998). "A novel approach to study the geometry of the water lumen of ion channels: colicin Ia channels in planar lipid bilayers." *J Membr Biol* **161**(1): 83-92.

Kuwana, T., Mackey, M. R., Perkins, G., Ellisman, M. H., Latterich, M., Schneiter, R., Green, D. R. and Newmeyer, D. D. (2002). "Bid, Bax, and lipids cooperate to form supramolecular openings in the outer mitochondrial membrane." *Cell* **111**(3): 331-342.

Kyriakis, J. M. (2007). "The integration of signaling by multiprotein complexes containing Raf kinases." *Biochim Biophys Acta* **1773**(8): 1238-1247.

Lackner, L. L., Horner, J. S. and Nunnari, J. (2009). "Mechanistic analysis of a dynamin effector." *Science* **325**(5942): 874-877.

Le Mellay, V., Troppmair, J., Benz, R. and Rapp, U. R. (2002). "Negative regulation of mitochondrial VDAC channels by C-Raf kinase." *BMC Cell Biol* **3**: 14.

Leber, B., Lin, J. and Andrews, D. W. (2007). "Embedded together: the life and death consequences of interaction of the Bcl-2 family with membranes." *Apoptosis* **12**(5): 897-911.

Lee, M. H., Lee, S. E., Kim, D. W., Ryu, M. J., Kim, S. J., Kim, Y. K., Park, J. H., Kweon, G. R., Kim, J. M., Lee, J. U., De Falco, V., Jo, Y. S. and Shong, M. (2010). "Mitochondrial Localization and Regulation of BRAFV600E in Thyroid Cancer: A Clinically Used RAF Inhibitor Is Unable to Block the Mitochondrial Activities of BRAFV600E." *J Clin Endocrinol Metab*.

Letai, A. (2006). "Growth factor withdrawal and apoptosis: the middle game." *Mol Cell* **21**(6): 728-730.

Letai, A., Bassik, M. C., Walensky, L. D., Sorcinelli, M. D., Weiler, S. and Korsmeyer, S. J. (2002). "Distinct BH3 domains either sensitize or activate mitochondrial apoptosis, serving as prototype cancer therapeutics." *Cancer Cell* **2**(3): 183-192.

Ley, R., Balmanno, K., Hadfield, K., Weston, C. and Cook, S. J. (2003). "Activation of the ERK1/2 signaling pathway promotes phosphorylation and proteasome-dependent degradation of the BH3-only protein, Bim." *J Biol Chem* **278**(21): 18811-18816.

Li, H., Zhu, H., Xu, C. J. and Yuan, J. (1998). "Cleavage of BID by caspase 8 mediates the mitochondrial damage in the Fas pathway of apoptosis." *Cell* **94**(4): 491-501.

Li, P., Nijhawan, D., Budihardjo, I., Srinivasula, S. M., Ahmad, M., Alnemri, E. S. and Wang, X. (1997). "Cytochrome c and dATP-dependent formation of Apaf-1/caspase-9 complex initiates an apoptotic protease cascade." *Cell* **91**(4): 479-489.

Light, Y., Paterson, H. and Marais, R. (2002). "14-3-3 antagonizes Ras-mediated Raf-1 recruitment to the plasma membrane to maintain signaling fidelity." *Mol Cell Biol* **22**(14): 4984-4996.

Liu, X., Kim, C. N., Yang, J., Jemmerson, R. and Wang, X. (1996). "Induction of apoptotic program in cell-free extracts: requirement for dATP and cytochrome c." *Cell* **86**(1): 147-157.

Lovric, J., Dammeier, S., Kieser, A., Mischak, H. and Kolch, W. (1998). "Activated raf induces the hyperphosphorylation of stathmin and the reorganization of the microtubule network." *J Biol Chem* **273**(35): 22848-22855.

Luciano, F., Jacquel, A., Colosetti, P., Herrant, M., Cagnol, S., Pages, G. and Auberger, P. (2003). "Phosphorylation of Bim-EL by Erk1/2 on serine 69 promotes its degradation via the proteasome pathway and regulates its proapoptotic function." *Oncogene* **22**(43): 6785-6793.

Luo, X., Budihardjo, I., Zou, H., Slaughter, C. and Wang, X. (1998). "Bid, a Bcl2 interacting protein, mediates cytochrome c release from mitochondria in response to activation of cell surface death receptors." *Cell* **94**(4): 481-490.

Macdonald, A., Campbell, D. G., Toth, R., McLauchlan, H., Hastie, C. J. and Arthur, J. S. (2006). "Pim kinases phosphorylate multiple sites on Bad and promote 14-3-3 binding and dissociation from Bcl-XL." *BMC Cell Biol* **7**: 1.

Maiuri, M. C., Le Toumelin, G., Criollo, A., Rain, J. C., Gautier, F., Juin, P., Tasdemir, E., Pierron, G., Troulinaki, K., Tavernarakis, N., Hickman, J. A., Geneste, O. and Kroemer, G. (2007). "Functional and physical interaction between Bcl-X(L) and a BH3-like domain in Beclin-1." *EMBO J* **26**(10): 2527-2539.

Majewski, M., Nieborowska-Skorska, M., Salomoni, P., Slupianek, A., Reiss, K., Trotta, R., Calabretta, B. and Skorski, T. (1999). "Activation of mitochondrial Raf-1 is involved in the antiapoptotic effects of Akt." *Cancer Res* **59**(12): 2815-2819.

Manich, M., Knapp, O., Gibert, M., Maier, E., Jolivet-Reynaud, C., Geny, B., Benz, R. and Popoff, M. R. (2008). "Clostridium perfringens delta toxin is sequence related to beta toxin, NetB, and Staphylococcus pore-forming toxins, but shows functional differences." *PLoS ONE* **3**(11): e3764.

Manning, G., Whyte, D. B., Martinez, R., Hunter, T. and Sudarsanam, S. (2002). "The protein kinase complement of the human genome." *Science* **298**(5600): 1912-1934.

Marani, M., Tenev, T., Hancock, D., Downward, J. and Lemoine, N. R. (2002). "Identification of novel isoforms of the BH3 domain protein Bim which directly activate Bax to trigger apoptosis." *Mol Cell Biol* **22**(11): 3577-3589.

Mark, G. E. and Rapp, U. R. (1984). "Primary structure of v-raf: relatedness to the src family of oncogenes." *Science* **224**(4646): 285-289.

Martinez-Senac Mdel, M., Corbalan-Garcia, S. and Gomez-Fernandez, J. C. (2002). "The structure of the C-terminal domain of the pro-apoptotic protein Bak and its interaction with model membranes." *Biophys J* **82**(1 Pt 1): 233-243.

Martinou, J. C. and Green, D. R. (2001). "Breaking the mitochondrial barrier." *Nat Rev Mol Cell Biol* **2**(1): 63-67.

Mason, C. S., Springer, C. J., Cooper, R. G., Superti-Furga, G., Marshall, C. J. and Marais, R. (1999). "Serine and tyrosine phosphorylations cooperate in Raf-1, but not B-Raf activation." *EMBO J* **18**(8): 2137-2148.

Masters, S. C., Yang, H., Datta, S. R., Greenberg, M. E. and Fu, H. (2001). "14-3-3 inhibits Bad-induced cell death through interaction with serine-136." *Mol Pharmacol* **60**(6): 1325-1331.

Mavria, G., Vercoulen, Y., Yeo, M., Paterson, H., Karasarides, M., Marais, R., Bird, D. and Marshall, C. J. (2006). "ERK-MAPK signaling opposes Rho-kinase to promote endothelial cell survival and sprouting during angiogenesis." *Cancer Cell* **9**(1): 33-44.

Mikula, M., Schreiber, M., Husak, Z., Kucerova, L., Ruth, J., Wieser, R., Zatloukal, K., Beug, H., Wagner, E. F. and Baccarini, M. (2001). "Embryonic lethality and fetal liver apoptosis in mice lacking the c-raf-1 gene." *EMBO J* **20**(8): 1952-1962.

Minn, A. J., Velez, P., Schendel, S. L., Liang, H., Muchmore, S. W., Fesik, S. W., Fill, M. and Thompson, C. B. (1997). "Bcl-x(L) forms an ion channel in synthetic lipid membranes." *Nature* **385**(6614): 353-357.

Moelling, K., Heimann, B., Beimling, P., Rapp, U. R. and Sander, T. (1984). "Serine- and threonine-specific protein kinase activities of purified gag-mil and gag-raf proteins." *Nature* **312**(5994): 558-561.

Molzan, M., Schumacher, B., Ottmann, C., Baljuls, A., Polzien, L., Weyand, M., Thiel, P., Rose, R., Rose, M., Kuhenne, P., Kaiser, M., Rapp, U. R. and Kuhlmann, J. (2010). "Impaired binding of 14-3-3 to C-RAF in Noonan syndrome suggests new approaches in diseases with increased Ras signaling." *Mol Cell Biol* **30**(19): 4698-4711.

Montal, M. and Mueller, P. (1972). "Formation of bimolecular membranes from lipid monolayers and a study of their electrical properties." *Proc Natl Acad Sci U S A* **69**(12): 3561-3566.

Morrison, D. K. (2001). "KSR: a MAPK scaffold of the Ras pathway?" *J Cell Sci* **114**(Pt 9): 1609-1612.

Morrison, D. K. and Davis, R. J. (2003). "Regulation of MAP kinase signaling modules by scaffold proteins in mammals." *Annu Rev Cell Dev Biol* **19**: 91-118.

Muchmore, S. W., Sattler, M., Liang, H., Meadows, R. P., Harlan, J. E., Yoon, H. S., Nettesheim, D., Chang, B. S., Thompson, C. B., Wong, S. L., Ng, S. L. and Fesik, S. W. (1996). "X-ray and NMR structure of human Bcl-xL, an inhibitor of programmed cell death." *Nature* **381**(6580): 335-341.

Muller, J., Ory, S., Copeland, T., Piwnica-Worms, H. and Morrison, D. K. (2001). "C-TAK1 regulates Ras signaling by phosphorylating the MAPK scaffold, KSR1." *Mol Cell* **8**(5): 983-993.

Muslin, A. J. and Xing, H. (2000). "14-3-3 proteins: regulation of subcellular localization by molecular interference." *Cell Signal* **12**(11-12): 703-709.

Nablo, B. J., Halverson, K. M., Robertson, J. W., Nguyen, T. L., Panchal, R. G., Gussio, R., Bavari, S., Krasilnikov, O. V. and Kasianowicz, J. J. (2008). "Sizing the Bacillus anthracis PA63 channel with nonelectrolyte poly(ethylene glycols)." *Biophys J* **95**(3): 1157-1164.

Nakano, K. and Vousden, K. H. (2001). "PUMA, a novel proapoptotic gene, is induced by p53." *Mol Cell* **7**(3): 683-694.

Nantel, A., Huber, M. and Thomas, D. Y. (1999). "Localization of endogenous Grb10 to the mitochondria and its interaction with the mitochondrial-associated Raf-1 pool." *J Biol Chem* **274**(50): 35719-35724.

Nechushtan, A., Smith, C. L., Lamensdorf, I., Yoon, S. H. and Youle, R. J. (2001). "Bax and Bak coalesce into novel mitochondria-associated clusters during apoptosis." *J Cell Biol* **153**(6): 1265-1276.

Nekhoroshkova, E., Albert, S., Becker, M. and Rapp, U. R. (2009). "A-RAF kinase functions in ARF6 regulated endocytic membrane traffic." *PLoS One* **4**(2): e4647.

Neuhoff, V., Arold, N., Taube, D. and Ehrhardt, W. (1988). "Improved staining of proteins in polyacrylamide gels including isoelectric focusing gels with clear background at nanogram sensitivity using Coomassie Brilliant Blue G-250 and R-250." *Electrophoresis* **9**(6): 255-262.

Nomura, M., Shimizu, S., Sugiyama, T., Narita, M., Ito, T., Matsuda, H. and Tsujimoto, Y. (2003). "14-3-3 Interacts directly with and negatively regulates pro-apoptotic Bax." *J Biol Chem* **278**(3): 2058-2065.

O'Connor, L., Strasser, A., O'Reilly, L. A., Hausmann, G., Adams, J. M., Cory, S. and Huang, D. C. (1998). "Bim: a novel member of the Bcl-2 family that promotes apoptosis." *EMBO J* **17**(2): 384-395.

O'Neill, E., Rushworth, L., Baccarini, M. and Kolch, W. (2004). "Role of the kinase MST2 in suppression of apoptosis by the proto-oncogene product Raf-1." *Science* **306**(5705): 2267-2270.

Obsil, T., Ghirlando, R., Klein, D. C., Ganguly, S. and Dyda, F. (2001). "Crystal structure of the 14-3-3zeta:serotonin N-acetyltransferase complex. a role for scaffolding in enzyme regulation." *Cell* **105**(2): 257-267.

Oda, E., Ohki, R., Murasawa, H., Nemoto, J., Shibue, T., Yamashita, T., Tokino, T., Taniguchi, T. and Tanaka, N. (2000). "Noxa, a BH3-only member of the Bcl-2 family and candidate mediator of p53-induced apoptosis." *Science* **288**(5468): 1053-1058.

Opferman, J. T. and Korsmeyer, S. J. (2003). "Apoptosis in the development and maintenance of the immune system." *Nat Immunol* **4**(5): 410-415.

Ory, S., Zhou, M., Conrads, T. P., Veenstra, T. D. and Morrison, D. K. (2003). "Protein phosphatase 2A positively regulates Ras signaling by dephosphorylating KSR1 and Raf-1 on critical 14-3-3 binding sites." *Curr Biol* **13**(16): 1356-1364.

Ottmann, C., Yasmin, L., Weyand, M., Veesenmeyer, J. L., Diaz, M. H., Palmer, R. H., Francis, M. S., Hauser, A. R., Wittinghofer, A. and Hallberg, B. (2007). "Phosphorylation-independent interaction between 14-3-3 and exoenzyme S: from structure to pathogenesis." *EMBO J* **26**(3): 902-913.

Pahl, H. L. (1999). "Activators and target genes of Rel/NF-kappaB transcription factors." *Oncogene* **18**(49): 6853-6866.

Pandit, B., Sarkozy, A., Pennacchio, L. A., Carta, C., Oishi, K., Martinelli, S., Pogna, E. A., Schackwitz, W., Ustaszewska, A., Landstrom, A., Bos, J. M., Ommen, S. R., Esposito, G., Lepri, F., Faul, C., Mundel, P., Lopez Siguero, J. P., Tenconi, R., Selicorni, A., Rossi, C., Mazzanti, L., Torrente, I., Marino, B., Digilio, M. C., Zampino, G., Ackerman, M. J., Dallapiccola, B., Tartaglia, M. and Gelb, B. D. (2007). "Gain-of-function RAF1 mutations cause Noonan and LEOPARD syndromes with hypertrophic cardiomyopathy." *Nat Genet* **39**(8): 1007-1012.

Panka, D. J., Wang, W., Atkins, M. B. and Mier, J. W. (2006). "The Raf inhibitor BAY 43-9006 (Sorafenib) induces caspase-independent apoptosis in melanoma cells." *Cancer Res* **66**(3): 1611-1619.

Pavey, S., Johansson, P., Packer, L., Taylor, J., Stark, M., Pollock, P. M., Walker, G. J., Boyle, G. M., Harper, U., Cozzi, S. J., Hansen, K., Yudt, L., Schmidt, C., Hersey, P., Ellem, K. A., O'Rourke, M. G., Parsons, P. G., Meltzer, P., Ringner, M. and Hayward, N. K. (2004). "Microarray expression profiling in melanoma reveals a BRAF mutation signature." *Oncogene* **23**(23): 4060-4067.

Pelkmans, L., Fava, E., Grabner, H., Hannus, M., Habermann, B., Krausz, E. and Zerial, M. (2005). "Genome-wide analysis of human kinases in clathrin- and caveolae/raft-mediated endocytosis." *Nature* **436**(7047): 78-86.

Pelkmans, L. and Zerial, M. (2005). "Kinase-regulated quantal assemblies and kiss-and-run recycling of caveolae." *Nature* **436**(7047): 128-133.

Peng, C. Y., Graves, P. R., Thoma, R. S., Wu, Z., Shaw, A. S. and Piwnica-Worms, H. (1997). "Mitotic and G2 checkpoint control: regulation of 14-3-3 protein binding by phosphorylation of Cdc25C on serine-216." *Science* **277**(5331): 1501-1505.

Peruzzi, F., Prisco, M., Morrione, A., Valentinis, B. and Baserga, R. (2001). "Anti-apoptotic signaling of the insulin-like growth factor-I receptor through mitochondrial translocation of c-Raf and Nedd4." *J Biol Chem* **276**(28): 25990-25996.

Petros, A. M., Medek, A., Nettesheim, D. G., Kim, D. H., Yoon, H. S., Swift, K., Matayoshi, E. D., Oltersdorf, T. and Fesik, S. W. (2001). "Solution structure of the antiapoptotic protein bcl-2." *Proc Natl Acad Sci U S A* **98**(6): 3012-3017.

Petros, A. M., Nettesheim, D. G., Wang, Y., Olejniczak, E. T., Meadows, R. P., Mack, J., Swift, K., Matayoshi, E. D., Zhang, H., Thompson, C. B. and Fesik, S. W. (2000). "Rationale for Bcl-xL/Bad peptide complex formation from structure, mutagenesis, and biophysical studies." *Protein Sci* **9**(12): 2528-2534.

Petros, A. M., Olejniczak, E. T. and Fesik, S. W. (2004). "Structural biology of the Bcl-2 family of proteins." *Biochim Biophys Acta* **1644**(2-3): 83-94.

Peyssonnaux, C. and Eychene, A. (2001). "The Raf/MEK/ERK pathway: new concepts of activation." *Biol Cell* **93**(1-2): 53-62.

Piazzolla, D., Meissl, K., Kucerova, L., Rubiolo, C. and Baccarini, M. (2005). "Raf-1 sets the threshold of Fas sensitivity by modulating Rok-alpha signaling." *J Cell Biol* **171**(6): 1013-1022.

Polo, S. and Di Fiore, P. P. (2006). "Endocytosis conducts the cell signaling orchestra." *Cell* **124**(5): 897-900.

Polzien, L., Baljuls, A., Rennefahrt, U. E., Fischer, A., Schmitz, W., Zahedi, R. P., Sickmann, A., Metz, R., Albert, S., Benz, R., Hekman, M. and Rapp, U. R. (2009). "Identification of novel in vivo phosphorylation sites of the human proapoptotic protein BAD: pore-forming activity of BAD is regulated by phosphorylation." *J Biol Chem* **284**(41): 28004-28020.

Polzien, L., Benz, R. and Rapp, U. R. (2009). "Can BAD pores be good? New insights from examining BAD as a target of RAF kinases." *Adv Enzyme Regul*.

Poulikakos, P. I., Zhang, C., Bollag, G., Shokat, K. M. and Rosen, N. (2010). "RAF inhibitors transactivate RAF dimers and ERK signalling in cells with wild-type BRAF." *Nature* **464**(7287): 427-430.

Prendergast, G. C., Khosravi-Far, R., Solski, P. A., Kurzawa, H., Lebowitz, P. F. and Der, C. J. (1995). "Critical role of Rho in cell transformation by oncogenic Ras." *Oncogene* **10**(12): 2289-2296.

Principato, M., Cleveland, J. L., Rapp, U. R., Holmes, K. L., Pierce, J. H., Morse, H. C., 3rd and Klinken, S. P. (1990). "Transformation of murine bone marrow cells with combined v-raf-v-myc oncogenes yields clonally related mature B cells and macrophages." *Mol Cell Biol* **10**(7): 3562-3568.

Principato, M., Klinken, S. P., Cleveland, J. L., Rapp, U. R., Holmes, K. L., Pierce, J. H. and Morse, H. C., 3rd (1988). "In vitro transformation of murine bone marrow cells with a v-raf/v-myc retrovirus yields clonally related mature B cells and macrophages." *Curr Top Microbiol Immunol* **141**: 31-41.

Pritchard, C. A., Bolin, L., Slattery, R., Murray, R. and McMahon, M. (1996). "Post-natal lethality and neurological and gastrointestinal defects in mice with targeted disruption of the A-Raf protein kinase gene." *Curr Biol* **6**(5): 614-617.

Puthalakath, H., Huang, D. C., O'Reilly, L. A., King, S. M. and Strasser, A. (1999). "The proapoptotic activity of the Bcl-2 family member Bim is regulated by interaction with the dynein motor complex." *Mol Cell* **3**(3): 287-296.

Puthalakath, H., Villunger, A., O'Reilly, L. A., Beaumont, J. G., Coultas, L., Cheney, R. E., Huang, D. C. and Strasser, A. (2001). "Bmf: a proapoptotic BH3-only protein regulated by interaction with the myosin V actin motor complex, activated by anoikis." *Science* **293**(5536): 1829-1832.

Qiu, R. G., Chen, J., Kirn, D., McCormick, F. and Symons, M. (1995). "An essential role for Rac in Ras transformation." *Nature* **374**(6521): 457-459.

Qiu, R. G., Chen, J., McCormick, F. and Symons, M. (1995). "A role for Rho in Ras transformation." *Proc Natl Acad Sci U S A* **92**(25): 11781-11785.

Raabe, T. and Rapp, U. R. (2002). "KSR--a regulator and scaffold protein of the MAPK pathway." *Sci STKE* **2002**(136): PE28.

Rajagopalan, H., Bardelli, A., Lengauer, C., Kinzler, K. W., Vogelstein, B. and Velculescu, V. E. (2002). "Tumorigenesis: RAF/RAS oncogenes and mismatch-repair status." *Nature* **418**(6901): 934.

Rajagopalan, S., Sade, R. S., Townsley, F. M. and Fersht, A. R. (2010). "Mechanistic differences in the transcriptional activation of p53 by 14-3-3 isoforms." *Nucleic Acids Res* **38**(3): 893-906.

Rajakulendran, T., Sahmi, M., Lefrancois, M., Sicheri, F. and Therrien, M. (2009). "A dimerization-dependent mechanism drives RAF catalytic activation." *Nature* **461**(7263): 542-545.

Rajalingam, K., Schreck, R., Rapp, U. R. and Albert, S. (2007). "Ras oncogenes and their downstream targets." *Biochim Biophys Acta* **1773**(8): 1177-1195.

Rajalingam, K., Wunder, C., Brinkmann, V., Churin, Y., Hekman, M., Sievers, C., Rapp, U. R. and Rudel, T. (2005). "Prohibitin is required for Ras-induced Raf-MEK-ERK activation and epithelial cell migration." *Nat Cell Biol* **7**(8): 837-843.

Rampino, N., Yamamoto, H., Ionov, Y., Li, Y., Sawai, H., Reed, J. C. and Perucho, M. (1997). "Somatic frameshift mutations in the BAX gene in colon cancers of the microsatellite mutator phenotype." *Science* **275**(5302): 967-969.

Rapp, U. R. (1994). Role of the RAF signal transduction pathway in Fos/Jun regulation and determination of cell fates. *The Fos and Jun families of transcription factors*. P. H. Angel, P. Boca Raton, CRC Press**:** 221-247.

Rapp, U. R., Cleveland, J. L., Brightman, K., Scott, A. and Ihle, J. N. (1985). "Abrogation of IL-3 and IL-2 dependence by recombinant murine retroviruses expressing v-myc oncogenes." *Nature* **317**(6036): 434-438.

Rapp, U. R., Cleveland, J. L., Fredrickson, T. N., Holmes, K. L., Morse, H. C., 3rd, Jansen, H. W., Patschinsky, T. and Bister, K. (1985). "Rapid induction of hemopoietic neoplasms in newborn mice by a raf(mil)/myc recombinant murine retrovirus." *J Virol* **55**(1): 23-33.

Rapp, U. R., Fensterle, J., Albert, S. and Gotz, R. (2003). "Raf kinases in lung tumor development." *Adv Enzyme Regul* **43**: 183-195.

Rapp, U. R., Fischer, A., Rennefahrt, U. E., Hekman, M. and Albert, S. (2007). "BAD association with membranes is regulated by Raf kinases and association with 14-3-3 proteins." *Adv Enzyme Regul* **47**: 281-285.

Rapp, U. R., Goldsborough, M. D., Mark, G. E., Bonner, T. I., Groffen, J., Reynolds, F. H., Jr. and Stephenson, J. R. (1983). "Structure and biological activity of v-raf, a unique oncogene transduced by a retrovirus." *Proc Natl Acad Sci U S A* **80**(14): 4218-4222.

Rapp, U. R., Gotz, R. and Albert, S. (2006). "BuCy RAFs drive cells into MEK addiction." *Cancer Cell* **9**(1): 9-12.

Rapp, U. R., Korn, C., Ceteci, F., Karreman, C., Luetkenhaus, K., Serafin, V., Zanucco, E., Castro, I. and Potapenko, T. (2009). "MYC is a metastasis gene for non-small-cell lung cancer." *PLoS One* **4**(6): e6029.

Rapp, U. R., Rennefahrt, U. and Troppmair, J. (2004). "Bcl-2 proteins: master switches at the intersection of death signaling and the survival control by Raf kinases." *Biochim Biophys Acta* **1644**(2-3): 149-158.

Razzaque, M. A., Nishizawa, T., Komoike, Y., Yagi, H., Furutani, M., Amo, R., Kamisago, M., Momma, K., Katayama, H., Nakagawa, M., Fujiwara, Y., Matsushima, M., Mizuno, K., Tokuyama, M., Hirota, H., Muneuchi, J., Higashinakagawa, T. and Matsuoka, R. (2007). "Germline gain-of-function mutations in RAF1 cause Noonan syndrome." *Nat Genet* **39**(8): 1013-1017.

Reed, J. C. (1999). "Dysregulation of apoptosis in cancer." *J Clin Oncol* **17**(9): 2941-2953.

Reed, J. C., Doctor, K. S. and Godzik, A. (2004). "The domains of apoptosis: a genomics perspective." *Sci STKE* **2004**(239): re9.

Reinders, J., Wagner, K., Zahedi, R. P., Stojanovski, D., Eyrich, B., van der Laan, M., Rehling, P., Sickmann, A., Pfanner, N. and Meisinger, C. (2007). "Profiling phosphoproteins of yeast mitochondria reveals a role of phosphorylation in assembly of the ATP synthase." *Mol Cell Proteomics* **6**(11): 1896-1906.

Ren, J. G., Li, Z. and Sacks, D. B. (2008). "IQGAP1 integrates Ca2+/calmodulin and B-Raf signaling." *J Biol Chem* **283**(34): 22972-22982.

Ritt, D. A., Monson, D. M., Specht, S. I. and Morrison, D. K. (2010). "Impact of feedback phosphorylation and Raf heterodimerization on normal and mutant B-Raf signaling." *Mol Cell Biol* **30**(3): 806-819.

Robertson, S. E., Setty, S. R., Sitaram, A., Marks, M. S., Lewis, R. E. and Chou, M. M. (2006). "Extracellular signal-regulated kinase regulates clathrin-independent endosomal trafficking." *Mol Biol Cell* **17**(2): 645-657.

Rogers, S., Wells, R. and Rechsteiner, M. (1986). "Amino acid sequences common to rapidly degraded proteins: the PEST hypothesis." *Science* **234**(4774): 364-368.

Roskoski, R., Jr. (2010). "RAF protein-serine/threonine kinases: structure and regulation." *Biochem Biophys Res Commun* **399**(3): 313-317.

Roux, P., Gauthier-Rouviere, C., Doucet-Brutin, S. and Fort, P. (1997). "The small GTPases Cdc42Hs, Rac1 and RhoG delineate Raf-independent pathways that cooperate to transform NIH3T3 cells." *Curr Biol* **7**(9): 629-637.

Roy, N., Deveraux, Q. L., Takahashi, R., Salvesen, G. S. and Reed, J. C. (1997). "The c-IAP-1 and c-IAP-2 proteins are direct inhibitors of specific caspases." *EMBO J* **16**(23): 6914-6925.

Roy, S. S., Madesh, M., Davies, E., Antonsson, B., Danial, N. and Hajnoczky, G. (2009). "Bad targets the permeability transition pore independent of Bax or Bak to switch between Ca2+-dependent cell survival and death." *Mol Cell* **33**(3): 377-388.

Rushworth, L. K., Hindley, A. D., O'Neill, E. and Kolch, W. (2006). "Regulation and role of Raf-1/B-Raf heterodimerization." *Mol Cell Biol* **26**(6): 2262-2272.

Saito, M., Korsmeyer, S. J. and Schlesinger, P. H. (2000). "BAX-dependent transport of cytochrome c reconstituted in pure liposomes." *Nat Cell Biol* **2**(8): 553-555.

Salomoni, P., Wasik, M. A., Riedel, R. F., Reiss, K., Choi, J. K., Skorski, T. and Calabretta, B. (1998). "Expression of constitutively active Raf-1 in the mitochondria restores antiapoptotic and leukemogenic potential of a transformation-deficient BCR/ABL mutant." *J Exp Med* **187**(12): 1995-2007.

Sattler, M., Liang, H., Nettesheim, D., Meadows, R. P., Harlan, J. E., Eberstadt, M., Yoon, H. S., Shuker, S. B., Chang, B. S., Minn, A. J., Thompson, C. B. and Fesik, S. W. (1997). "Structure of Bcl-xL-Bak peptide complex: recognition between regulators of apoptosis." *Science* **275**(5302): 983-986.

Schaeffer, H. J., Catling, A. D., Eblen, S. T., Collier, L. S., Krauss, A. and Weber, M. J. (1998). "MP1: a MEK binding partner that enhances enzymatic activation of the MAP kinase cascade." *Science* **281**(5383): 1668-1671.

Scheid, M. P., Schubert, K. M. and Duronio, V. (1999). "Regulation of bad phosphorylation and association with Bcl-x(L) by the MAPK/Erk kinase." *J Biol Chem* **274**(43): 31108-31113.

Schendel, S. L., Azimov, R., Pawlowski, K., Godzik, A., Kagan, B. L. and Reed, J. C. (1999). "Ion channel activity of the BH3 only Bcl-2 family member, BID." *J Biol Chem* **274**(31): 21932-21936.

Schendel, S. L., Montal, M. and Reed, J. C. (1998). "Bcl-2 family proteins as ion-channels." *Cell Death Differ* **5**(5): 372-380.

Schendel, S. L., Xie, Z., Montal, M. O., Matsuyama, S., Montal, M. and Reed, J. C. (1997). "Channel formation by antiapoptotic protein Bcl-2." *Proc Natl Acad Sci U S A* **94**(10): 5113-5118.

Schlesinger, P. H., Gross, A., Yin, X. M., Yamamoto, K., Saito, M., Waksman, G. and Korsmeyer, S. J. (1997). "Comparison of the ion channel characteristics of proapoptotic BAX and antiapoptotic BCL-2." *Proc Natl Acad Sci U S A* **94**(21): 11357-11362.

Schreck, R. and Rapp, U. R. (2006). "Raf kinases: oncogenesis and drug discovery." *Int J Cancer* **119**(10): 2261-2271.

Schulte, T. W., Blagosklonny, M. V., Romanova, L., Mushinski, J. F., Monia, B. P., Johnston, J. F., Nguyen, P., Trepel, J. and Neckers, L. M. (1996). "Destabilization of Raf-1 by geldanamycin leads to disruption of the Raf-1-MEK-mitogen-activated protein kinase signalling pathway." *Mol Cell Biol* **16**(10): 5839-5845.

Schumacher, B., Mondry, J., Thiel, P., Weyand, M. and Ottmann, C. (2010). "Structure of the p53 C-terminus bound to 14-3-3: implications for stabilization of the p53 tetramer." *FEBS Lett* **584**(8): 1443-1448.

Schurmann, A., Mooney, A. F., Sanders, L. C., Sells, M. A., Wang, H. G., Reed, J. C. and Bokoch, G. M. (2000). "p21-activated kinase 1 phosphorylates the death agonist bad and protects cells from apoptosis." *Mol Cell Biol* **20**(2): 453-461.

Seeliger, M. A., Ranjitkar, P., Kasap, C., Shan, Y., Shaw, D. E., Shah, N. P., Kuriyan, J. and Maly, D. J. (2009). "Equally potent inhibition of c-Src and Abl by compounds that recognize inactive kinase conformations." *Cancer Res* **69**(6): 2384-2392.

Seimiya, H., Sawada, H., Muramatsu, Y., Shimizu, M., Ohko, K., Yamane, K. and Tsuruo, T. (2000). "Involvement of 14-3-3 proteins in nuclear localization of telomerase." *EMBO J* **19**(11): 2652-2661.

Shaul, Y. D. and Seger, R. (2006). "ERK1c regulates Golgi fragmentation during mitosis." *J Cell Biol* **172**(6): 885-897.

Shaw, R. J. and Cantley, L. C. (2006). "Ras, PI(3)K and mTOR signalling controls tumour cell growth." *Nature* **441**(7092): 424-430.

She, Q. B., Ma, W. Y., Zhong, S. and Dong, Z. (2002). "Activation of JNK1, RSK2, and MSK1 is involved in serine 112 phosphorylation of Bad by ultraviolet B radiation." *J Biol Chem* **277**(27): 24039-24048.

She, Q. B., Solit, D. B., Ye, Q., O'Reilly, K. E., Lobo, J. and Rosen, N. (2005). "The BAD protein integrates survival signaling by EGFR/MAPK and PI3K/Akt kinase pathways in PTEN-deficient tumor cells." *Cancer Cell* **8**(4): 287-297.

Shimamura, A., Ballif, B. A., Richards, S. A. and Blenis, J. (2000). "Rsk1 mediates a MEK-MAP kinase cell survival signal." *Curr Biol* **10**(3): 127-135.

Shinjyo, T., Kuribara, R., Inukai, T., Hosoi, H., Kinoshita, T., Miyajima, A., Houghton, P. J., Look, A. T., Ozawa, K. and Inaba, T. (2001). "Downregulation of Bim, a proapoptotic relative of Bcl-2, is a pivotal step in cytokine-initiated survival signaling in murine hematopoietic progenitors." *Mol Cell Biol* **21**(3): 854-864.

Simons, K. and Toomre, D. (2000). "Lipid rafts and signal transduction." *Nat Rev Mol Cell Biol* **1**(1): 31-39.

Smart, E. J., Graf, G. A., McNiven, M. A., Sessa, W. C., Engelman, J. A., Scherer, P. E., Okamoto, T. and Lisanti, M. P. (1999). "Caveolins, liquid-ordered domains, and signal transduction." *Mol Cell Biol* **19**(11): 7289-7304.

Solit, D. B., Garraway, L. A., Pratilas, C. A., Sawai, A., Getz, G., Basso, A., Ye, Q., Lobo, J. M., She, Y., Osman, I., Golub, T. R., Sebolt-Leopold, J., Sellers, W. R. and Rosen, N. (2006). "BRAF mutation predicts sensitivity to MEK inhibition." *Nature* **439**(7074): 358-362.

Stancato, L. F., Silverstein, A. M., Owens-Grillo, J. K., Chow, Y. H., Jove, R. and Pratt, W. B. (1997). "The hsp90-binding antibiotic geldanamycin decreases Raf levels and epidermal growth factor signaling without disrupting formation of signaling complexes or reducing the specific enzymatic activity of Raf kinase." *J Biol Chem* **272**(7): 4013-4020.

Stoka, V., Turk, B., Schendel, S. L., Kim, T. H., Cirman, T., Snipas, S. J., Ellerby, L. M., Bredesen, D., Freeze, H., Abrahamson, M., Bromme, D., Krajewski, S., Reed, J. C., Yin, X. M., Turk, V. and Salvesen, G. S. (2001). "Lysosomal protease pathways to apoptosis. Cleavage of bid, not pro-caspases, is the most likely route." *J Biol Chem* **276**(5): 3149-3157.

Storm, S. M., Cleveland, J. L. and Rapp, U. R. (1990). "Expression of raf family proto-oncogenes in normal mouse tissues." *Oncogene* **5**(3): 345-351.

Subramanian, R. R., Masters, S. C., Zhang, H. and Fu, H. (2001). "Functional conservation of 14-3-3 isoforms in inhibiting bad-induced apoptosis." *Exp Cell Res* **271**(1): 142-151.

Sutrave, P., Bonner, T. I., Rapp, U. R., Jansen, H. W., Patschinsky, T. and Bister, K. (1984). "Nucleotide sequence of avian retroviral oncogene v-mil: homologue of murine retroviral oncogene v-raf." *Nature* **309**(5963): 85-88.

Sutton, V. R., Davis, J. E., Cancilla, M., Johnstone, R. W., Ruefli, A. A., Sedelies, K., Browne, K. A. and Trapani, J. A. (2000). "Initiation of apoptosis by granzyme B requires direct cleavage of bid, but not direct granzyme B-mediated caspase activation." *J Exp Med* **192**(10): 1403-1414.

Tait, S. W. and Green, D. R. (2008). "Caspase-independent cell death: leaving the set without the final cut." *Oncogene* **27**(50): 6452-6461.

Tait, S. W. and Green, D. R. (2010). "Mitochondria and cell death: outer membrane permeabilization and beyond." *Nat Rev Mol Cell Biol* **11**(9): 621-632.

Tan, K. O., Tan, K. M. and Yu, V. C. (1999). "A novel BH3-like domain in BID is required for intramolecular interaction and autoinhibition of pro-apoptotic activity." *J Biol Chem* **274**(34): 23687-23690.

Tang, Y., Zhou, H., Chen, A., Pittman, R. N. and Field, J. (2000). "The Akt proto-oncogene links Ras to Pak and cell survival signals." *J Biol Chem* **275**(13): 9106-9109.

Tatton, N. A. (2000). "Increased caspase 3 and Bax immunoreactivity accompany nuclear GAPDH translocation and neuronal apoptosis in Parkinson's disease." *Exp Neurol* **166**(1): 29-43.

Taylor, R. C., Cullen, S. P. and Martin, S. J. (2008). "Apoptosis: controlled demolition at the cellular level." *Nat Rev Mol Cell Biol* **9**(3): 231-241.

Teis, D., Taub, N., Kurzbauer, R., Hilber, D., de Araujo, M. E., Erlacher, M., Offterdinger, M., Villunger, A., Geley, S., Bohn, G., Klein, C., Hess, M. W. and Huber, L. A. (2006). "p14-MP1-MEK1 signaling regulates endosomal traffic and cellular proliferation during tissue homeostasis." *J Cell Biol* **175**(6): 861-868.

Townsend, K. J., Trusty, J. L., Traupman, M. A., Eastman, A. and Craig, R. W. (1998). "Expression of the antiapoptotic MCL1 gene product is regulated by a mitogen activated protein kinase-mediated pathway triggered through microtubule disruption and protein kinase C." *Oncogene* **17**(10): 1223-1234.

Treisman, R. (1996). "Regulation of transcription by MAP kinase cascades." *Curr Opin Cell Biol* **8**(2): 205-215.

Troppmair, J. and Rapp, U. R. (2003). "Raf and the road to cell survival: a tale of bad spells, ring bearers and detours." *Biochem Pharmacol* **66**(8): 1341-1345.

Tzivion, G., Gupta, V. S., Kaplun, L. and Balan, V. (2006). "14-3-3 proteins as potential oncogenes." *Semin Cancer Biol* **16**(3): 203-213.

Udell, C. M., Rajakulendran, T., Sicheri, F. and Therrien, M. (2011). "Mechanistic principles of RAF kinase signaling." *Cell Mol Life Sci* **68**(4): 553-565.

van Hemert, M. J., Steensma, H. Y. and van Heusden, G. P. (2001). "14-3-3 proteins: key regulators of cell division, signalling and apoptosis." *Bioessays* **23**(10): 936-946.

Vander Heiden, M. G. and Thompson, C. B. (1999). "Bcl-2 proteins: regulators of apoptosis or of mitochondrial homeostasis?" *Nat Cell Biol* **1**(8): E209-216.

Verhagen, A. M., Ekert, P. G., Pakusch, M., Silke, J., Connolly, L. M., Reid, G. E., Moritz, R. L., Simpson, R. J. and Vaux, D. L. (2000). "Identification of DIABLO, a mammalian protein that promotes apoptosis by binding to and antagonizing IAP proteins." *Cell* **102**(1): 43-53.

Vila, M., Jackson-Lewis, V., Vukosavic, S., Djaldetti, R., Liberatore, G., Offen, D., Korsmeyer, S. J. and Przedborski, S. (2001). "Bax ablation prevents dopaminergic neurodegeneration in the 1-methyl-4-phenyl-1,2,3,6-tetrahydropyridine mouse model of Parkinson's disease." *Proc Natl Acad Sci U S A* **98**(5): 2837-2842.

Vincenz, C. and Dixit, V. M. (1996). "14-3-3 proteins associate with A20 in an isoform-specific manner and function both as chaperone and adapter molecules." *J Biol Chem* **271**(33): 20029-20034.

Virdee, K., Parone, P. A. and Tolkovsky, A. M. (2000). "Phosphorylation of the pro-apoptotic protein BAD on serine 155, a novel site, contributes to cell survival." *Curr Biol* **10**(18): 1151-1154.

von Gise, A., Lorenz, P., Wellbrock, C., Hemmings, B., Berberich-Siebelt, F., Rapp, U. R. and Troppmair, J. (2001). "Apoptosis suppression by Raf-1 and MEK1 requires MEK- and phosphatidylinositol 3-kinase-dependent signals." *Mol Cell Biol* **21**(7): 2324-2336.

Voncken, J. W., Niessen, H., Neufeld, B., Rennefahrt, U., Dahlmans, V., Kubben, N., Holzer, B., Ludwig, S. and Rapp, U. R. (2005). "MAPKAP kinase 3pK phosphorylates and regulates chromatin association of the polycomb group protein Bmi1." *J Biol Chem* **280**(7): 5178-5187.

Vousden, K. H. (2000). "p53: death star." *Cell* **103**(5): 691-694.

Wan, P. T., Garnett, M. J., Roe, S. M., Lee, S., Niculescu-Duvaz, D., Good, V. M., Jones, C. M., Marshall, C. J., Springer, C. J., Barford, D. and Marais, R. (2004). "Mechanism of activation of the RAF-ERK signaling pathway by oncogenic mutations of B-RAF." *Cell* **116**(6): 855-867.

Wang, C. and Youle, R. J. (2009). "The role of mitochondria in apoptosis*." *Annu Rev Genet* **43**: 95-118.

Wang, C. Y., Mayo, M. W., Korneluk, R. G., Goeddel, D. V. and Baldwin, A. S., Jr. (1998). "NF-kappaB antiapoptosis: induction of TRAF1 and TRAF2 and c-IAP1 and c-IAP2 to suppress caspase-8 activation." *Science* **281**(5383): 1680-1683.

Wang, G., Chen, G., Wang, X., Zhong, J. and Lu, J. (2001). "[The polymorphism of (CAG)n repeats within androgen receptor gene among Chinese male population]." *Zhonghua Yi Xue Yi Chuan Xue Za Zhi* **18**(6): 456-458.

Wang, H. G., Rapp, U. R. and Reed, J. C. (1996). "Bcl-2 targets the protein kinase Raf-1 to mitochondria." *Cell* **87**(4): 629-638.

Wang, X. (2001). "The expanding role of mitochondria in apoptosis." *Genes Dev* **15**(22): 2922-2933.

Weber, C. K., Slupsky, J. R., Kalmes, H. A. and Rapp, U. R. (2001). "Active Ras induces heterodimerization of cRaf and BRaf." *Cancer Res* **61**(9): 3595-3598.

Wei, M. C., Lindsten, T., Mootha, V. K., Weiler, S., Gross, A., Ashiya, M., Thompson, C. B. and Korsmeyer, S. J. (2000). "tBID, a membrane-targeted death ligand, oligomerizes BAK to release cytochrome c." *Genes Dev* **14**(16): 2060-2071.

Wellbrock, C., Karasarides, M. and Marais, R. (2004). "The RAF proteins take centre stage." *Nat Rev Mol Cell Biol* **5**(11): 875-885.

Wiese, S., Pei, G., Karch, C., Troppmair, J., Holtmann, B., Rapp, U. R. and Sendtner, M. (2001). "Specific function of B-Raf in mediating survival of embryonic motoneurons and sensory neurons." *Nat Neurosci* **4**(2): 137-142.

Wilhelm, S. M., Adnane, L., Newell, P., Villanueva, A., Llovet, J. M. and Lynch, M. (2008). "Preclinical overview of sorafenib, a multikinase inhibitor that targets both Raf and VEGF and PDGF receptor tyrosine kinase signaling." *Mol Cancer Ther* **7**(10): 3129-3140.

Wilhelm, S. M., Carter, C., Tang, L., Wilkie, D., McNabola, A., Rong, H., Chen, C., Zhang, X., Vincent, P., McHugh, M., Cao, Y., Shujath, J., Gawlak, S., Eveleigh, D., Rowley, B., Liu, L., Adnane, L., Lynch, M., Auclair, D., Taylor, I., Gedrich, R., Voznesensky, A., Riedl, B., Post, L. E., Bollag, G. and Trail, P. A. (2004). "BAY 43-9006 exhibits broad spectrum oral antitumor activity and targets the RAF/MEK/ERK pathway and receptor tyrosine kinases involved in tumor progression and angiogenesis." *Cancer Res* **64**(19): 7099-7109.

Willis, S. N., Chen, L., Dewson, G., Wei, A., Naik, E., Fletcher, J. I., Adams, J. M. and Huang, D. C. (2005). "Proapoptotic Bak is sequestered by Mcl-1 and Bcl-xL, but not Bcl-2, until displaced by BH3-only proteins." *Genes Dev* **19**(11): 1294-1305.

Willis, S. N., Fletcher, J. I., Kaufmann, T., van Delft, M. F., Chen, L., Czabotar, P. E., Ierino, H., Lee, E. F., Fairlie, W. D., Bouillet, P., Strasser, A., Kluck, R. M., Adams, J. M. and Huang, D. C. (2007). "Apoptosis initiated when BH3 ligands engage multiple Bcl-2 homologs, not Bax or Bak." *Science* **315**(5813): 856-859.

Wilm, M., Shevchenko, A., Houthaeve, T., Breit, S., Schweigerer, L., Fotsis, T. and Mann, M. (1996). "Femtomole sequencing of proteins from polyacrylamide gels by nano-electrospray mass spectrometry." *Nature* **379**(6564): 466-469.

Wojnowski, L., Stancato, L. F., Larner, A. C., Rapp, U. R. and Zimmer, A. (2000). "Overlapping and specific functions of Braf and Craf-1 proto-oncogenes during mouse embryogenesis." *Mech Dev* **91**(1-2): 97-104.

Wojnowski, L., Zimmer, A. M., Beck, T. W., Hahn, H., Bernal, R., Rapp, U. R. and Zimmer, A. (1997). "Endothelial apoptosis in Braf-deficient mice." *Nat Genet* **16**(3): 293-297.

Wolfman, J. C., Planchon, S. M., Liao, J. and Wolfman, A. (2006). "Structural and functional consequences of c-N-Ras constitutively associated with intact mitochondria." *Biochim Biophys Acta* **1763**(10): 1108-1124.

Wolter, K. G., Hsu, Y. T., Smith, C. L., Nechushtan, A., Xi, X. G. and Youle, R. J. (1997). "Movement of Bax from the cytosol to mitochondria during apoptosis." *J Cell Biol* **139**(5): 1281-1292.

Yang, E., Zha, J., Jockel, J., Boise, L. H., Thompson, C. B. and Korsmeyer, S. J. (1995). "Bad, a heterodimeric partner for Bcl-XL and Bcl-2, displaces Bax and promotes cell death." *Cell* **80**(2): 285-291.

Yang, J. (2009). "Molecular modeling of human BAD and its interaction with PKAc or PP1c." *J Theor Biol* **257**(1): 159-169.

Yang, Q. H., Church-Hajduk, R., Ren, J., Newton, M. L. and Du, C. (2003). "Omi/HtrA2 catalytic cleavage of inhibitor of apoptosis (IAP) irreversibly inactivates IAPs and facilitates caspase activity in apoptosis." *Genes Dev* **17**(12): 1487-1496.

Yang, X., Lee, W. H., Sobott, F., Papagrigoriou, E., Robinson, C. V., Grossmann, J. G., Sundstrom, M., Doyle, D. A. and Elkins, J. M. (2006). "Structural basis for protein-protein interactions in the 14-3-3 protein family." *Proc Natl Acad Sci U S A* **103**(46): 17237-17242.

Yeang, C. H., McCormick, F. and Levine, A. (2008). "Combinatorial patterns of somatic gene mutations in cancer." *FASEB J* **22**(8): 2605-2622.

Yin, X. M., Wang, K., Gross, A., Zhao, Y., Zinkel, S., Klocke, B., Roth, K. A. and Korsmeyer, S. J. (1999). "Bid-deficient mice are resistant to Fas-induced hepatocellular apoptosis." *Nature* **400**(6747): 886-891.

Yokoyama, T., Takano, K., Yoshida, A., Katada, F., Sun, P., Takenawa, T., Andoh, T. and Endo, T. (2007). "DA-Raf1, a competent intrinsic dominant-negative antagonist of the Ras-ERK pathway, is required for myogenic differentiation." *J Cell Biol* **177**(5): 781-793.

Yoshida, H., Kong, Y. Y., Yoshida, R., Elia, A. J., Hakem, A., Hakem, R., Penninger, J. M. and Mak, T. W. (1998). "Apaf1 is required for mitochondrial pathways of apoptosis and brain development." *Cell* **94**(6): 739-750.

Youle, R. J. and Strasser, A. (2008). "The BCL-2 protein family: opposing activities that mediate cell death." *Nat Rev Mol Cell Biol* **9**(1): 47-59.

Yu, C., Minemoto, Y., Zhang, J., Liu, J., Tang, F., Bui, T. N., Xiang, J. and Lin, A. (2004). "JNK suppresses apoptosis via phosphorylation of the proapoptotic Bcl-2 family protein BAD." *Mol Cell* **13**(3): 329-340.

Yu, J., Zhang, L., Hwang, P. M., Kinzler, K. W. and Vogelstein, B. (2001). "PUMA induces the rapid apoptosis of colorectal cancer cells." *Mol Cell* **7**(3): 673-682.

Yuryev, A., Ono, M., Goff, S. A., Macaluso, F. and Wennogle, L. P. (2000). "Isoform-specific localization of A-RAF in mitochondria." *Mol Cell Biol* **20**(13): 4870-4878.

Zahedi, R. P., Lewandrowski, U., Wiesner, J., Wortelkamp, S., Moebius, J., Schutz, C., Walter, U., Gambaryan, S. and Sickmann, A. (2008). "Phosphoproteome of resting human platelets." *J Proteome Res* **7**(2): 526-534.

Zamzami, N. and Kroemer, G. (2003). "Apoptosis: mitochondrial membrane permeabilization--the (w)hole story?" *Curr Biol* **13**(2): R71-73.

Zamzami, N., Marchetti, P., Castedo, M., Hirsch, T., Susin, S. A., Masse, B. and Kroemer, G. (1996). "Inhibitors of permeability transition interfere with the disruption of the mitochondrial transmembrane potential during apoptosis." *FEBS Lett* **384**(1): 53-57.

Zamzami, N., Susin, S. A., Marchetti, P., Hirsch, T., Gomez-Monterrey, I., Castedo, M. and Kroemer, G. (1996). "Mitochondrial control of nuclear apoptosis." *J Exp Med* **183**(4): 1533-1544.

Zha, J., Harada, H., Yang, E., Jockel, J. and Korsmeyer, S. J. (1996). "Serine phosphorylation of death agonist BAD in response to survival factor results in binding to 14-3-3 not BCL-X(L)." *Cell* **87**(4): 619-628.

Zha, J., Weiler, S., Oh, K. J., Wei, M. C. and Korsmeyer, S. J. (2000). "Posttranslational N-myristoylation of BID as a molecular switch for targeting mitochondria and apoptosis." *Science* **290**(5497): 1761-1765.

Zhang, J., Liu, J., Yu, C. and Lin, A. (2005). "BAD Ser128 is not phosphorylated by c-Jun NH2-terminal kinase for promoting apoptosis." *Cancer Res* **65**(18): 8372-8378.

Zhang, L., Chen, J. and Fu, H. (1999). "Suppression of apoptosis signal-regulating kinase 1-induced cell death by 14-3-3 proteins." *Proc Natl Acad Sci U S A* **96**(15): 8511-8515.

Zhang, P., Chan, S. L., Fu, W., Mendoza, M. and Mattson, M. P. (2003). "TERT suppresses apoptotis at a premitochondrial step by a mechanism requiring reverse transcriptase activity and 14-3-3 protein-binding ability." *FASEB J* **17**(6): 767-769.

Zhong, J., Troppmair, J. and Rapp, U. R. (2001). "Independent control of cell survival by Raf-1 and Bcl-2 at the mitochondria." *Oncogene* **20**(35): 4807-4816.

Zhou, L. and Chang, D. C. (2008). "Dynamics and structure of the Bax-Bak complex responsible for releasing mitochondrial proteins during apoptosis." *J Cell Sci* **121**(Pt 13): 2186-2196.

Zhu, J., Balan, V., Bronisz, A., Balan, K., Sun, H., Leicht, D. T., Luo, Z., Qin, J., Avruch, J. and Tzivion, G. (2005). "Identification of Raf-1 S471 as a novel phosphorylation site critical for Raf-1 and B-Raf kinase activities and for MEK binding." *Mol Biol Cell* **16**(10): 4733-4744.

Zoratti, M. and Szabo, I. (1995). "The mitochondrial permeability transition." *Biochim Biophys Acta* **1241**(2): 139-176.

6. Appendix

6.1. Abbreviations

AIF	Apoptosis inducing factor
Akt/PKB	Acutely transforming retrovirus in rodent T cell lymphoma/ Protein kinase B
Apaf-1	Apoptotic protease activating factor-1
APS	Ammonium peroxydisulfate
ATP	Adenosine-5'-triphosphate
BAD	Bcl-2 associated death promoter Bcl-2 antagonist of cell death
Bak	Bcl-2 homologous antagonist/killer
Bax	Bcl-2–associated X protein
Bcl-2	B-cell lymphoma 2
Bcl-X_L	B-cell leukemia XL
BH	Bcl-2 homology domain
Bid	Bcl-2 interacting domain
Bik	Bcl-2-interacting killer
Bmf	Bcl-2-modifying factor
Bok	Bcl-2-related ovarian killer
bp	Base pairs
BSA	Bovine serum albumin
CD	Circular dicroism
cDNA	Complementary DNA
CDS	Coding sequence
C-terminal	Carboxy-terminal
CytC	Cytochrome C
ca.	Circa
cAMP	Cyclic adenosine monophosphate
Da	Dalton
ddH_2O	Double distilled water
DiphPC	Diphytanoylphosphatidylcholine
DMEM	Dulbecco's Modified Eagle Medium
DMSO	Dimethyl sulfoxide
DNA	Deoxyribonucleic acid
dNTP	Deoxyribonucleoside triphosphate
dsDNA	Double-stranded DNA
DTT	Dithiothreitol
E. coli	*Escherichia coli*
ECL	Enhanced chemiluminescence
EDTA	Ethylenediaminetetraacetic acid-disodium salt
e. g.	*exempli gratia*
EGF	Epidermal growth factor
EGFR	Epidermal growth factor receptor
EGTA	Ethylene glycol tetraacetic acid
ER	Endoplasmic reticulum
ERK	Extracellular signal-regulated protein kinase
ESI	Electrospray ionization
FASL	Ligand of apoptosis stimulating factor
FCS	Fetal calf serum
et al.	*et alii*
GCWN	Graduate college Würzburg Nice
GDP	Guanosine diphosphate
GEF	Guanine nucleotide exchange factor
GPCR	G-protein-coupled receptor
Grb2	Growth-factor-receptor-binding protein 2

GRE	Glucocorticoid response element
GST	Glutathione *S*-transferase
GTP	Guanosine-5'-triphosphate
h	Hours
hBAD	Human BAD
Hrk	Harakiri
IAP	Inhibitor of apoptosis protein
IB	Immunoblot
IP	Immunoprecipitation
JNK	c-Jun N-terminal kinases
kb	Kilobase
kDa	Kilodalton
L	Liter
LB	Luria Bertani
LBD	Lipid binding domain
KSR	Kinase suppressor of Ras
MALDI	Matrix Assisted Laser Desorption Ionization
MAPK	Mitogen-activated protein kinase
MAP2K	MAPK kinase
MAP3K	MAPK kinase kinase
mBAD	Mouse BAD
MEK	Mitogen-activated protein kinase/extracellular signal-regulated kinase kinase
MEKK	MAPK kinase kinase
min	Minutes
MOI	Multiplicity of infection
MP1	MEK-partner 1
mRNA	Messenger RNA
MS	Mass spectrometry
MW	Molecular weight
NMR	Nuclear magnetic resonace
N-terminal	Amino-terminal
NGF	Nerve growth factor
NP-40	Nonidet P-40
OD	Optical density
PAK	p21-activated kinases
PARP	Poly-[ADP-ribose]-polymerase
PBS	Phosphate buffered saline
PI3K	Phosphatidylinositol 3-kinase
PKA	Protein kinase A
PKB	Protein kinase B
PKC	Protein kinase C
PUMA	p53-upregulated modulator of apoptosis
pS (pSer)	Phosphoserine
PA	Phosphatidic acid
PCR	Polymerase chain reaction
pfu	Plaque forming unit
PMSF	Phenylmethylsulfonylfluorid
PVDF	Polyvinylidene difluoride
RAS	*Rat* sarcoma
RAF	Rapidly growing fibrosarcoma/*rat* fibrosarcoma
RNA	Ribonucleic acid
Rpm	Rotations per minute
RSK	Ribosomal S6 kinase
RT	Room temperature
RTK	Receptor tyrosine kinase

RU	Resonance unit
SAPK	Stress activated protein kinase
SDS	Sodium dodecyl sulfate
SDS-PAGE	Sodium dodecyl sulfate polyacrylamide gel electrophoresis
sec	Seconds
Ser	serine
SFB	Sonderforschungsbereich
Shc	Src homology and collagen
SOS	"Son of sevenless"
SPR	Surface plasmon resonance
Src	Rous sarcoma oncogene cellular homolog
SUR-8	Suppressor of Ras-8
TEMED	N,N,N',N'-Tetramethylethylenediamine
TERT	Telomerase reverse transcriptase
TFE	Trifluoroethanol
TGF-β	Transforming growth factor-β
T_m	Melting temperature
TM	Transmembrane domain
U	Unit
UV-light	Ultraviolet light
vs.	*versus*
v/v	Volume/Volume
v	Viral
WT	Wild type
w/v	Weight/Volume

6.2. List of Figures

6.3. ACKNOWLEDGMENTS

I want to thank Prof. Dr. Ulf R. Rapp for giving me the opportunity to start my PhD in the Institute for Medical Radiation and Cell Research and for his support during my thesis.

Many thanks go also to Prof. Dr. Thomas Rudel for helping me to reach my goals efficiently. I am grateful that he admitted me to the Microbiological Department. I enjoyed the interesting seminars and the social and scientific events that provided a constructive and stimulating environment.

Special thanks go to my supervisor PD Dr. Mirko Hekman, for his strong guidance during this work. I am thankful for the excellent supervision I received. He was a great aid in so many situations during all periods of my dissertation.

I want to gratefully acknowledge Prof. Dr. Dr. h.c. Roland Benz for his helping hand. He was supporting me and was taking care of me in an uncomplicated and trustful way leading to high productivity and a wonderful cooperation. Additionally, I want to thank him and the members of his group for giving me the opportunity to work in their laboratories for many times.

I am thankful to Dr. Angela Baljuls who provided me a high quality research group that excellently combined a goal orientated and challenging research mentality with an independent, faithful and motivating teamwork. Additionally, I want to thank her for standing behind me in and besides the lab.

I am especially grateful to Marco Albrecht whose innovative ideas brought my research work further several times. His great technical and scientific knowledge enriched and improved my everyday life in many aspects.

I enjoyed the contact to all of my co-authors, cooperation partners and co-workers from the Microbiological Department and the Institute for Medical Radiation and Cell Research. I am thankful for the nice and friendly atmosphere, the helpful discussions and for the time we shared outside of the institute. Special thanks go to Laura Goldberg for excellent cooperativeness and proof reading. Renate Metz made an important contribution to my dissertation by providing excellent technical assistance and many constructive suggestions. I also want to acknowledge Dr. Birgit Bergmann for her persistent readiness to help, for offering her administrative skills and for doing a great job in desperate situations. Many thanks go also to Hartmut Mull for struggling a lot to provide necessary cells and for many inspiring inputs.

My final acknowledgment goes to my family for their everlasting love and support.

6.4. LIST OF PUBLICATIONS

Research Papers:

1. Baljuls A, Mahr R, Schwarzenau I, Müller T, **Polzien L**, Hekman M, Rapp UR (2011) Single substitution within the RKTR motif impairs kinase activity but promotes dimerization of RAF, *J. Biol. Chem.* (in revision)

2. **Polzien L**, Baljuls A, Albrecht M, Hekman M, Rapp UR (2011) BAD contributes to RAF-mediated proliferation and cooperates with B-RAF-V600E in cancer signaling, *J. Biol. Chem*. [Epub ahead of print]

3. **Polzien L**, Baljuls A, Roth HM, Kuper J, Benz R, Schweimer K, Hekman M, Rapp UR (2010) Pore-forming activity of BAD is regulated by specific phosphorylation and structural transitions of the C-terminal part, *Biochim. Biophys. Acta*. **1810,** 162-169

4. Molzan M, Schumacher B, Ottmann C, Baljuls A, **Polzien L**, Weyand M, Thiel P, Rose R, Rose M, Kuhenne P, Kaiser M, Rapp UR, Kuhlmann J, Ottmann C (2010) Impaired binding of 14-3-3 to C-RAF in Noonan syndrome suggests new approaches in diseases with increased Ras signaling, *Mol. Cell. Biol*. **30,** 4698-4711

5. **Polzien L**, Benz R, Rapp UR (2010) Can BAD pores be good? New insights from examining BAD as a target of RAF kinases, *Adv. Enzyme Regul*. **50**, 147-159

6. **Polzien L**, Baljuls A, Rennefahrt UE, Fischer A, Schmitz W, Zahedi RP, Sickmann A, Metz R, Albert S, Benz R, Hekman M, Rapp UR (2009) Identification of novel *in vivo* phosphorylation sites of the human proapoptotic protein BAD: pore-forming activity of BAD is regulated by phosphorylation, *J. Biol. Chem*. **284**, 28004-28020

7. Niewiadomska E, **Polzien L**, Desel C, Rozpadek P, Miszalski Z, Krupinska K (2009) Spatial patterns of senescence and development-dependent distribution of reactive oxygen species in tobacco (*Nicotiana tabacum*) leaves, *J. Plant Physiol*. **166**, 1057-1068

Oral Presentations:

Feb 2009 International research training group 1141/1 prolongation review University of Würzburg, Germany "Specific phosphorylation of BAD: contribution of RAF kinases, effects on BAD's pore forming abilities and impact on cell survival"

Jul 2010 Collaborative Research Centre 487 Convention 2010, Bad Brückenau, Germany "Controlling Cell Survival and Proliferation by BAD Phosphorylation"

Sep 2010 Symposium of the International Max Planck Research School for Molecular Biology 2010: Horizons in Molecular Biology, University of Göttingen, Germany "BAD phosphorylation: A Checkpoint for Cell Death or Survival"

Poster Presentations:

Sep 2009 International Symposium of the Graduate School of Life Science, University of Würzburg, Germany "Specific phosphorylation of BAD: contribution of RAF kinases, effects on BAD's pore forming abilities and impact on cell survival" **Lisa Polzien**, Ulrike Rennefahrt, Mirko Hekman, Ulf R. Rapp, and Roland Benz

Oct 2009 2nd Symposium of the Research Training Group 1048 - Molecular Basis of Organ Development in Vertebrates, University of Würzburg, Germany "Apoptosis protein BAD is directly regulated by tumour kinases" **Lisa Polzien**, Angela Baljuls, Mirko Hekman, Ulf R. Rapp, and Roland Benz

Sep 2010 Symposium of the International Max Planck Research School for Molecular Biology 2010: Horizons in Molecular Biology, University of Göttingen, Germany "BAD phosphorylation: A Checkpoint Between Cell Death and Survival" **Lisa Polzien**, Angela Baljuls, Mirko Hekman, Marco Albrecht, Roland Benz, and Ulf R. Rapp

Oct 2010 Integrated Graduate College of the SFB Transregio 17, Autumn School: The Puzzling World of Cancer, University of Würzburg, Germany "BAD: A Node of the RAF and PI3K/Akt Pathway" **Lisa Polzien**, Angela Baljuls, Mirko Hekman, Marco Albrecht, Roland Benz, and Ulf R. Rapp

Oct 2010 International Symposium of the Graduate School of Life Science, University of Würzburg, Germany "BAD phosphorylation: A Checkpoint Between Cell Death and Survival" **Lisa Polzien**, Angela Baljuls, Mirko Hekman, Marco Albrecht, Roland Benz, and Ulf R. Rapp

6.5. DECLARATION

Affidavit
(Eidesstattliche Erklärung)

I hereby declare that my thesis entitled " BAD Phosphorylation: A Novel Link between Apoptosis and Cancer" is the result of my own work. I did not receive any help or support from commercial consultants. All sources and/or materials applied are listed and specified in the thesis.

This work is based on four publications that are specified within this thesis. Apart from that, I verify that this thesis has not yet been submitted as part of another examination process neither in identical nor in similar form.

Würzburg

……..

Date Signature